PTEN inactivation has distinct effects on the signalling properties of EGFR and MET and their response to kinase inhibitors

Irene Matucci

The Institute of Cancer Research
and
University of London

PhD Supervisor: Igor Vivanco

A thesis submitted for the degree of
Doctor of Philosophy

June 2020

Declaration

I Irene Matucci confirm that the work presented in this thesis is my own. Where information has been derived from other sources, I confirm that this has been indicated in the thesis.

Abstract

Receptor tyrosine kinases (RTKs) are a family of cell-surface receptors that play a major role in regulating pro-proliferative and pro-survival signalling pathways, such as the Phosphoinositide 3-kinase (PI3K/Akt) pathway. When aberrantly activated, RTKs can promote oncogene addiction, causing tumour cells to develop exquisite dependency on their activity. Consequently, various RTK inhibitors are approved for the targeted treatment of cancers with aberrant RTK activation. However, both *de novo* and acquired mechanisms of drug resistance pose challenges to such treatments. The loss of the tumour suppressor Phosphatase and Tensin Homolog (PTEN), a negative regulator of the PI3K/Akt pathway, is a common molecular dysfunction associated with resistance to inhibitors of Epidermal Growth Factor Receptor (EGFR) and Human Epidermal Growth Factor Receptor 2 (HER2). Despite the irrefutable role of PTEN in tumorigenesis, our understanding of how PTEN regulates tyrosine kinase inhibitor (TKI) responses remains limited. This thesis investigates the molecular consequences of PTEN inactivation on EGFR and Mesenchymal to Epithelial Transition Receptor (MET) inhibitor responses, providing evidence that complete PTEN-inactivation is an RTK-selective mechanism of TKI resistance. As such, we find that PI3K/Akt pathway activation in relation to TKI resistance varies based on the identity of the driver RTK. Specifically, while MET-TKI resistance may be PI3K/Akt pathway-dependent, EGFR-TKI resistance appears to be at least partially PI3K/Akt-independent. We also provide some evidence that PTEN could modulate the abundance of certain RTK conformations, as well as affect receptor cellular localisation. Finally, through molecular profiling, new mediators of EGFR and MET inhibitor responses are identified. In particular, PIKfyve emerges as a potential therapeutic target in MET-driven cancers.

Acknowledgement

This page is probably the most important section of the thesis, as I would have not been here without the help and support of a lot of people, to whom I am extremely grateful.

To start off, a big thank you goes to my team, Igor, Alice, Lefteris, Sara, Niamh and Glori, and to those who joined us only briefly. Without you there would have been no PhD, and I would have probably given up a long time ago. Thank you all for not killing me despite my innumerable complaints and for listening to my endless rants. Lefteris and Sara, thank you for teaching me science and sharing your knowledge with me.

Thank you Rita, Henry, Selby and George for letting me train your abs and for coming with me to the gym; smashing some weights may still be the best way to get through a PhD. Thank you Marco for all the scientific and non-scientific support, and thank you, Kostas, for the endless chats, the caring smile and the supportive presence. It would have been no fun without you guys, you made the journey a lot more pleasant and I will be forever grateful for your friendship.

To my boxing crew, and in particular to Chloe, thank you. Thank you for holding the pads, thank you for the pizzas, thank you for your wonderful friendship. Chloe, thank you for those heart-to-heart Aperitivo's that put a smile back on my face.
One more friend to thank is Elisa, my life-long support. You saved me and put me back on track on a few occasions; your presence has often given me strength throughout this journey.

Another thank you goes to my Italian family: to my aunties, uncles, cousins and grandparents. You have never had a clue what I was doing, but you were there to support me whatever, whenever and wherever. I'd like to thank Nicola in particular. Your inspirational figure has added depth to every step of this journey and has left a light on for what the future could hold.

I could have not finished this PhD, nor written a page of this thesis without the presence and support of my partner, Dan. You have kept my insanity at bay, and somehow managed to keep me relatively sane. You have silenced my fears and you have given me courage. You have dried my tears and made me laugh. If I am putting a full stop to this PhD, and I do it in my full capabilities, it is mainly because of you and I am forever grateful.

Finally, the biggest thank you of all goes to my family: dad, mum and Mati. You three are the ones that have allowed me to be here today. You are my biggest fans, and your faith in me is what has often driven me to push through. Your constant and kind presence in my life has given me the strength I needed to start and finish this. Mati, you are all the good things I am not, the most important human in my life, and believe it or not, but your existence has made these four years a lot more worthy. Thank you.

Per aspera ad astra

Table of Contents

Table of figures

Table of Supplementary Figures

List of tables

Abbreviations

AKT – AKR thyoma, also known as PKB – Protein Kinase B

ALK – Anaplastic Lymphoma Kinase

AMP – adenosine monophosphate

AMPK – Adenosine Monophosphate-activated Protein Kinase

AP-1 – Activator Protein 1

AP-2 – Activator Protein 2

AREG – Amphiregulin

Asp, D – Aspartic Acid

Atg – Autophagy Related

ATP – Adenosine Triphosphate

Bcl-2 – B-cell lymphoma 2

BTC – Betacellulin

CBL – Casitas B-lineage Lymphoma

CCP – Clathrin Coated Pit

CDR – Circular Dorsal Ruffles

CIE – Clathrin Independent Endocytosis

CME – Clathrin Mediated Endocytosis

CRISPR – Clustered Regularly Interspaced Short Palindromic Repeats

Crk – CT10 Regulator of Kinase

DCTN2 – dynactin subunit 2

DFG – Aspartic Acid (Asp), Phenylalanine (Phe), Glycine (Gly)

EE – Early Endosome

EEA1 – Early Endosome Antigen 1

EGF – Epidermal Growth Factor

EGFR – Epidermal Growth Factor Receptor

EGFRvIII – EGFR variant III

EPG – Epigen

EPR – Epiregulin

Eps15 – EGFR Pathway Substrate 15

ER – Endoplasmic Reticulum

ErbB – Erythroblastic Oncogene B

Erk1/2 – Extracellular signal Regulated Kinase 1 and 2

FBS – Foetal Bovine Serum

FYVE – Fab1p-YOTB-Vac1P-EEA1

Gab1 – Grb2 Associated Binder

GBM – Glioblastoma Multiforme

GDP – Guanosine Diphosphate

Gly, G – Glycine

GOF – Gain of Function

Grb2 – Growth Factor Receptor Bound Protein 2

GTP – Guanosine Triphosphate

h – hour/hours

HBEGF – Heparin-binding EGF-like Growth Factor

HER2 – Human Epidermal Growth Factor Receptor 2

HER3 – Human Epidermal Growth Factor Receptor 3

HGF – Hepatocyte Growth Factor

HRAS – Harvey Ras

Hsc70 – Heat Shock Cognate 70 kDa

IF – Immunofluorescence

IL – Interleukin

ILV – intraluminal Vesicles

$Ins(1,3,4,5)P_4$ – Inositol 1,3,4,5-tetrakisphosphate

IPT – Immunoglobulin-Plexin-Transcription factor

JAK – Janus Kinases

JM – Juxtamembrane Domain

JNK – cJun N-terminal Kinase

KRAS – Kirsten Ras

LAMP1 – Lysosome Associated Membrane Protein 1

LC3B - microtubule-associated protein Light Chain 3

LE – Late Endosome

LOF – Loss of function

mAb – monoclonal Antibodies

MAPK – Mitogen-Activated Protein Kinase

MAPKKK – MAPK Kinase Kinase

MEK – MAPK/Erk kinase

MET – Mesenchymal to Epithelial Transition Receptor

min – minute/minutes

mPTEN – mouse PTEN

mTOR – mechanistic Target of Rapamycin

mTORC – mTOR Complex

MVBs – Multivesicular Bodies

NHEJ – Non-Homologous End Joining

NRAS – Neuroblastoma Ras

NSCLC – Non Small Cell Lung Cancer

p – Phosphorylated

PAM – Protospacer-Adjacent Motif

PDGF – Platelet-derived Growth Factor

PDK – 3'-Phosphoinositide-Dependent Kinase 1

PDZ – Post synaptic density protein (PSD95), Drosophila disc large tumour suppressor (Dlg1) and Zonula occludens-1 protein (Zo-1)

PH – Pleckstrin Homology

Phe, F – Phenylalanine

PI – Phosphoinositide

PIKfyve – Phosphoinositide Kinase for five position containing a Fyve finger

PIP_2 – Phosphatidylinositol 4,5-bisphosphate

PIP_3 – Phosphatidylinositol 3,4,5-triphosphate

PI3K – Phosphoinositide 3-kinase

PKC – Protein Kinase C

PLC – Phospholipase Cγ

PP2A – Protein Phosphatase 2A

PRAS40 – Prolin-rich Akt substrate of 40 kDa

PS – Phosphatidylserine

PTB – Phosphotyrosine binding domain

PTEN – Phosphatase and Tensin Homolog

Rab - Ras-associated binding protein

Raf – Rapidly Accelerated Fibrosarcoma

Ras – Rat Sarcoma

Rb1 – Retinoblastoma protein 1

RE – Recycling Endosomes

RNAi – RNA interference

ROS – Reactive Oxygen Species

RTK – Receptor Tyrosine Kinase

SAPK – Stress Activated Protein Kinase

Ser – Serine

SGK1 – Serum- and Glucocorticoid-inducible kinase 1

sgRNA – single guided RNA

SH2 – Src-Homology 2 domain

SHP1 – SH2 domain containing protein tyrosine phosphatase 1

SHP2 – SH2 domain containing protein tyrosine phosphatase 2

shRNA – small hairpin RNA

SOS – Son Of Sevenless

Src – Sarcoma

STAT – Signal Transducer and Activator of Transcription

S6K – S6 Kinase

TGFα – Transforming Growth Factor-α

Th – T helper (cells)

Thr – Threonine (T)

TK – Tyrosine Kinase Domain

TKI – Tyrosine Kinase Inhibitor

TSC2 – Tuberous Sclerosis protein 2

Tyr – Tyrosine (Y)

UV – Ultraviolet

Vps34 – Vacuolar protein sorting 34

4EBP1 – 4E Binding Protein 1

Chapter 1. Introduction

1.1 Introduction to Receptor Tyrosine Kinases (RTKs)

Multicellular organisms are constantly interacting with the environment that surrounds them. In order to do so, their cells are equipped with surface receptors that can capture and translate signals and stimuli (Schlessinger, 2000; Uings and Farrow, 2000).

One large family of cell-surface receptors is the Receptor Tyrosine Kinase (RTK) group. RTKs are type I transmembrane proteins with intrinsic protein tyrosine kinase activity (Schlessinger, 2000). They receive and transduce extracellular signals, including hormones, growth factors and cytokines, to regulate intracellular processes such as cell proliferation, survival, death, movement and differentiation. Due to the essential role these receptors play in cellular homeostasis, their dysregulation can lead to disease, most prominently cancer. Not surprisingly, several RTKs have extensively been pursued as cancer therapeutic targets.

There are 58 human RTKs, grouped into 20 families based on differences in their kinase domain (Lemmon and Schlessinger, 2010), such as the Epidermal Growth Factor (EGF), the Hepatocyte Growth Factor (HGF), the platelet-derived growth factor (PDGF) and the insulin receptor family . Despite this diversity, RTK overall structure and mechanism of action are evolutionarily conserved (Lemmon and Schlessinger, 2010). RTKs are single-pass transmembrane enzymes that catalyze the transfer of the γ-phosphate from adenosine triphosphate (ATP) molecules onto the tyrosine (Tyr, Y) residues of substrates (Hubbard, 1999). Upon ligand binding to the extracellular domain, RTKs undergo receptor dimerization and *trans*-phosphorylation on key tyrosine residues. Phosphorylated RTKs in turn act as docking platforms for downstream effectors that initiate signalling cascades, such as the activation of phospholipase C-γ (PLCγ), the Mitogen-Activated Protein Kinase (MAPK), the Janus kinases (JAK)-signal transducer and activator of transcription (STAT) and the Phosphoinositide 3-Kinase (PI3K/Akt) pathways (Carrasco-García et al., 2014; Leatherbarrow and Halfon, 2009).

1.2 RTK Structure and activation mechanisms

The majority of RTKs exist in a monomeric state when unstimulated and consists of a single polypeptide chain. RTK structure can be simplified into three main units: an extracellular glycosylated domain that interacts with ligands, a transmembrane helix that anchors the receptor to the plasma membrane, and a cytoplasmic portion, which acts as a site for protein-protein interactions and catalytic activity (Figure 1.1).

The extracellular domain that drives ligand recognition varies across RTK families; it often contains regions such as immunoglobin-like domains or EGF-like domains. The intracellular structure of RTK is instead more conserved. Following a transmembrane α-helix, the cytoplasmic section consists of a juxtamembrane (JM) portion, a tyrosine kinase (TK) catalytic domain and a C-terminal region (Hubbard, 1999). The TK domain has a two-lobe structure formed by a smaller N-terminal (N-lobe) and a larger C-terminal (C-lobe) subdomain, with an ATP binding site between the two (Ung and Schlessinger, 2015) (Figure 1.1).

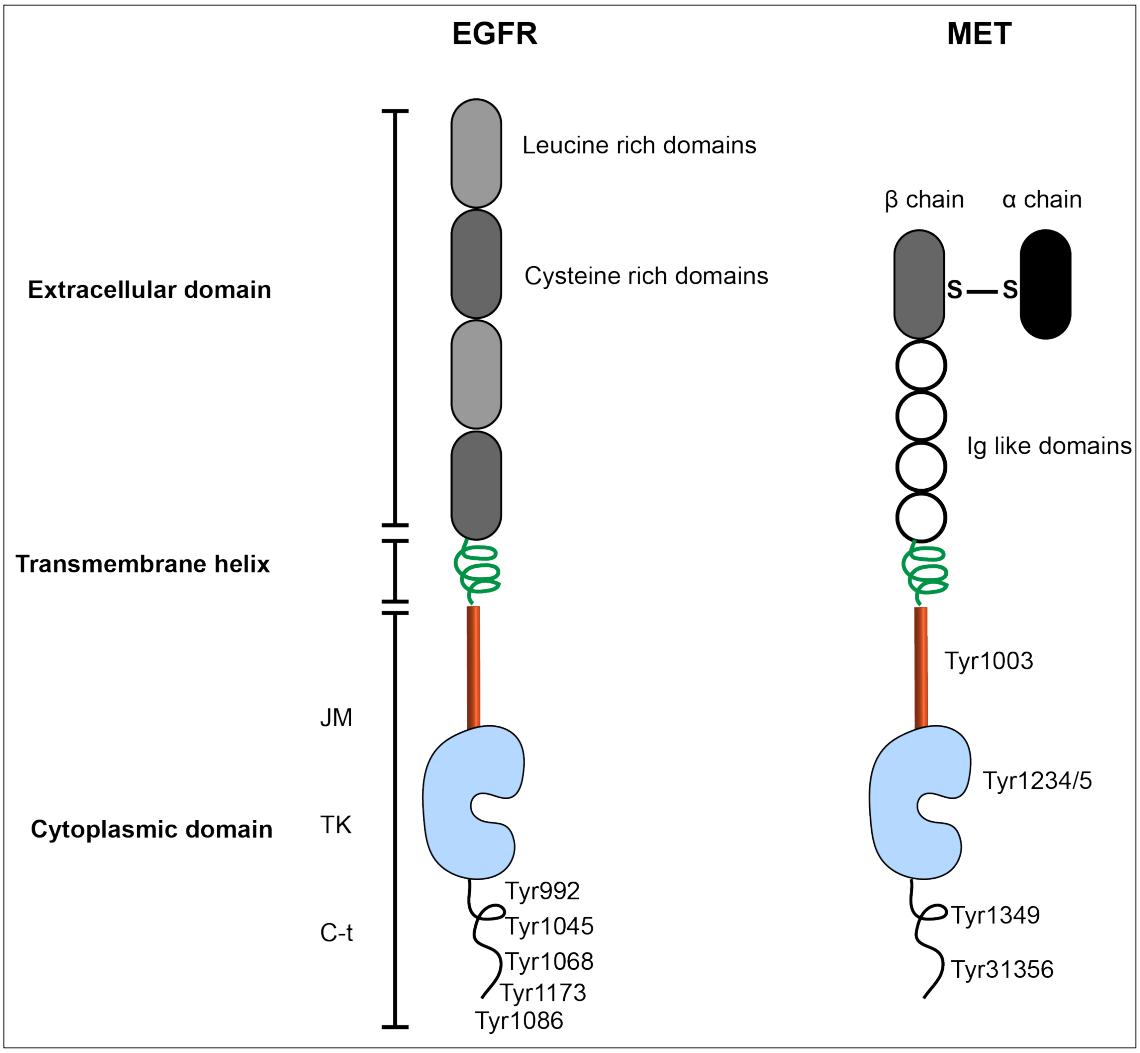

Figure 1.1 RTK structure

The above diagram is a schematic description of the main domains of EGFR and MET, including the main tyrosine phosphorylation sites. RTK overall structure is composed of an extracellular domain, a transmembrane helix and a cytoplasmic domain. The cytoplasmic domain is formed by the Juxtamembrane domain (JM), the tyrosine kinase domain (TK) and the C-terminal region (C-t).

RTKs exist at the plasma membrane in equilibrium between monomeric and oligomeric forms (Schlessinger, 2000). What drives RTK activation is a combination of conformational and oligomeric changes that enable the receptor to carry out its function (Westerfield and Barrera, 2019).

The canonical mechanism of RTK activation postulates that ligand binding to the extracellular domain stabilizes the formation of active homo or hetero dimers by juxtaposing the TK domains of each monomer. This newly acquired positioning within the dimer allows for *trans*-autophosphorylation of key tyrosine residues

within the cytoplasmic domain (Heldin, 1995; Ullrich and Schlessinger, 1990). The exact steps required to generate a fully signalling-competent RTK differ between RTK family members. However, the *trans*-phosphorylation events catalyse four conserved processes: destabilisation of auto-inhibitory conformations, rotation of the Aspartic acid (Asp, D)-Phenylalanine (Phe, F)-Glycine (Gly, G) (DFG) motif, enhancement of tyrosine kinase activity and recruitment of downstream signalling proteins.

RTK's auto-inhibitory conformations are mainly mediated by the JM domain and by C-terminal regions, in particular the activation loop found within the C-lobe of the catalytic domain. These regions adopt conformations that block substrate and/or ATP access in an inactive RTK. For instance the activation loop of Mesenchymal to Epithelial Transition Receptor (MET, also known as hepatocyte growth factor receptor) makes numerous interactions with N-lobe residues repressing the RTK catalytic activity (Wang et al., 2006a). Phosphorylation on key tyrosines within these domains triggers a conformational change that facilitates substrate access (Hubbard, 2004). As we will discuss later in more detail, Epidermal Growth Factor Receptor (EGFR) is an exception, as it does not depend on the phosphorylation of the activation loop for full activation (Stamos et al., 2002). Furthermore, the JM region of EGFR acts as an activator rather than an autoinhibitory domain. It in fact helps establishing important contacts within the dimer and holds it in an active conformation (Aifa et al., 2005; Thiel and Carpenter, 2007).

Rotation of the DFG motif is another important step towards a fully activated RTK. This motif is located at the beginning of the activation loop and can acquire an "in" or an "out" conformation, directly contributing to the active and inactive RTK states, respectively. In the "out" state, the ATP pocket is occupied by phenylalanine, preventing ATP access and receptor activation. In the "in" conformation the phenylalanine is packed in a hydrophobic pocket within the N-C-lobe junction, stabilising the ATP binding pocket. At the same time, the aspartic acid, faces outward to coordinate the interaction with a magnesium ion, allowing ATP binding and receptor activation (Modi and Dunbrack, 2018; Ung and Schlessinger, 2015). The rotation of the DFG motif also contributes to the repositioning of the αC helix, a helical structure within the N-lobe of the catalytic domain. A conserved glutamic

acid within the αC helix contributes to the phosphate transfer from the molecule of ATP to the kinase's substrate (Palmieri and Rastelli, 2013).
Importantly, the DFG motif is not restricted to the "in" and "out" conformations only, and can sample many intermediary states. In particular, it can have many inactive conformations, given that the inactive catalytic domain does not face the chemical constraints that an active catalytic site has (Modi and Dunbrack, 2018).

Phosphorylation in *trans* of the activation domain within an RTK dimer enhances the kinase catalytic activity by placing the domain in a catalytically favourable position (Johnson et al., 1996). How *trans* phosphorylation helps RTK catalytic activity is still subject to debate. It could support an optimal conformation for signalling due to the physical proximity of the cytoplasmic domains within a dimer, as well as help with the recruitment of a higher number of intracellular substrates (Hubbard, 2004). With the exception of the EGFR family of receptors, *trans* phosphorylation is a necessary step for the activation of an RTK. However, the TK domain is believed to have sufficient kinase activity to *trans*-phosphorylate even when in an autoinhibited conformation. Due to the dynamic nature of those interactions that keep RTK molecules in an "off' state, TK domains are believed to "breathe", relaxing and tightening those inhibitory bonds (Lemmon and Schlessinger, 2010). Inactive RTKs are therefore, for a portion of the time, capable of allosteric activation and can result in receptor dimer activation in the absence of ligand (Lemmon and Schlessinger, 2010). Although these events are likely to contribute minimally to an RTK's overall activity, they may become significant in cells with RTK overexpression. A rise in local RTK concentrations in fact increases the probability of a transiently active TK domain encountering another TK domain and promoting its activation.

An auto-phosphorylated RTK is primed for binding substrates containing a phospho-tyrosine recognition domain, such as SRC-Homology 2 (SH2) or PhosphoTyrosine Binding (PTB) domains (Lemmon and Schlessinger, 2010). Among these interactors, there are several accessory or adaptor proteins, such as Growth Factor Receptor-bound protein 2 (Grb2) and Grb2 Associated Binder 1 (Gab1) that are recruited at active RTK sites, and facilitate the formation of large

multiprotein complexes. This is the first step for an intracellular signalling cascade (Pawson, 1995).

Despite the similarity in the overall structure and the main steps that initiate signal propagation, each RTK is unique, especially in its activation mechanism (Schlessinger, 2000). It is important that we appreciate the complexity of each RTK individually, particularly as receptor conformation can significantly affect the efficacy of targeted treatments. For the purpose of this thesis, we will focus on EGFR and MET only.

1.2.1 EGFR activation mechanism and main phosphorylation sites

EGFR is the most well-studied RTK; it was the first receptor to be characterised with tyrosine kinase activity and linked to its ligand, EGF (Carpenter et al., 1978). At least seven EGFR ligands have now been identified: EGF, transforming growth factor-α (TGFα), heparin-binding EGF-like growth factor (HBEGF), amphiregulin (AREG), betacellulin (BTC), epiregulin (EPR) and epigen (EPG) (Harris et al., 2003).

It is also now recognised that EGFR activation mechanism differs from that of other RTKs, and aspects of it are still subject of research. For instance, it is yet unclear whether EGFR is activated by the dimerization of monomers upon EGF binding or by a rotation of the monomers within an inactive dimer upon ligand stimulation (Moriki et al., 2001). Research has in fact demonstrated how EGFR can live in symmetric unliganded inactive dimeric conformations (Jura et al., 2009; Yu et al., 2002).

As previously mentioned, phosphorylation of the activation domain is a necessary step for receptor catalytic activity. EGFR is, however, an exception. Its activation domain, in fact, sits in a catalytically competent orientation even in the absence of phosphorylation (Stamos et al., 2002). Nonetheless, the receptor has a rigorous form of autoinhibition.
Unlike other RTKs, EGFR possesses a dimerization arm, a region of the receptor's extracellular domain that sits right at the dimer interface (Dawson et al., 2005;

Freed et al., 2017). The dimerization arm remains deeply buried within the monomer structure in the absence of EGF (Burgess et al., 2003). Binding of the growth factor causes a conformational change that leads to the release of the dimerization arm, which then mediates the dimerization with another monomer (Burgess et al., 2003).

Another peculiar aspect of EGFR activation mechanism is that there is no direct contribution of the growth factor towards the dimerization interface itself, as seen in the case of other RTKs. EGF instead contacts two sites within a single monomer, and it is this binding that triggers the conformational change that leads to receptor activation. It is still subject of debate whether the second monomer is also required to be bound to an EGF molecule, as a single ligand has been shown capable of activating EGFR dimers (Liu et al., 2012).

It is also yet unclear how the binding of EGF actually propagates the conformational change to the catalytic domain; the conformation of the extracellular domain in fact does not change substantially upon binding of EGF (Ferguson et al., 2003; Ogiso et al., 2002). It has been hypothesised that a movement in the TM domain is what propagates the conformational change to the overall receptor structure. EGFR is in fact believed to exist in a very dynamic equilibrium, constantly sampling different conformations (Figure 1.2). Under steady state conditions, EGF binds weakly to the tethered EGFR conformation, with 2-5% of growth factor binding strongly to the more extended EGFR conformation (Ullrich and Schlessinger, 1990). The latter is an energy favourable event, so, in the presence of increasing concentrations of ligand, the EGFR equilibrium will shift towards the extended, dimerization-prone conformation (Burgess et al., 2003). The extracellular domain rearrangement triggered by this event allows for the dimerization arm on EGFR to reach out and dimerize with the second EGFR molecule (Gotoh et al., 1992; Stamos et al., 2002). This binding triggers a change of conformation in the “receiving” monomer, which releases the autoinhibitory interactions (Zhang et al., 2006), rotating the transmembrane domains into the ideal position for the cytoplasmic domain dimerization (Figure 1.2).

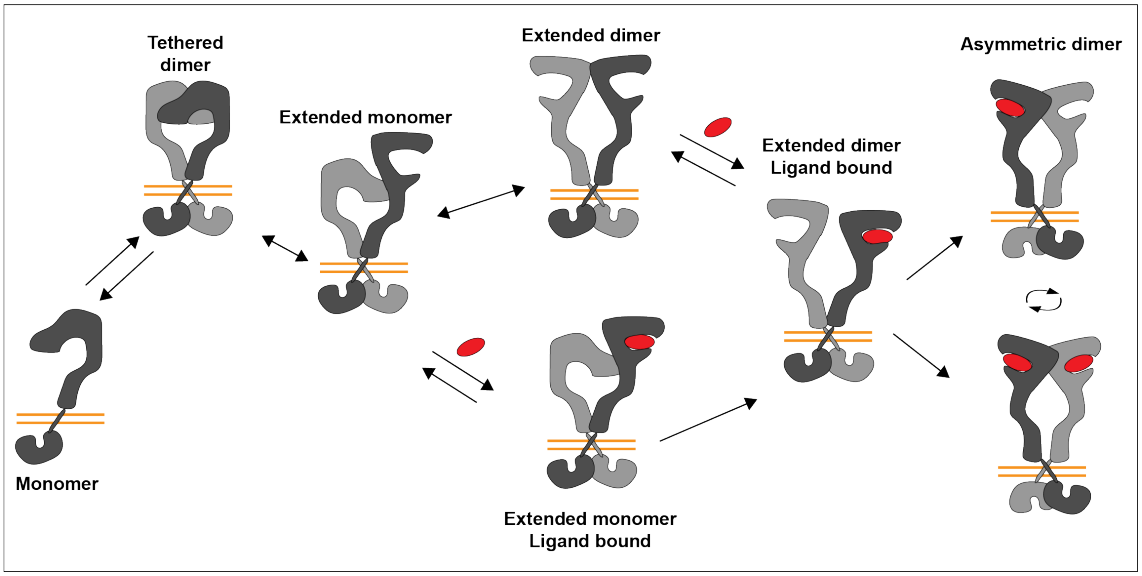

Figure 1.2 EGFR activation mechanism

EGFR can be found in either a monomeric or a dimeric form. The extracellular domain constantly samples different conformations. EGF (red) preferentially binds to the extended conformation; this energy favourable event stabilises the monomer and induces a conformational change. The dimerization arm reaches out for the other EGFR monomer and triggers a conformational change in the receiver. As a consequence, the dimer rotates to form an asymmetric dimer, and positions the intracellular domains in the perfect orientation for full activation.

The JM domain, which in other RTKs often inhibits kinase activity, contributes to EGFR activation upon EGF binding (Thiel and Carpenter, 2007). It does so by forming an alpha helix structure that interacts with the JM domain of the receiver monomer and wraps around the C-terminal lobe of the activator (Gajiwala, 2013). This newly formed interaction connects to the transmembrane domain, stabilising the dimer (Jura et al., 2009). In the absence of EGF, JM domains are prevented from forming activating alpha helices structures by the interaction with the C-terminal regions (Figure 1.3). Ultimately, the structural changes propelled by EGF binding result in the phosphorylation of the C-terminal tail (Figure 1.3).

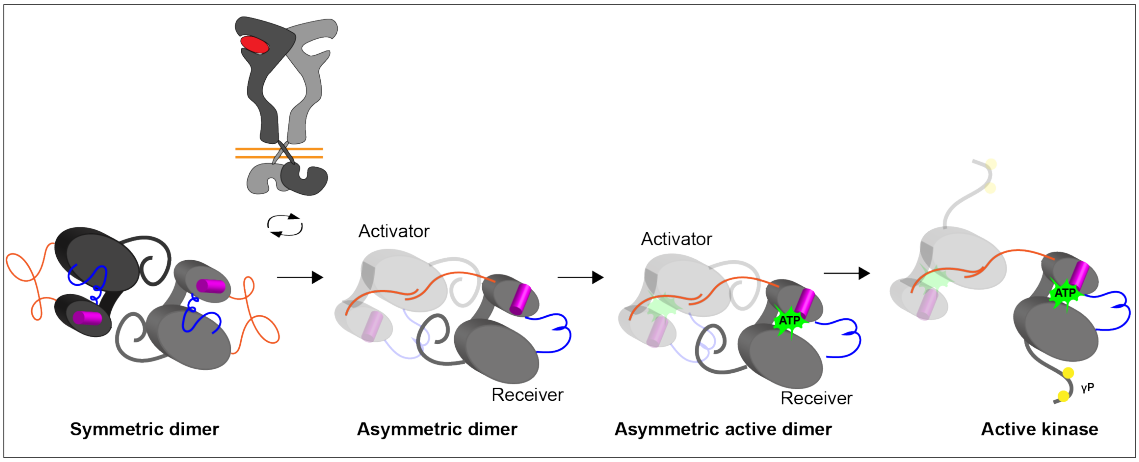

Figure 1.3 EGFR JM domain contributes to receptor activation

In an EGFR inactive dimer, the cytoplasmic domains are in a symmetric conformation. Upon conformational change of the extracellular domain, the receptors undergo a rotation that breaks the auto-inhibitory conformation of the receiver. The JM domains (orange) are dislodged from their interactions with the C-terminal lobes and bind together. The αC helix (magenta) acquires a DFG-in conformation. The conformational change results in the dislocation of the activation loop (blue) and primes the receptor for ATP binding. C-terminal tails are phosphorylated and the EGFR dimer is ready to carry out its kinase activity.

The C-terminal tail contains 5 tyrosine residues that become phosphorylated upon activation, and are highly conserved in the EGFR subfamily: Tyr992, Tyr1045, Tyr1068, Tyr1086 and Tyr1173 (Figure 1.1) (Ullrich and Schlessinger, 1990; Wee and Wang, 2017; Yarden and Ullrich, 1988). Tyr1068 is responsible for Gab1 binding and phosphorylation, resulting in the activation of downstream signalling cascades, such as the PI3K/Akt pathway (Mattoon et al., 2004; Rodrigues et al., 2000). Tyr1045 is an important phosphorylation site for the regulation of EGFR activity via the ubiquitin ligase Casitas B-lineage Lymphoma protein c (c-Cbl) (Levkowitz et al., 1998). Tyr992 and Tyr1173 play an important role as sites for PLCγ and Shc binding, thus being involved in MAPK pathway activation (Vega et al., 1992). These sites are also key for the binding of phosphatases, which, in turn, modulate EGFR activity (Agazie and Hayman, 2003; Sturla et al., 2005). Tyr1068, Tyr1086 and, indirectly, Tyr1173 mediated the binding of Grb2 and, consequently, the activation of Rat Sarcoma (Ras) and Extracellular signal Regulated Kinase 1 and 2 (Erk1/2) (Batzer et al., 1994).

Despite the presence of auto-inhibitory features, several cancers show autonomous unliganded EGFR phosphorylation. This can occur due to mutations that favour an active conformation (Shan et al., 2012), or because of increased

levels of EGFR cell-surface concentrations. Interestingly, when EGFR cell-surface levels reach a critical density (~2000 receptors per μm^2), receptor activation is comparable to the EGF-induced level, based on the quantification of Tyr1068 phosphorylation (Endres et al., 2013). This amount of receptor on the surface is present in cancer cells that tend to overexpress EGFR (Haigler et al., 1978) and it is therefore likely that in these systems EGF-independent activation of EGFR is present at basal levels.

1.2.2 MET activation mechanism and main phosphorylation sites

Receptors in the MET family, unlike EGFR, are heterodimeric RTKs characterised by a short extracellular α-chain that links to the main receptor β-chain via disulfide bridges (Hubbard, 1999). The extracellular portion of the receptor comprises of a Semaphorin (Sema) domain, a plexin-semaphorin-integrin (PSI) domain, and four immunoglobulin-plexin-transcription factor (IPT) domains (Zhang et al., 2018). The rest of the receptor, similarly to other RTKs, is characterized by a TM, a JM and a TK domain, followed by a C-terminal tail (Figure 1.1).

In the absence of ligand, MET exists on the cell-surface in a monomeric unphosphorylated form or as unliganded MET dimers (Koschut et al., 2016). Unphosphorylated MET predominantly exists in an autoinhibited conformation with the activation loop folding against the kinase active sites (Wang et al., 2006b). Tyr1234 thus remains hidden, and, the other conserved catalytic residue, Tyr1235, is only partially solvent-exposed (Wang et al., 2006b). MET can also exist in a rare monomeric, phosphorylated, signaling-competent conformation, although this is a thermodynamically unfavourable state (Sheth et al., 2008). Phosphorylation events alone are in fact not sufficient to fully enable MET kinase activity, and the dimerized receptor is more efficient than the monomeric phosphorylated version of MET (Hays and Watowich, 2003). On the other hand, MET crosslinking has been observed in the absence of HGF, suggesting that the RTK can dimerize without ligand stimulation (Kong-Beltran et al., 2004). Similar to EGFR, this event is likely to become relevant in an oncogenic setting, in which there is an increased local concentration of MET.

Binding of the sole MET ligand, HGF (Nakamura, 1994; Naldini et al., 1991), to MET extracellular domain triggers a thermodynamically favourable conformational change and induces dimerization (Sheth et al., 2008). Particularly important for binding the growth factor is the Sema domain (Stamos et al., 2004), which also aids crosslinking of MET monomers (Kong-Beltran et al., 2004).

There are two main hypotheses that describe the dimerization of MET triggered by HGF binding; the topic is in fact still an active subject of research. The first model proposes that a single HGF molecule binds to two MET monomers with different affinities; interaction between the two monomers then stabilizes the dimeric structure (de Vos et al., 1992). The second model instead maintains the idea of a 2:2 stoichiometry, with two MET monomers surrounding a two-molecule HGF dimer (Ferraris et al., 2010; Gherardi et al., 2006). However, both models of MET dimer activation agree on the necessary receptor *trans*-autophosphorylation event on the conserved catalytic residues, Tyr1234 and Tyr1235 (Komada and Kitamura, 1994; Rodrigues and Park, 1994; Zhen et al., 1994). Given that Tyr1235 is the more exposed residue between the two, phosphorylation at this site is considered to precede phosphorylation on Tyr1234 (Wang et al., 2006b). These two residues are located on the activation loop and their phosphorylation is key to release the autoinhibitory conformation, thus making the ATP-binding site accessible (Rickert et al., 2011).

Two other residues, located in the C-terminal tail become phosphorylated upon MET activation; Tyr1349 and Tyr1356. Phosphorylation of these sites has a dual function. First of all, it releases an inhibitory conformation; in an inactive receptor the C-terminal tail is in fact believed to fold onto the receptor's catalytic domain thus inhibiting its activity (Bardelli et al., 1999). Secondly, these sites serve as docking sites for adaptor proteins and downstream signalling effectors (Ponzetto et al., 1994). When phosphorylated Tyr1349 and Tyr1356 can directly bind PLCγ, PI3K, Grb2, Signal Transducer and Activator of Transcription 3 (Stat3), Son Of Sevenless (SOS) and Sarcoma (Src) (Birchmeier et al., 2003; Furge et al., 2000). This docking site is unique to the MET receptor and has a strategic conformation. Two substrates in fact cannot simultaneously bind to Tyr1349 and Tyr1356 on the same MET monomer. However, they can bind to Tyr1349 on one MET molecule

and to Tyr1356 on the second monomer (Birchmeier et al., 2003). This bidentate motif of the C-terminal MET tail thus constitutes a multifunctional docking site which can mediate simultaneous interactions with multiple proteins (Ponzetto et al., 1994).

A very important molecular adaptor recruited on the activated MET receptor, both directly and indirectly, is Gab1. Gab1 can bind multiple effector proteins, among which PI3K, SH2 domain containing protein tyrosine phosphatase 2 (SHP2) (Schaeper et al., 2000; Wang et al., 2015b) and CT10 Regulator of Kinase (Crk). Crk is key for the activation of the downstream c-Jun N-terminal kinase (JNK) pathway (Garcia-Guzman et al., 1999). Gab1 mediates the majority of MET activation responses (Sachs et al., 2000). The biological relevance of this interaction is evidenced by the existence of a unique MET-binding sequence in Gab1. This sequence is different from the SH2 and PTB domains and it is unique to MET binding, allowing for a robust interaction between the two proteins and prolonging MET-driven signalling responses (Birchmeier et al., 2003).

Another important MET phosphorylation site is Tyr1003, in the JM domain, that serves as a negative regulatory site via binding of c-Cbl (Abella et al., 2005). Point mutations in the JM domain of MET are common alterations in MET-driven lung cancer (Krishnaswamy et al., 2009). Also, somatic mutations affecting exon 14, which encodes for the JM domain, have been shown to occur in approximately 3% of lung adenocarcinoma cases (Cancer Genome Atlas Research Network, 2014; Okuda et al., 2008; Onozato et al., 2009; Seo et al., 2012). Exon 14 mutations have also been observed in neuroblastoma (Yan et al., 2013), gastric cancers (Asaoka et al., 2010) and glioblastoma multiforme (GBM) (Hu et al., 2018). Mutations in exon 14 cause the phenomenon known as exon 14-skipping that results in a truncated MET. This version of MET lacks Tyr1003 and is therefore unable to efficiently recruit c-Cbl. Ultimately this results in sustained MET activation and oncogenesis (Kong-Beltran et al., 2006).

Another residue that contributes to MET downregulation is juxtamembrane Serine (Ser) 985 (Gandino et al., 1994) (Figure 1.1). This site is regulated by the activity of Protein Kinase C (PKC) and Protein Phosphatase 2A (PP2A). Phosphorylation of Ser985 is associated with a decrease in receptor's tyrosine phosphorylation and

HGF stimulation responsiveness. It has been proposed that phosphorylation at this site is dependent on extracellular factors, such as oxidative stress, and that this is a very unique mechanism that allows the receptor to adapt its activation to best respond to extracellular conditions (Hashigasako et al., 2004).

1.3 RTK signalling

RTKs sit at the top of complex signalling networks that receive extracellular stimuli and translate them into cellular responses. The multiple phosphotyrosines, and their interaction with various docking proteins, allow for amplification and diversification of signalling outputs (Lemmon and Schlessinger, 2010).

SH2 and PTB domains containing proteins, as previously mentioned, are recruited and activated by RTKs. They tend to be modular in structure. Each module has been associated with a particular protein function, summarised in Figure 1.4, and can explain the propagation of the signal downstream of an RTK (Schlessinger, 2000). For instance, Pleckstrin Homology (PH) modules are characteristic of those proteins that can bind phospholipids and interact with membranes. FYVE (an acronym for Fab1p-YOTB-Vac1P-EEA1) domains specifically recognise phosphatidylinositol 3-phosphate (PI(3)P), while PDZ (an acronym for post synaptic density protein (PSD95), Drosophila disc large tumour suppressor (Dlg1) and Zonula occludens-1 protein (Zo-1)) domains specifically bind to the C-termini of their target proteins. Importantly, some SH2 domain-containing proteins also have intrinsic enzymatic activities, such as Src (Wagner et al., 2013).

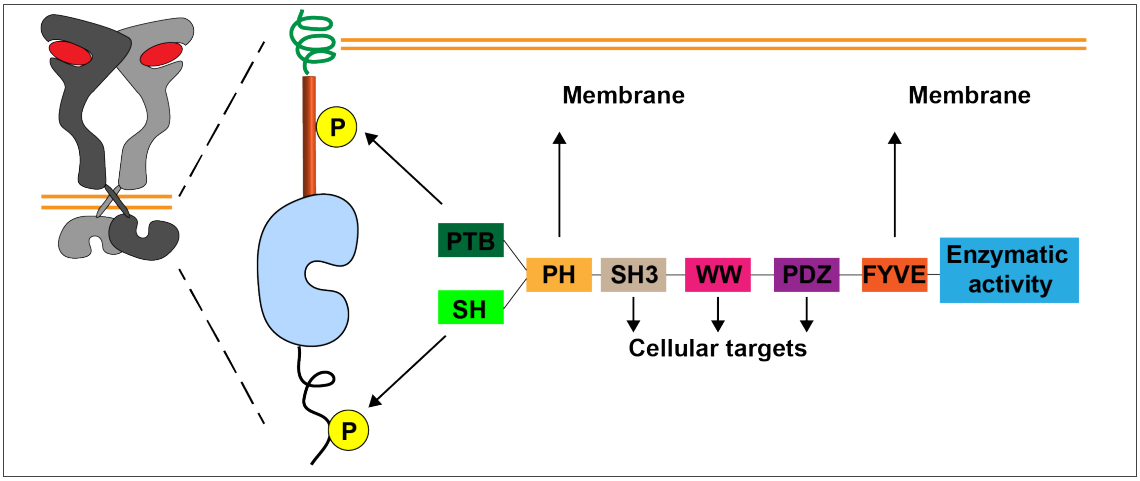

Figure 1.4 Modular structure of PTB and SH containing proteins

PTB and SH2 domain-containing proteins interact with active RTK via phosphorylated tyrosine sites (P). These proteins are often modular in structure. PH and FYVE domains bind to phospholipids in membranes, SH3 and WW domains bind to proline-rich sequences in target proteins. PDZ domains bind to hydrophobic residues in the C-terminus of substrates. Some signalling proteins can also contain additional domains that have enzymatic activity (e.g. kinase).

Adaptor and docking proteins also participate in RTK-driven signalling networks, thanks to SH and PTB domains. They lack intrinsic catalytic activity, but are able to assemble signalling-competent protein complexes (Wagner et al., 2013). Some adaptor proteins contain a transmembrane domain or a myristyl anchor to associate with membranes. Others have a PH domain, that mediates their recruitment to an activated RTK site by interacting with phospholipids, in particular with phosphatidylinositol (3,4,5)-trisphosphate ($PI(3,4,5)P_3$), product of PI3K activation. Gab1 is such an adaptor protein, crucial in mediating RTK signalling and, as previously discussed, particularly important for the activation of MET-driven signalling pathways (Birchmeier et al., 2003).

Importantly, despite often being depicted as linear for simplicity, signalling pathways are functionally interconnected. Furthermore, similar signalling cascades can be engaged by different RTKs and yet result in distinct cellular outcomes. Therefore, identifying the components of a signalling pathway may not be sufficient to predict the qualitative output of receptor activation. The level, kinetics and location of RTK activation all help determine the signalling outcome, in addition to the identity of the RTK and the molecular components of the pathway (Lemmon and Schlessinger, 2010).

The two major RTK-dependent signalling arms that will be discussed in more detail are the MAPK and the PI3K/Akt pathway.

1.3.1 MAPK pathway

MAPK pathways contribute to the control of metabolic processes, cell cycle, migration, proliferation and differentiation. In mammalian cells there are three sub-families of MAPK pathways: the classical MAPK/Erk1/2 pathway, C-Jun N-terminal kinase/stress-activated protein kinase (JNK/SAPK) and p38 kinase (Zhang and Liu, 2002).

In the classical and best-studied MAPK pathway, the MAPK/Erk1/2 cascade, the adaptor protein Grb2 plays the first central role in activation. Grb2, by virtue of its SH2-binding domain, is recruited to RTKs at the plasma membrane with its binding partner SOS, a guanine nucleotide exchange factor. This translocation brings SOS in close proximity with Ras, a small GTPase located at the plasma membrane (Margolis and Skolnik, 1994), and SOS can thus favour the exchange of guanosine diphosphate (GDP) for guanosine triphosphate (GTP) on Ras (Schlessinger, 2000). Ras is a family of three proteins, Harvey Ras (HRAS), Kirsten Ras (KRAS) and Neuroblastoma Ras (NRAS), that act downstream of all RTKs (McCain, 2013). Once activated, Ras can interact with several effector proteins such as Rapidly Accelerated Fibrosarcoma (Raf) and PI3K. Raf phosphorylates MAPK/Erk1/2 kinase (MEK) proteins, which in turn activate Extracellular signal-Regulated Kinase (Erk)1 and Erk2 (or p44 and p42 MAPK) (Figure 1.5) (Schlessinger, 2000). Erk1/2 have several downstream substrates, among which a number of transcription factors that control cell cycle progression and proliferation (Zhang and Liu, 2002).

The second MAPK signalling cascade is the JNK pathway. Several MAPK kinase kinases (MAPKKKs) are responsible for its activation. They can respond to a large number of stimuli, such as environmental stresses, inflammatory cytokines, as well as growth factors. The central member of this second branch of MAPK pathways is JNK. JNK pathway activation results in the activation of several substrates, among which the dimeric transcription factor Activator Protein 1 (AP-1), of which c-Jun is

one component, plays a prominent role in cell proliferation and apoptosis (Figure 1.5) (Zhang and Liu, 2002).

While the Erk1/2 and JNK branches of the MAPK pathway are mainly activated by growth factor stimulation, the p38 pathway contributes to responses to stress signals, such as ultraviolet (UV) radiation and inflammatory cytokines (Figure 1.5). One of these responses involves the endocytosis of EGFR in the presence of extracellular stress, such as X-rays or UV radiation (Tomas et al., 2017). Importantly, the p38 pathway is involved in cell cycle arrest at the G1/S phase transition and plays a major role in triggering apoptosis (Zhang and Liu, 2002).

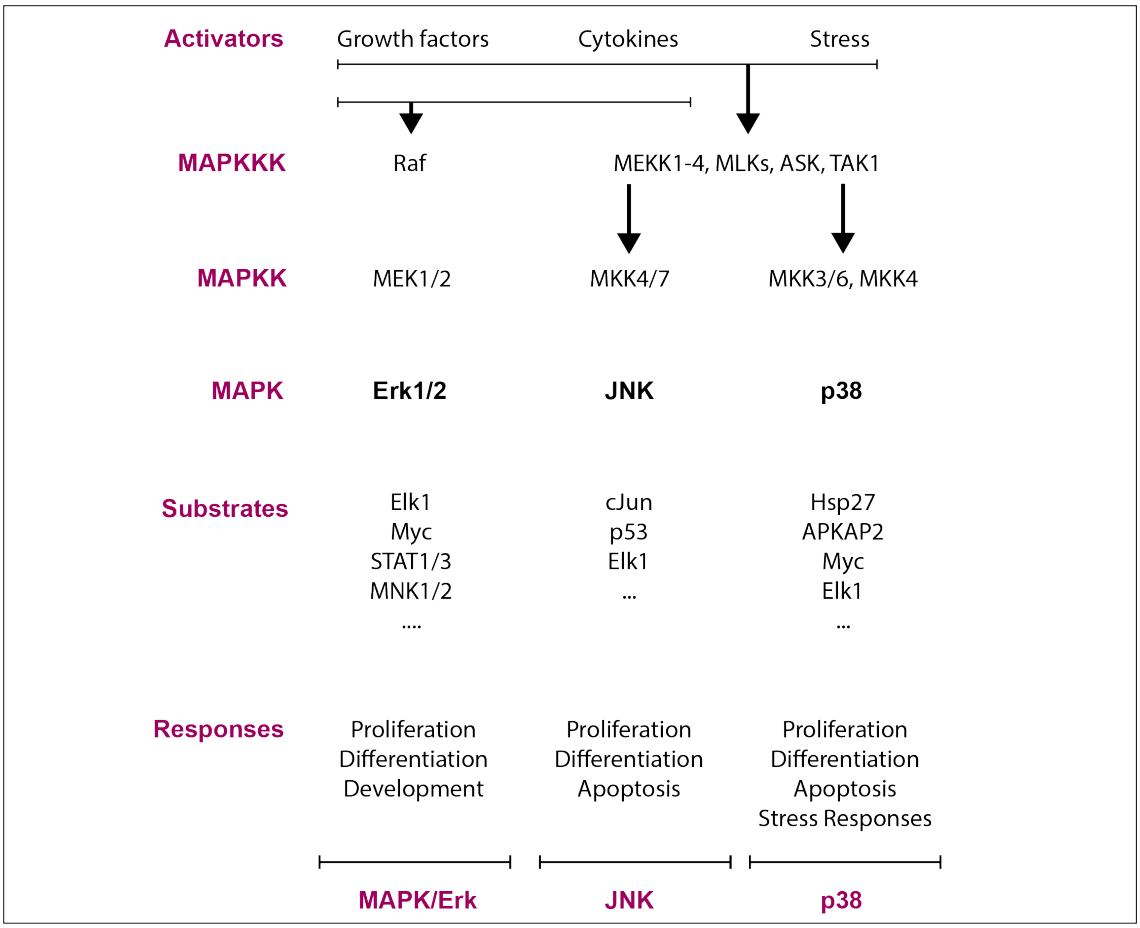

Figure 1.5 MAPK pathways

Schematic of the three main MAPK pathways, namely MAPK/Erk, JNK and p38. Only some of the substrates are listed.

Abnormalities in the MAPK pathways play a critical role in the development and progression of cancer. In particular the Erk1/2 signalling pathway (hereafter

referred to simply as MAPK pathway) is deregulated in approximately one-third of all human cancers (Dhillon et al., 2007).

1.3.2 PI3Ks and the PI3K/Akt pathway

The PI3K/Akt pathway is a key downstream effector of RTK signalling for cell survival and proliferation, and the most frequently altered pathway in cancer (Mayer and Arteaga, 2016).

The first player in the PI3K/Akt signalling cascade belongs to the PI3K family, a group of plasma membrane-associated lipid kinases. The PI3K family is composed of eight members, grouped into three classes. Class I comprises four isoforms, α, β, γ and δ. They all exist as obligate heterodimers composed of a regulatory subunit and a catalytic subunit from which each isoform gets its name (p110α, p110β, p110γ, p110δ) (Yang et al., 2019). The regulatory subunit harbors SH2 domains, key for lipid interactions (Vanhaesebroeck et al., 2010). The regulatory subunit is also responsible for the recruitment of PI3K at RTK-active site, either via direct interaction with RTK phosphotyrosines (Burke and Williams, 2013) or via adaptor proteins, such as Ras (Jean and Kiger, 2014). This interaction breaks the inhibitory contacts between the regulatory and the catalytic subunits and allows for PI3K to carry out its function (Burke and Williams, 2013). All activated dimeric PI3Ks can catalyse the phosphorylation of phosphatidylinositol 4,5-bisphosphate ($PI(4,5)P_2$, or simply PIP_2), producing the second messenger $PI(3,4,5)P_3$ (or simply PIP_3) molecule. Nonetheless, each isoform has distinct biological functions (Fruman and Rommel, 2014). While PI3Kγ and PI3Kδ play critical roles in immune functions, where they have been explored as therapeutic targets for immune diseases, PI3Kα is often mutated in cancer. The precise contribution of PI3Kβ to tumour initiation and/or maintenance remains unclear, although the occurrence of some rare PI3Kβ mutations have been linked to tumour development (Nakanishi et al., 2016).

The other two PI3K classes, class II and III, have three (PI3KC2α, β and γ) and one (vacuolar protein sorting 34, Vps34) isoforms, respectively. Unfortunately, the physiological functions of both these classes have been less well studied (Engelman et al., 2006; Vanhaesebroeck et al., 2010). PI3KC2α and β contain a

clathrin-binding domain, and, as such, have been implicated in endocytosis. They also have a Ras binding domain, although it is unclear which signalling pathways they modulate (Jean and Kiger, 2014). Class II PI3K can also bind $PI(4,5)P_2$ (Stahelin et al., 2006) and PI3KC2β has been shown to promote PI(3)P synthesis (Das et al., 2007). The activity of Vps34 has been linked to intracellular vesicle trafficking and mainly been implicated in autophagy induction, via the synthesis of PI(3)P (Kim et al., 2013; Simonsen and Tooze, 2009).

It is class I PI3K (hereafter referred to as PI3K), which initiate the PI3K/Akt cascade. The formation of PIP_3 in fact recruits pleckstrin homolog (PH) domain-containing proteins to cellular membranes, which triggers their subsequent activation.

The serine-threonine kinase, Akt (also known as protein kinase B, PKB), is one such PH-domain containing protein. It mediates many of PI3K physiological functions including cell survival, proliferation, motility and metabolism through direct and indirect regulation of downstream effector molecules such as mechanistic target of rapamycin (mTOR) complex 1 (mTORC1) (Figure 1.6) (Wee et al., 2008). Given PI3K association with tumour development, Akt-associated pathways are also frequently altered in human cancers (Liu et al., 2009).

Akt binding to PIP_3 via its PH domain causes a conformational change that exposes two critical amino acids for phosphorylation, Threonine (Thr) 308 and Serine (Ser) 473 (Liu et al., 2009). 3'-phosphoinositide-dependent kinase 1 (PDK1) is responsible for Akt phosphorylation on Thr308, which yields a partially activated form of Akt that can negatively regulate Prolin-rich Akt Substrate of 40 kDa (PRAS40) and Tuberous Sclerosis protein 2 (TSC2), resulting in mTORC1 activation (Figure 1.6). Maximal activation of Akt, however, requires phosphorylation on Ser473 by mTORC2 (Manning and Toker, 2017).

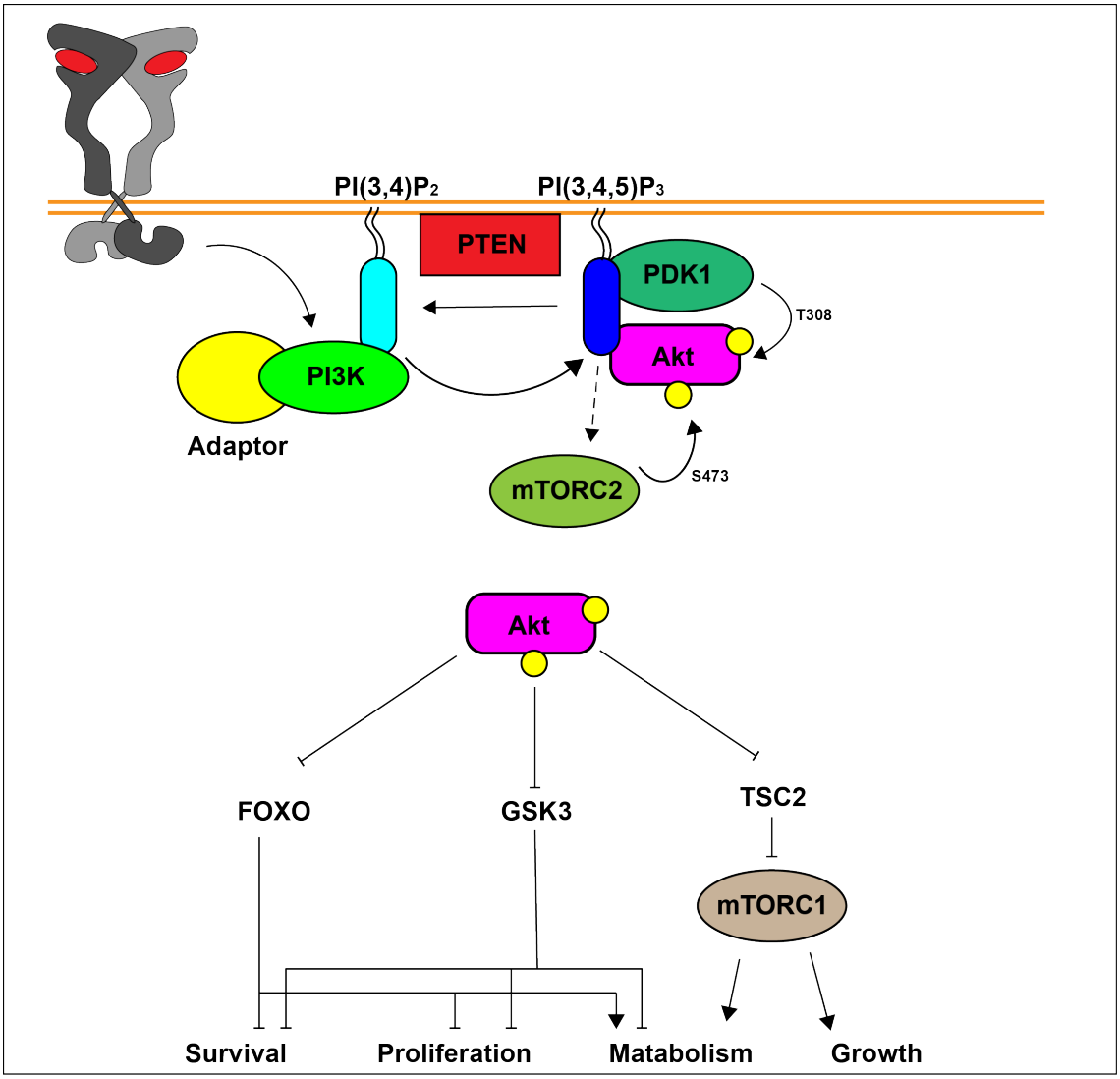

Figure 1.6 The PI3K/Akt pathway

PI3K is activated by RTKs directly, or indirectly via adaptor proteins. PI3K catalyses the phosphorylation of $PI(3,4)P_2$ to $PI(3,4,5)P_3$ phospholipids and is antagonised by PTEN. Akt is recruited to the plasma membrane via its PH domain and phosphorylated by PDK1 on Thr308 and by mTORC2 on Ser473. Active Akt then has multiple downstream substrates. Three are illustrated here which are negatively regulated by Akt. TSC2 inhibition via Akt results in the activation of mTORC1 which promotes metabolism and growth.

Akt is a major signalling hub for a wide plethora of cellular functions; in fact more than 200 Akt substrates have been identified (Toker, 2012). Among downstream signalling substrates of Akt are eukaryotic translation initiation factor 4E binding protein 1 (4EBP1) and ribosomal protein S6 kinase (S6K). Both of these are activated by mTORC1 and result in phosphorylation of ribosomal protein S6, ultimately promoting protein synthesis and cellular proliferation (Hemmings and Restuccia, 2012).

1.3.3 PTEN in the PI3K/Akt pathway

The PI3K/Akt pathway controls many functions that are critical for cellular homeostasis; as such its activity is tightly controlled. A direct regulator of PI3K function is the tumour suppressor phosphatase and tensin homolog (PTEN). PTEN is a lipid phosphatase that directly antagonizes PI3K action by dephosphorylating PIP_3 to generate PIP_2 (Figure 1.6). An imbalance in this phosphoinositide equilibrium can have a detrimental effect on cells, triggering uncontrolled cell proliferation.

PTEN tumour suppressor function is generally accredited to its intrinsic lipid phosphatase activity and its inactivation via deletion, inactivating mutations and epigenetic silencing is considered to be the leading cause of PI3K/Akt pathway activation in human cancers (Parsons, 2004).

In vitro studies have identified $PI(3,4,5)P_3$ and $PI(3,4)P_2$ as PTEN most important physiological substrates, although at lower efficiency, PTEN also demonstrates activity on PI(3)P, inositol 1,3,4,5-tetrakisphosphate ($Ins(1,3,4,5)P_4$) and possibly phosphatidylinositol 3,5-bisphosphate ($PI(3,5)P_2$) (McConnachie et al., 2003).

PTEN also possesses a polypeptide phosphatase activity against Tyrosine, Serine and Threonine phosphorylated polypeptides *in vitro* (Myers et al., 1997), a function that may be particularly relevant for PTEN pools located in the nucleus where the phosphatase cannot readily target $PI(3,4,5)P_3$ molecules. A lack of PTEN pools in the nucleus has been associated with worse cancer prognosis, suggesting the importance of the lipid phosphatase-independent function of PTEN (Song et al., 2012). The protein phosphatase activity of PTEN has been demonstrated towards non-receptor tyrosine kinase, SRC, in a cell line study (Zhang et al., 2011). Loss of PTEN in this setting contributes to Trastuzumab resistance in both Trastuzumab resistant cell lines and mouse models. PTEN activity on SRC appears to be PI3K/Akt pathway independent (Zhang et al., 2011). Unfortunately, it is yet unclear how much and in what context PTEN protein phosphatase activity contributes to tumour-associated phenotypes.

There is evidence suggesting that PTEN status influences cellular responses to PI3K class I isoform-selective inhibitors (Berenjeno et al., 2012). For instance, cell lines harboring PTEN-inactivating mutations respond particularly well to PI3Kβ inhibitors, perhaps owing to the fact that in these cells PI3Kβ seems to be the primary source of PIP_3 production, for as yet unknown reasons (Torbett et al., 2008). However, in some PTEN-null cases treated with PI3Kβ inhibitors, PI3K/Akt signalling rebound occurs via PI3Kα-directed activity (Schwartz et al., 2015). It would therefore appear that PI3Kα and PI3Kβ play distinct yet somehow interchangeable roles. In EGFR-amplified, PTEN-null cell lines (MDA-MB-468), inhibition of both PI3Kα and β in fact demonstrates more potency than a PI3Kα only inhibitor (Schwartz et al., 2015).

It is clear that we still do not hold a complete picture of the relationship between RTKs, PI3K isoforms and PTEN; a better understanding of the subject would be pivotal to the clinical development of more efficient targeting strategies.

1.3.4 Phospholipids: an overview

Phosphoinositides (PIs) are a minor class of phospholipids that control almost all aspects of a cell's life and death (Balla, 2013) and more specifically play a major role in cell signalling and trafficking (Marat and Haucke, 2016).

Phosphorylation of PIs occurs in one of the –OH groups of their inositol ring (Balla, 2013). In the case of PI-3 phosphates, the inositol ring is phosphorylated at the 3-position. PIs main phosphorylation events and some of the kinases and phosphatases involved are summarised in Figure 1.7.

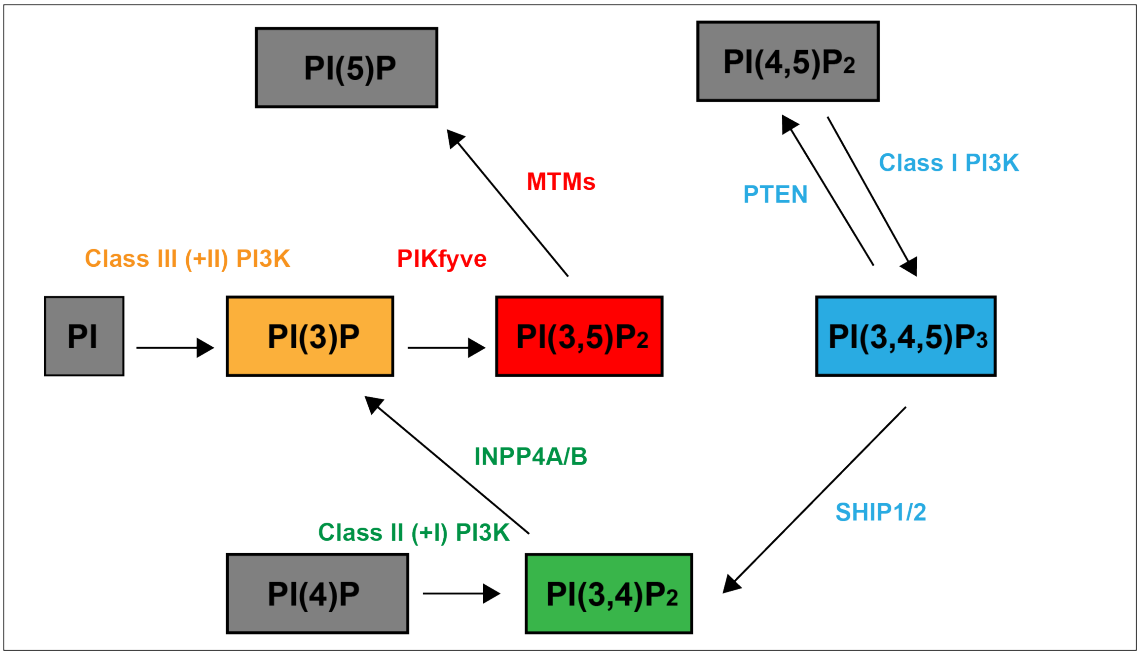

Figure 1.7 Main steps in Phosphoinositides-3 phosphates conversion

A schematic of the interconversion of PI 3-phosphates via kinases and phosphatases.

Generally speaking, PI4-phosphates can be found at the plasma membrane and along the exocytic pathway. PI3-phosphates are also found at the plasma membrane, as well as in endosomal membranes, since they are crucial components of the endosomal system (Balla, 2013; Raiborg et al., 2013).
Each PI, however, can be found enriched at specific subcellular location; this trait allows PIs to be central regulators of intracellular membranes (Marat and Haucke, 2016).

$PI(3,4,5)P_3$ and $PI(3,4)P_2$ are found at the plasma membrane and are generated upon responses to extracellular stimuli (Vanhaesebroeck et al., 2010). $PI(3,4)P_2$ is also present in endomembranes, but its function there is unclear (Marat and Haucke, 2016). Important at early endosomes and for autophagy is PI(3)P, while $PI(3,5)P_2$ is found at late endocytic vesicles, multivesicular bodies (MVBs) and, again, autophagic compartments (Mayinger, 2012).

The abundance of PIs varies with tissues, cell types and stimuli, but they are estimated to represent ~10-20% of total phospholipids (Balla, 2013). Thanks to their rapid generation and equally fast de-phosphorylation, PIs are a crucial and

incredibly versatile tool for regulation of intracellular signalling and membrane trafficking.

Given the link between PIs and both the PI3K pathway and RTK endocytosis, we are increasingly appreciating the central role that PIs play in cancer biology (Bunney and Katan, 2010). However, we are still lacking a complete understanding of the underlying principle of how PIs work and dynamically interact with other cellular entities.

1.4 RTK degradation and endocytic trafficking

RTK signalling is modulated at the receptor level by ubiquitin-induced degradation and through endocytic and recycling processes (Mosesson et al., 2008; Shinde and Maddika, 2016).

Several factors can affect receptor degradation, endocytosis and recycling. First of all, turnover times of receptors vary between different family members and are accelerated by ligand engagement. Internalisation rates also positively correlate with RTK expression levels (Goh and Sorkin, 2013), and therefore, in cells with RTK overexpression, the turnover rates are much longer (Stoscheck and Carpenter, 1984). Additionally, the duration of ligand occupancy and the pattern of receptor ubiquitination are critical factors in determining receptor post-endocytic fate (i.e. degradation vs recycling), which is decided within intraluminal vesicles (ILVs) (Ebner and Derynck, 1991; Huang et al., 2006; Sigismund et al., 2008).

Although the spatiotemporal constrains of RTK ubiquitination are unclear, mediators of RTK ubiquitination have been identified. Casitas B-lineage Lymphoma (Cbl), a family of E3 ubiquitin ligases, c-Cbl, Cbl-b and Cbl-3, is responsible for the ubiquitination of several RTKs including EGFR and MET. In the case of EGFR, ubiquitination is crucial for degradation, as non-ubiquitinated EGFR fails to traffic into ILVs (Eden et al., 2012). All the three Cbl members exclusively target protein tyrosine kinases, but structurally, they differ in their protein-protein interactions C-terminal domain (Mohapatra et al., 2013). Both Cbl-b and c-Cbl can participate in RTK degradation, although Cbl-b activity does not always result in substrate

degradation (Thien and Langdon, 2005). On the contrary, a loss of c-Cbl causes a decrease in RTK internalisation (Zeng et al., 2005), and an increase in cell migration (Mohapatra et al., 2013), accompanied by a decrease in receptor downregulation, in the case of EGFR (Levkowitz et al., 1998; Yokouchi et al., 1999). Although some evidence suggests that c-Cbl may be the main contributor to RTK degradation, other data point towards a complex interplay between Cbl-b and c-Cbl, with contributions from both isoforms to EGFR downregulation (Pennock and Wang, 2008).

Cbl binds to RTKs either directly at phosphotyrosine motifs in the cytoplasmic tails of RTKs, or indirectly through adaptor proteins, such as Grb2. Binding to Tyr1045 on the EGFR receptor has been shown to be key for EGFR downregulation (Yarden, 2001). A similar site, Tyr1003, has been identified for the MET receptor (Abella et al., 2005).
Cbl activity can also be modulated via its interactions with accessory proteins, such as Sprouty2 (Okur et al., 2014). These interactions have been shown to contribute to RTK degradation by stabilizing the newly formed ubiquitin chain until an ILV is formed, thus targeting the receptors for their final destination (Marmor and Yarden, 2004). The mechanism of RTK degradation is generally shared by all RTK, but components of the molecular machinery that helps E3-multicomplex formation may vary between receptors (Goh and Sorkin, 2013).

Deregulation of RTK degradation is associated with cancer development. For instance, loss of function (LOF) mutations of c-Cbl correlate with myeloid neoplasms. These mutants interfere with wild type c-Cbl and Cbl-b E3-ligases in cells, reducing the overall levels of cytokine receptor degradation and causing sustained signalling (Sanada et al., 2009).

Mutations within RTK that disrupt Cbl binding have also been implicated in cancer. The previously discussed exon-14-skipping activating mutation in MET (Onozato et al., 2009) has for instance been associated with lung adenocarcinoma (Kong-Beltran et al., 2006; Ma et al., 2003, 2005). Expression of this mutant has also been linked with positive responses to MET inhibitors Crizotinib and Cabozantinib (Jorge et al., 2015; Paik et al., 2015). Recently, more potent and selective MET-

targeting TKI, Capmatinib (Schuler et al., 2016) and Tepotinib (Falchook et al., 2019), have also demonstrated promising clinical efficacy against non-small-cell lung cancer (NSCLC) harbouring exon 14 MET mutation (Heist et al., 2019; Paik et al., 2019).

Our understanding of RTK degradation is still incomplete and primarily based on studies carried out on EGFR as a prototypical model system. Expanding our understanding of the molecular mechanisms underlying this regulation and the specific context in which they function is therefore warranted.

Along with receptor ubiquitination, RTK endocytosis is a mechanism that allows for intracellular signal modulation. RTKs are subjected to both slow but continuous clathrin-independent (CIE) endocytosis, and faster ligand-induced clathrin-mediated endocytosis (CME). Both of these processes contribute to cell-surface receptor levels and signalling strength. Like other integral membrane proteins, RTKs are also subjected to rapid basal levels of recycling to the cell-surface. Growth factor stimulation increases turnover rates and ultimately results in signalling downregulation (Goh and Sorkin, 2013). Receptor interaction with lipids, lipid membrane components and cytoskeleton can influence the rate of endocytosis. For instance Human Epidermal Growth Factor Receptor 2 (HER2) interaction with membrane protrusions has been shown to lengthen receptor residency at the plasma membrane (Hommelgaard et al., 2004).

The current model of receptor endocytosis is based on EGFR. Upon EGF stimulation, EGFR clusters to plasma membrane areas, also known as clathrin coated pits (CCPs). CCPs are enriched in PIP_2 and adaptor proteins with phosphoinositide-binding sites (such as adaptor protein-2, AP-2) and get quickly coated on the cytosolic side with clathrin, a triskelion-shaped scaffolding protein. Clathrin functions to reinforce the membrane invagination and help it mould into an intracellular vesicle. Its joint action with dynamin, a GTPase, allows for efficient scission of the vesicle from the plasma membrane (Mousavi et al., 2004).

What causes the formation of CCPs is still subject to debate, but there is evidence supporting that ligand-induced EGFR activity is an essential trigger. The adaptor

protein Grb2, as well as epidermal growth factor receptor pathway substrate 15 (Eps15), recruited to the plasma membrane by active EGFR, could both contribute to receptor endocytosis (Confalonieri et al., 2000; van Delft et al., 1997; Jiang et al., 2003).

RTKs can also endocytose following a CIE route, especially in cases of receptor overexpression. Both increased number of EGFR receptors at the cell-surface and sustained EGF stimulation have been shown to saturate CME and trigger the slower CIE internalisation (Wiley, 1988). In fact, we now know that CIE makes up 50% of all cellular endocytic activity (Gong et al., 2008). CIE has received more attention since EGFR circular dorsal ruffles (CDR)-dependent endocytosis was discovered (Orth et al., 2006). CDR has been observed after growth factor stimulation and described as a dynamic membrane structure, containing key RTKs. These membrane sites appear straight after growth factor stimulation and disappear after 10-20 minutes. They do not require clathrin, but they positively correlate with PI3K, dynamin and PIP_2 (Orth et al., 2006). The contribution of CDR endocytosis to RTK signalling is an active subject of research.

Once receptors have been endocytosed, they are collected within acidic early endosomes (EE). From here, RTKs can follow different fates, and the residency time of growth factor on the receptor plays an important role. Ligand-free RTKs tend to recycle to the plasma membrane. Ligand-bound RTKs instead are usually considered destined for degradation. In reality, the fate of ligand-bound receptors is far more complex, and it is cell-type, as well as receptor, specific. EGF-bound EGFR, for instance, has been shown to still recycle via both a slow and a fast recycling pathway (Sorkin et al., 1991) up to 3-5 times before proceeding onto late endocytic compartments (Clague and Urbé, 2001). The slow recycling pathway involves a specialised form of endosomes, also known as recycling endosomes (RE) (Naslavsky and Caplan, 2018). Receptors that have not yet left EEs will continue their intracellular journey to MVBs and, ultimately, late endosomes (LE). The fusion with lysosomes, which contain proteolytic enzymes, signals the end of the RTK journey (Figure 1.8) (Goh and Sorkin, 2013; Naslavsky and Caplan, 2018).

The length of time that it takes for a receptor to go through the entire cycle is receptor, and possibly cell type, dependent. The rough timings of RTK endocytosis (based on EGFR dynamics) are highlighted in Figure 1.8 (Yarden, 2001).

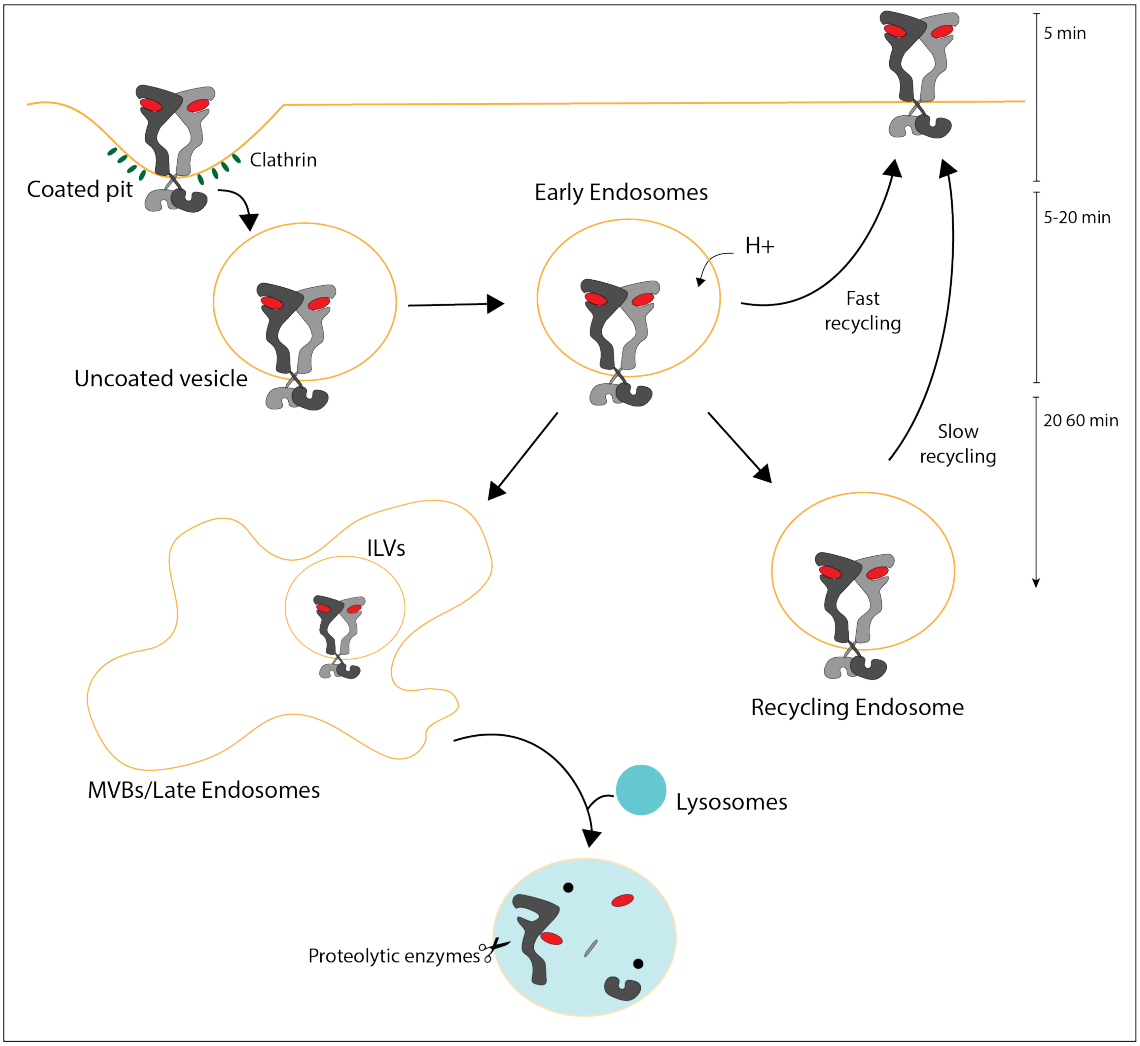

Figure 1.8 RTK endocytosis

Clathrin-mediated endocytosis of receptors is characterised by the formation of a clathrin-coated pit. RTKs are thus internalised and vesicles are rapidly uncoated after scission with the cell-surface. Vesicles then fuse to form an early endosome (EE), also referred to as sorting endosome (SE). From here receptors can return to the cell-surface either via a fast recycling route or via a slow recycling pathway by trafficking to recycling endosomes (RE). RTKs ubiquitinated by cCbl remain on early endosomes that soon mature into multivesicular bodies (MVBs) and late endosomes (LE). Fusion with lysosomes carrying proteolytic enzymes ultimately results in RTK and growth factors degradation.

Each one of the endosomal compartments is characterised by the presence of integrins, adaptor proteins and GTPases that contribute to their proper functionality. In particular, EEs are characterised by the presence of Early Endosome Antigen 1 (EEA1) and Ras-associated binding (Rab) protein 5. Rab7 and Rab9 aid EEs

maturation into late endosomes and fusion with lysosomes. Rab11 and Rab4 instead promote the slow and the fast recycling pathways, respectively (Miaczynska et al., 2004; Wandinger-Ness and Zerial, 2014).

Internalisation of receptors is generally linked to signal downregulation. However, this concept can be misleading as RTKs are still capable of signalling from endocytic vesicles; endocytosis is in fact a mechanism of signalling compartmentalisation, and, in some cases, even of signalling amplification (McPherson et al., 2001; Miaczynska et al., 2004). The spatial and temporal dimensions of the endocytic network allow for signalling specificity and regulation (Miaczynska et al., 2004). For instance, specific protein complexes have been shown to form mainly on early endosomes, ensuring that signal propagation happens only when activated RTKs reach a specific cellular compartment (Sadowski et al., 2009). For instance, MET-dependent STAT3 phosphorylation occurs almost exclusively from perinuclear endomembrane compartments (Kermorgant et al., 2003; Trusolino et al., 2010). Furthermore, at steady state, it has been shown that almost 80% of EGF-bound EGFR is internalised, and signalling molecules, such as Grb2, follow the receptor to early endosomes (Clague and Urbé, 2001), becoming important signalling hubs. Indeed one of the most striking cases of signalling from endocytic vesicles is the MAPK pathway, which RTK activate from intracellular vesicles, thus prolonging signal activation (Schoeberl et al., 2002; Trusolino et al., 2010). Akt can also be locally activated in a $PI(3,4,5)P_3$-dependent manner from $PI(3,4,5)P_3$ enriched early endosomal compartments (Jethwa et al., 2015).

As our appreciation for the spatio-temporal regulation of RTK signalling grows, its connection to oncogenesis and TKI responses is progressively emerging (Casaletto and McClatchey, 2012).

1.5 RTKs and Cancer

1.5.1 RTK aberrant activation by mutations or overexpression

RTKs are aberrantly activated in a variety of human cancers. The two most common mechanisms of aberrant RTK activation are gain-of-function (GOF)

mutations and overexpression. GOF mutations often lead to the formation of constitutive dimers by disrupting the ability of RTKs to engage in an autoinhibitory conformation (Ludes-Meyers et al., 1996).

EGFR oncogenic mutations characterize a limited set of tumours, mainly NSCLC and GBM. They also tend to localise in specific areas, known as “hot spots”, such as the TK domain in NSCLC, as well as the C-tail and the ligand binding domain in GBM (Pines et al., 2010). An important feature of EGFR mutants is their ability to escape degradation by reducing their interaction with c-Cbl. This is usually achieved by keeping Tyr1045 weakly phosphorylated, while allowing the phosphorylation of other tyrosine residues, resulting in an uncontrolled downstream signalling (Carey et al., 2006; Lee et al., 2006; Shtiegman et al., 2007). A peculiar EGFR mutant is EGFR variant III (EGFRvIII), which lacks the ligand-binding domain (Ekstrand et al., 1992). Its oncogenic features derive from the fact that EGFRvIII is found in a dimeric form with constitutive basal activity (Huang et al., 1997; Moscatello et al., 1996; Prigent et al., 1996), and reduced downregulation (Grandal et al., 2007).

MET mutations on the other hand have been identified in numerous types of human cancers, such as breast, colorectal, head and neck and gastric carcinomas. Additionally, they can be localised in several protein domains (Tovar and Graveel, 2017). Often mutations in the TK domain render MET constitutively active, independently of HGF stimulation (Jeffers and Vande Woude, 1999; Jeffers et al., 1998). As previously discussed, mutations in the JM domain affect ligand degradation by impairing its interaction with c-Cbl (Tovar and Graveel, 2017), while Sema domain mutations likely alter the structure of the ligand-binding domain rendering MET activation independent of growth factor stimulation (Kong-Beltran et al., 2006).

Often oncogenic driver mutations in RTKs are a predictor of sensitivity to specific TKIs. For instance, in NSCLC, small in-frame deletions in exon 19 and missense mutations in exon 21 (L858R or L861Q) of the EGFR protein are associated with favourable responses to TKIs, while T750M mutation in exon 20 often marks resistance to EGFR inhibitors, such as Erlotinib (Luo and Lam, 2013). This is not the case for MET, as many of the TKIs targeting this RTK have failed in clinical

trials (Hughes and Siemann, 2019). Recently, the clinical success of MET inhibitors in treating NSCLC with exon 14 MET alterations has led to renewed interest in MET TKIs. In particular, clinicians are now starting to recognise the lack of appropriate patient selection criteria in past MET inhibitor trials (Hughes and Siemann, 2018, 2019). More evidence may therefore emerge in the near future to shed more light on MET and MET mutations as predictors of TKI sensitivity.

Aberrant RTK activation can also be caused by RTK overexpression. The main mechanism of RTK overexpression is gene amplification, which causes increased localised concentration of the receptor, resulting in elevated downstream signalling (Du and Lovly, 2018). Importantly, gene amplification of an RTK can occur in the context of a wild type, as well as of a mutant allele. Alternatively, a similar result is achieved with RTK overproduction via transcriptional enhancement, for instance via the activity of p53 (Ludes-Meyers et al., 1996).

Gene amplification drives activation of EGFR in nearly half the cases of glioblastoma (GBM) (Brennan et al., 2013), and 10-20% of NSCLC, HER2 in approximately 20-30% of breast cancer cases (Slamon et al., 1987) and MET in approximately 3% of NSCLC and gastric cancer cases (Sierra and Tsao, 2011) and in 1% of breast cancer cases (The Cancer Genome Atlas). In approximately 3% of NSCLC cases, chromosomal translocations lead to the production of constantly activated anaplastic lymphoma kinase (ALK) fusion proteins (Koivunen et al., 2008).

Unlike oncogenic driver mutations, wild type RTK overexpression, with the exception of HER2 (Connell and Doherty, 2017), is not a good predictor of TKI sensitivity and is often associated with poor prognosis. For instance, EGFR amplification is associated with negative treatment outcomes in triple-negative breast cancers (Lehmann et al., 2011; Masuda et al., 2012; Rakha et al., 2007), GBM (Frederick et al., 2000), lung (Hirsch et al., 2009), colorectal (Ooi et al., 2004) and oesophageal cancers (Hanawa et al., 2006). Similarly MET gene amplification is associated with bad prognosis in gastric cancers (Catenacci et al., 2017; Lee et al., 2016; Liu et al., 2014), breast carcinomas (Veenstra et al., 2016) and gliomas (Kwak et al., 2015).

1.5.2 Oncogene addiction

"Oncogene addiction" is defined as a cellular condition wherein tumour cell survival becomes dependent on the activity of a single oncogene (Weinstein, 2002). From a therapeutic standpoint, the manifestation of oncogene addiction is induction of cell death, or terminal differentiation, upon oncogene-targeted inhibition (Weinstein, 2002). RTKs are known oncogenic drivers that, when constitutively activated, can render tumour cells addicted to their activity. Consequently, RTKs have been attractive therapeutic targets. Both small molecule inhibitors and monoclonal antibodies have become standard of care in the treatment of a few RTK-dependent cancers. Unfortunately, despite initial good responses, these cancers almost invariably develop drug resistance. Improving our understanding of RTK signalling mechanisms will allow us to identify additional drug targets and/or optimise our targeting strategies so as to render them more effective.

Drug resistance and progression to more aggressive disease can be attributed to three main mechanisms: a change in RTK-dependent signalling, a change in membrane composition and/or receptor dynamics, and the accumulation of additional mutations.

RTK-dependent signalling is often altered in the case of oncogene addiction, resulting in an over-activation of the canonical pathways (PI3K/Akt and MAPK). However, recent studies have shown how non-canonical pathways can also play an important role. For instance, ligand-independent EGFR (wild type) activation in cancer (glioblastoma and NSCLC) leads to non-canonical signalling networks that are mutually exclusive with ligand-induced Akt and Erk1/2 activation (Chakraborty et al., 2014). The impact of the non-canonical signalling pathways in Tyrosine Kinase Inhibitor (TKI) responses has not been assessed yet. However, given the frequency of RTK wild type overexpression (especially EGFR) in cancer without significant co-expression of ligand, the possibility that non-canonical RTK signalling may modulate TKI-responses cannot be excluded (Guo et al., 2015).

Additionally, it has been shown that EGFR can have oncogenic activity independently of its kinase activity (Cho et al., 2018). This non-canonical function

of RTKs is often overlooked when assessing TKI-resistance mechanisms, but may nonetheless play an important role.

Another mechanism of cancer cells to alter cellular signalling and escape targeted therapies is RTK heterodimerization. Heterodimerization between RTKs is a normal mean of signal amplification and diversification (He and Hristova, 2012). Heterodimers in fact have a weaker binding to ligands, and are less targeted by c-Cbl, often resulting in an overall prolonged and stronger signalling (Sigismund et al., 2018). Nonetheless, heterodimerization of RTKs can have oncogenic effects. This mechanism is well documented for the Erythroblastic Oncogene B (ErbB) family of receptors; for instance, resistance to HER2 TKIs is often observed with the activation of other members of this RTK family via heterodimerization (Yamaoka et al., 2018). Heterodimerization of RTKs, especially in cancer cells, is not limited to members of the same family and for instance MET is known to heterodimerize with members of the ErbB family (Jo et al., 2000). Heterodimers of MET with EGFR, HER2 or Human Epidermal Growth Factor Receptor 3 (HER3) all have differential roles in tumour development (Tanizaki et al., 2011).

Changing membrane composition or receptor trafficking dynamics are two other general mechanisms, often observed in cancer, which provide resistance to treatment. It has been shown that oncogene amplification can render cancer cells dependent on membrane lipid remodelling (Bi et al., 2019). Additionally, defects in phosphoinositide metabolism and localisation can contribute to cancer development (Jethwa et al., 2015).

Inappropriate receptor activation and/or RTK-dependent signalling can result from derailed endocytosis and trafficking. This has been shown to be the case for both MET (Joffre et al., 2011) and EGFR (Mellman and Yarden, 2013). Changes in membrane composition and RTK trafficking can also alter responses to TKI, by activating mechanisms such as autophagy or by physically relocating receptors to separate cellular compartments (Sigismund et al., 2018).

Finally, accumulation of additional mutations can aid cancer cells in escaping TKI inhibition. PTEN loss is one of the most common events observed in many types of

cancer (Álvarez-Garcia et al., 2019). Loss of PTEN is a particularly important event as it has been shown to regulate TKI-responses. In particular, it is associated with clinical resistance to EGFR (Fenton et al., 2012; Mellinghoff et al., 2005; Sos et al., 2009) and HER2 inhibitors (Esteva et al., 2010; Razis et al., 2011). Little is known, however, about its role in the responses to other inhibitors of different RTKs. Partial loss of PTEN, has been shown to correlate with opposite responses to TKI in the case of EGFR and MET addiction (Vivanco et al., 2010), but the mechanism behind this PTEN-mediated effect remains unclear.

1.6 Rationale

Since the discovery of EGF in the 1960's (Levi-Montalcini and Booker, 1960), a vast amount of research has been undertaken to unveil the complex network of RTKs and their signalling pathways. Their central role in cancer development and progression is now clear and strategies, such as TKIs, have been developed to target RTKs when they are oncogenic drivers. Nonetheless, cancer cells almost invariably develop resistance to such targeted treatments and escape therapies. Central to TKI-resistance mechanisms are the activation of the PI3K pathway and the loss of PTEN, historically considered predictive markers of responses to TKIs.

The connection between TKI responses, PI3K pathway activation and PTEN loss is however still unclear and, given their central role in human cancers, warrants further research. The current scientific model suggests that the identity of the RTK itself influences its activation, signalling and trafficking processes. Similarly, we hypothesise that the mechanisms of TKI-resistance, in particular loss of PTEN, depend on the identity of the RTK.

With a focus on RTK-addiction, we therefore seek to a) provide proof-of-concept evidence that PTEN differentially affects TKI responses, and that it does so differently depending on the RTK; b) thoroughly investigate the mechanisms behind this effect; and c) identify distal mediators of drug resistance caused by PTEN loss that could, in the future, aid the clinical development of new therapeutic strategies.

Chapter 2. Materials and Methods

2.1 Cell lines

A431, A549, Hs746T, H1993 and HEK-293T were obtained from the American Type Culture Collection (ATCC) (Manassas, VA). EBC1 and SBC5 cells were obtained from the Japanese Collection of Research Bioresources Cell Bank (JBC). KYSE-30 cells were obtained from the German Collection of Microorganisms and Cell Cultures (DSMZ). GTL16 cells were a kind gift from Dr. Silvia Giordano (University of Torino). MDA-MB-468 was a kind gift of Prof Bart Vanhaesebroeck (UCL Cancer Institute). H596 were kindly provided by Dr Anne Bowcock (Icahn School of Medicine at Mount Sinai). Cell lines were maintained in DMEM (Sigma Aldrich, D5796) supplemented with 10% FBS (Life Science, 10270106) and antibiotics (Normocin and Primocin, InvivoGen, ant-nr-2 and ant-pm-2). PTEN lox/lox Mouse Embryonic Fibroblasts (MEFs) were kindly provided by Dr Hong Wu (Peking University) and maintained in DMEM (Sigma Aldrich, D5796) supplemented with 5% FBS (Life Science, 10270106) and antibiotics (Normocin and Primocin, InvivoGen, ant-nr-2 and ant-pm-2). SNU-638, and NUGC4 were obtained from ATCC and maintained in RPMI-1640 (Sigma Aldrich, R8758) supplemented with 10% foetal bovine serum (FBS) (Life Science, 10270106) and antibiotics (Normocin and Primocin, InvivoGen, ant-nr-2 and ant-pm-2).

All cells, if not otherwise indicated, were grown in standard conditions of 5% CO_2, 90% humidity and 37°C. Trypsin-EDTA (0.25%) (Sigma, T3924) was used to detach cells from plates.

2.1.1 PTEN KO EGFR wild type stable cell lines and PTEN reconstitution of MDA-MB-468

Gateway cloning with Gateway LR Clonase II Enzyme Mix (Invitrogen, 11791-020 and 11791-100) was used to clone the donor vector pDONR223 EGFR (Addgene, 23935) or pDONR223 PTEN (Addgene, 81737) in the destination vector pLenti PGK Hygro DEST (Addgene, 1906). The cloning procedure was carried out according to the manufacturer's instruction. Successful cloning was confirmed via sequencing using PGKforw primer (CATTCTGCACGCTTCAAAAG).

Lentiviruses were generated with the calcium phosphate transfection method by transfecting psPAX2, pMD2.G (Addgene, 12260 and 12259) and the vector of interest into HEK-293T cells in a 3:1:5 ratio, for a total of 30 µg of DNA. Virus was collected 36 and 56 hours post-transfection and filtered (0.45 µm). PTEN lox/lox MEFs and MDA-MB-468 were then infected for 12 hours with each virus collection and selected with 500 µg/mL Hygromycin B (Invitrogen, 10687010). EGFR (in MEFs) and PTEN (in MDA-MB-468 cells) expression was tested by western blotting.

In order to knockout PTEN in MEFs, retroviruses were generated with the calcium phosphate transfection method by transfecting retroviral packaging vector (pCL-Ampho Retrovirus Packaging Vector, novus Biologicals, NBP2-29541) and WZL Neo-Cre (Addgene, 34568) into HEK- 293T cells in a 1:1 ratio, for a total of 30 µg of DNA. Virus was collected 36 hours post-transfection and filtered (0.45 µm). Cell lines were then infected for 12 hours and selected with 800 µg/mL of G418 (Sigma Aldrich, A1720-5G). Loss of PTEN expression was confirmed by western blotting.

2.1.2 Stable cell lines

Retroviruses were generated following the above-described method with pLNCX mPTEN wt (Vivanco et al., 2010) or pLP-LNCX-PIK3CA-H1047R (AddGene, 25635). Cell lines were then infected for 12 hours and selected with 800 µg/mL of G418 (Sigma Aldrich, A1720-5G). PTEN or p110α expression, with concomitant increase in phosphorylated Akt was confirmed by western blotting.

2.1.3 shRNA PTEN knock down

Retroviruses were generated following the above-discussed method with pSIREN PTEN sh Puro (Vivanco et al., 2007). Cell lines were then infected for 12 hours and selected with 5 µg/mL of Puromycin (Gibco, A11130-03). PTEN knockdown was confirmed by western blotting.

2.1.4 CRISPR/Cas9 cell lines

To generate PTEN knockout (KO) cells, three PTEN single guide RNAs (sgRNAs) CRISPR/Cas9 All-in-One Lentivector (Abm, K1749406, K1749407, K1749408)

were used. Lentiviruses were generated with the calcium phosphate transfection method already described. Virus for the three sgRNAs was collected 36 and 56 hours post-transfection, filtered (0.45 µm) and mixed in equal proportions. Cell lines were then infected with the mix for 12 hours with each virus collection and selected with 5µg/mL Puromycin (Gibco, A11138-03). PTEN KO was assessed by western blotting.

2.1.5 Single cell cloning

Single cell cloning was carried out on a MoFloAstrios machine (Beckman Coulter). 0.45 micron filtered 50% conditioned media was used for 96-well (Corning) plating.

2.1.6 Apilimod Resistant Cell Lines

125 x 10^6 GTL16 and EBC1 cells were seeded in a Hyper Flask (Corning) and Cell maintained in DMEM (Sigma Aldrich, D5796) supplemented with 10% FBS (Life Science, 10270106), antibiotics (Normocin and Primocin, InvivoGen, ant-nr-2 and ant-pm-2) and 200 nM Apilimod (AI Therapeutics, under NDA) for three months, with media and drug being refreshed every other week. Resistance was assessed by trypan blue exclusion method (ViCell).

2.1.7 Apilimod Resistant N1939K stable cell lines

PJ[puro, PIKfyve-N1939K] plasmid was obtained from AI Therapeutics (Guilford, CT) (Gayle et al., 2017) under NDA. Cells were transfected with Lipofectamine 3000 (ThermoFisher Scientific, L3000015) following the manufacturer's instructions.

2.1.8 mCherry-EGF-LC3B stable cell lines

To generate mCherry-EGFP-LC3B GTL16 and EBC1 cell lines, pBABE-puro mCherry-EGFP-LC3B plasmid was purchased from Addgene (22418). Retroviruses were generated with the calcium phosphate transfection method already discussed. Cell lines were infected for 12 hours and selected with 5 µg/mL Puromycin (Gibco, A11138-03).

2.2 General techniques, drug treatments and storage conditions

Distilled water was used to prepare all stock solutions and reactions, unless otherwise stated. All small volume centrifugation steps were carried out at room temperature using a desktop centrifuge (Eppendorf) and at 4°C in a refrigerated centrifuge (Eppendorf), if required. DNA containing solutions were stored at -20°C and their glycerol stocks at -80°C. All antibodies were stored in the short term at -20°C (unless otherwise stated by the manufacturer's guidelines), and, if necessary, in the dark.

All drugs (Table 2.1) were prepared under sterile conditions in a cell culture-hood. Unless otherwise stated, drugs were dissolved in DMSO (Sigma-Aldrich, D2438) and diluted according to the manufacturer's instructions and used at the indicated concentrations.

Drug	Manufacturer	Cat. number
Afatinib	LC Laboratories	A-8644
Apilimod (LAM-002)	AI Therapeutics (Guilford, CT)	under NDA
APY-0201	Insight Biotech Limited	HY-15982
ARQ-092	Medkoo Biosciences	200281
AZD-6482	Cambridge Bioscience	CAY15250
Bafilomycin A1	MedChem Express	HY-100558
BMS-777607	MedChem Express	HY-12076
BYL-719	LC Laboratories	A4477
Cabozantinib	Selleck Chemicals	S1119
Crizotinib	Selleck Chemicals	S1068
CX-4945	ApexBio Technology	A8330
Cycloheximide	Sigma Aldrich	C4859
EKB-569	Pelitinib, Medkoo Biosciences Inc.	202190
Erlotinib	LC Laboratories	E-4007
GDC-0068	Startech Scientific	S2808-SEL
GDC-0941	LC Laboratories	G9252
Idelalisib	LC Laboratories	I7447
JNJ-38877605	Selleck Chemicals	S1114
Lapatinib	LC Laboratories	L-4899

MK2206	Selleck Chemicals	S1078
SAR405	Axon Medchem	2716
Torin1	Selleck Chemicals	S2827
Trametinib	LC Laboratories	T-8123
YM-201636	ApexBio Technology	B2189

Table 2.1 Drugs used in the study

The drugs used in the study are listed in this table. Information regarding the manufacturer and the catalogue number are indicated.

Please see the main text for the final drug concentrations. The following table indicates the known binding affinities (*in vitro*) and selectivity of the main inhibitors used (Table 2.2).

Drug	Main Target (IC50)	Other Targets (IC50)
Afatinib	EGFR (0.5 nM)	HER2 (14 nM), HER4 (1 nM)
Apilimod	PIKfyve (14 nM)	Inhibits IL-12/23 production
BMS-777607	MET (3.9 nM)	Axl (1.1 nM),Ron (1.8 nM), Tyro3 (4.3 nM)
Cabozantinib	MET (1.3 nM)	VEGFR2 (0.035 nM), et (4 nM), Kit (4.6 nM), Flt-1/3/4 (12/11.3/6 nM), Tie2 (14.3 nM), AXL (7 nM)
Crizotinib	MET (11 nM)	ALK (24 nM), ROS1 (Ki<0.025 nM)
EKB-569	EGFR (38.5 nM)	n/a
Erlotinib	EGFR (2 nM)	c-Src, v-Abl (>1000-fold)
GDC-0068	Akt1/2/3 (5/18/8 nM)	PKA (620-fold)
GDC-0941	PI3Kα/δ (3 nM)	PI3Kβ/γ (11/25-fold)
JNJ-38877605	MET (4 nM)	600-fold selectivity for MET compared with more than 200 other diverse tyrosine and serine-threonine kinases
Lapatinib	EGFR (10.8 nM)	HER2 (9.2 nM)
MK2206	Akt1/2/3 (8/12/65 nM)	n/a

Table 2.2 Binding affinities and specificities of main drugs used in the study

The binding affinities (IC50) and specificity (IC50 or fold increase compared to main target) of the main drugs used in the study are listed in this table.

2.3 Assessment of cell death induction

Cell viability was determined with a Vi-CELL Cell Viability Analyzer (Beckman Coulter, Brea, CA, USA) according to the manufacturer's instructions. Cells were seeded in 3 replicates on day 0 on 60mm dishes (Corning). On day 1 cell counts were assessed and treatments started. Treatments were carried out in full serum

unless otherwise indicated. Cell death was determined 72 hours after treatment. Both attached and floating cells were harvested and counted. The instrument uses trypan blue to assess cell death. Cell death was expressed as the fraction of trypan-blue-positive cells over the total number of cells.

All growth assays have been performed a minimum of two times. Shown are results from one representative experiment, unless otherwise indicated. Statistical significance was performed using either one- or two-way analysis of variance (GraphPad Prism). Symbols ns, *, **, ***, **** represent values that are not significant or having a *P* value <0.05, <0.01, <0.001 or <0.0001, respectively.

In few instances, cell viability was assessed with CellTiter-Glo Luminescent cell viability Assay (Promega, G7570) as per manifacturer's instructions. Briefly, 5 x 10^3 A431 or 2.5 x 10^3 GTL16 cells were seeded in 96 wells. Following treatments with different drug concentrations, CTG (Promega, G7570) was added and the plates were read in Spectramax I3 reader. Background noise (i.e. readings derived from control wells with no cells) was subtracted before proceeding to analyse the results. The curves were created using GraphPad Prism [nonlinear regression, log(inhibitor) vs. response – variable slope (four parameters)].

2.4 Western Blot

Cells were starved overnight (GTL16) or for 4 hours (A431) for growth factor stimulation. Growth factor stimulation was carried out in serum free media, while TKI experiments were carried out in DMEM supplemented with 5% FBS, unless otherwise indicated.
Cells were harvested on ice directly on tissue culture plates. 1% triton X lysis buffer (Cell Signaling Technologies, 9803) supplemented with protease and phosphatase inhibitors (Millipore, 539131, 524627) was used.

Lysates were sonicated, cleared by centrifugation and normalized to equal amounts of total protein using the DC protein assay (Bio-Rad, 5000111).

Proteins were run on Tris-Glycine TGX 4-20% gels (Bio-Rad, 567-1095) using 1X SDS Tris-Glycine Running buffer (Fisher Scientific), and transferred to nitrocellulose membrane (Bio-Rad, 1704271) using 1X transfer buffer (25 mM Tris-HCl (pH 7.6), 192 mM glycine, 20% methanol, 0.03% sodium dodecyl sulfate) with the Trans-Blot Turbo Transfer System (Bio-Rad, 1704150). Membranes were blocked for 1 hour in 5% milk at room temperature and subsequently incubated overnight at 4°C with primary antibodies (Cell Signaling if not otherwise indicated): AKT (1:1000, 4685), pAkt S473, T308 (1:1000, 4060,13038), CK2α (1:1000, 2656), pCK2 substrate (1:1000, 8738), cMyc (1:1000, 5605), CoxIV (1:10000, 4850), cyclinD1 (1:1000, 2978), EGFR (1:5000, 4267), pEGFR Y1068, Y1045, Y1173 (1:1000, 2234, 2237, 4407), Erk1/2 (1:5000, 9102), pErk1/2 (1:1000, 9101), Gab (1:1000, 3232), pGab (1:1000, 3233), GAPDH (1:10000, 5174), Hsc70 (1:10000, Santa Cruz, sc-7298), LC3B (1:500, 2775), MET (1:10000, 8198), pMET Y1234/1235, Y1349, Y1003 (1:10000, 3077, 3121, 3135), NDRG1 (1:1000, 5196), pNDRG1 (1:1000, 5482), PIKfyve (1:100, Biorbyt, orb255387), PTEN (1:1000, 9559), p62 (1:1000, 8025), pP62 (1:1000, 95697), Rb1 (1:1000, 9309), pRb1 (1:1000, 8516), Src (1:1000, 2108), Transferrin (1:500, ThermoFisher Scientific, MA1-20106), Vinculin (1:10000, 13901), total p-tyrosine (pY) (1:500, ThermoFisher Scientific, 14-5001-82), βActin (1:5000, Merck, MABT825). The following day, membranes were incubated with a horseradish peroxidase (HRP) conjugated anti-rabbit or anti-mouse secondary (1:5000, Jackson ImmunoResearch, 111-035-144 and 315-035-003) for 1 hour and developed using Amersham ECL (GE Healthcare, RPN 2106).

Band intensity was quantified with the gel analyser function of the ImageJ software (Schneider et al., 2012). For this purpose, developed films were scanned with an Epson scanner (Epson, Perfection V370) at 1200 pixels per inches (ppi) and images converted to 8-bit format in order to perform uncalibrated optical density. Western blot analysis was performed on a single representative experiment.

Western blot experiments have been performed a minimum of two times with identical conditions/treatments, unless otherwise stated. Shown are results from one representative experiment.

2.5 Immunoprecipitation

Cells were harvested on ice directly on tissue culture plates. 50 mM HEPES (pH 7.4), 150 mM NaCl, 1mM EDTA, 1 mM EGTA, 1% Nonidet P-40, 1% glycerol lysis buffer supplemented with protease and phosphatase inhibitors (Millipore 539131, 524627) was used. Lysates were normalized to equal amounts of total protein using the DC protein assay (Bio-Rad, 5000111).

Lysates underwent a 30-minute pre-clearing step with 20 µL protein A Agarose beads (50% slurry, Cell Signaling Technology, 9863) at 4˚C, followed by MET pulldown using the Immunoprecipitation Kit Dynabeads protein A, according to manufacturer's instructions (Thermo Scientific, 10006D). Dynabeads were crosslinked to MET antibody (Cell Signaling Technology, 8198) using BS_3, as per manufacturer's instructions (Thermo Scientific, 10006D).

Proteins were eluted as per manufacturer's instructions (Thermo Scientific, 10006D) and analysed on Tris-Glycine TGX 4-20% gels (Bio-Rad, 567-1095), as previously described.

2.6 Cell-surface Biotinylation

Cells were plated on 100 mm dishes and incubated to reach 80% confluency prior to procedure. If starved, GTL16 cell lines were starved overnight, while A431 were starved for 4 hours. The procedure was performed on ice. On day of procedure, cells were washed twice with ice-cold PBS (with $CaCl_2$, $MgCl_2$) and incubated in 2.5 mg/mL biotin reagent, Sulfo-NHS-SS-Biotin (ThermoFisher Scientific, 21331), for 30 minutes on ice with gentle rocking. Biotin was quenched with 1 mL of 200 mM glycine in PBS for 10 minutes on ice with gentle rocking. After incubation, cells were washed with 100 mM glycine in PBS three times and lysed with 200 µL of 1% triton X lysis buffer (Cell Signaling Technologies, 9803) supplemented with protease and phosphatase inhibitors (Millipore, 59131, 524627). Following sonication and 30 minutes incubation on ice, lysates were cleared by centrifugation and normalized to equal amounts (2 mg/mL in 500 µL) of total protein using the DC protein assay (Bio-Rad, 5000111). 20 µL of each sample were transferred to a new

tube and saved as whole cell lysates (WCL). 80 µL per sample of streptavidin agarose slurry was prepared as follows: the slurry was transferred to an Eppendorf tube and spun at 800 × g for 1 minute. The supernatant was discarded and beads were washed two more times with 300 µL of Lysis Buffer. Samples were added to packed beads and incubated with an end over end rotation for 1 hour at room temperature. Lysates were spun at 800 × g for 1 minute. 100 µL of each supernatant was transferred to a new tube and saved as unbound eluate (UE). Beads were washed 1X with Lysis Buffer containing 300 mM NaCl and 2X with Lysis Buffer. Pull-down, WCL and UE samples were incubated using 3X Laemmli buffer with 50 mM DTT at 30°C for 30 minutes with brief vortexing every 10 minutes. Western blotting was performed on samples as described above.

2.7 Kinase Enrichment Assay

The ability of TKIs to compete with ATP for binding to receptors and the ability of receptors to bind increasing concentrations of ATP was measured using the Pierce Kinase Enrichment Kit with ATP probe (ThermoFisher Scientific, 88310) and was conducted according to the manufacturer's protocol following the modifications described in (Vivanco et al., 2012). To summarize, cells were harvested and lysed 24 hours after seeding. Lysates were passed through a de-salting column to remove ATP. Lysates were incubated with a premade mixture of inhibitors at the desired concentrations and desthiobiotin-ATP probe to a final concentration of 5 µM. Alternative, lysates were incubated with different concentrations of desthiobiotin-ATP probe alone. The incubation time was of 5 minutes at room temperature, the reaction was terminated by addition of 4M urea. Avidin agarose beads were then added to the reaction mixtures and allowed to pull down biotinylated proteins for 1 hour at room temperature with end over end rotation. Beads were washed 3X and eluted with 3X Laemmi sample buffer. Pulldowns were analysed by western blotting.

2.8 Proteomics and phosphoproteomics profiling experiments and KSEA analysis

Treatments were carried out for 4 hours in 5% DMEM at the following concentration: 20 nM Cizotinib, 2 µM Erlotinib and 2 µM Lapatinib. Treatment with

200 nM Apilimod was carried out for 24 hours. For each treatment condition, five independent biological replicates were performed.

Plates were washed 3 times with 3 mL ice-cold PBS containing protease and phosphatase inhibitors (2% (v/v) NaF and 10% (v/v) Na_3VO_4). Cells were harvested on ice, directly on tissue culture plates, with 300 µL lysis buffer (250 mM $Na_2H_2P_2O_7$, 1 M β-glycerol phosphate, 500 mM NaF, 100 mM Na_3VO_4, 8 M Urea in 20 mM HEPES pH 8.0). Cells were sonicated, while on ice, 3 times at 20% intensity for 10 seconds with a 10 seconds rest in a Diagenode Bioruptor® Plus. Cell suspensions were centrifuged at 20000 × g for 10 minutes at 5°C. Protein was quantified by the BCI assay. Supernatant was recovered in 1.5 mL Eppendorf Protein Lo-bind tube. Lysates were snap frozen in dry ice before sending to the phosphoproteomics facility for further processing. All of the processing and analysis steps were carried out by Dr Cutillas's team in Queen Mary University of London.

For each replicate, 325 µg of protein was reduced, alkylated and digested with TLCK-trypsin (Thermo-Fisher Scientific) as previously described (Casado et al., 2013). The resultant peptide solutions were desalted with C18-Oasis cartridges (Waters, Manchester, UK) as indicated by the manufacturer with slight modifications as previously described (Casado et al., 2018). For phosphoproteomics analyses, peptides were eluted with 500 µL of glycolic acid buffer (1 M glycolic acid, 50% ACN, 5% TFA) and subjected to phosphoenrichment. For proteomics analyses peptides were eluted with 500 µL of ACN solution (30% ACN, 0.1% TFA), dried in a speed vac (RVC 2-25, Martin Christ Gefriertrocknungsanlagen GmbH, Osterode am Harz, Germany) and stored at -80 ^{o}C. For phosphoproteomics, enrichment of phosphorylated peptides was performed with TiO2 as previously described (Casado et al., 2013, 2018).

For phosphoproteomics, phosphopeptides were resuspended in 12 µL of reconstitution buffer (20 fmol/µL enolase in 3% ACN, 0.1% TFA) and 5.0 µL were loaded onto a liquid chromatography with tandem mass spectrometry (LC-MS/MS) system consisting of a Dionex UltiMate 3000 RSLC directly coupled to an Orbitrap Q-Exactive Plus mass spectrometer (Thermo Fisher Scientific) through an EasySpray system. LC-MS/MS was performed as previously described (Casado et

al., 2013). For proteomics, pellets were resuspended in reconstitution buffer (0.5 µg/µL) and 2 µL were injected.

Mascot Daemon 2.5.0 was used to automate peptide identification from MS data as indicated before (Casado et al., 2013). Label-free peptide quantification was performed using Pescal, an in-house developed software, that constructed of XICs for all identified peptides across all samples (±7 ppm mass and ±2 min retention time windows) and calculated the peak areas of the generated XICs (Casado et al., 2013, 2018). Normalized peak areas of peptides (proteomics) or phosphopeptides (phosphoproteomics) were used to calculate fold change and statistical significance between conditions.

Kinase activity was estimated from phosphoproteomics data using a kinase substrate enrichment analysis (KSEA) approach (Casado et al., 2013, 2018; Montoya et al., 2011). Briefly, phosphorylated peptides were grouped into substrate groups associated to particular kinases as annotated in the PhosphoSite database. Z-scores for each kinase were calculated as (mS−mP) *m1/2/d, where mS is the $\log_2$ of the mean abundances for each kinase group, mP is the $\log_2$ of the mean abundances of the whole data set, m is the size of each substrate group and d is the SD of the mean abundances of the entire data set. Excel software was used to transform Z-scores into *P*-values. For statistical analysis only *P* values < 0.05 were considered along with a fold change threshold = 0.75.

2.9 Immunmofluorescence staining and confocal analysis

For the immunofluorescence (IF) procedure, 10^5 cells were plated onto coverslips. After 24 hours, cells underwent fixation with 4% paraformaldehyde in PBS for 10 minutes at room temperature. Subsequently, paraformaldehyde was quenched using 50 mM NH_4Cl in PBS for 10 minutes, followed by three consecutive PBS washes. Next, cells were permeabilised using 0.1% Triton X-100 in PBS for 15 minutes at room temperature. After three washes with PBS, non-specific antibody binding sites were blocked by incubating cells in blocking solution (1% BSA, 0.1% Tween 20 in PBS) for 30 minutes at room temperature. Next, cells were incubated with 30 µL of pre-diluted antibodies in blocking solution (Human MET Antibody (10

μg/mL, R & D, AF276), EGFR (10 μg/mL, R & D, AF231), EEA1 (1:100, Cell Signalling Technologies, 3288), LAMP1 (1:100, Cell Signalling Technologies, 15665)) overnight at 4°C. Afterwards, cells were washed with PBS three times. Dye-coupled secondary antibodies in blocking solution were incubated 1 hour at room temperature in a dark chamber (donkey anti-goat AlexaFluor568 (Invitrogen, A11057), donkey anti-mouse AlexaFluor488 (Invitrogen, A21202), donkey anti-rabbit AlexaFluor488 (Invitrogen, A32790) and goat anti-rabbit AlexaFluor555 (Invitrogen, A21429). After three washes with PBS, nuclei were stained with DAPI (1:5000, Sigma-Aldrich, D9542) for 5 minutes in PBS. Finally, after three washes in PBS and one in water, cells were mounted in Mowiol (ThermoFisher, P36961). Cells were examined under a 63x magnification lens and pictures were acquired using a Zeiss LSM700 Confocal. Co-localisation was determined by Manders' coefficient using JACoP plugin (Bolte and Cordelières, 2006) in Fiji (Schindelin et al., 2012). The quantification of MET-positive structures was achieved by counting the circular structures in 74 parental and 60 PTEN KO cells.

2.10 Flow cytometry

Cells were seeded in 6-well plates at a density of 5 x 10^5 cells/well and incubated overnight to attach and reach a 1 x 10^6 confluency. Before drug treatments, cells were washed twice with Ca^{2+}-Mg^{2+}-free PBS (Sigma-Aldrich, D8537). mCherry-EGFP-LC3 GTL16 cells were starved in DMEM FBS free media for 2 hours prior the following treatments: DMSO (Sigma-Aldrich, D2438), Bafilomycin A1 (200 nM), Torin-1 (250 nM). After treatments, cells were washed with Ca^{2+}-Mg^{2+}-free PBS twice and trypsinized, at 37ºC for 5 minutes. Cells were centrifuged at 189 × g for 5 minutes and the pellet was resuspended in 1 mL of FACS buffer (3% FBS containing Ca^{2+}-Mg^{2+}-free PBS). DAPI (5 mg/mL) (Sigma-Aldrich, D9542) was added to each sample in order to analyze the cell viability by FACS. Samples were stored on ice and foil wrapped until analysed.

BeckmanCoulter MoFlo Astrios flow cytometry analyzer was used to analyze cell suspensions. In order to measure the effect of the different drugs on autophagy, changes in mCherry and GFP signals were analysed (Gump and Thorburn, 2014). After gating singlets and live cells (DAPI negative cells), mCherry versus GFP dot plot was generated, and a derived parameter mCherry/GFP (561-614/20-Height-

Log/488-513/26-Height- Log) was calculated. mCherry-GFP high-expressing cells were gated, and a histogram of cell count on the derived parameter was generated. Basal autophagy was set as a baseline on the control and DMSO conditions. High autophagy flux was described as the percentage of the gated mCherry-GFP high-expressing cells displaying a higher mCherry/GFP ratio than the basal autophagy mCherry/GFP ratio (this value being the mean of the derived parameter, mCherry signal/GFP signal respectively). Changes on mCherry/GFP ratio were compared in order to assess the effect of the drugs on autophagy. Inhibition of autophagy is represented as a small increase or no increase in mCherry/GFP ratio, since both mCherry and GFP signals are stabilized. Induction of autophagy results in an increase of mCherry/GFP ratio, since GFP is quenched at the lysosomal pH when autophagy is induced, while mCherry is stabilized. Histogram overlays were created using FlowJo® (Tree Star Inc., Ashland, Oregon, USA).

2.11 Mouse Experiment

Mouse experiments were carried out by Dr Gabriela Kramer's team at The Institute of Cancer Research. 3 mice (male, 6-7 weeks, BALB/c nude, Charles River) per treatment group were used. Apilimod (AI Therapeutics) was administered at 60 mg/Kg or 30 mg/Kg, daily by oral gavage. A vehicle control group was included. Mice's weight was monitored daily. The experiment was terminated after 14 days.

Chapter 3. PTEN loss differentially affects EGFR and MET inhibitor responses

3.1 Introduction

3.1.1 PTEN loss in RTK addiction

PTEN has been shown to modulate TKI responses. For instance, PTEN loss contributes to Trastuzumab resistance in HER2-amplified tumours (Berns et al., 2007). Similarly, loss of PTEN in tumours with EGFR amplification, as found in 50% of adult glioblastoma (GBM) patients (Brennan et al., 2013), is associated with clinical *de novo* resistance to EGFR inhibitors (Bianco et al., 2003; Mellinghoff et al., 2005).

Despite significant efforts to understand the role of PTEN in cancer, the particular aspects of PTEN function, which are involved in TKI responses, remain vaguely defined. Existing evidence suggests that PTEN loss, by causing unopposed PIP_3 accumulation and enhanced downstream signalling, may provide survival signals that bypass the need for single RTK input (Stommel et al., 2007). Given that most RTKs generate survival signals through PI3K activation, PTEN inactivation might be predicted to act as a general mechanism of TKI resistance. However, this concept has only been extensively evaluated in EGFR and HER2-dependent tumours (Berns et al., 2007; Bianco et al., 2003; Mellinghoff et al., 2005). Interestingly, there is some evidence that, unlike EGFR/HER2-dependent cells, MET-addicted cell line models with PTEN inactivation display increased cell death in response to MET inhibitors (Vivanco et al., 2010). These data, therefore, supports the hypothesis that loss of PTEN affects TKI responses in vastly different ways, depending on the identity of the RTK.

PTEN can be lost or inactivated by several mechanisms, including mutations, deletions, transcriptional silencing and alteration in protein stability. Monoallelic or biallelic inactivation of PTEN can occur clonally via focal gene deletions of one or both copies of PTEN, phosphatase-inactivating mutations, and/or through whole chromosomal loss. The different mechanisms of PTEN inactivation lead to

variations in the tumour suppressor expression levels. There is genetic evidence from mouse models that subtle differences in PTEN protein leads to differences in cancer susceptibility (Alimonti et al., 2010; Trotman et al., 2003).

While several studies have shown that haploinsufficiency of the PTEN gene can promote tumour progression, the significance of complete loss of PTEN is not entirely clear (Salmena et al., 2008). Complete loss of PTEN, in fact, can trigger p53-dependent cellular senescence; a potential disadvantage for early-stage tumour development (Chen et al., 2005). Nonetheless, endometrial cancer, glioblastoma, and many other cancers in the advanced and metastatic stage present high frequencies of complete loss of PTEN (Salmena et al., 2008). It is therefore evident that more studies are needed to better understand how the quantitative aspect of PTEN status impacts tumour development.

Previous work linking loss of PTEN activity to TKI responses relied on RNAi-mediated PTEN knockdown (KD) (Vivanco et al., 2010). With this approach, however, it is difficult to assess how or whether any residual PTEN activity could affect cellular responses. Given that subtle differences in PTEN levels can have significant effects on the biology of certain tissues (Alimonti et al., 2010; Trotman et al., 2003), cellular models with complete PTEN gene inactivation are needed to better understand the effects of PTEN loss on RTK inhibitor responses.

3.1.2 Cell lines selection and single cell cloning

Since there is some evidence of PTEN loss having opposite effects on the response to EGFR versus MET inhibitors (Vivanco et al., 2010), we reasoned these two RTK were a valid starting point to assess the selective effect of PTEN loss on RTK physiology.

The most used scientific model system to analyse phenomena in an EGFR overexpressed and amplified setting is A431, an epidermoid carcinoma cell line (Ullrich et al., 1984). GTL16 on the other hand, is a clone derived from MKN45 (Rege-Cambrin et al., 1992). It is a gastric adenocarcinoma cell line, in which the MET oncogene has been activated and overexpressed, following a relocation of the un-mutated coding sequence (Rege-Cambrin et al., 1992). Given the absence of

further mutations affecting the PI3K/Akt pathway in A431 and GTL16, we thought of these two cell lines as well suited for the study, and chose them as our main two *in vitro* models.

It is widely accepted that cancer cell lines are genetically heterogenous (Ben-David et al., 2018). Minimising the potential confounding effects of heterogeneity when working with isogenic lines is therefore critical for the robustness of the model. To this end, isolating single cell clones from the parental cell population, from which all subsequent cell lines will be derived, is a strategy that can partially restrict the effects of genetic variability, by providing an identical subclonal population of cells as starting material.

When generating a knockout (KO) of a protein of interest, single-cell-derived subclonal populations become an effective tool to identify and isolate lines with a complete KO (Giuliano et al., 2019). This is particularly relevant given the potential heterogeneity of protein expression or gene dosage of the gene of interest.

This approach, however, is not without drawbacks. For example, generating an entire cell line from a single cell progenitor may trigger the selection and subsequent accumulation of genetic alterations that facilitate clonal expansion. Additionally, interclonal heterogeneity, has been reported, causing clones derived from the same parental line to display different phenotypes, such as variation in drug treatments and proliferation (Khan et al., 2017). Therefore, it is essential to confirm that a) the clone selected as the 'parental control' retains the phenotypic trait of the original population (e.g. drug sensitivity), and b) phenotypes observed in sub-lines derived by gene editing of the parental clone can be observed in multiple subclones (Giuliano et al., 2019).

3.1.3 CRISPR Cas9

The generation of a complete PTEN KO is a critical step in the study of the role of true homozygous loss of PTEN in TKI responses. However, sufficient efficiency and precision of the knockout is required to generate a strong cellular model. Originally identified in *Escherichia coli* as a bacterial naturally occurring anti-viral

defence mechanism, the Clustered Regularly Interspaced Short Palindromic Repeats (CRISPR)/Cas9 tool has since been extensively studied and adapted to be used in eukaryotic cells. It has now proven its efficacy in genome editing of mammalian cells and has become a standard choice for somatic gene editing (Cong et al., 2013; Jinek et al., 2013; Mali et al., 2013). This method has many advantages compared to older RNAi and transcription activator-like effector nucleases (TALENs) systems because of its ease of design, high efficiency and cost-effectiveness (Gupta and Musunuru, 2014; Loureiro and da Silva, 2019).

The CRISPR system used for gene editing is composed of a Cas9 nuclease protein and a 20-nucleotide long single guide RNA (sgRNA). The sgRNA is engineered to match the target sequence of interest. This helps target recognition and direct base-pairing with the correct DNA locus. The sgRNA-Cas9 complex locks onto the protospacer-adjacent motif (PAM); a short DNA sequence at the 3' end of the DNA target locus necessary for Cas9 to start unwind the DNA. Once both sgRNA-DNA binding and PAM recognition have occurred, Cas9 endonuclease activity is triggered, resulting in double-stranded DNA breaks. The cellular machinery will then attempt to repair the DNA breaks, often by the error-prone non-homologous end-joining (NHEJ) mechanism. This typically results in non-reversible insertion or indel mutations ultimately causing a gene knockout (Hsu et al., 2014).

One concern with CRISPR/Cas9 tool is its off-target effects. Increasing target specificity of the system is therefore an active subject of research, but there are already efficient strategies in place. For instance, careful design of the PAM sequence, optimization of sgRNAs (Fu et al., 2013) and introduction of multiple guide RNAs can improve specificity up to 15000x compared to the naturally occurring form of Cas9 (Ran et al., 2013).

An additional drawback in the use of the CRISPR/Cas9 system is the potential generation of alternative isoforms of the original protein that still retain partial function. Although the frequency of such occurrence is unclear and seems to be linked to the use of a single sgRNA, CRISPR/Cas9 target modification of mammalian exon sequences can lead to exon skipping. The resulting messenger RNAs can in some cases encode functional or partially functional proteins (Mou et

al., 2017). It is therefore important to document the complete loss of the protein of interest in the knockout population.

More problematic is the observation that occasionally, indel mutations can have long-read sequence effects, away from the target locus, therefore interfering with neighbouring genes (Kosicki et al., 2018). Ideally, sequencing nearby regions of the target locus could provide reassurance of on-target genetic modification, although it is unclear as to what region one should look at.

Finally, there is evidence that CRISPR/Cas9 site directed mutagenesis can trigger a p53-mediated DNA damage response. This can result in cell cycle arrest and therefore indirectly select for cells with non-functional p53. A clonal population thus selected could carry additional mutations due to inefficient p53 activity that may affect experimental outcomes (Haapaniemi et al., 2018). There is no evidence for this effect in cancer cell lines, and, given the efficiency of recombination-based editing in cancer cell lines, CRISPR/Cas9 remains a valid and efficient tool for gene editing.

Our choice to use CRISPR/Cas9 technology to knockout PTEN in the cell lines of interest was dictated by the three main strengths of this technology, namely ease of design, high efficiency and cost-effectiveness (Gupta and Musunuru, 2014; Loureiro and da Silva, 2019). To maximise the efficiency of this gene-editing tool we designed the introduction of three guide RNAs, while we documented the complete loss of PTEN protein via western blotting to address potential technical drawbacks. To minimise the risk of off-target effects and false positive observations regarding the PTEN KO phenotype, we also resolved to, whereas possible, replicate the data obtained for the KO lines in correspondent PTEN KD cells, obtained via small hairpin (sh) RNAs. Additionally, we aimed to rescue the phenotype displayed by PTEN KO cells by reconstituting them with a CRISPR/Cas9 resistant mouse (m) PTEN cDNA. Finally, we hoped to replicate our observations in multiple cell lines, dependent on the same RTK, with either a complete PTEN KO or a PTEN KD.

3.2 Results

3.2.1 A431 and GTL16 cell lines establishment

To evaluate the effects of PTEN inactivation on EGFR and MET inhibitor responses, A431 and GTL16 were chosen as EGFR-addicted and MET-addicted models, respectively Supplementary Figure 1). Having chosen to minimise clonal heterogeneity in the parental control population via single cell cloning, multiple clonal lines of the A431 population were derived. A similar approach was unnecessary for GTL16, which is already a clonal line derived from MKN45 cells (Rege-Cambrin et al., 1992). A431 clones 4 and 6 were picked for further validation in EGFR inhibitor sensitivity assays (Figure 3.1a). Given the different levels of EGFR inhibitor sensitivity and EGFR expression, as well as activation, of the two subclones (Figure 3.1a), we reasoned that comparing clone 4 and 6 in further experiments would more accurately represent the parental population.

CRISPR/Cas9 technology was then used to knockout PTEN in A431 and GTL16 cell lines. PTEN KO was carried out on single cell clones of parental cell lines (clone 4 and 6 in Figure 3.1a); a subsequent round of single cell cloning allowed clones with a complete PTEN loss to be obtained. A single clone, highlighted in Figure 3.1b with an arrow, was chosen from both GTL16 (clone 11) and A431 (clone 3) for further experiments (henceforth referred to as PTEN knockout (KO), Figure 3.1b). Other A431 and GTL16 PTEN KO clones were later used to validate the PTEN KO phenotypes.

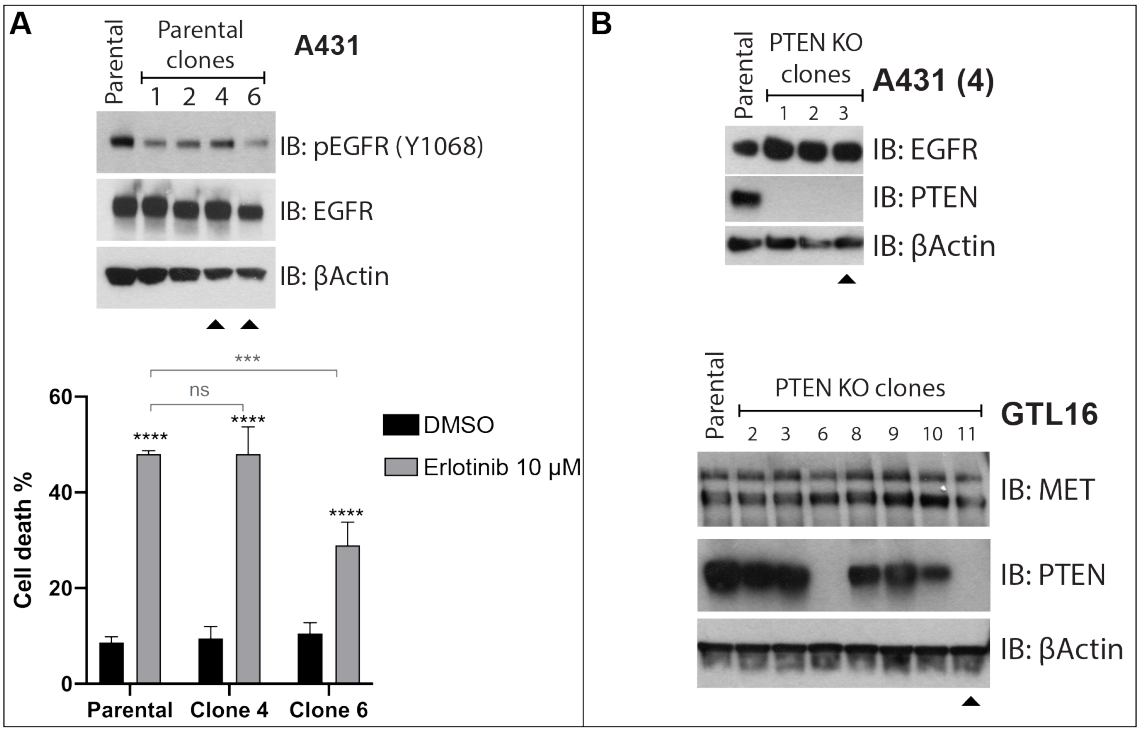

Figure 3.1 A431 and GTL16 PTEN KO generation(A) Western blot analysis (n=1) of A431 (EGFR amplified) subclonal populations. Single cell clones have been named with a number. The two clones indicated with an asterisk were chosen for further validation (bottom). Their responses to the EGFR inhibitor Erlotinib were assessed via automated trypan blue exclusion method (ViCell). Cell death percentages (mean ± SD) in response to 72 h treatment with 10 μM Erlotinib are plotted in the graph. n=3. ns, not significant; *** significant at *P*<0.001; **** significant at *P*<0.0001. **(B)** Western blot analysis of PTEN knockout in A431 subclone 4 (top) and GTL16 (bottom) (n=1). The arrows indicate the PTEN KO clones that were chosen for further experiments.

3.2.2 PTEN loss causes resistance to EGFR inhibitors in EGFR-addicted cancer cells, but sensitises MET-addicted cancer cells to MET inhibition

To assess the impact of PTEN loss on TKI treatments, responses in parental single cell clones (henceforth referred to as 'parental') to the appropriate RTK inhibitor were compared to those in the PTEN KO clones. The clinically approved EGFR inhibitors Erlotinib and Lapatinib were tested in the A431 cell lines. In GTL16 cells, responses were tested against a clinical MET/ALK inhibitor, Crizotinib, and a MET-selective inhibitor, JNJ38877605. The results showed that PTEN loss caused resistance to EGFR inhibitors in EGFR-addicted cancer cells (A431), while further sensitising MET-addicted cancer cells (GTL16) to MET inhibitors (Figure 3.2). The data were collected using two different experimental methods, the trypan blue exclusion method (Figure 3.2a and Supplementary Figure 2a and b) and the

CellTiter-Glo Luminescent cell viability Assay (Figure 3.2b), in order to assess the effects of TKI on cell death and viability, respectively. Nonetheless, based on the oncogene addiction paradigm, oncogene inhibition is manifested when cell death is induced (Weinstein, 2002). Consequently, direct assessment of cell death by trypan blue exclusion method is the preferred strategy.

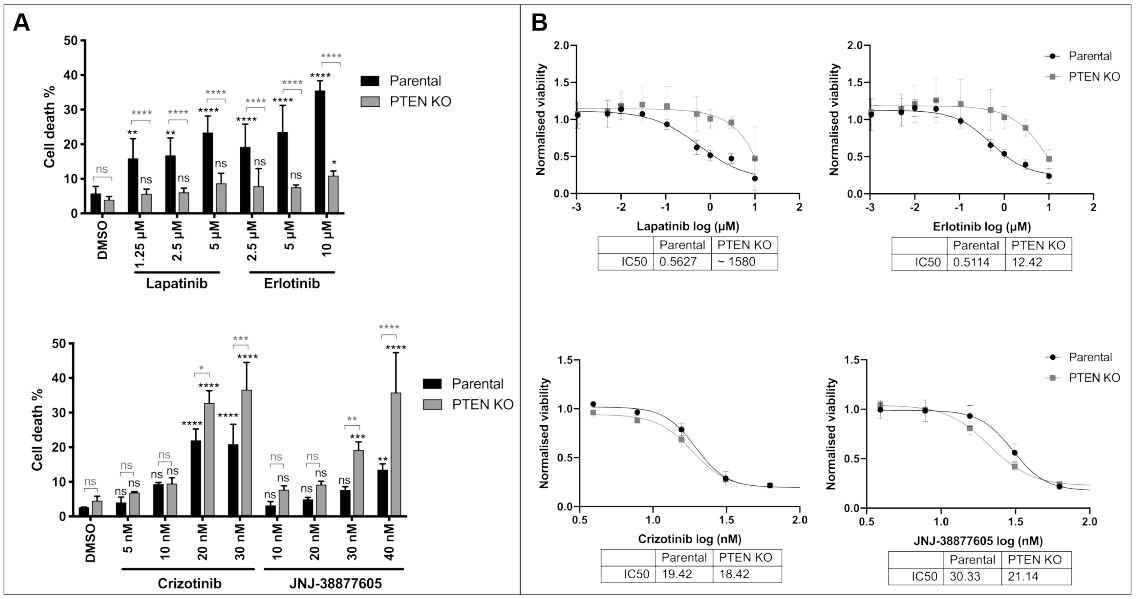

Figure 3.2 PTEN loss differentially affects inhibitor cell responses in EGFR and MET amplified cell lines

(A, B) Analysis of the responses of GTL16 parental and PTEN KO (clone 11) and A431 (clone 4) and PTEN KO (clone 3) to 72 h treatment with EGFR (Lapatinib and Erlotinib) and MET (Crizotinib and JNJ38877605) inhibitors. Cell death percentages (mean ± SD) were assessed via automated trypan blue exclusion method (ViCell, **(A)**); cell viability was assessed via CellTiter-Glo Luminescent cell viability assay **(B)**. n=3. ns, not significant; * significant at $P<0.05$; ** significant at $P<0.01$; *** significant at $P<0.001$; **** significant at $P<0.0001$.

The TKI resistance phenotype observed in A431 PTEN KO cells was validated in a different A431 clonal line (clone 6) and its respective PTEN KO subclone (clone 2), as well as in an A431 PTEN knock down line generated with shRNA (Figure 3.3a and Supplementary Figure 2c). Additionally, A431 PTEN KO cells were resensitised to EGFR inhibition through PTEN reconstitution using a mPTEN cDNA (Figure 3.3b). An EGFR-amplified oesophageal cancer cell line, KYSE-30, also demonstrated resistance to an EGFR inhibitor following RNAi-mediated knockdown of PTEN, further confirming the EGFR-dependency of the phenotype (Figure 3.3c).

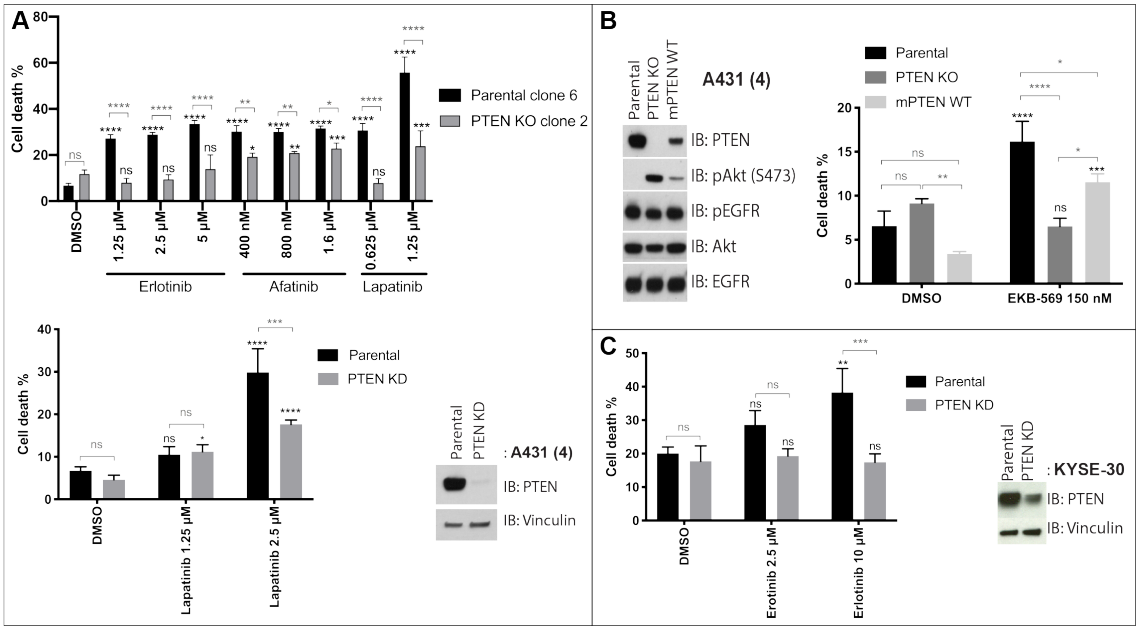

Figure 3.3 Validation of A431 PTEN KO TKI resistance phenotype

(A) Analysis of the responses of A431 (clone 6) and PTEN KO (clone 2) to 72 h treatment with EGFR (Afatinib, Erlotinib and Lapatinib) inhibitors (top). Analysis of the responses of A431 (clone 4) and the correspondent PTEN knockdown (KD) cell line to Lapatinib (bottom), along with western blots confirmation of PTEN KD (n=1). **(B)** Analysis of the responses to an EGFR inhibitor (EKB-569, 72 h) of the A431 (clone 4) PTEN KO (clone 3) reconstituted with murine (m) PTEN wild type (WT) protein along with western blot confirmation of mPTEN reconstitution (n=1). **(C)** Analysis of the responses of EGFR-amplified KYSE-30 cell line and its correspondent PTEN KD line to a 72 h treatment with an EGFR inhibitor (Erlotinib). Western blot n=1. Cell death percentages (mean ± SD) were assessed via automated trypan blue exclusion method (ViCell). ns, not significant; * significant at $P<0.05$; ** significant at $P<0.01$; *** significant at $P<0.001$; **** significant at $P<0.0001$.

To validate the MET TKI hypersentivity phenotype of the GTL16 PTEN KO model, a second PTEN KO clone (clone 6) (Figure 3.1b) was used to assess responses to MET inhibitors. GTL16 PTEN KO clone 6 also showed hypersenstisation to MET inhibitors (Figure 3.4a). Additionally, another MET-addicted cancer line model, EBC1, reproduced the hypersensitisation to MET TKI phenotype after PTEN inactivation via CRISPR/Cas9 technology (Figure 3.4b). Importantly, the hypersenstisation to MET inhibitors was rescued in GTL16 PTEN KO cells when reconstituted with a mPTEN construct (Figure 3.4c).

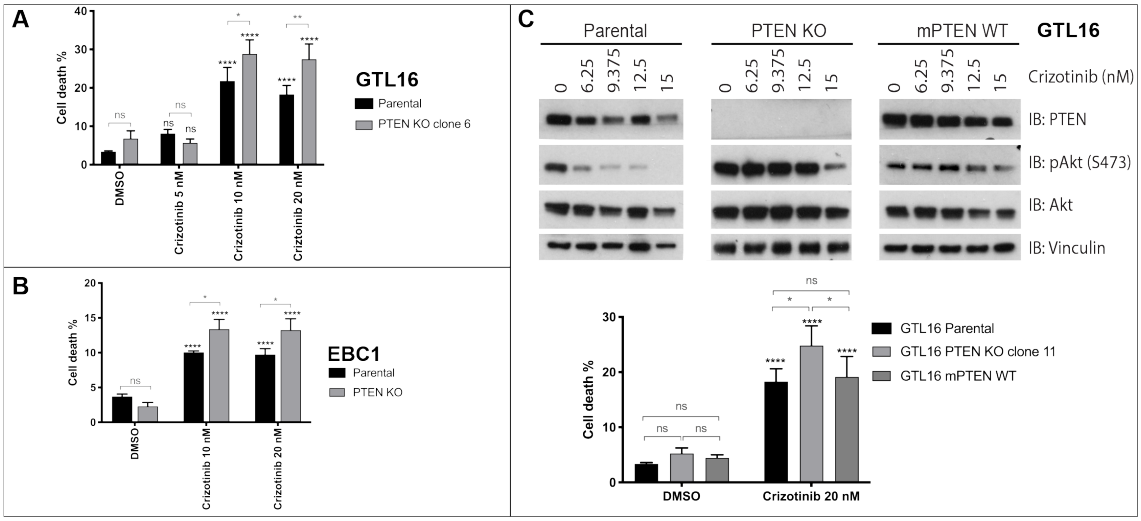

Figure 3.4 Validation of GTL16 PTEN KO TKI hypersensitivity phenotype

(A) Analysis of the responses of GTL6 and GTL16 PTEN KO (clone 6) to 72 h treatment with a MET inhibitor (Crizotinib). **(B)** Analysis of the responses of EBC1 and EBC1 PTEN KO to 72 h treatment with a MET inhibitor (Crizotinib). **(C)** Analysis of the responses of GTL6 parental, GTL16 PTEN KO (clone 11) and GTL16 PTEN KO (clone 11) reconstituted with murine (m) PTEN wild type (WT) protein to an overnight (Western blot, n=1) and a 72 h (growth assay) treatment with the MET inhibitor Crizotinib. Cell death percentages (mean ± SD) were assessed via automated trypan blue exclusion method (ViCell). ns, not significant; * significant at $P<0.05$; ** significant at $P<0.01$; *** significant at $P<0.001$; **** significant at $P<0.0001$.

3.2.3 PTEN loss is associated with increased PI3K and MAPK pathway signalling

We then investigated the effects of PTEN loss on RTK downstream signalling, namely on the PI3K/Akt and MAPK pathways. Despite differences in cell survival triggered by the loss of PTEN, western blot analysis of A431 and GTL16 showed that in both cases, PTEN inactivation was associated with increased TKI-resistant signalling through PI3K, as evidenced by higher phosphorylation (p) of Akt (pAkt S473) (Figure 3.5 a and b).

Nonetheless, while EGFR TKIs failed to inhibit Akt phosphorylation in A431 PTEN KO cells, MET TKIs in GTL16 PTEN KO cells retained the ability to inhibit pAkt (Figure 3.5 a and b). Interestingly, the phosphorylation levels of the MAPK pathway marker, Erk1/2 (pErk1/2), were also basally increased in both PTEN KO lines (Figure 3.5a and b). EGFR inhibitors had an effect on the MAPK pathway, as demonstrated by the reduction in pErk1/2 levels, however, they were unable to completely suppress pErk1/2 signal in the A431 PTEN KO line (Figure 3.5a).

The TKIs also caused a reduction in overall phosphorylation levels of both MET and EGFR in the PTEN KO lines (Figure 3.5a), however, both receptors retained growth factor-induced phosphorylation (Figure 3.5b).

Interestingly, EGF-induced EGFR phosphorylation in A431 cells did not show a time-dependent increase, similar to pGab and pErk (Figure 3.5b). Perhaps EGFR in this specific cell line reaches a maximum threshold of activation as early as 5 minutes after stimulation. However, more data is needed to clarify this hypothesis.

MET phosphorylation was similarly regulated by HGF in both GTL16 parental and PTEN KO lines. However, with the exception of Tyr1349, none of the MET phosphorylation sites investigated (i.e. Tyr1003, Tyr1234/5) showed a clear time-dependent increase (Figure 3.5b). It is unclear why we were unable to detect HGF-induced MET phosphorylation when looking at tyrosine residues within the activation loop or the kinase domain. We can hypothesise that either in GTL16 MET phosphorylation on Tyr1234/5 is close to its maximum levels, perhaps due to high basal levels of receptor *trans*-autophosphorylation in these cells, or that MET activation in GTL16 cells is insensitive to HGF stimulation. Additionally, GTL16 cells may have very high levels of MET, which could hinder the detection of small changes in phosphorylation levels.

Interestingly, pAkt signal failed to show a growth factor-induced increase in either PTEN KO lines (Figure 3.5b). The phosphorylation levels of Erk1/2 (pErk1/2) also failed to respond to growth factor stimulation in the GTL16 PTEN KO cells (Figure 3.5b), but not in A431 PTEN KO cells (Figure 3.5b).

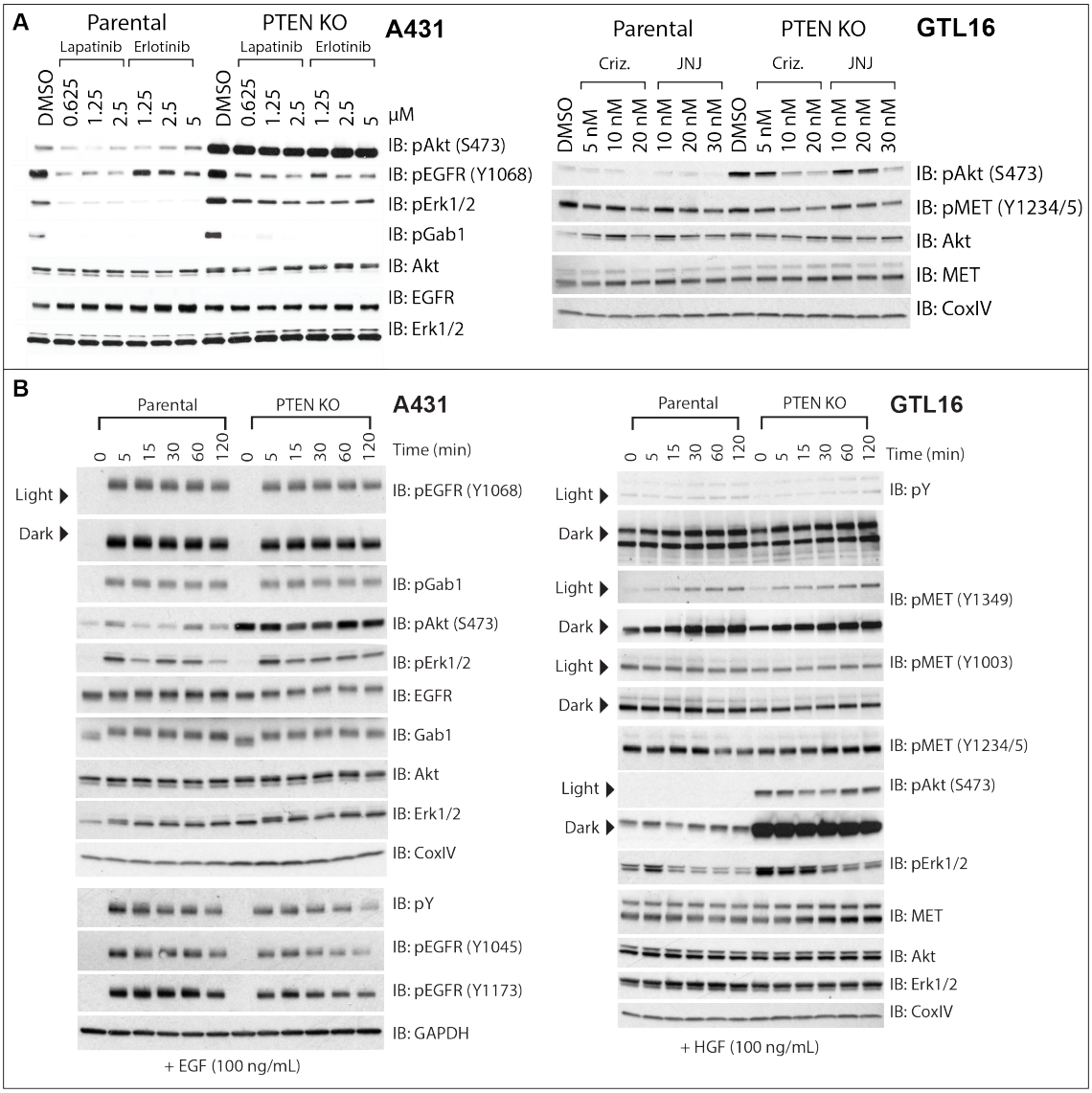

Figure 3.5 PTEN loss causes upregulation of the PI3K/Akt pathway (A) Western blot analysis of A431 (left) and GTL16 (right) responses to 3 h treatment with EGFR (Lapatinib and Erlotinib) and MET (Crizotinib – Criz and JNJ38877605 - JNJ) inhibitors. **(B)** Western blot analysis of A431 responses to EGF (left) and GTL16 responses to HGF (right). Growth factors were used at a concentration of 100 ng/mL after a 4 h (A431) or overnight (GTL16) starvation period.

PTEN tumour suppressor function is thought to be primarily driven by its ability to antagonise PI3K signalling (Parsons, 2004). Indeed, increased phosphorylation of Akt (pAkt S473) was observed in both A431 and MET PTEN KO lines (Figure 3.5 a and b). We therefore hypothesised that pharmacological normalisation of PI3K function via PI3K inhibitor treatment would reverse the effects of PTEN loss on RTK inhibitor response. Interestingly, MET and EGFR addicted cell lines responded differently to combined RTK and PI3K inhibitor treatments, in the context of PTEN deficiency.

Treatment with the pan-class I PI3K inhibitor, GDC-0941, or with the isoform-selective PI3K-targeting compounds (AZD6482, BYL-719 and Idelalisib for PI3Kβ, PI3Kα, and PI3Kδ, respectively) in combination with an EGFR inhibitor (either Afatinib or Lapatinib) elicited increased cell death compared to the individual treatments in parental A431 cells (Figure 3.6a and b and Supplementary Figure 3a). However, the combination of EGFR and PI3K inhibitors failed to completely overcome the EGFR inhibitor resistance phenotype of the PTEN KO line (Figure 3.6a Supplementary Figure 3a). This was observed with all PI3K inhibitors tested (Figure 3.6b), and despite re-establishing PI3K/Akt pathway activation levels (as determined by pAkt levels) in PTEN KO cells similar to those in parental cells (Figure 3.6a).

In contrast, inhibition of PI3K activity alone or in combination with a MET inhibitor in GTL16 cells had little to no impact on cell death. Nonetheless, the combination of MET and PI3K inhibitors in the GTL16 PTEN KO line partially reversed the MET inhibitor hypersensitisation phenotype, flattening the difference in cell death between parental and PTEN KO cell lines (Figure 3.6a and Supplementary Figure 3b). This could suggest that in MET-addicted cells, PTEN loss promotes sensitisation through PI3K activation. PI3K activation may therefore be sufficient to increase the sensitivity of MET-addicted cells to a MET inhibitor. Consistent with this hypothesis, expression of a constitutively active PI3Kα variant (PIK3CA-H1047R) in GTL16 cells promoted sensitisation to Crizotinib (Figure 3.6c).

Because the Serine/Threonine kinase Akt is one of the most important PI3K effectors, it was interesting to test whether Akt inhibition would be sufficient to reverse MET inhibitor sensitisation in GTL16 PTEN KO cells. Indeed, the Akt inhibitor GDC-0068 caused a reversal in Crizotinib sensitisation (Figure 3.6d and Supplementary Figure 3c). On the other hand, a similar experiment carried out in A431 cells failed to fully overcome the EGFR inhibitor resistant phenotype of A431 PTEN KO cells, as expected (Figure 3.6d and Supplementary Figure 3c).

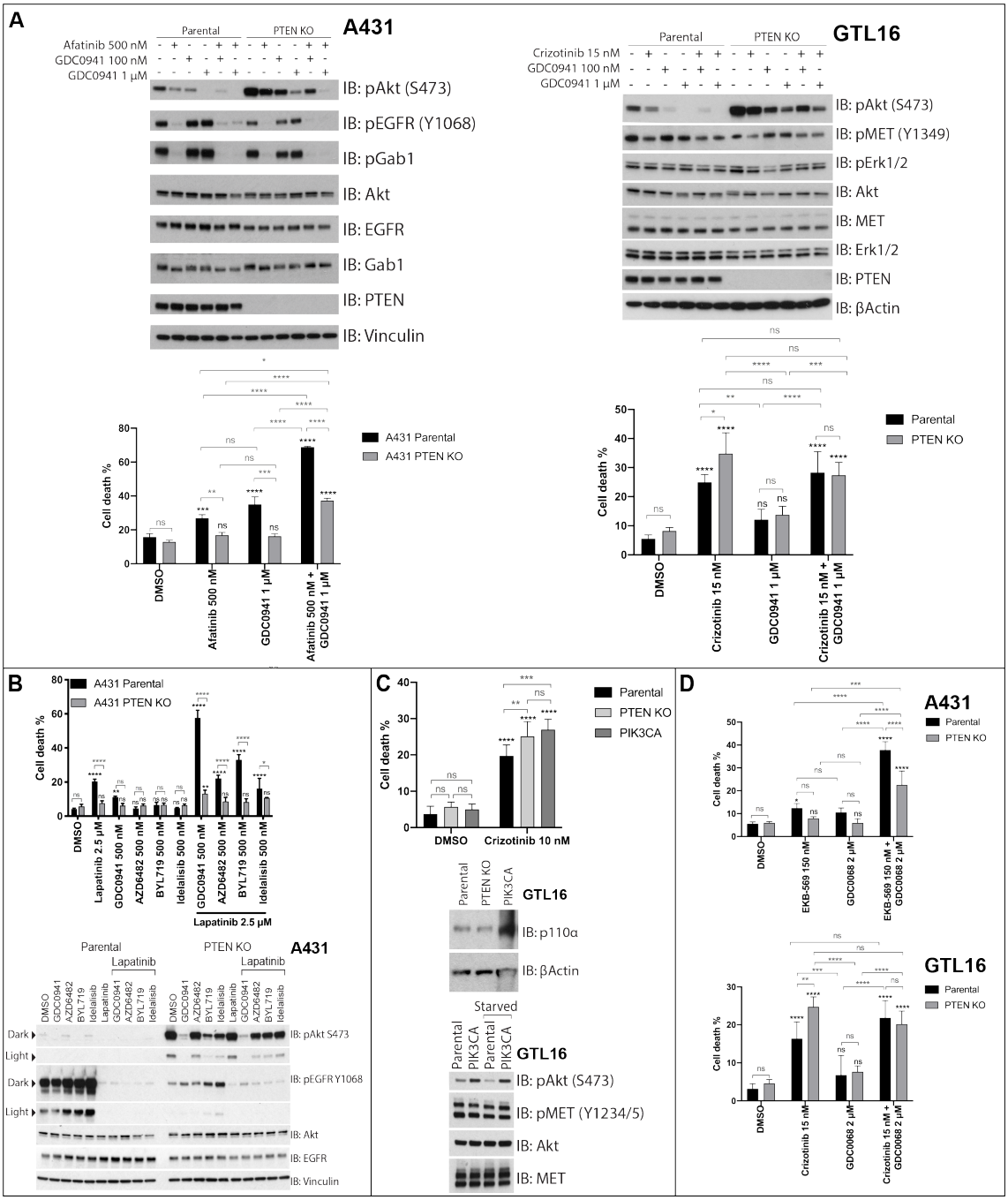

Figure 3.6 PI3K pathway inhibition differentially affects MET and EGFR inhibitor responses in the context of PTEN loss

(A) Analysis of the responses of A431 (left) and GTL16 (right) to 3 h (Western blots) or 72 h (growth assay) treatment with a PI3K class I inhibitor (GDC0941) alone or in combination with an EGFR (Afatinib) or MET (Crizotinib) inhibitor. For the western blots cells were pre-treated with GDC0941 for 24 h before treatment with TKI. n=3. **(B)** Analysis of the responses of A431 to 72 h (growth assay) or 3 h (western blot, n=1) treatment with an EGFR (Lapatinib, 2.5 µM) inhibitor alone or in combination with class-specific PI3K inhibitors (500 nM). **(C)** Western blot analysis (n=1) of PIK3CA overexpression in GTL16. Analysis of the responses of GTL16, GTL16 PTEN KO and GTL16 PIK3CA to 72 h treatment with Crizotinib. n=3 **(D)** Analysis of the responses of A431 (top) and GTL16 (bottom) to 72h treatment with EGFR (EKB-569) and MET (Crizotinib) inhibitors alone or in combination with an Akt inhibitor (GDC0068). Cell death

percentages (mean ± SD) were assessed via automated trypan blue exclusion method (ViCell). ns, not significant; * significant at *P*<0.05; ** significant at *P*<0.01; *** significant at *P*<0.001; **** significant at *P*<0.0001.

Given the molecular upregulation of the MAPK pathway (as determined by changes in pErk1/2 signal in western blots) (Figure 3.5), inhibitors of the MAPK pathway were also used to assess the involvement of this pathway in the response to TKI in the context of PTEN loss. Combination of the MEK inhibitor Trametinib and the EGFR inhibitor Erlotinib failed to overcome the EGFR inhibitor resistance phenotype of the A431 PTEN KO cells, which showed resistance to the treatment compared to parental A431 cells (Figure 3.7). Intriguingly, in the GTL16 model, PTEN loss appeared to increase sensitivity to single agent MEK inhibition and to the combination of Crizotinib and Trametinib (Figure 3.7). These results would suggest that MAPK pathway activation in the PTEN KO models does not directly contribute to the TKI-responses phenotypes observed in both A431 and GTL16 PTEN KO cells.

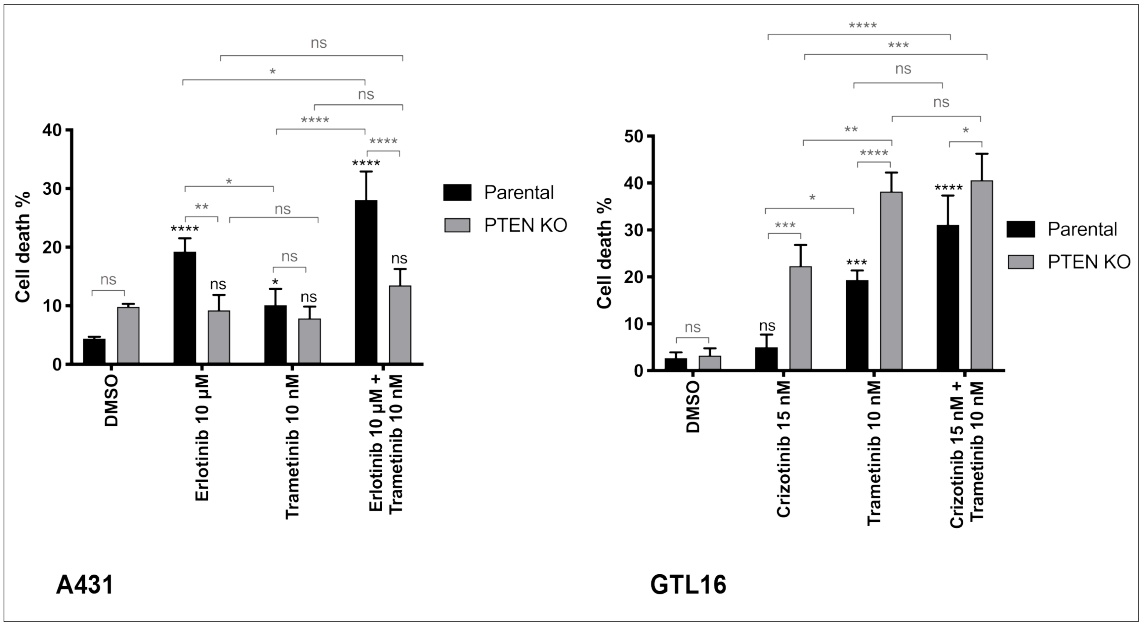

Figure 3.7 MAPK pathway inhibition differentially affects MET and EGFR inhibitor responses in the context of PTEN loss

Analysis of the responses of A431 (left) and GTL16 (right) to 72 h treatment with EGFR (Erlotinib) and MET (Crizotinib) inhibitors alone or in combination with a MEK inhibitor (Trametinib). Cell death percentages (mean ± SD) were assessed via automated trypan blue exclusion method (ViCell). ns, not significant; * significant at *P*<0.05; ** significant at *P*<0.01; *** significant at *P*<0.001; **** significant at *P*<0.0001.

3.3 Discussion

The data presented in this chapter characterise the differential effects of PTEN inactivation on RTK inhibitor responses, which appear to be dependent on the identity of the driver RTK. This is consistent with some early indication that RNAi-mediated knockdown of PTEN showed a trend towards sensitisation to a multi-kinase inhibitor with potent activity towards MET (Vivanco et al., 2010). Given the significance of PTEN allele dose in its tumour suppressive activity (Ali et al., 1999), these data are highly relevant to cancer biology, and have important translational implications for the development of therapeutic strategies that involve targeting of RTKs.

Given the importance of improving our current understanding of the true biological consequences of homozygous PTEN inactivation (Milella et al., 2015), the use of CRISPR/Cas9 technology was critical in developing appropriate PTEN knockout models (Figure 3.1b). One outstanding question, which was not covered during this project, was how heterozygous loss of PTEN or phosphatase inactivating mutations affect the response to EGFR or MET TKIs. Given the allelic-dose-dependent contribution of PTEN to tumour progression (Alimonti et al., 2010; Trotman et al., 2003), profiling the effects of different levels of PTEN inactivation on responses to RTK inhibitors would be a very interesting line of future investigation, and could add further translational value.

Having chosen to subject the cell lines of choice (i.e. A431 and GTL16) to single cell cloning both prior to and after PTEN KO (Figure 3.1), the potentially confounding effects of well-established genetic heterogeneity of cancer cell lines was minimised, thus increasing the robustness of our models.

However, single cell cloning can also increase the potential for clonal artefacts. To control for this, the relevant phenotypes were assessed in multiple clones and validated using RNAi-mediated knockdown (in A431) (Figure 3.3, Figure 3.4 and Supplementary Figure 2). The strongest evidence against potential clonal artefacts is the rescue of the observed phenotype with the reconstitution of a CRISPR-resistant form of PTEN in the same cell lines (Figure 3.3 and Figure 3.4). Ideally,

the phenotype would be replicated in a vast panel of cell lines, characterised by the same EGFR/MET dependency and PTEN loss, in order to rule out cell line-specific effects. This aspect was only partially covered by looking at the KYSE-30 (EGFR amplified) cell line, following RNAi-mediated PTEN KD (Figure 3.3) and EBC1 (MET amplified) cell line, following CRISPR/Cas9 mediated PTEN KO (Figure 3.4). The results continue to strengthen the evidence that PTEN loss drives resistance to EGFR inhibitors and hypersensitisation to MET TKI, according to the identity of the driver RTK.

Limiting the analysis to EGFR and MET is partially restricting the scope of the study which could benefit in the future from expanding the investigation to a panel of different RTKs. In fact, many additional PTEN KO models of cell lines with other driver RTKs (e.g. HER2 and PDGFR) have been generated (Supplementary Figure 4). Some preliminary data shows that the loss of PTEN in a HER2-addicted line (AU565) resembles the A431 model. The loss of the tumour suppressor triggers resistance to HER2 inhibitors, namely Lapatinib, Afatinib and Neratinib (Supplementary Figure 4). Future work will define the molecular details of PTEN loss in AU565 and its contributions in other cell lines will be further validated.

Nonetheless, the strong phenotype observed in GTL16 and A431 provides proof-of-concept evidence that PTEN can differentially affect TKI responses, and that it does so differently depending on the driver RTK.

The striking difference in responses to the inhibitors (Figure 3.2) prompted more questions regarding the signalling downstream of EGFR and MET, in the absence of PTEN.

As expected, loss of PTEN resulted in an increase of Akt phosphorylation, even in the absence of growth factor, in both A431 and GTL16 (Figure 3.5). Akt activation as a consequence of PTEN inactivation characterises the majority of GBM cases (Li et al., 1997) and has been observed in the case of some MET-dependent tumours (Xu et al., 2018). Despite the similarity in terms of PI3K/Akt pathway molecular upregulation (increase in pAkt, Figure 3.5), direct inhibition of the same pathway revealed an additional difference between MET and EGFR models.

Inhibition of the PI3K/Akt pathway in A431 PTEN KO failed to rescue the resistance phenotype, even when combined with an EGFR inhibitor, independently of the PI3K class targeted (Figure 3.6a and b). This would suggest that in the EGFR model, PTEN loss causes changes in signalling networks that appear to be independent of class I PI3Ks.

The combination of MET and PI3K/Akt inhibitors also failed to show synergy between the two drugs, instead showing an antagonistic behaviour in the PTEN KO line. This combination reversed MET-inhibitor sensitivity to the level observed in the GTL16 parental line (Figure 3.6a). In contrast to A431, this result would therefore suggest that the effect of PTEN loss in a MET-addicted setting is primarily dictated by activation of the PI3K/Akt pathway. Expressing a constitutively active version of PI3K in the GT16 parental line did reproduce the MET inhibitor response phenotype observed in the PTEN KO, strengthening the hypothesis of a PI3K/Akt pathway-dependent effect (Figure 3.6c). Inhibition of Akt, a major signalling effector downstream of PI3K activation, also reversed MET inhibitor sensitivity in PTEN KO GTL16 cells, while having no effect in the A431 model (Figure 3.6d).

Interestingly, an upregulation of the MAPK signalling pathway was also observed upon loss of PTEN in both models, with increased levels of Erk1/2 phosphorylation (Figure 3.5). While the link between PTEN and the PI3K/Akt pathway is well established, the connection with the MAPK pathway is ill defined. There is evidence from prostate cancer studies that PTEN reconstitution in PTEN null HER2 or EGFR overexpressing cells decreases the levels of Erk1/2 phosphorylation (Bouali et al., 2009; Chetram et al., 2011), while PTEN inactivation by reactive oxygen species (ROS) accumulation has the opposite effect (Chetram et al., 2011). Knockdown of PTEN resulted in upregulation of Erk1/2 phosphorylation also in HER-2 addicted breast cancer samples (Ebbesen et al., 2016). Additionally, increased phosphorylation of Erk1/2 has been reported in a MET-dependent PTEN KO hepatocellular carcinoma line (Xu et al., 2018).

Our data indicate that in GTL16 upregulation of Erk1/2 phosphorylation is a PTEN dependent effect (Figure 3.5). Additionally, this increase is associated with an increase in sensitivity to both a PI3K inhibitor alone (Figure 3.6a) and to a MEK

inhibitor either alone or in combination with a MET TKI (Figure 3.7). Our current data, is consistent with a model in which PTEN loss, perhaps through PI3K/Akt-dependent activation of Erk1/2, leads to an increased reliance on MET-driven survival signals. However, more data is needed to better understand the functional relationship between PI3K/Akt and MAPK in the context of MET dependence.

In A431 cells, upregulation of the MAPK pathway appears to be EGFR-dependent, given pErk1/2 induction upon EGF stimulation (Figure 3.5b). However, the increased phosphorylation detected in the PTEN KO cells, is only marginally responsive to EGFR inhibitors, which fail to fully suppress MAPK signalling and rescue the EGFR inhibitor resistant phenotype of the PTEN KO (Figure 3.7).

Together with the PI3K/Akt pathway data, the observations regarding the MAPK pathway suggest that the effect on EGFR inhibitor resistance, triggered by the loss of PTEN, cannot be simply explained by an upregulation of the canonical PI3K/Akt pathway, nor of the MAPK pathway; a non-canonical downstream effector of PI3K. An explanation to the resistance phenotype can therefore be sought upstream, by assessing the impact of PTEN loss on receptor physiology, or downstream, by identifying novel signalling pathways upregulated with the loss of PTEN.

Chapter 4. PTEN loss differentially affects the physiology of EGFR and MET

4.1 Introduction

4.1.1 RTK and membranes: two players in a dynamic system

RTKs are dynamic entities that constantly sample different conformations in a fluid membrane system (Kaplan et al., 2016). In order to generate a complete understanding of the complexity of RTK signalling two closely interlinked factors should be taken into consideration; a) the plasticity of RTK conformation changes and b) the molecular environment surrounding the receptors.

The dynamic nature of RTKs is evident in both their inactive and active states. In the absence of growth factors, receptors on the cell-surface continuously transition between multiple inactive conformations. This has been investigated for EGFR, but it is potentially relevant to all RTKs (Kaplan et al., 2016; Lemmon and Schlessinger, 2010; Shan et al., 2013). The plasticity of the extracellular domain and the flexible hinge that connects it to the TM domain would in fact support this model. According to this hypothesis, ligand binding triggers the active conformation by restricting the movement of the extracellular domain, locking the dimer in a low-entropy position (Kaplan et al., 2016) (Figure 4.1a).

Full receptor activation is achieved thanks to the movement and flexibility of some intracellular domains. In particular, the positioning of the DFG motif, along with the αC helix, contributes to the different active and inactive states (Roskoski, 2016) (Figure 4.1b). In a DFG-in conformation, commonly defined as “active”, the catalytic site is perfectly positioned for ATP binding and substrate phosphorylation. On the contrary, a DFG-out conformation marks the inactive kinase state. Between these two extreme positions of the DFG motif, there are other intermediate states that a receptor can sample (Figure 4.1b). For instance, RTKs can exist in a non-autoinhibited DFG-out conformation, which is overall inactive, but can still allow for ATP binding. Similarly, the DFG motif can be in an inward positioning, typical of an active RTK, but unable to efficiently bind ATP, due to the positioning of the αC helix

and of other amino acids surrounding the DFG motif (Modi and Dunbrack, 2018). Therefore, beyond the canonical active and inactive states, RTKs have shown to present a series of intermediate conformations, the signalling relevance of which is not entirely understood (Shan et al., 2013) (Figure 4.1).

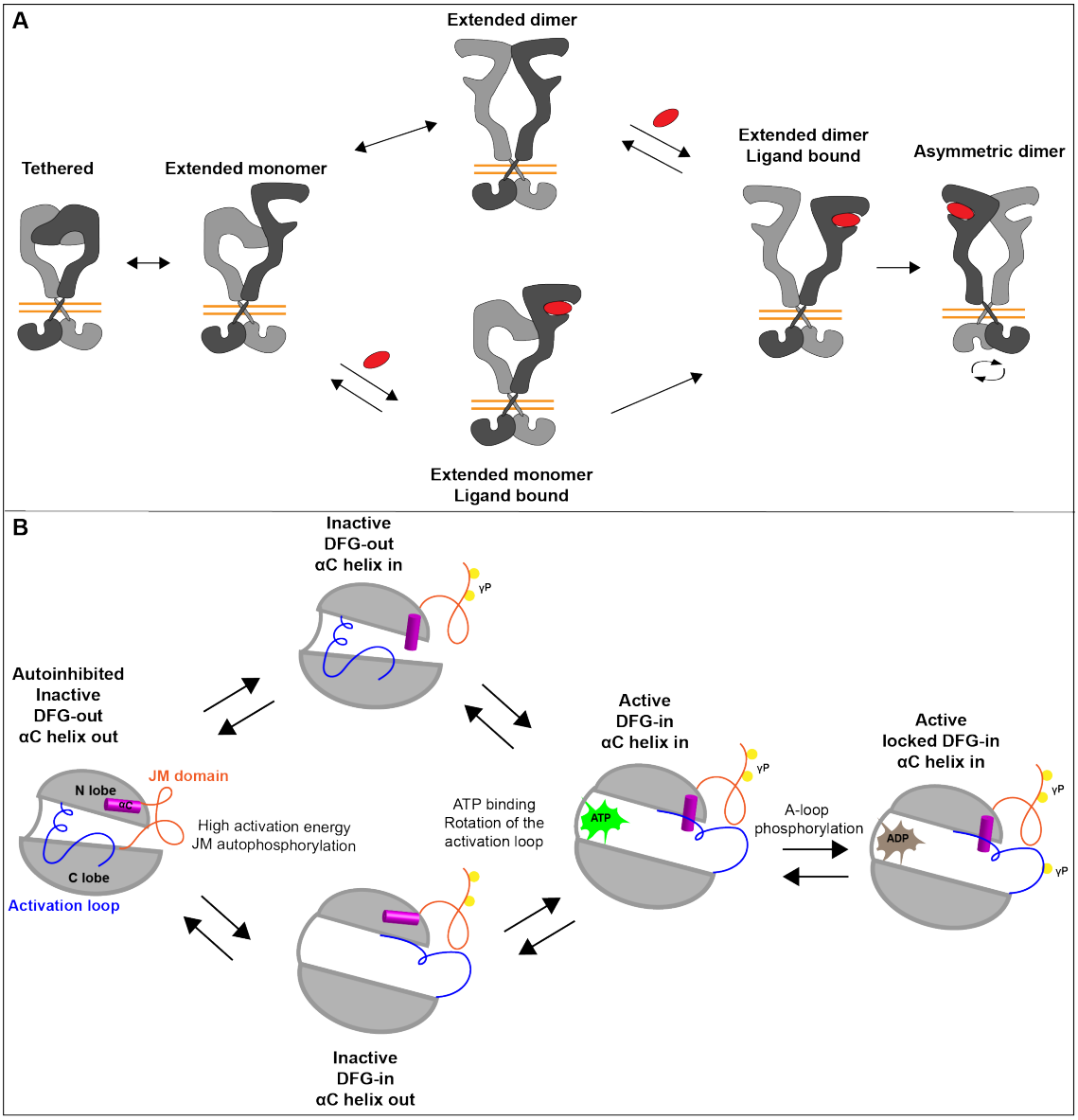

Figure 4.1 The model of RTK dynamic conformational sampling

(A) RTK extracellular domain can sample different conformations. It can be found in the classical inactive tethered conformation, or in different inactive states in which one or both monomers acquire more extended conformations. Ligands (red) preferentially bind to the extended form of RTK. Ligand binding stabilizes the extracellular conformation and prepares the dimer for activation. **(B)** The intracellular motif of RTK is also of a dynamic nature. Various inactive conformations have been studied based on the orientation of the DFG motif (within the activation loop, blue) along with the αC helix (magenta). The classical active conformation sees the ATP binding pocket exposed with the DFG motif and the αC helix oriented inwards. The JM (orange) domain inhibits the movement of the intracellular elements when interacting with the C-lobe in the autoinhibited conformation.

The model of dynamic conformational sampling also provides an explanation for ligand-independent dimerization and activation of receptors, commonly observed in RTK overexpressing cancers (Kaplan et al., 2016).

In addition to the intrinsically dynamic nature of RTKs, the environment that surrounds a receptor also deeply affects its activation and signalling. This dynamic environment is characterised by the plasma membrane (PM), the cytoskeleton and various cytosolic components (Bocharov et al., 2017). These elements can have a deep influence on RTK network dynamics.

Particularly relevant in modulating RTK-dependent signalling is the organisation of the PM in different domains. These domains are classified based on their composition, and serve to locally and dynamically increase the concentrations of biomolecules, creating local hubs for cellular activities (Eggeling et al., 2009). Among these domains, lipid rafts are enriched with cholesterol and sphingolipids, caveolae with cholesterol and glycolipids and cholesterol-low domains are characterised by the low abundance of the cholesterol molecule (Bag et al., 2015). Membrane domains are connected to intracellular cytoskeletal elements that help to further create zones of low membrane diffusion, in which biomolecules get trapped (Kusumi et al., 2011). RTKs are constantly interacting with these elements to modulate their signalling capabilities and interaction with substrates. For instance, there is extensive evidence supporting the role of membranes in mediating RTK dimerization. Membrane components contribute to this process by directly interacting with receptor's TM domains (Bocharov et al., 2008; Cymer and Schneider, 2010; Li and Hristova, 2010).

Particularly relevant in the context of PTEN loss is the phospholipid composition of membranes surrounding RTK, which has been shown to influence the signalling properties of transmembrane receptors (Sunshine and Iruela-Arispe, 2017). Both the TM and JM regions of RTK have been shown to interact with membrane lipids, such as phosphatidylserine (PS) and PIPs (Hedger et al., 2015; McLaughlin et al., 2005). For instance, it is known that in EGFR the JM helix closely interacts with the PM's lipids when the receptor is inactive, causing the helix to be buried in the membrane (Endres et al., 2013). To allow for receptor activation, the interaction

between membrane lipids and the JM helix needs to be broken via the rotation of the TM domain. At the same time, EGFR interaction with lipids after EGF binding is key to stabilize the dimer (Arkhipov et al., 2013; Endres et al., 2013).

Among all PIPs, the phospholipid PIP_2 has been shown to preferentially cluster around the JM regions of all 58 known RTKs. Given PIP_2 involvement in downstream signalling pathways, it has been proposed that these highly clustered structures may affect receptor signalling properties and, consequently, cellular functions (Hedger et al., 2015). It has been shown that PIP_2 directly facilitates the dimerization of EGFR JM domains (Maeda et al., 2018) and participates in receptor autophosphorylation and initiation of downstream signalling (Michailidis et al., 2011). There is also evidence that EGFR clustering and PIP_2 interaction contribute to the malignant phenotype of lung cancer. JM binding to PIP_2 is in fact associated with increased receptor clustering at the membrane. This has been shown to cause deregulated downstream signalling and to mediate EGFR inhibitor resistance (Wang et al., 2014).

The link between RTK activity and membranes is not limited to the PM, but it extends to include intracellular vesicles. The interaction of receptors with different intracellular lipid bilayers is dictated by increasing doses and length of growth factor stimulation (Bag et al., 2015). For instance, low-level EGF stimulation causes EGFR to undergo endocytosis and recycling to the PM. Increasing EGF doses instead cause receptor clustering and internalisation, with an overall increased diffusion of EGFR in the lipid bilayer (Sigismund et al., 2008). These receptor movements have all been shown to be dependent on membrane composition and cytoskeletal interactions (Bag et al., 2015).

Importantly, one of the lipids involved in receptor endocytic trafficking is PIP_2, which is enriched at endocytic sites and quickly removed for the completion of the process (Williams, 2007). PIP_3 has also been recently involved in endocytosis, as it is found in higher quantities at the site of short-lived CCPs. Loss of PTEN has been linked to an increase of these signalling-capable CCPs, which have also been proposed as mediators of the more aggressive phenotype of PTEN null cancers (Rosselli-Murai et al., 2018).

The latest evidence supporting the role of PIP_3 and PIP_2 in RTK trafficking and signalling therefore tightly links PTEN lipid phosphatase activity to these cellular events. Nonetheless, PTEN protein phosphatase activity has also been linked to RTK trafficking. PTEN in fact mediates the dephosphorylation of Rab7, a GTPase that contributes to the maturation of EGFR-positive early endosomes into late endosomal vesicles. Loss of PTEN could therefore promote deregulated EGFR signalling via disrupting receptor downregulation (Shinde and Maddika, 2016).

One aspect of PTEN contribution to RTK signalling that has not been extensively investigated is the possibility of its impact on RTK conformational shifts, and subsequent signalling capabilities, via the modulation of PIP_3/PIP_2 ratio. This line of investigation is particularly relevant considering TKIs are designed to inhibit specific receptor conformations, and, vice versa changes in RTK conformation could influence sensitivity to TKIs. The lipid composition of membranes is known to act as mediator of RTK conformational changes (Coskun et al., 2011), but it is unknown whether it significantly influences TKI responses and generates indirect alternative mechanisms of drug resistance.

4.1.2 Type I and II RTK inhibitors

TKIs are small molecule inhibitors and a type of targeted therapy against RTKs activity. They are particularly relevant for treating tumours with RTK addiction. TKIs have been classified based on their mode of binding to receptors; the vast majority of available TKIs are ATP-competitive compounds that directly compete with ATP for binding to the receptor's catalytic site. Type I inhibitors preferentially bind to the ATP pocket with a DFG-in conformation, when the kinase is in its fully active state. Type I½ inhibitors also bind to the DFG-in conformation, but when the RTK is inactive. Type II inhibitors instead occupy the ATP pocket when the DFG motif is in the "out" conformation, and they also contact sites outside the ATP pocket (Roskoski, 2016). There are two more classes of non-ATP-competitive compounds. Rare type III inhibitors bind away from the active site and act like allosteric inhibitors, while type IV inhibit RTK interaction with regulatory proteins (Modi and Dunbrack, 2018; Zhang et al., 2010).

In the case of MET, there is a further sub-classification for type I inhibitors, which are divided into type I A and I B. All type I MET inhibitors bind to the autoinhibited conformation of the receptor by contacting Tyr1230 in the activation loop. This interaction, however, is stronger in type I B inhibitors compared to type I A, and results in type I B inhibitors being more specific towards MET (Reungwetwattana et al., 2017).

TKIs are also classified as reversible or irreversible inhibitors based on their mode of binding to the ATP-binding pocket of the receptors.

Binding of an inhibitor to the receptor stabilises its active (type I) or inactive (type I½, type II) conformation, depending on the inhibitor class (Martin-Fernandez et al., 2019). Table 4.1 illustrates the classification of the inhibitors used in this study.

Drug	Target	Type	Binding
Erlotinib	EGFR	I	Reversible
Lapatinib	EGFR, HER2	I½	Reversible
Afatinib	ErbB family	I	Irreversible
Crizotinib	MET, ALK	I A	Reversible
JNJ-38877605	MET	I	Reversible
Cabozantinib	MET, VEGFR2	II	Reversible

Table 4.1 Classification of tyrosine kinase inhibitors

The table illustrates the classification of EGFR and MET inhibitors used in the study, based on type and generation.

Detailing the existence of the predominant conformation of the target RTK in a tumour sample can aid the strategic choice of the inhibitor to use. For instance, EGFR mutations in NSCLC destabilise EGFR autoinhibited conformation, causing the majority of receptors to live in an active conformation. In this case a type I inhibitor, such as Erlotinib, is the better treatment option (Ferguson, 2008).

It is unknown whether there is a predominant receptor conformation in cancers with wild type RTK overexpression, but it is a compelling hypothesis. Both MET and EGFR ability to dimerize and activate dependently and independently of ligand binding have been shown to change in cancer cell lines with RTK overexpression

(Chung, 2017). It would be interesting to document whether these changes are connected to a shift in receptor conformation. This could provide new explanations for TKI resistant phenotypes and aid with the choice of RTK targeted therapies.

4.2 Results

4.2.1 Modulation of RTK signalling by different classes of inhibitors is affected by the loss of PTEN

The upregulation of PI3K/Akt and MAPK signalling pathways upon loss of PTEN is insufficient to explain the EGFR inhibitor resistance phenotype observed in A431 PTEN KO cells (Chapter 3). As mentioned, an explanation for the resistance phenotype can be sought upstream, by assessing the impact of PTEN loss on receptor physiology. One possibility is that the deregulation of PIP_2/PIP_3 ratios caused by the loss of the tumour suppressor affects RTK conformational dynamics, thus providing a mechanism for EGFR-driven TKI resistance.

The study of receptor conformation relies on complex techniques such as X-ray crystallography, cryo-EM and NMR-spectroscopy (Martin-Fernandez et al., 2019). We hypothesised that type I, type I½ and type II inhibitors, along with the relevant growth factors, can be used as an indirect methodology to infer information about RTK conformational equilibrium. Based on this model, type I TKIs and binding of the growth factor to the target RTK can inform about the active conformation, while type I½ and type II inhibitors can probe for the inactive receptor conformation. We tested this method in A431 and GTL16 to derive evidence regarding the conformational equilibrium of the target RTKs, namely EGFR and MET, and test the hypothesis of the existence of a predominant receptor conformation in cancers with wild type RTK overexpression.

Both type I (Erlotinib) and I½ (Lapatinib) EGFR inhibitors caused a similar level of dose-dependent pEGFR reduction in A431 cells, in the absence of EGF. Based on this evidence, it therefore appears that EGFR lives in equilibrium between the active and inactive state. In the PTEN KO cells, under similar conditions, no dose-dependent pEGFR reduction was observed with the type I inhibitor, Erlotinib.

Lapatinib, on the other hand, was more efficient at reducing EGFR activation (as determined by the decreasing pEGFR levels) (Figure 4.2a). Therefore, loss of PTEN caused a sensitisation to type I½ inhibitors, suggesting that overall more of EGFR resides in an inactive state (Figure 4.2a).

Stimulation with EGF in the parental A431 line shifted the sensitivity to type I TKI, suggesting that EGFR preferentially resides in an active conformation in the presence of the growth factor, as expected. At low doses and under EGF stimulation, the type I inhibitor, Erlotinib, was also better than Lapatinib (type I½) at reducing pEGFR in the PTEN KO cells. Nonetheless, the effects of Erlotinib on EGFR phosphorylation seemed to reach a plateau at 0.5 μM, in contrast to Lapatinib, which exhibited a dose-dependent effect in the same dosage range (Figure 4.2a).

Overall the western blot data supports a model for which the loss of PTEN sensitizes cells to a type I½ inhibitor, such as Lapatinib. This hypothesis is strengthened by the anti-proliferative activity of high doses of Lapatinib in A431 PTEN KO cells, under low serum conditions (Figure 4.2b). Additionally, a natural cell line model for EGFR-addiction and PTEN-inactivation, MDA-MB-468, also showed a more pronounced decrease in EGFR phosphorylation when treated with a high dose of Lapatinib compared to Erlotinib, after an overnight starvation period (Figure 4.2c). These results are consistent with a role for PTEN in regulating EGFR conformational equilibrium.

An unexpected, yet relevant, observation that emerged from this experiment was the fact that PTEN inactivation reduced total EGFR levels. Additionally, the levels of total receptor were unaffected by TKI treatments. This prompted us to investigate RTK stability, which will be discussed in the next section.

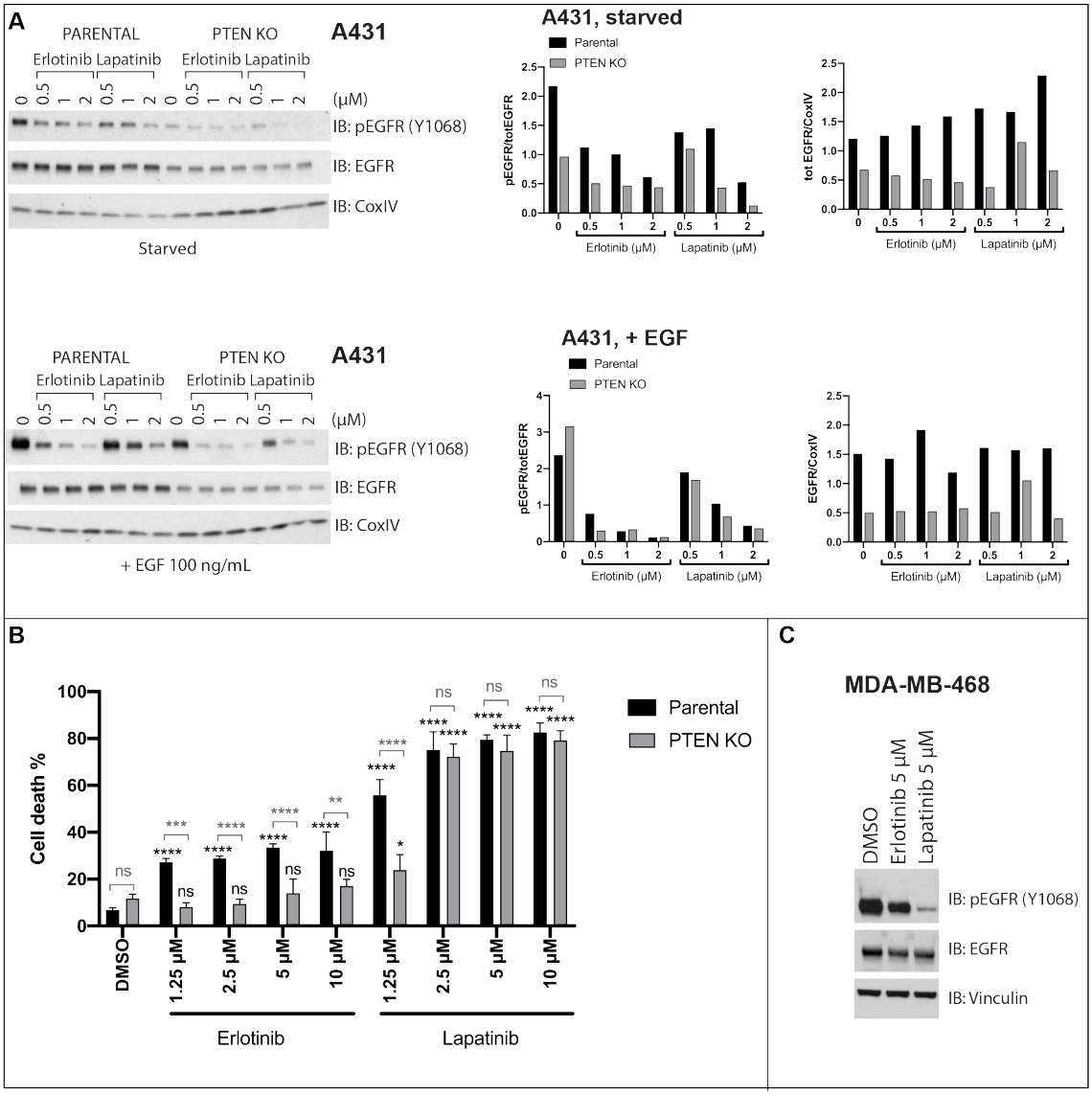

Figure 4.2 PTEN loss sensitizes EGFR to type II TKI

(A) Western blot analysis of A431 parental and A431 PTEN KO responses to 20 min treatment with a type I, Erlotinib, and a type I½, Lapatinib inhibitors. Cells were starved for 4 h and pre-stimulated for 5 min with EGF (100 ng/mL, bottom) or vehicle (top). Western blot quantification by ImageJ (right) of phosphorylated EGFR (pEGFR) values normalised against total EGFR (EGFR) levels, and of total EGFR levels normalised against the loading control. **(B)** Analysis of the responses of A431 and PTEN KO to 72 h treatment in reduced serum conditions (2.5 % FBS) with type I EGFR inhibitor, Erlotinib, and type I½ EGFR inhibitor, Lapatinib. Cell death percentages (mean ± SD) were assessed via automated trypan blue exclusion method (ViCell). n=3. ns, not significant; * significant at $P<0.05$; ** significant at $P<0.01$; *** significant at $P<0.001$; **** significant at $P<0.0001$. **(C)** Western blot analysis (n=1) of MDA-MB-468 cells starved overnight and treated with 5 μM of a type I, Erlotinib, and a type I½, Lapatinib inhibitor.

In order to confirm the effects of PTEN inactivation on pEGFR levels, non-transformed mouse embryonic fibroblasts (MEFs) with a floxed allele of PTEN were used. These cells were engineered to overexpress EGFR (Parental) and, through expression of a Cre recombinase, to lose PTEN (PTEN KO) (Figure 4.3). A

complete loss of PTEN in this model also resulted in lower pEGFR basal levels. Similarly to Figure 4.2a PTEN-inactivation accelerated EGFR dephosphorylation dynamics in the presence of increasing doses of Lapatinib. However, no changes in total receptor levels were identified (Figure 4.3), unlike the previous observation that PTEN KO in A431 reduces total EGFR levels (Figure 4.2a).

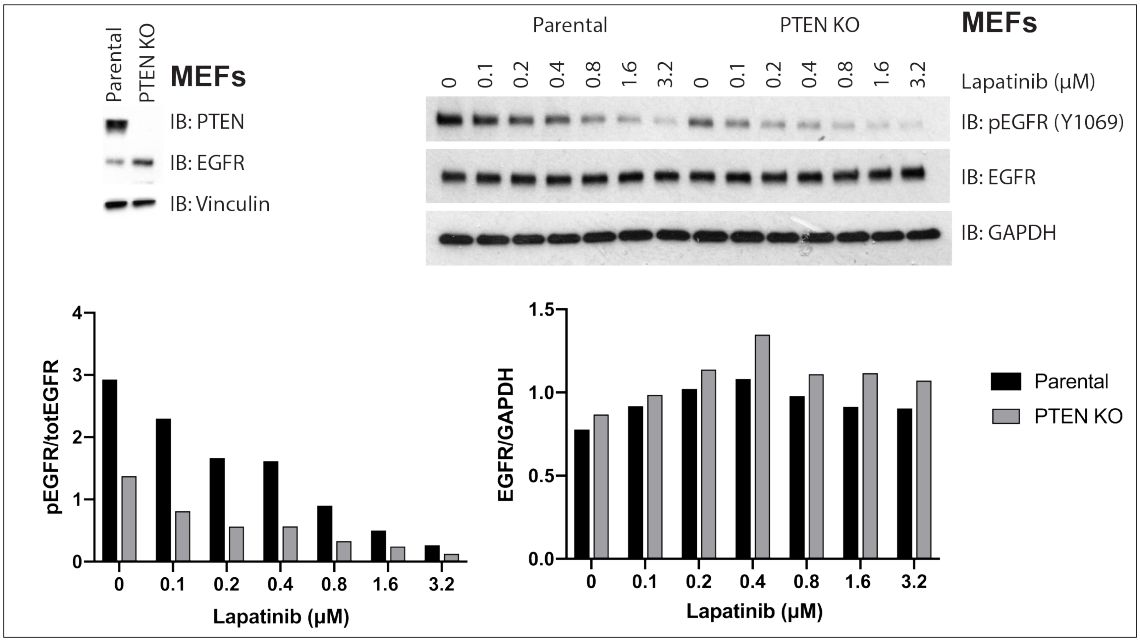

Figure 4.3 PTEN loss affects EGFR phosphorylation levels in MEFs

Western blot analysis of the responses of mouse embryonic fiibroblasts (MEFs) to Lapatinib treatment (right). The parental MEF line overexpresses EGFR, and the PTEN KO line was derived by expression of Cre recombinase (left, n=1). Western blot quantification by ImageJ of phosphorylated EGFR (pEGFR) values normalised against total EGFR (totEGFR) and of total EGFR levels normalised against the loading control.

With the same rationale, we investigated the conformational equilibrium and TKI sensitivity of the MET receptor in the GTL16 cell lines.

In the absence of HGF, the type I MET inhibitor, Crizotinib, was more efficient than the type II inhibitor, Cabozantinib, at suppressing MET activation (as determined by pMET levels). This effect was documented in both the parental and the isogenic PTEN KO cell line, suggesting that under these conditions MET is preferentially found in an active conformation. The addition of HGF caused the parental line to become slightly more resistant to Crizotinib inhibition, and strongly resistant to Cabozantinib treatment (as determined by pMET levels). The loss of PTEN, on the

other hand, did not influence the dose-dependent effect of either types of TKI (Figure 4.4a).

The data supports a model for which, in the context of MET wild type amplification, MET receptor is predominantly found in an active conformation, independently of growth factor stimulation. The loss of PTEN, however, re-establishes the equilibrium between active and inactive receptor, as determined by the sensitivity to both Crizotinib and Cabozantinib (Figure 4.4a). This could also cause what seemed to be a re-sensitization to HGF stimulation in GTL16 PTEN KO cells (based on pMET levels in Figure 4.4a). This hypothesis would support the increased anti-proliferative effects that both drugs, Crizotinib (Figure 3.2) and Cabozantinib (Figure 4.4b), had in the PTEN KO cells compared to the parental line.

Unlike A431, total RTK levels in GTL16 remained unaffected by the loss of PTEN. Nonetheless, similar to the EGFR model, TKIs did not cause a reduction in total MET levels.

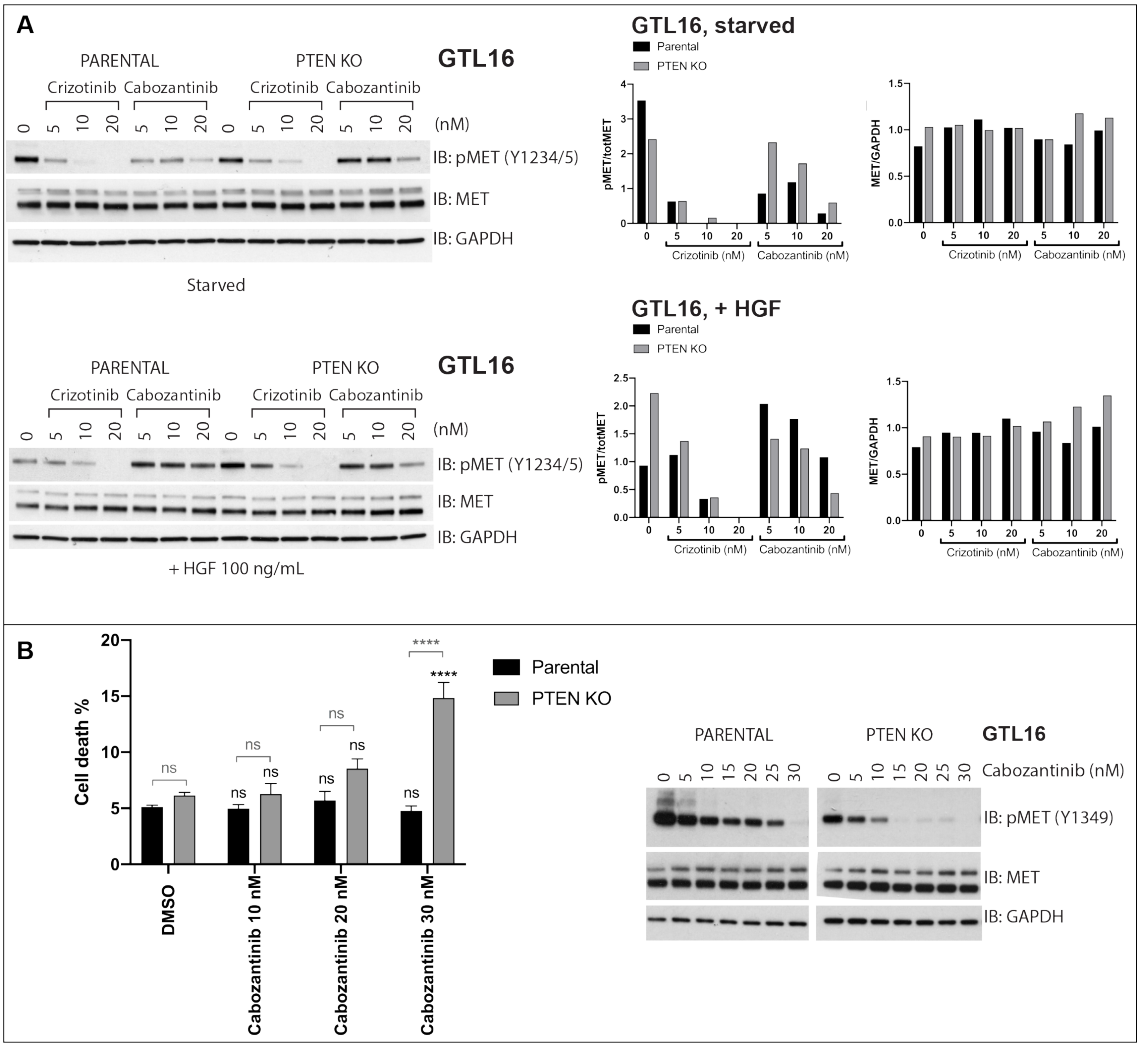

Figure 4.4 PTEN loss re-sensitizes MET to HGF stimulation and TKI inhibition

(A) Western blot analysis of GTL16 parental and GTL16 PTEN KO responses to 20 min treatment with a type I, Crizotinib, and a type II, Cabozantinib inhibitors. Cells were starved for 4 h and pre-stimulated for 5 min with HGF (100 ng/mL, bottom) or vehicle (top). Western blot quantification by ImageJ (right) of phosphorylated MET (pMET) values normalised against total MET (MET) levels and of total MET levels normalised against the loading control. **(B)** Analysis of the responses of GTL16 parental and PTEN KO to 3 h (western blot) or 72 h (growth assay) treatment with MET inhibitor Cabozantinib. Cell death percentages (mean ± SD) were assessed via automated trypan blue exclusion method (ViCell). ns, not significant; * significant at $P<0.05$; ** significant at $P<0.01$; *** significant at $P<0.001$; **** significant at $P<0.0001$.

The data presented so far propose a role for PTEN in regulating TKI responses by directly influencing RTK conformational equilibrium. Interestingly, the effects of the loss of the tumour suppressor differ between A431 and GTL16 cells. This would suggest that the nature of the RTK is key in determining the phenotype of an otherwise identical genetic loss.

4.2.2 PTEN loss does not affect receptor degradation

As previously mentioned, an important observation that emerged from the analysis of the western blots in Figure 4.2 and Figure 4.4 was the lack of a significant reduction of total EGFR and total MET levels upon TKI treatment. This prompted the question of RTK stability that was investigated by the use of cycloheximide, a protein synthesis inhibitor.

In A431 parental cells a mild reduction in total EGFR levels was detected after 8 hours of combined growth factor and cycloheximide treatment. Total EGFR levels in the PTEN KO cells, although overall lower compared to the parental line, remained unchanged (Figure 4.5a). Phosphorylation of EGFR on Tyr1045 instead increased with the treatment in a time dependent manner, and reached a plateau at 6 hours, independently of PTEN status. However, PTEN inactivation caused the levels of EGFR phosphorylation on Tyr1045 to be overall lower compared to the parental cell line. A perfect comparison of pEGFR levels within the isogenic pair was, however, hindered by the overall lower levels of total EGFR in the PTEN KO cells (Figure 4.5a). Nonetheless, phosphorylation on Tyr1045 is an important event as it allows for the interaction of EGFR with cCbl, an E3 ubiquitin ligase that is responsible for downregulating EGFR signalling. We hypothesised that the observed overall lower levels of Tyr1045 phosphorylation in A431 PTEN KO cells (Figure 4.5a) may result in lower EGFR-cCbl binding.

Interestingly, even after 8 hours of growth factor and cycloheximide-combined treatment, the levels of MET remained largely unchanged, independently of PTEN status (Figure 4.5b). In GTL16, no difference in pMET levels was detected across the treatment period in the parental cell line. In the PTEN KO cells, however, a clear shift of the pMET band was detected after 1 hour of combined HGF stimulation and cycloheximide treatment (Figure 4.5b). In line with some previous results (Figure 4.4a), this evidence supports a model for which the loss of PTEN in GTL16 may re-sensitize the MET receptor to HGF stimulation.

Finally, in both A431 and GTL16 cells, PTEN inactivation caused an increase in c-Myc levels. This is in line with previous evidence that PTEN acts as a negative

regulator of c-Myc (Ghosh et al., 1999; Kaur and Cole, 2013; Lee et al., 2019; Schubbert et al., 2014; Zheng et al., 2008). Cyclin D1 levels were also increased in PTEN KO GTL16 cells. This confirms that PTEN is a negative regulator of cyclin D1 in our model, as it has been previously shown to be the case in some glioblastoma cell lines (Radu et al., 2003).

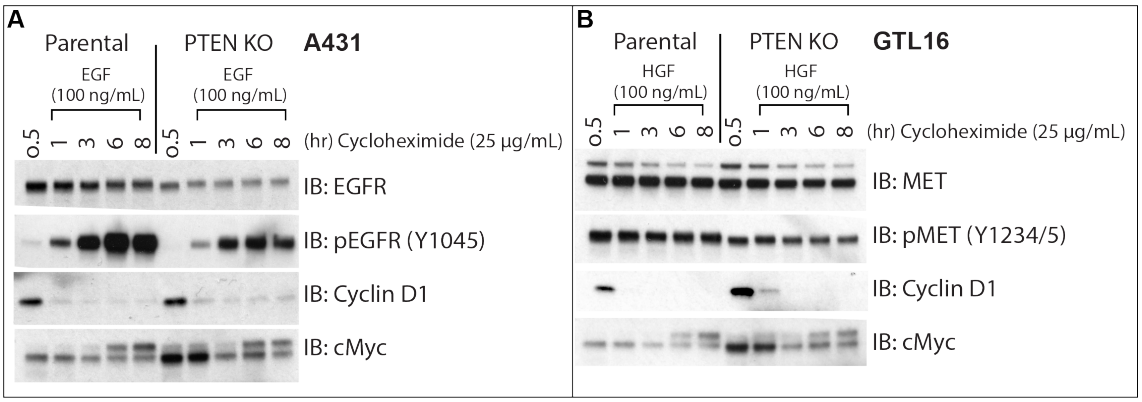

Figure 4.5 EGFR and MET protein stability in A431 and GTL16

(A, B) Western blot analysis of receptor turnover rates in A431 (A) and GTL16 (B) parental and PTEN KO lines. Cells were pre-treated with cycloheximide for 30 min prior stimulation with growth factor (EGF and HGF, 100 ng/mL).

Various interpretations could be derived from the cycloheximide experiment. Firstly, it could be hypothesised that both RTKs are extremely stable proteins and the time span chosen (8 hours) is not enough to see a significant decrease in total protein levels. Another explanation could also be that the overexpression of EGFR and MET characterising A431 and GTL16 hinders the detection of a reduction in RTK levels, at least by western blotting. However, big changes, as would be expected with the combined ligand stimulation, should still be detectable, unless A431 and GTL16 are less sensitive to ligand-induced degradation. This could happen because of RTK enhanced recycling or impaired lysosomal/proteosomal targeting. The lack of comparison with a non-RTK-overexpressing cell line leaves this subject open for further investigation.

The reduced phosphorylation of EGFR on Tyr1045 observed in A431 PTEN KO cells is in line with some previously published data. PTEN inactivation has in fact been shown to raise EGFR activity by impairing ligand-induced ubiquitylation and degradation of the activated receptor, through the destabilization of cCbl-EGFR complexes. This was shown to be linked to TKI resistance (Vivanco et al., 2010). Nonetheless, we have no evidence directly supporting this phenotype in our A431

isogenic model. Some preliminary data point towards a potential link between PTEN inactivation and cCbl activation in the GTL16 model (Supplementary Figure 5b, c and d). However, these data remain to be validated. Additionally, it is yet to be investigated whether alterations in receptor ubiquitylation are at all responsible for MET TKI responses.

4.2.3 PTEN loss affects RTK ability to bind ATP

Another aspect that can be exploited to probe for receptor conformation is RTK ability to bind ATP. Kinase enrichment assays can be used to assess ATP binding and indirectly infer information regarding a receptor's ATP binding pocket. During this assay, cell lysates are incubated with an ATP-desthiobiotin probe, which binds to the ATP binding pocket and selectively biotinylates lysines in the active kinase site. Biotinylated proteins are then captured in a Streptavidin column, analysed by SDS-PAGE and subsequently detected with target specific antibodies. Concurrent incubation of the samples with TKIs that compete for the ATP active site allows to determine the inhibitor binding affinity (Figure 4.6).

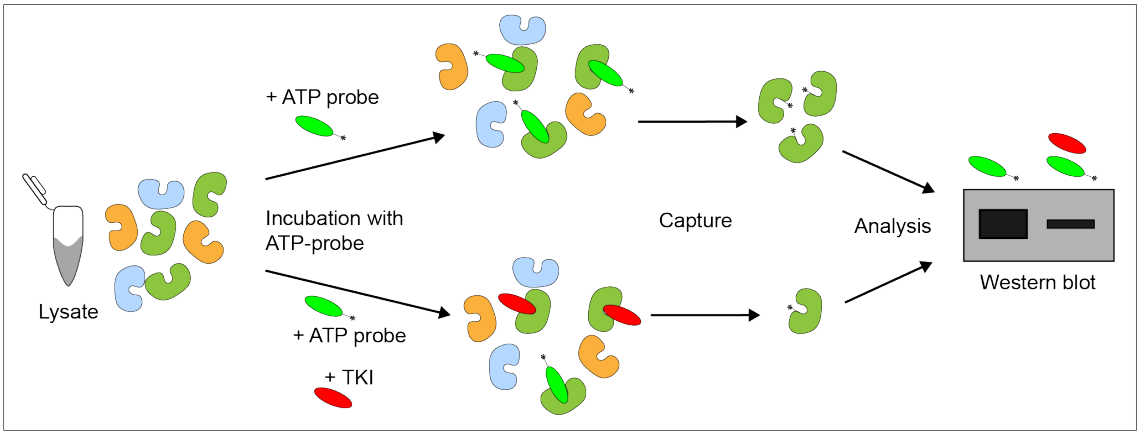

Figure 4.6 Kinase enrichment assay

Cell lysates are incubated with an ATP-desthiobiotin probe alone or in combination with a Tyrosine kinase inhibitor (TKI) against the kinase one wishes to study. Kinases that use the ATP will be biotinylated. This allows for their capture onto resins and further analysis. TKI compete with ATP for binding to the kinase and will reduce the amount of biotinylated protein.

A kinase enrichment assay was carried out in A431 and GTL16 to assess whether loss of PTEN in either cell line causes a change in the ability of the RTK to bind ATP, or in its interactions with TKIs.

In A431 cells, PTEN KO caused reduced RTK-ATP binding compared to the parental lines, while both GTL16 lines displayed a similar affinity for ATP (Figure 4.7a). Furthermore, in A431, ATP displacement with Erlotinib was more rapid in the PTEN KO cells compared to the parental line. However, beyond 8 μM of Erlotinib no dose-dependent effect was detectable (Figure 4.7b). This is suggestive of a PTEN-dependent change in accessibility to the receptor's ATP-binding pocket.

On the other hand, the loss of PTEN in GTL16 did not affect Crizotinib-mediated displacement of ATP. This argues against a dramatic change of MET ability to engage ATP and/or MET TKI upon loss of PTEN (Figure 4.7a and b).

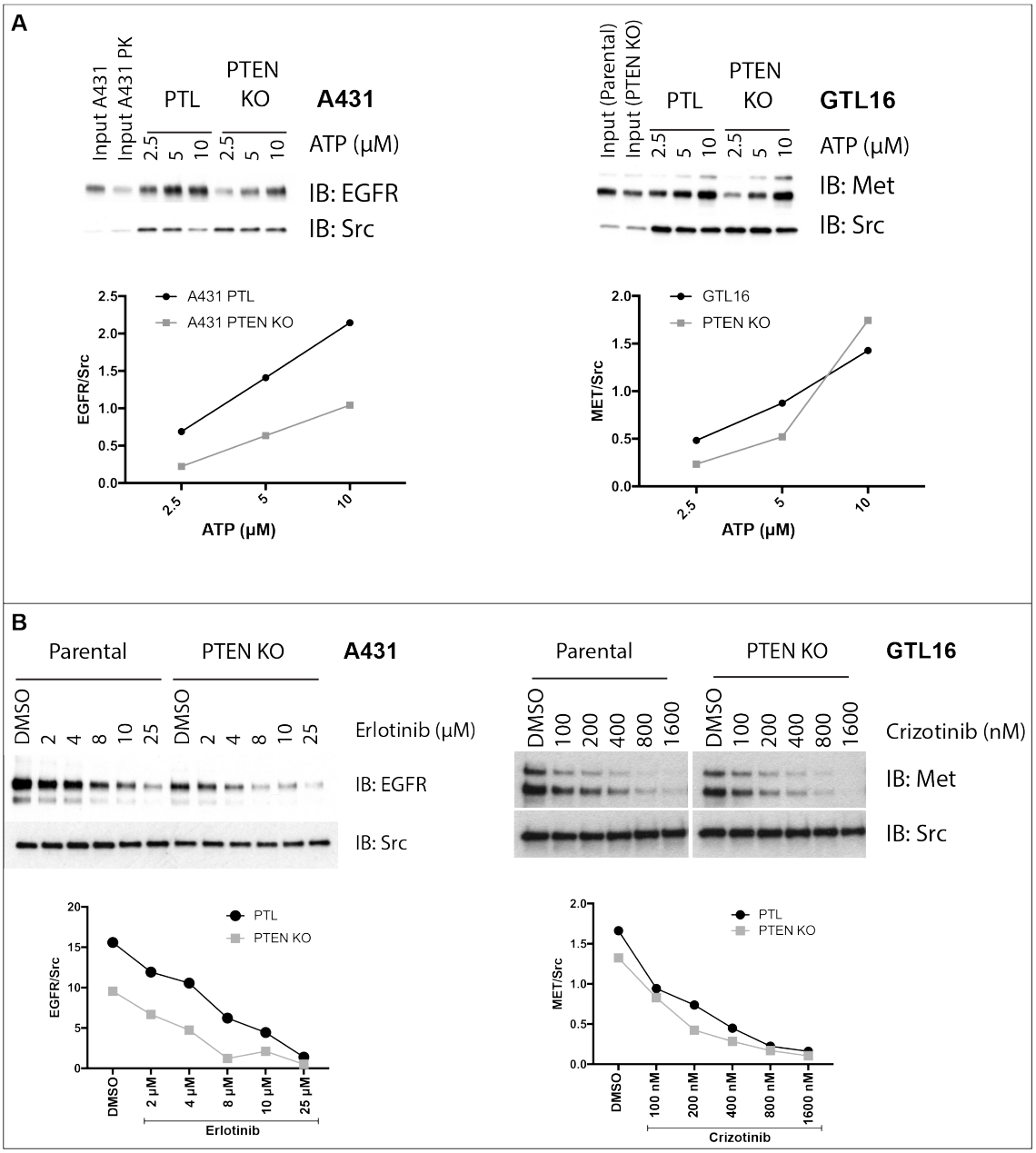

Figure 4.7 PTEN loss effects on RTK ability to bind ATP

(A) Western blot analysis (n=4) of a kinase enrichment assay looking at PTEN KO effects on ATP binding to EGFR (A431, left) and MET (GTL16, right). Western blot quantification via ImageJ of RTK (EGFR or MET) normalised against the loading control Src. **(B)** Western blot (n=3) analysis of a kinase enrichment assay looking at the displacement of 10 μM ATP from the EGFR (A431, left) and MET (GTL16, right) receptors with increasing doses of RTK inhibitors (Erlotinib, Crizotinib). Western blot quantification via ImageJ of RTK (EGFR or MET) normalised against the loading control Src.

4.2.4 PTEN loss affects the cell-surface distribution of RTKs

The data so far support a role for PTEN in modulating RTK conformational dynamics. However, an additional hypothesis is that the loss of the tumour

suppressor has an effect on localised RTK pools. This model could provide an explanation for some results that have emerged so far. For instance, the re-sensitisation of MET to HGF stimulation upon PTEN loss could be explained by changes in RTK localisation. Similarly, the relocation of RTK to intracellular compartments or a change in receptor trafficking could partially explain the MET and EGFR protein stability, as observed in the combined growth factor-cycloheximide experiment (Figure 4.5).

We decided to first assess the cell-surface-localised RTK pool, via cell-surface biotinylation. In this method, live cells are incubated with a cell-impermeable biotin solution. Cell-surface proteins are thus biotinylated and, after lysing, column purified. The cell-surface proteins can then be studied via SDS-PAGE and detected with target-specific antibodies (Figure 4.8).

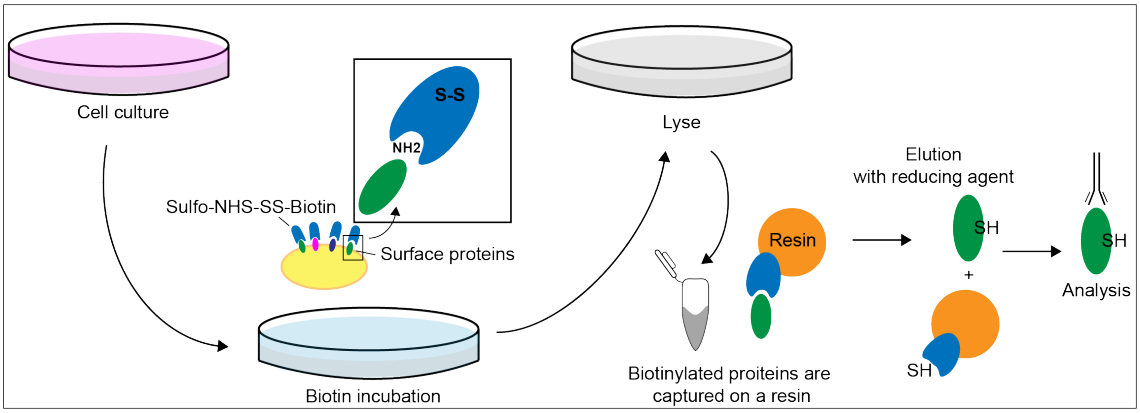

Figure 4.8 Biotinylation assay

Cells cultures are washed and incubated with a thiol-cleavable amine-reactive biotinylation reagent. Surface proteins are thus biotinylated at primary amino groups. After lysing biotinylated proteins are captured on a resin and eluted for further analysis.

Based on the cell-surface biotinylation assay carried out in the A431 model, we found cell-surface levels of EGFR to be similar between the parental and the PTEN KO cells. However, if taking into account the total EGFR content of the whole cell lysate (WCL) prior to pulldown, then we found that in the PTEN KO sample a greater proportion of the EGFR receptor was localised at the cell-surface compared to the parental cells (Figure 4.9a). Nonetheless, the levels of phosphorylation of the cell-surface receptor were overall lower in the PTEN KO cells compared to the parental line (Figure 4.9a). This observation was particularly evident in full serum, where the differences between the parental and the PTEN KO lines, as determined by pEGFR levels, were more pronounced (Figure 4.9a). Overall, the shift from

starved to full serum conditions triggered a more pronounced increase in pEGFR in the parental A431 line, compared to the PTEN KO cells (Figure 4.9a). This result would suggest that, the parental A431 cells are more sensitive to changes in the extracellular environment, which trigger EGFR to shift to an active conformation, providing that pEGFR is generally indicative of an active receptor.

Overall, we can conclude that upon loss of PTEN, a bigger proportion of EGFR is cell-surface localised. This pool is, however, less phosphorylated than in the parental cells, suggesting less of a shift towards the active receptor conformation. EGFR is in fact not particularly affected by changes in the extracellular environment, as provided by media supplemented with serum.

A similar analysis of the GTL16 model revealed quite a few differences compared to the A431 cell lines. First of all, the pool of cell-surface-localised MET was higher in the parental cells, compared to the PTEN KO line. Secondly, the PTEN KO, but not the parental cells, were sensitive to changes in the extracellular environment, as determined by a slight increase in total and phosphorylated MET levels in the full serum samples. Thirdly, the overall levels of cell-surface phosphorylated receptor did not change significantly between the parental and the PTEN KO lines, when the total MET levels (WCL) were taken into account (Figure 4.9b).

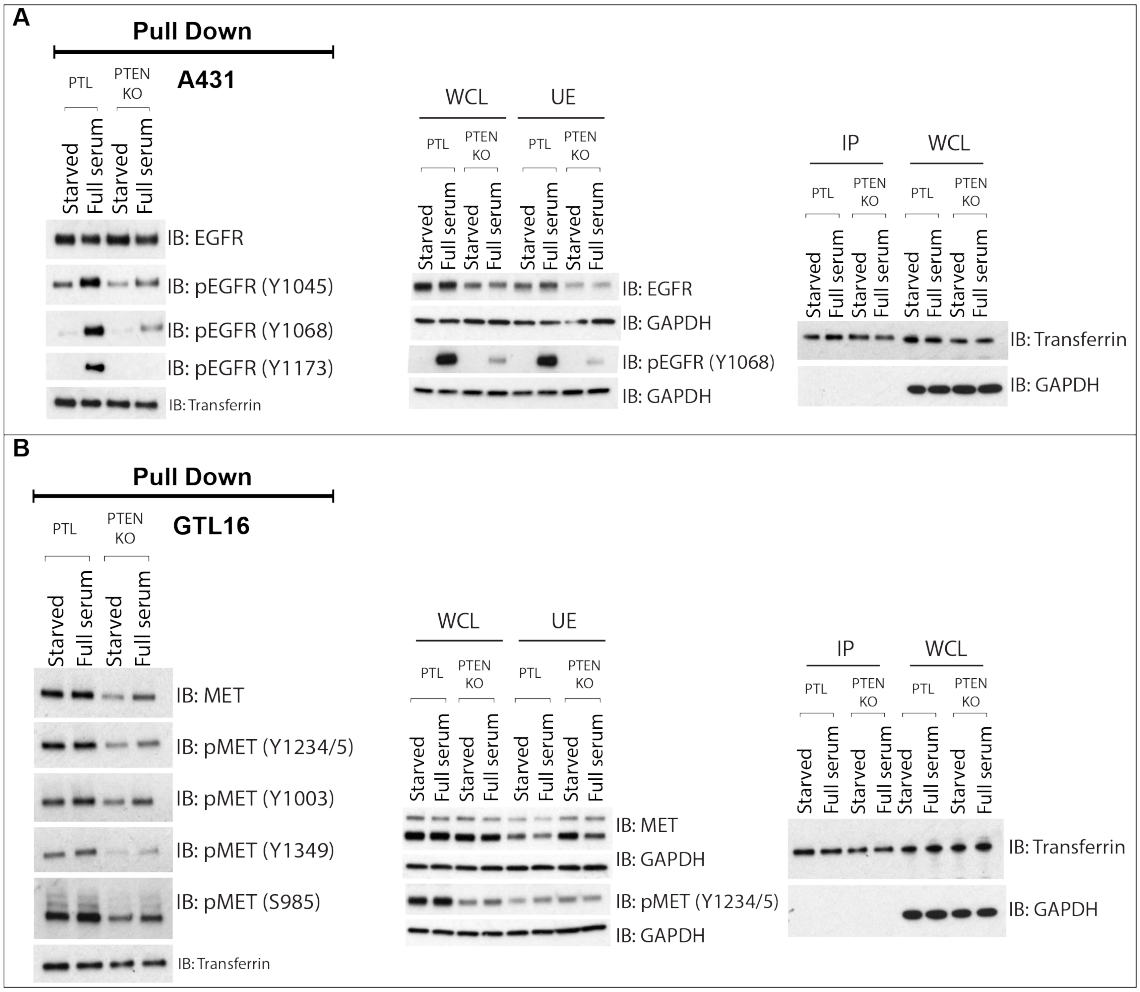

Figure 4.9 PTEN loss affects RTK cell-surface localisation

(A, B) Western blot analysis of cell-surface biotinylation assays. Cells were incubated with 10% FBS enriched media (full serum) or starved for 4 h (A, A431) or overnight (B, GTL16) prior to biotinylation (IP). Whole cell lysate (WCL) and unbound eluate (UE) are run as controls.

The data therefore depicted a different scenario for the A431 isogenic pair compared to the GTL16 model. Firstly, if EGFR responded to changes in the extracellular environment by shifting towards an active conformation, MET in GTL16 was mostly found in an active conformation, and only minimal increases in pMET levels were observed. Secondly, PTEN inactivation caused an increase in cell-surface-localised EGFR, while it resulted in a significant reduction of cell-surface-localised MET. Finally, following the loss of PTEN, the EGFR that was localised on the cell-surface was overall less phosphorylated and the shift towards an active conformation was minimal. Cell-surface total and phosphorylated MET levels instead increased with changes in the extracellular environment in PTEN KO cells compared to the parental, potentially indicating changes in receptor trafficking.

4.2.5 PTEN loss affects the intracellular localisation of RTKs

Granted differences in the cell-surface-localised RTK pool, we then sought to understand the intracellular distribution of the two RTKs via confocal imaging. To this end, co-localisation of the RTK of interest, namely EGFR and MET, with markers of early endosomes (EEA1) and lysosomes (Lysosome Associated Membrane Protein 1(LAMP1)) was used.

In A431 parental cells, EGFR co-localised with the early endocytic marker EEA1 prior to EGF stimulation and only mildly increased with the addition of the growth factor (Figure 4.10). A more drastic EGF-dependent EGFR-EEA1 co-localisation was observed in the PTEN KO A431 cells (Figure 4.10).

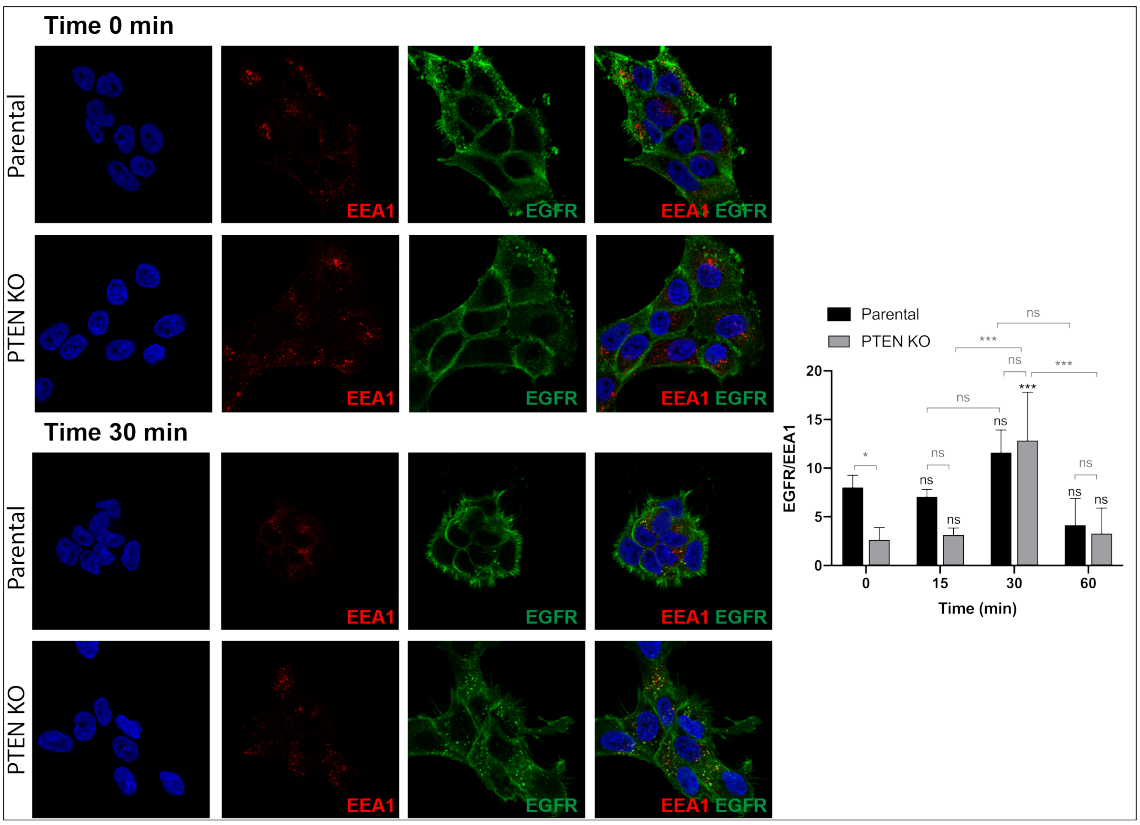

Figure 4.10 PTEN effects on EGFR-EEA1 co-localisation

Confocal microscopy of A431 parental and PTEN KO lines. Cells were starved overnight and treated with EGF (100 ng/mL) for 15, 30, 120 min and co-stained with anti-EGFR (green) or anti-EEA1 (red) antibodies. Images for time 0 and 30 min are shown. On the right, analysis of co-localisation (mean ± SD) of EGFR with EEA1. Average cells counted: 48. ns, not significant; * significant at $P<0.05$; ** significant at $P<0.01$; *** significant at $P<0.001$; **** significant at $P<0.0001$.

The lysosomal marker, LAMP1, also co-localised with EGFR in the A431 parental line in an EGF-independent fashion. In the PTEN KO cells, however, the EGFR-LAMP1 co-localisation pattern was lost (Figure 4.11). Interestingly, LAMP1 distribution throughout the cell also changed in the PTEN KO A431 line. The protein seemed to localise in circular structures, as opposed to exhibiting the more dispersed pattern observed in the parental A431 line (Figure 4.11).

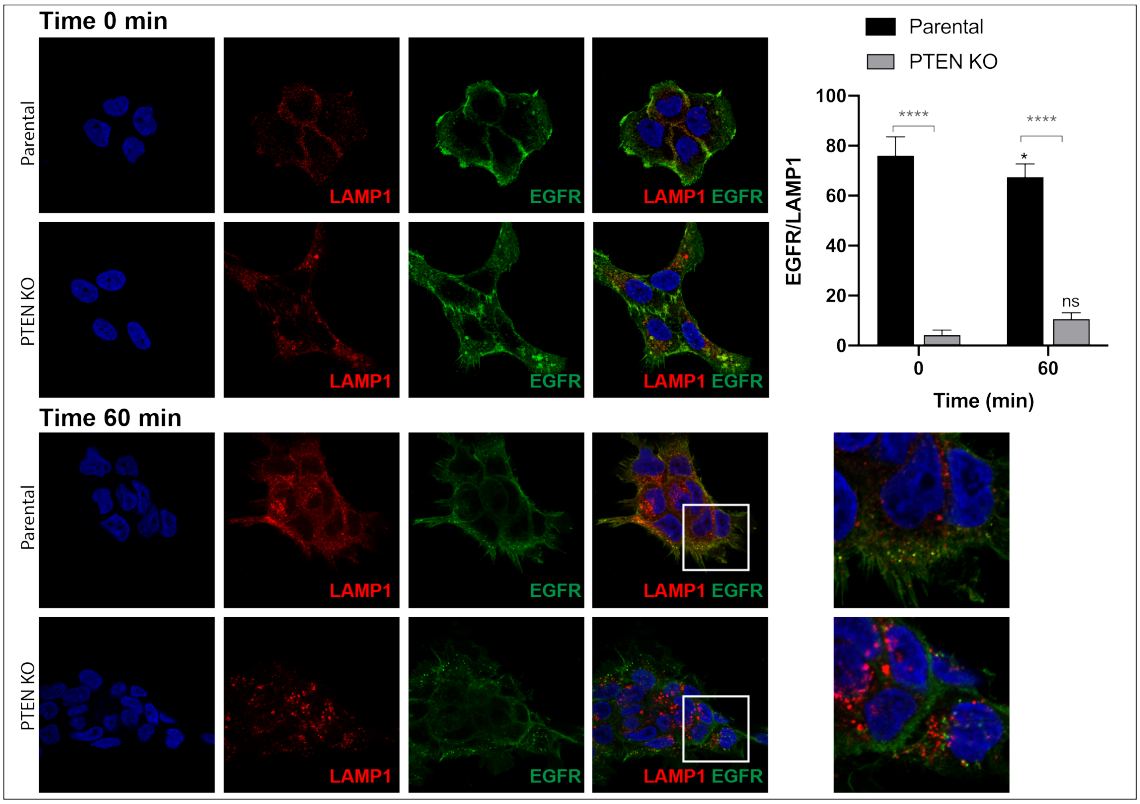

Figure 4.11 PTEN loss disrupts LAMP1 co-localisation

Confocal microscopy of A431 parental and PTEN KO lines. Cells were starved overnight and treated with EGF (100 ng/mL) for 15, 30, 120 min and co-stained with anti-EGFR (green) or anti-LAMP1 (red) antibodies. Images for time 0 and 60 min are shown. On the right, analysis of co-localisation (mean ± SD) of EGFR with LAMP1. Average cells counted: 58. ns, not significant; * significant at $P<0.05$; **** significant at $P<0.0001$.

The removal of PTEN in the A431 line therefore sensitized cells to EGF-induced EGFR-EEA1 co-localisation, and deregulated LAMP1 cellular localisation, and its co-localisation pattern with EGFR.

In both parental and PTEN KO GTL16 cells, we failed to detect a clear co-localisation of MET with EEA1 or LAMP1, at both early and late time points (Figure 4.12a). Nonetheless, a clear difference in MET intracellular distribution emerged from this analysis. In the GTL16 parental cells, MET was localised both at the cell-

surface, and in round intracellular structures (Figure 4.12 a and b). The nature of these intracellular structures is unknown, given the lack of co-localisation with the known endocytic markers EEA1 and LAMP1. Upon loss of PTEN, there was a marked reduction of MET-positive intracellular structures, and the majority of the receptor appeared to be localised at the cell-surface (Figure 4.12 a and c).

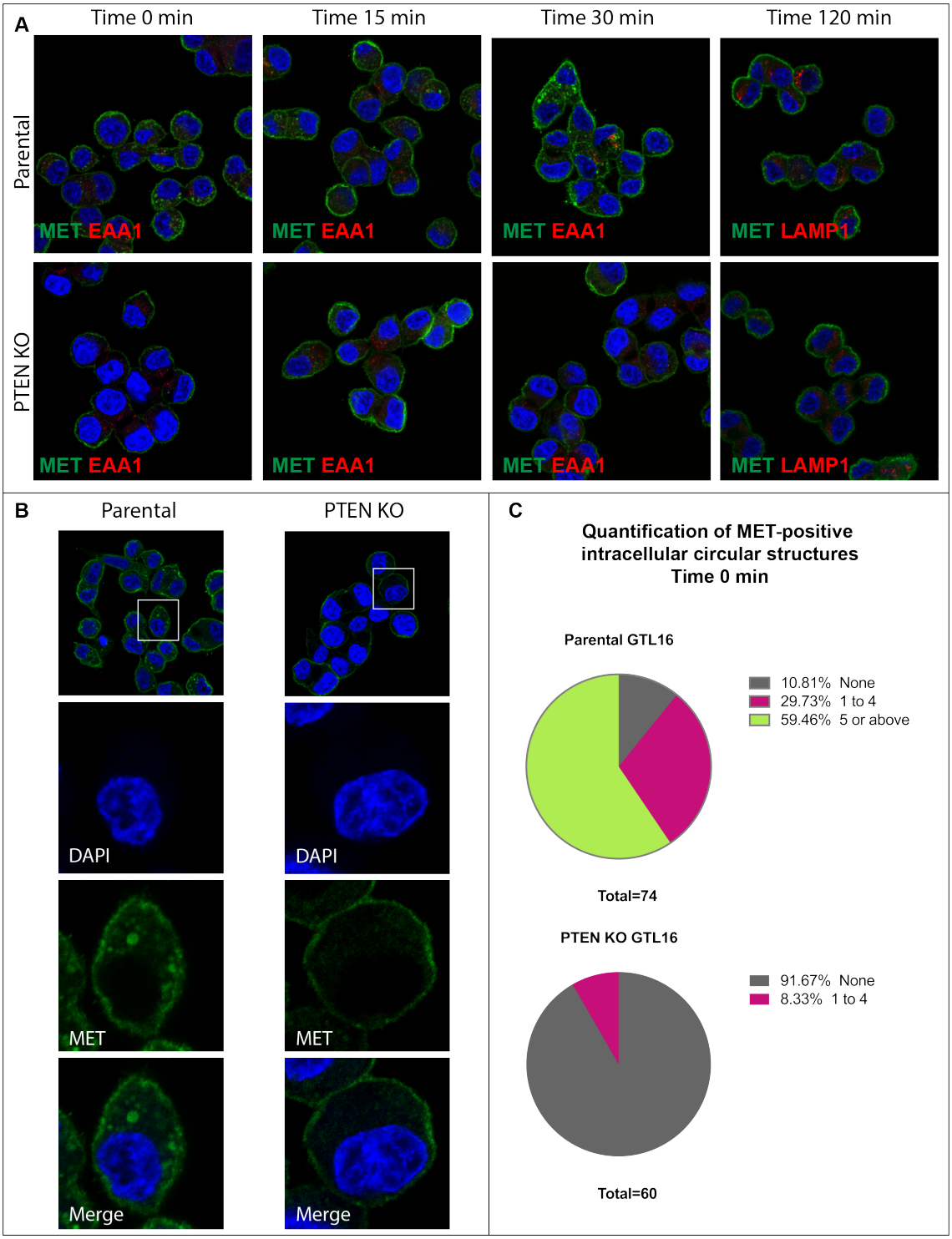

Figure 4.12 PTEN loss changes MET internal localisation

(A) Confocal microscopy of GTL16 parental and PTEN KO lines. Cells were starved overnight and treated with HGF (100 ng/mL) for 15, 30, 120 min and co-stained with anti-MET (green), anti-EEA1 (red) or anti-LAMP1 (red) antibodies. **(B)** Confocal microscopy of GTL16 parental and PTEN KO cells after overnight starvation. Cells were stained with anti-MET (green) antibodies. **(C)** Quantification of MET-positive intracellular structures in GTL16 parental and PTEN KO cell lines. A total of 74 (parental) and 60 (PTEN KO) cells were taken into consideration for the analysis.

Although the link between MET TKI responses and receptor localisation remains to be investigated, the marked differences in the intracellular MET localisation, along with those of the cell-surface-localised receptor, could provide an explanation for the hypersensitisation to MET TKI and ligand displayed by the PTEN KO cells.

4.3 Discussion

PTEN loss is known to affect the PIP_2/PIP_3 phospholipids ratio in cell membranes. PIP_2 and PIP_3 relevance in cellular signalling is well-established and their roles in receptor activation mechanisms are just starting to emerge. To the best of our knowledge, however, this is the first time that the loss of PTEN is linked to changes in RTK conformational equilibrium.

Unfortunately, the methodology available to us only allowed for the generation of indirect evidence of conformational changes of RTK. As such, there are drawbacks related to the use of different classes of TKIs as a tool to study RTK conformation. First of all, despite choosing all first generation drugs, the pharmacokinetics of the inhibitors were not taken into account in the study. Therefore, the doses chosen are comparable in terms of anti-proliferative effects, but may have different rate constants and drug-target binding characteristics. Additionally, receptors do not simply alternate between an inactive and an active state, but rather acquire a variety of conformations in between. This can affect TKI binding. For instance, it has been shown that a proportion of inactive RTKs do not bind to type II inhibitors, despite having a DFG-out conformation. Type I TKI binding to the DFG-in conformation is also often not as specific as expected, and these dugs have shown to bind to DFG-out states too (Vijayan et al., 2015).

Obtaining more direct evidence of RTK conformational changes is a challenging task. Cryogenic electron microscopy (cryoEM) is probably the only technique that would allow to do so by preserving the local RTK environment. Despite other complex techniques such as x-ray crystallography, magnetic resonance spectroscopy and transmission electron microscopy could allow the study of RTK conformation (Martin-Fernandez et al., 2019), they would all fail to capture the

dynamicity of RTK conformational change. At any given time, in fact, RTKs are expected to sample a mix of different conformations (Kaplan et al., 2016). In an attempt to minimise this variability, we used growth factors prior TKI treatments to push the RTK conformational equilibrium towards an active (growth factor stimulated) or inactive (starved cells) state. This solution allowed for a clearer detection of TKI effects on RTKs, without preventing their dynamic movements. Growth factor stimulation, in fact, did result in a higher sensitivity to type I inhibitors, as expected when RTKs are in an active, DFG-in, conformation (Figure 4.2 and Figure 4.4).

Differences between parental and PTEN KO lines also emerged. For instance, type I½ inhibitors worked better in the PTEN KO A431 cells, as determined by pEGFR levels. Interestingly, higher doses of Lapatinib (type I½) also rescued the TKI-resistant phenotype of A431 PTEN KO cells (Figure 4.2). It remains to be determined whether the Lapatinib effect observed is solely an EGFR-driven one. Lapatinib is in fact a dual EGFR, HER2 inhibitor (Medina and Goodin, 2008). Although A431 cells have only low levels of HER2 expression (Ma et al., 2014), HER2-mediated resistance to EGFR inhibitors has been shown to occur in cancer (Hirsch et al., 2009; Kong et al., 2008). We can't therefore exclude that Lapatinib-driven toxicity in A431 occurs via HER2 inhibition. However, lower doses of Lapatinib have molecular effects on EGFR directly, as demonstrated by pEGFR immunoblotting, and these are different between the parental and the PTEN KO cells (Figure 4.2). Additionally, our preliminary results in MDA-MB-468, a HER2-negative breast cancer cell line (Dai et al., 2017), would suggest that in the context of PTEN-inactivation Lapatinib is indeed more efficient at inhibiting EGFR activity (Figure 4.2). Reconstitution of PTEN in MDA-MB-468 cells (Supplementary Figure 5a) will help determine the PTEN-dependency of the phenotype.

Overall our results are proof-of-concept evidence that the loss of PTEN can affect EGFR conformational equilibrium. However, further experiments with additional inhibitors, including type II EGFR inhibitors, are necessary. At the same time, this model is supported by the kinase enrichment assay that shows how the ATP, and consequently the TKI, binding capacity of the receptor has also changed upon

PTEN loss (Figure 4.7a). We hypothesise that this effect is driven by PTEN lipid phosphatase activity, but this hypothesis still awaits validation.

The influence of PTEN on RTK conformational dynamics is likely to depend on the identity of the RTK. Major differences in sensitivity or binding to type I and II MET TKIs are in fact not present in the GTL16 model lines (Figure 4.4 and Figure 4.7b). However, the loss of PTEN, unlike in A431, seem to sensitize cells to growth factor stimulation (Figure 4.4 and Figure 4.5b).

We hypothesise that this re-sensitization phenotype is linked to a difference in MET cellular localisation, rather than in MET conformational shift. We indeed found cell-surface MET levels to decrease with PTEN inactivation and to change depending on the extracellular environment (i.e. increase in full serum, decrease with serum starvation), suggesting a change in MET trafficking. Unfortunately, we were unable to demonstrate this hypothesis by studying the co-localisation with known endocytic markers (EEA1 and LAMP1). Nonetheless, confocal analysis revealed a clear PTEN-dependent change of MET intracellular localisation (Figure 4.12). The nature of the MET-positive intracellular structures that disappear with the loss of PTEN remains to be determined.

We are currently hypothesising that the intracellular MET-positive structures are important endocytic hubs for MET signalling. Although RTK endocytosis is generally linked to receptor down regulation, it is also known that MET endocytosis and MET degradation constitute two separate processes (Li et al., 2007). For instance, the signalling that defines the migration phenotype observed in invasive breast cancers has been proposed to be driven by MET-positive perinuclear endosomes (Ménard et al., 2014).
The hypothesis that MET-positive intracellular structures are sites of alternative signalling mechanism, rather than part of the MET downregulation process (Miaczynska et al., 2004), is also supported by the lack of co-localisation with known endocytic markers (EEA1 and LAMP1, Figure 4.12).

The complete lack of co-localization of MET with endocytic markers is surprising, but could also be explained by the highly dynamic nature of the endocytic

trafficking vesicles. However, little is known about the dynamics of MET endocytosis in cellular models with MET overexpression, such as GTL16, and other cell lines with similar MET expression levels should be used for comparison.

Although the nature of the MET-positive intracellular structures remains unknown, they are clearly PTEN dependent. Our current hypothesis is that changes in these structures contribute to the MET TKI hypersensitivity phenotype of the PTEN KO cells. Going forward we would like to test the contribution of the lipid phosphatase activity of PTEN to the phenotype, in order to investigate the role of PIP_2/PIP_3 phospholipids.

We found that both the cell-surface and intracellular localisation of EGFR was affected by PTEN, although differently compared to the MET receptor.
In A431, EGFR is localised at the cell-surface, in EEA1-positive and LAMP1-positive endocytic vesicles (Figure 4.10 and Figure 4.11). The loss of PTEN increases receptor localisation at the cell-surface (Figure 4.9) and reduces receptor localisation at the intracellular sites (Figure 4.10 and Figure 4.11), and only co-localisation with EEA1, is rescued by EGF stimulation. We hypothesise that PTEN has an important role in EGFR-positive endocytic vesicles trafficking. The dramatic effect of PTEN loss on LAMP1 distribution is supportive of a role for PTEN in the endocytic trafficking (Figure 4.11).

The link between PTEN and endocytic vesicles remains to be investigated in our model system. While the protein phosphatase activity of PTEN has previously been linked to the maturation of EGFR-positive endocytic vesicles (Shinde and Maddika, 2016), the role of the lipid phosphatase activity of PTEN in RTK trafficking is unclear. An increase in PIP_3 levels is, however, known to positively correlate with signalling-capable short-lived CCPs and cancer aggressiveness (Rosselli-Murai et al., 2018). The high levels of PIP_3 that follow the loss of PTEN could therefore cause increased levels of CCPs-resident EGFR molecules and explain the decrease of surface EGFR that we observe in A431 PTEN KO cells. Unfortunately, we were unable to test this hypothesis and quantify differences in cell-surface versus internalised EGFR, due to the lack of a cell-surface staining in our immunofluorescence samples.

A role for PTEN lipid phosphatase activity in EGFR trafficking could also find an explanation for the dramatic changes of LAMP1 co-localisation observed with the loss of PTEN. PIP_2 has in fact been shown to reside in LAMP1-positive compartments and play a critical role for their fusion with lysosomes (Li et al., 2013). It is, however, unclear if the changes in LAMP1 co-localisation pattern observed upon the loss of PTEN play a role in the TKI resistant phenotype displayed by A431 PTEN KO cells.

One hypothesis is that loss of PTEN causes the disruption of EGFR late endocytic events, as determined by the loss of EGFR-LAMP1 co-localisation (Figure 4.11). EGFR downregulation would thus fail and cells would rely on sustained EGFR signalling to overcome TKI toxicity. PTEN, by virtue of its protein phosphatase activity, has indeed been shown to regulate late endosomal maturation of EGFR-positive vesicles (Shinde and Maddika, 2016)

Another possibility is that the co-localisation of LAMP1 with EGFR is a marker for PTEN-dependent signalling hubs, rather than late endocytic vesicles. LAMP1 localisation is, in fact, more widespread than what it is traditionally believed (Cheng et al., 2018). Despite it being enriched in late endosomes, LAMP1 presence has also been reported on plasma membranes and early endosomes (Cook et al., 2004). Determining the nature of LAMP1-positive structures is pivotal to understand the dynamics of EGFR trafficking, and additional markers, including a lysotracker, should be used in the future.

There may indeed be a role for receptor degradation in mediating EGFR inhibitor resistance phenotype when PTEN is lost (Vivanco et al., 2010). This is supported by the marked difference in Tyr1045 phosphorylation of EGFR within the A431 isogenic pair (Figure 4.5a). However, we detected no marked total EGFR or MET downregulation in the cycloheximide experiments (Figure 4.5).

We find that two main explanations could address for this apparent stability of both receptors. Firstly, A431 and GTL16 could be not as sensitive to growth factor stimulation, perhaps due to RTK enhanced recycling or impaired lysosomal/proteosomal targeting. This could reduce the extent of RTK

downregulation and lengthen the half-life of the protein. Secondly, the time-span chosen (8 hours) may not be enough to see a significant decrease in total protein levels. EGFR, for instance, has a turnover rate of 28 hours in A431 (Greig et al., 2015). By choosing to extend the treatment to a maximum of 8 hours, we probably failed to observe the relevant time point. However, less is known about EGFR turnover rates in the absence of PTEN. MDA-MB-468, a cell line that naturally harbours EGFR amplification and PTEN loss, when reconstituted with PTEN, has shown sustained levels of EGFR signalling, even with the addition of cycloheximide. Furthermore, PTEN knockdown in HeLa cells abolishes cycloheximide-driven reduction of receptor levels (Shinde and Maddika, 2016). Therefore, this particular method of assessing EGFR degradation is probably not well suited for RTK-overexpression models, and other methods, such as pulse chase experiments, should be used in the future.

It therefore remains to confirm the relevance of EGFR degradation in mediating TKI responses in our PTEN KO model, as well as to investigate whether alterations in MET degradation at all drive MET inhibitor toxicity in the context of PTEN inactivation. To this end, cCbl conditional KO lines for both GTL16 and A431 models have been generated, and will be used in the future to assess the relation between TKI responses and RTK degradation.

One aspect that remains unexplained, even when considering the differences in EGFR degradation and localisation following the PTEN KO, is the overall lower level of total and phosphorylated EGFR (Figure 4.2).

A potential explanation is that A431 PTEN KO cells have lost the dependency on EGFR as oncogenic driver. Some Gefitinib-resistant lung cancer lines with loss of PTEN show EGFR-independent activation of Akt (Kokubo et al., 2005). MDA-MB-468 cells have also shown sustained EGFR-inhibitor resistant Akt signalling. This would suggests that the loss of PTEN can result in RTK-independent downstream signalling (Bianco et al., 2003). Unfortunately, there is not sufficient data to rule this hypothesis out in the A431 model, and, going forward, removing EGFR in the PTEN KO line may be necessary to establish their continued dependency on the RTK.

However, if A431 PTEN KO cells have retained their EGFR dependency, as we expect, the decrease in pEGFR we observe (Figure 4.2) could represent a mechanism of drug resistance. A decrease in levels of EGFR in the DFG-in conformation could theoretically result in a reduction of type I TKI binding, and consequently diminish EGFR inhibition by this specific class of TKIs. This model is supported by the kinase enrichment assay that shows decreased binding of EGFR to type I inhibitors (Figure 4.7).

How PTEN modulates the total and activated levels of EGFR is unclear. If EGFR half-life does not change as a function of PTEN, as suggested by our cycloheximide experiments (Figure 4.5), lower levels of total EGFR protein could be the result of changes in EGFR transcription levels. PTEN could, for example, indirectly modulate EGFR levels by controlling the activity of transcription factors involved in transcription of EGFR. Messenger RNA levels and rate of transcription should therefore be assessed to test this possibility. On the other hand, PTEN could also indirectly modulate EGFR activation by affecting the local abundance of PIP_2. PIP_2 has in fact been shown to contribute to receptor activation (Maeda et al., 2018; Michailidis et al., 2011). A local decrease in PIP_2 due to the loss of PTEN could therefore mediate EGFR activation.

Considering our model, it still unclear how EGFR can act as a strong oncogenic driver, despite modest levels of activation. A possible explanation is that a low but constant level of EGFR activity is sufficient to confer oncogenic potential. The existence of a natural EGFR mutant with such characteristics, EGFR variant III (vIII), supports this model. EGFRvIII lacks the extracellular domain and is insensitive to growth factor stimulation. Nonetheless, it has oncogenic potential by virtue of its low-level constitutive signalling, due to EGF-independent receptor dimerization and activation. EGFRvIII activation is also aided by decreased internalisation and downregulation (Huang et al., 1997; Hwang et al., 2011).

A second possibility, that does not exclude the first hypothesis, is that the EGFR receptor does not need to be active to have oncogenic potential. Ligand independent EGFR signalling has previously been shown, as well as the existence of EGFR kinase independent pro-survival functions in cancer cells (Guo et al.,

2015; Weihua et al., 2008). Additionally, EGFR autophosphorylation is not always required for mutant EGFR tumorigenic activity (Cho et al., 2018). It is not known whether, in the context of PTEN deficiency, EGFR kinase independent functions become more relevant. However, this hypothesis could provide an explanation for the reduced pEGFR levels detected in the A431 PTEN KO cells.

It is clear that the documented effects of the loss of PTEN on MET and EGFR physiology in GTL16 and A431 cell lines, respectively, are very different. Recapitulating the phenotypes in other MET and EGFR addicted models will be necessary to strengthen the study and help our understanding of PTEN-dependent RTK physiology. Indeed several important questions remain to be answered, such as the intracellular localisation of the phosphorylated receptors, and RTK degradation patterns.

Nonetheless, this is the first time that TKI responses have been linked to PTEN-driven changes in RTK conformation and cellular localisation. The dramatic differences between A431 and GTL16 once again underline the importance of re-considering PTEN as a general marker for TKI resistance. The identity of the RTK is key in defining the resulting phenotype. Understanding the molecular mechanisms behind the regulation of each RTK will eventually help choosing the most suitable therapeutic strategy.

Chapter 5. PTEN loss differentially affects EGFR and MET signalling pathways

5.1 The rationale behind phosphoproteomics

We have shown how the loss of PTEN has extremely different effects on EGFR and MET physiology and how these can impact TKI responses (Chapter 3, Chapter 4). Given the observed changes in receptor conformation and localisation as a consequence of PTEN loss, it is reasonable to predict that these changes would result in difference in signalling properties. Supporting this hypothesis, it has been shown that PTEN loss can have wide effects on the overall gene expression. For instance, DNA microarrays in human glioblastoma cells have reported on dramatic changes in HGF-induced gene expression following PTEN inactivation (Abounader et al., 2004).

Our focus has so far remained on the canonical PI3K/Akt pathway and the closely related MAPK pathway. However, it is clearly important to gain a wider perspective on the PTEN-dependent signalling network. To this end, “omics” technologies can provide an unbiased approach to characterising global molecular changes caused by PTEN inactivation.

Gene arrays were among the first platforms capable of profiling global changes in a specific type of “cellular content”, namely gene expression, which is what we currently refer to as “omics” (Hasin et al., 2017). The types of content that omics platforms can currently profile are diverse and include genes, RNA, proteins, metabolites or even specific chemical modifications on any of these molecules.

Each “omic” technique is able to answer different questions. For instance, genomics will inform on the genetic make up and variations of cells, while proteomics will assess the protein makeup of a cell, or proteome. Therefore, it is key to choose the right “omic” technique based on the scientific question one aims to address.

In our case, we sought to identify PTEN-dependent targets involved in TKI responses that could help explain the TKI resistant (A431) or hypersensitivity (GTL16) phenotype. The “omic” that we saw best suited for the study was phosphoproteomics, which quantifies the cellular phosphoproteome.

Phosphorylation, the addition of a phosphate group to a residue (mainly serine, threonine or tyrosine), is a type of posttranslational modification (PTM). PTMs are chemical modifications added onto proteins (e.g. phosphorylation, ubiquitylation, glycosylation, etc.), which generally have an impact on the function of the target protein. This highly dynamic and often reversible process allows to add another layer of complexity to the regulation of protein activity (Deribe et al., 2010). As mentioned earlier, phosphorylation is an important regulatory modification that facilitates signal transduction. Protein phosphorylation governs cellular processes such as growth, survival, proliferation, protein synthesis and cell division (Ardito et al., 2017; Humphrey et al., 2015).

Therefore, given the critical role of phosphorylation in signal transduction, we decided that phosphoproteomics could provide us with information that would be most proximal to cellular function (Doll et al., 2019).

Often, phosphorylation of kinases (by auto-phosphorylation) and/or their substrates is used as a readout of kinase activation, while the removal of the phosphate group, or de-phosphorylation, is used as a marker of kinase inactivation or signal downregulation. However, phosphorylation is not limited to acting as a molecular switch for the target, but has a wider spectrum of effects in cells. For instance, it can modulate protein-protein interactions, affect subcellular localisation, regulate the production and recycling of ATP, and it can promote removal of other PTMs (Ardito et al., 2017).

Quantitative mass spectrometry (MS)-based phosphoproteomics is a high throughput strategy that allows studying the phosphoproteome. From this analysis, it is possible to search for potential therapeutic targets, identify downstream effectors of kinases of interest, and map out pathways associated with a specific phenotype (Harsha and Pandey, 2010).

Given the therapeutic relevance of RTK addiction in cancer and the link between deregulation of signalling pathways and oncogenic behaviours, focussing on the phosphorylation patterns in these cells can be highly informative (Harsha and Pandey, 2010). Phosphoproteomics was therefore chosen to investigate the molecular underpinnings of PTEN-dependent regulation of TKI responses in both A431 and GTL16.

5.2 (MS)-based Phosphoproteomics and KSEA analysis

MS-phosphoproteomics starts with cell lysis and protein extraction; particular attention is paid not to disrupt the PTM. This is followed by the digestion of proteins with a protease and the enrichment of the phosphopeptides. There are different enrichment methods, such as immobilized metal affinity chromatography or metal oxide affinity chromatography, but they all use the affinity between metal ions and the phosphorylated peptide. Once this step is concluded, the enriched peptides are separated via chromatography, often reversed phase liquid chromatography, and then analysed with a mass spectrometer (Wirbel et al., 2017).

This method allows for the collection of a vast amount of information about the protein samples collected. Nonetheless it has its pitfalls. The technique essentially takes a snapshot of the phosphoproteome at a single time point. Protein phosphorylation is, however, dependent on various factors, such as life cycle and extracellular stimuli, and, as such, varies in time. Therefore, phosphoproteomics is unable to provide an absolute description of the cell. However, biological replicates and the presence of experimental controls can minimise this effect (Wirbel et al., 2017).

Additionally, although PTMs are a better biomarker for biological effects than genomic changes, they are still an indirect readout of cell activity. For instance, it is known that a fraction of cellular phosphorylation events is non-functional, and we have yet to establish a comprehensive picture for all the functional phosphorylation events (Landry et al., 2009; Lienhard, 2008). This imposes an issue when analysing the data gathered with MS-based phosphoproteomics. Those phosphorylation events that remain un-linked to a cellular function cause the

generation of background noise that disturbs the computational analysis (Beltrao et al., 2012; Landry et al., 2009; Wirbel et al., 2017).

Different methods can be used to derive information regarding kinase activity. However, one method in particular aims to reduce the background noise, the Kinase-Substrate Enrichment Assay (KSEA) (Casado et al., 2013). KSEA infers pathway activity by calculating the statistical probability that a specific group of phosphopeptides (grouped based on the presence of phosphorylation sites known to be substrates of a specific kinase or a shared phosphorylation motif) is enriched in a phosphoproteomics data set (Casado et al., 2013; Wirbel et al., 2017). In this way, the noise is reduced and scientists get access to a simplified yet very informative analysis of the kinase signatures that have emerged from phosphoproteomics.

KSEA is extremely useful when comparing two datasets, for instance a treated and an untreated sample, because clear differences between the two can be picked up. In a comparative KSEA analysis, three main metrics become available: the main activity score of a substrate set (kinase signature), the phosphosites with a significant fold change, and the occurrence of significantly upregulated phosphosites (Casado et al., 2013). This method extrapolates from the phosphoproteomics data a manageable amount of kinase signatures potentially involved in the phenotype, without loosing access to the changes in single phosphopeptides.

5.3 Results

5.3.1 Phosphoproteomics analysis

MS-phosphoproteomics, followed by KSEA analysis, was used to identify PTEN-dependent effectors of TKI responses in A431 and GTL16.

First, EGFR and MET-dependent phosphorylation signatures were generated. These were defined as those phosphopeptides subjected to change in response to RTK-selective TKIs. Changes in the MET and EGFR signatures as a function of PTEN were then studied in the isogenic PTEN KO lines.

The MET signature consisted of 285 phosphopeptides (167 down and 118 up) of which 91 were similarly affected by MET inhibitor (Crizotinib) treatment and loss of PTEN (Figure 5.1a, b and c). PTEN loss alone generated a signature of almost 1500 phosphopeptides (745 down and 728 up), documenting significant cellular rewiring (Figure 5.1b); 189 of these phosphopeptides (60 down and 129 up) were sensitive to MET inhibition (Figure 5.1b).

Accordingly to KSEA analysis, the signatures for Akt and Erk1/2 signalling activity were upregulated with the loss of PTEN and remained high even after Crizotinib treatment (Figure 5.1d). This confirmed previous experimental results (Figure 3.5).

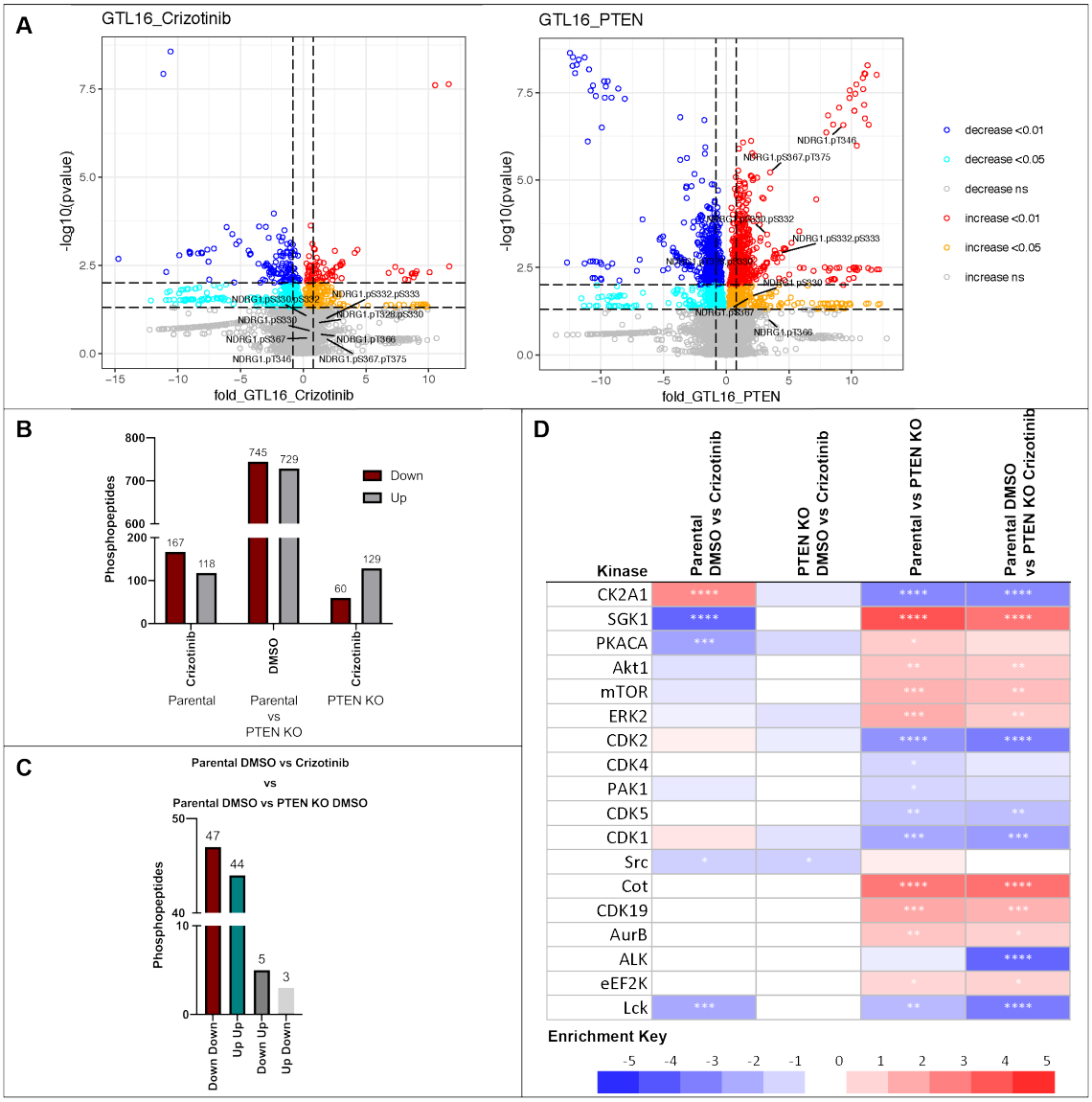

Figure 5.1 Generation of MET and PTEN signatures via a phosphoproteomics analysis

(A) Volcano plots representing phosphopeptides analysed via phosphoproteomics of GTL16 parental versus GTL16 treated with Crizotinib samples (left) and GTL16 parental versus GTL16 PTEN KO samples. Significance of *P* values is shown on the right hand side. **(B)** Quantification of significant phosphopeptides (*P* value < 0.05, fold change threshold = 0.75) emerging from the following comparison of GTL16 samples: Parental DMSO vs Parental Crizotinib, Parental DMSO vs PTEN KO DMSO and PTEN KO DMSO vs PTEN KO Crizotinib. Those peptides which presented a decrease in phosphorylation within the comparison groups are labelled as "down", those that showed an increase in phosphorylation are labelled as "up". n=5 **(C)** Comparison of the phosphopeptides (p value < 0.05, fold change threshold = 0.75) in common between the "Parental DMSO versus Parental Crizotinib" and the "Parental DMSO versus the PTEN KO DMSO" comparison groups. "Down" and "Up" refer to the phosphorylation pattern of the peptides within each comparison group; "down" refers to a decrease in phosphorylation and "up" to an increase in phosphorylation. n=5 **(D)** Heatmap of fold change of KSEA analysis of the top 18 hits. n=5. * significant at *P* <0.05; ** significant at *P* <0.01; *** significant at *P* <0.001; **** significant at *P* <0.0001.

As mentioned, when the Crizotinib signature (Parental DMSO vs Parental Crizotinib) was compared to the PTEN KO signature (Parental DMSO vs PTEN KO

DMSO), the majority of the phosphopeptides were similarly regulated; 8 phosphopeptides, however, were differentially regulated, increasing in one dataset and decreasing in the other, or vice versa (Figure 5.1c).

Unfortunately, it was not possible to perform a KSEA analysis on this subset, due to the small number of phosphopeptides. Despite the lack of a statistically supported analysis, the algorithm used was still capable of linking these phosphopeptides to the activity of six main kinases, via the presence of a shared consensus motif. The six kinases were the following: cyclin dependent kinase 1 and 2 (CDK1 and CDK2), casein kinase 2 subunit alpha (CK2A1), cAMP-dependent protein kinase catalytic subunit alpha (PKACA), Serum- and Glucocorticoid-inducible kinase 1 (SGK1) and proto-oncogene tyrosine-protein kinase (Src). The fact that CK2A1 was also present in the general KSEA analysis made this hit a strong candidate for further validation.

Similarly, no KSEA analysis could be run for the 91 phosphopeptides similarly affected by Crizotinib treatment and PTEN loss. The results of a gene ontology (GO) analysis using DAVID, however, revealed a potential link between some of these hits and Cbl, the E3 ubiquitin ligase responsible for RTK downregulation, and dynactin subunit 2 (DCTN2) involved in endocytosis.

Two EGFR signatures were generated using a type I (Erlotinib) and a type I½ (Lapatinib) inhibitors; the datasets comprised a total of 565 and 658 phosphopeptides, respectively (Figure 5.2 a and b). The two signatures had a total of 403 hits in common, all affected in an identical manner. Out of the 565 phosphopeptides of the Erlotinib signature, 104 were in common with the PTEN KO signature (A431 Parental Erlotinib vs A431 PTEN KO), 54 of which were differentially regulated by the inhibitor and by the loss of the tumour suppressor (Figure 5.2c). A similar comparison with the Lapatinib signature revealed that 111 phosphopeptides were in common between the Lapatinib and the PTEN KO signature; 64 of the phosphopeptides were differentially regulated (Figure 5.2c). PTEN inactivation alone, however, affected over 1100 phosphopeptides, suggesting an extensive signalling rewiring (Figure 5.2b). Out of these hits, 335 were sensitive to Erlotinib and 241 to Lapatinib (Figure 5.2b). In the PTEN KO cells,

therefore, ~50% of the effect of the inhibitors (in terms of phosphopeptides targeted) was lost (Erlotinib in parental targeted 565 phosphopeptides against the 335 targeted in the PTEN KO cells; Lapatinib targeted 658 phosphopeptides against the 271 targeted in the PTEN KO cells).

The KSEA analysis did not report an upregulation of Akt and Erk1/2 signatures in A431 PTEN KO cells, despite the phosphorylation levels of these two proteins had previously been found to be upregulated (Figure 3.5). As we will discuss in more details later, this is probably due to the nature of KSEA, which analyses an entire group of phosphopeptides linked to a kinase signature, rather than the kinase alone.

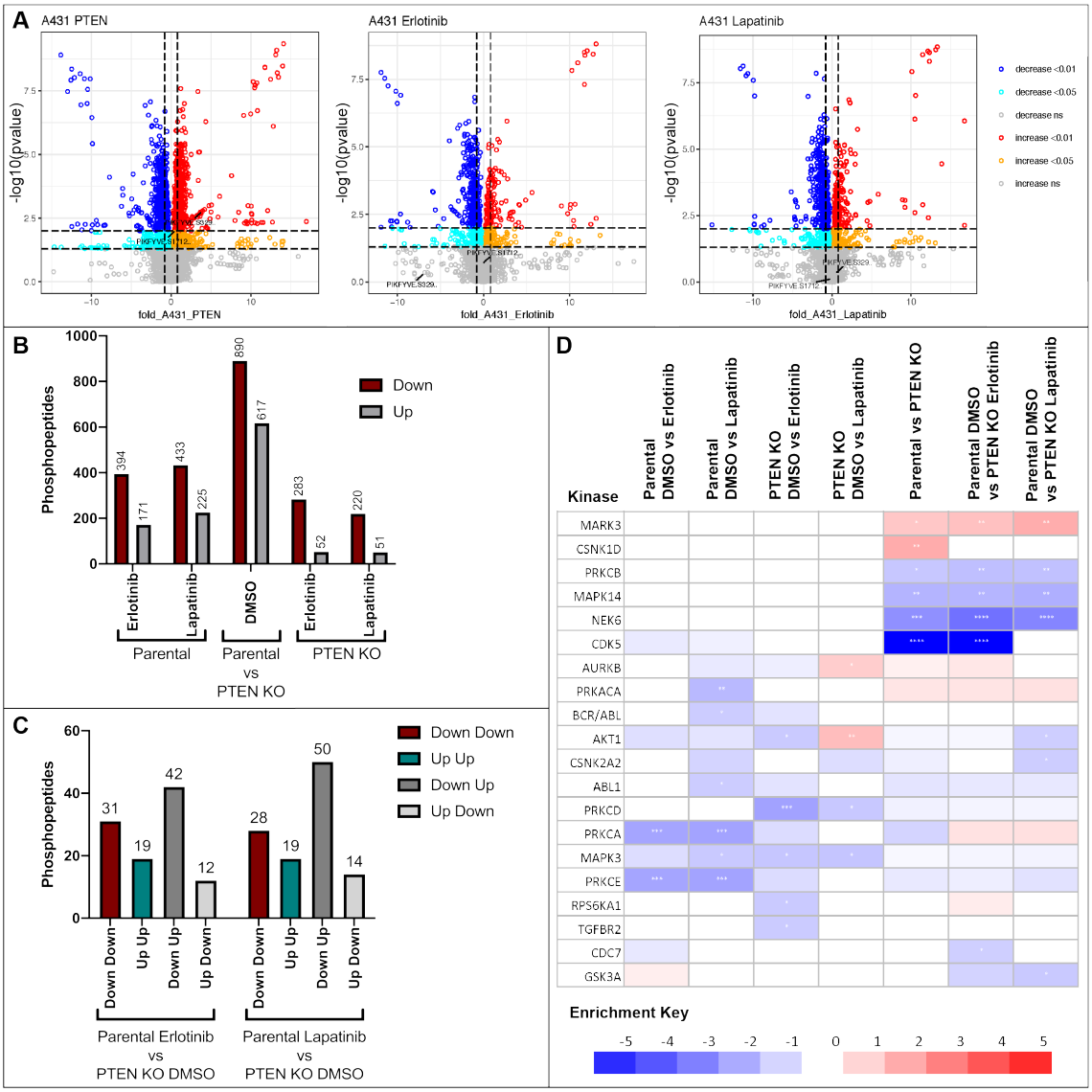

Figure 5.2 Generation of EGFR and PTEN signatures via a phosphoproteomics analysis

(A) Volcano plots representing phosphopeptides analysed via phosphoproteomics of A431 parental versus A431 PTEN KO samples (left), A431 Parental versus A431 treated with Erlotinib samples (middle) and A431 parental versus A431 treared with Lapatinib samples. Significance of p values is shown on the right hand side. **(B)** Quantification of significant phosphopeptides (*P* value < 0.05, fold change threshold = 0.75) emerging from the following comparison of A431 samples: Parental DMSO vs Parental Erlotinib or Lapatinib, Parental DMSO vs PTEN KO DMSO and PTEN KO DMSO vs PTEN KO Erlotinib or Lapatinib. Those peptides which presented a decrease in phosphorylation within the comparison groups are labelled as “down”, those that showed an increase in phosphorylation are labelled as “up”. n=5. **(C)** Comparison of the phosphopeptides (*P* value < 0.05, fold change threshold = 0.75) in common between the “Parental DMSO versus Parental Erlotinib” or the “Parental DMSO versus Parental Lapatinib” and the “Parental DMSO versus the PTEN KO DMSO” comparison groups. “Down” and “Up” refer to the phosphorylation pattern of the peptides within each comparison group; “down” refers to a decrease in phosphorylation and “up” to an increase in phosphorylation. n=5. **(D)** Heatmap of fold change of KSEA analysis of the top 20 hits. n=5. * significant at *P* <0.05; ** significant at *P* <0.01; *** significant at *P* <0.001; **** significant at *P* <0.0001.

A high level comparison between the analyses carried out for GTL16 and A431 cells thus revealed that, while the loss of PTEN deeply affected the phosphoproteome of both cell lines, it did so in a very different manner. In the case of GTL16, the PTEN KO signature shared more than 30% of the MET inhibitor signature, and 92% of these phosphopeptides were identically regulated. Therefore, PTEN inactivation affected part of phosphoproteome similarly to a MET inhibitor, potentially providing an explanation for the hypersensitisation to TKIs demonstrated by GTL16 PTEN KO cells. The same comparison in A431 cells instead showed that only 17-18% of the EGFR TKI signature was shared with the PTEN KO dataset, and only half of this subset of phosphopeptides was regulated in a similar manner by PTEN inactivation and treatment with a TKI.

5.3.2 Phosphoproteomics analysis validation

KSEA analysis revealed CK2, a serine/threonine kinase with a central role in cell viability, as a potential contributor to the TKI hypersensitivity phenotype of GTL16 PTEN KO cells. Western blot analysis indeed confirmed differences in the phosphorylation patterns of CK2 substrates between parental and PTEN KO GTL16 cells. The use of a CK2 inhibitor (CX-4945) overall reduced phosphorylation of CK2 substrates, as expected. However, CX-4945 treatment alone did not affect the survival of GTL16 PTEN KO cells, and its combination with a MET inhibitor did not differ from the single agent Crizotinib treatment. Only in the parental line, the combined treatment of a MET inhibitor and CX-4945 modestly increased cell death (Figure 5.3). Although the reduction in CK2 signature was associated with the loss of PTEN by phosphoproteomics analysis, our data do not support a role of CK2 in mediating responses to TKI in GTL16 PTEN KO cells. Nonetheless, CK2 is clearly a PTEN-dependent protein and its role in MET addicted tumours may be an interesting subject for further research.

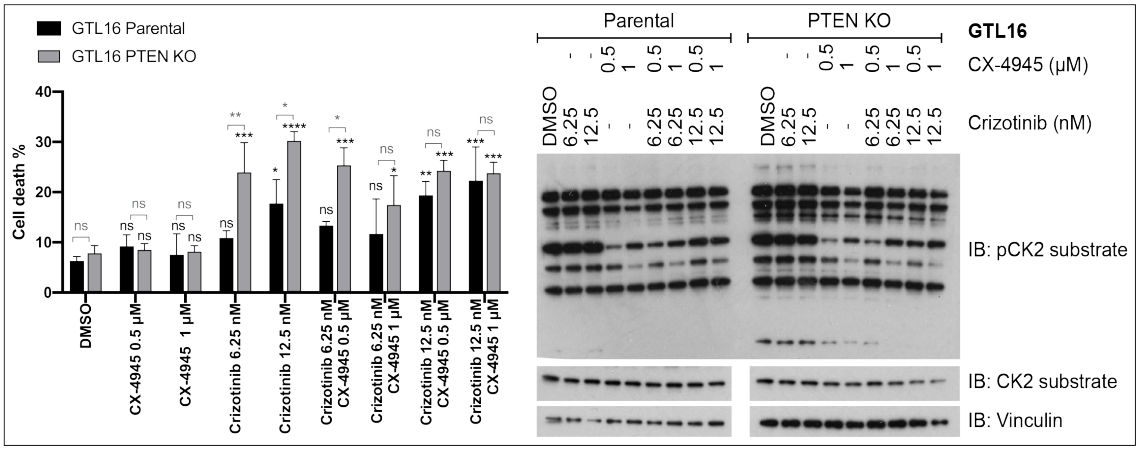

Figure 5.3 CK2 is a PTEN-dependent protein that is not involved in mediating TKI responses

On the left, analysis of the responses of GTL16 parental and PTEN KO to 72 h treatment with MET inhibitor Crizotinib, CK2 inhibitor CX-4945 and the combination of the two inhibitors. Cell death percentages (mean ± SD) were assessed via automated trypan blue exclusion method (ViCell). ns, not significant; * significant at *P* <0.05; ** significant at *P* <0.01; *** significant at *P* <0.001; **** significant at *P* <0.0001. On the right, western blot analysis (n=1) of GTL16 parental and GTL16 PTEN KO responses to 6 h treatment with Crizotinib, CK2 inhibitor CX-4945 and the combination of the two inhibitors.

Another phosphopeptide that emerged from phosphoproteomics analysis was N-myc downstream-regulated gene1 (NDRG1). NDRG1 appeared to be strongly associated with the PTEN signature; phosphopeptides related to NDRG1 were upregulated with PTEN inactivation and only mildly responsive to MET inhibition (Figure 5.4a). This made NDRG1 an interesting hit to explain the hypersensitivity of the PTEN KO line to Crizotinib.

Western blot analysis confirmed the phosphoproteomics data, as pNDRG1 levels were higher with PTEN inactivation. NDRG1 phosphorylation was also susceptible to Crizotinib treatment in the PTEN KO line, but, in line with the phosphoproteomics analysis, pNDRG1 levels in the treated sample remained higher than the vehicle parental sample (Figure 5.4b). Interestingly, total NDRG1 protein levels increased in PTEN KO cells (Figure 5.4c). This would suggest that NDRG1 has separate functions in its phosphorylated and unphosphorylated forms, although both are dependent on PTEN. Furthermore, the levels of pNDRG1 appeared to be marginally dependent on HGF stimulation in both parental and PTEN KO line, with an increase in signal after 60 minutes of stimulation (Figure 5.4c).

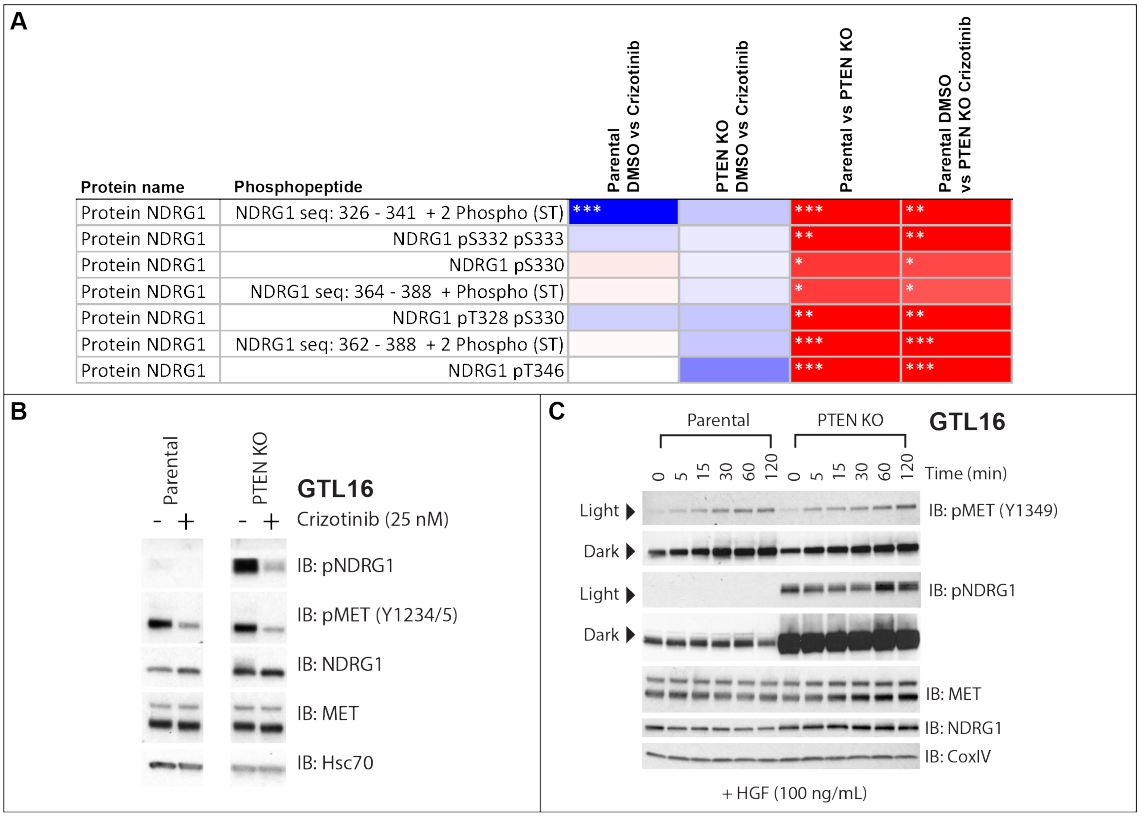

Figure 5.4 NDRG1 is a PTEN-dependent MET effector upregulated upon PTEN loss

(A) Heatmap of fold change of KSEA analysis of NDRG1. n=5. * significant at P <0.05; ** significant at P <0.01; *** significant at P <0.001; **** significant at P <0.0001. **(B)** Western blot analysis of GTL16 parental and GTL16 PTEN KO responses to 6 h treatment with Crizotinib. **(C)** Western blot analysis of GTL16 responses to HGF. HGF was used at a concentration of 100 ng/mL after a 4 h starvation period.

Similarly to GTL16, we sought to identify a few phosphopeptides within the EGFR signature that are affected by the loss of PTEN, yet contribute to TKI response. Among the ~ 50 phosphopeptides that were found to be downregulated by EGFR inhibitors treatment and upregulated by the loss of PTEN (Figure 5.2), an interesting hit was Phosphoinositide Kinase for five position containing a Fyve finger (PIKfyve) (Figure 5.5a). PIKfyve phosphorylates the D-5 position of phosphatidylinositol (PI) and phosphatidylinositol-3-phosphate (PI(3)P) to make phosphatidylinositol-5-phosphate (PI(5)P) and phosphatidylinositol-3,5-bisphosphate ($PI(3,5)P_2$), respectively.

We investigated the role of PIKfyve in modulating TKI responses by using Apilimod, a selective PIKfyve inhibitor (Gayle et al., 2017). Both parental and PTEN KO A431 cells were sensitive to Apilimod single agent treatment, albeit the latter showed a modest increase in sensitivity. Pronounced induction of cell death was observed

with the combination of Apilimod and an EGFR inhibitor (EKB-569), in both parental and PTEN KO lines. Nonetheless, the combinatorial treatment still failed to fully overcome the EGFR inhibitor resistance phenotype of the PTEN KO cells (Figure 5.5b).

The efficient induction of cell death by PIKfyve and EGFR inhibition in the context of EGFR addiction and PTEN inactivation was confirmed in MDA-MB-468 cells, using a combination of an EGFR inhibitor and Apilimod (Figure 5.5b), as well as two additional PIKfyve inhibitors, APY-0201 and YM-201636 (Figure 5.5c). At the molecular level, PIKfyve inhibition had a small effect on suppressing EGFR phosphorylation, and minimal to no effect on PI3K/Akt and MAPK activation (Figure 5.5b and c).

Importantly, the activity of Apilimod was PIKfyve specific, as the MDA-MB-468 line ectopically expressing an Apilimod resistant PIKfyve cDNA (N1939K) was resistant to an EGFR and PIKfyve combinatorial treatment (Figure 5.5d).

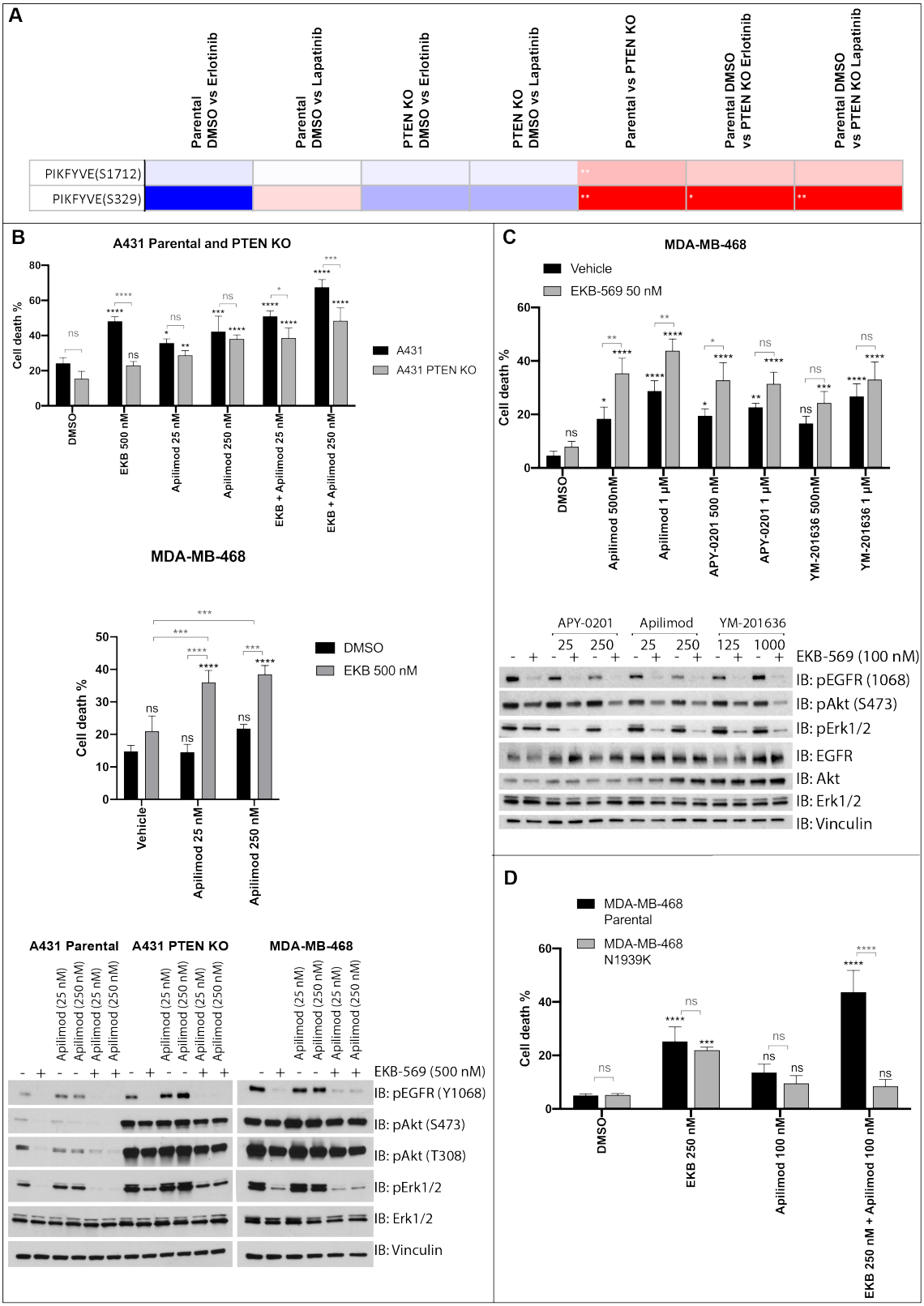

Figure 5.5 PIKfyve is a PTEN-dependent protein and its inhibition anti-proliferative effects in EGFR-addicted cells

(A) Heatmap of fold change of KSEA analysis of PIKfyve. n=5. * significant at *P* <0.05; ** significant at *P* <0.01; *** significant at *P* <0.001; **** significant at *P* <0.0001. **(B)** Analysis of

the responses of A431 parental, A431 PTEN KO and MDA-MB-468 to 72 h (growth assay) or 6 h (western blot, n=1) treatment with EGFR inhibitor EKB-569, PIKfyve inhibitor Apilimod and the combination of the two inhibitors. **(C)** Analysis of the responses of MDA-MB-468 to 72 h treatment with combination of EKB-569 and a PIKfyve inhibitor. Western blot analysis of MDA-MB-468 responses to 6 h treatment with EKB-569, Apilimod, APY-0201 or YM-201636, and the combination of EKB-569 and a PIKfyve inhibitor. **(D)** Analysis of the responses of MDA-MB-468 and Apilimod-resistant MDA-MB-468 N1939K cells to 72 h treatment with EGFR inhibitor EKB-569, PIKfyve inhibitor Apilimod and the combination of the two drugs. Cell death percentages (mean ± SD) were assessed via automated trypan blue exclusion method (ViCell). ns, not significant; * significant at P <0.05; ** significant at P <0.01; *** significant at P <0.001; **** significant at P <0.0001.

The combination of Apilimod with a TKI delivered quite promising results in the A431 PTEN KO cells, however, it still failed to completely overcome the EGFR inhibitor resistance phenotype of the PTEN KO line. We also noticed that Akt phosphorylation in this sample was resistant to all treatments (Figure 5.5b) and therefore hypothesised that the combined inhibition of the PI3K pathway and PIKfyve could successfully overcome the effects of PTEN loss.

The combination of a PI3K and a PIKfyve inhibitor in MDA-MB-468, induced cell death (Figure 5.6a) and reduced PI3K pathway activation in a dose-dependent manner (Figure 5.6b). This would suggest that, when PTEN is inactivated, PIKfyve contributes to the regulation of the PI3K/Akt pathway and could potentially play a role in the TKI resistance displayed by the PTEN null cells. The combined inhibition of PI3K and PIKfyve was, however, insufficient to fully overcome the resistant phenotype of PTEN KO cells (Figure 5.6c). Nonetheless, it remains to be investigated if this combination of drugs is effective in overcoming the resistance to TKI. Preliminary data of the combined inhibition of EGFR, PI3K and PIKfyve in MDA-MB-468 showed that these cells were sensitive to the treatment. Furthermore, the data pointed towards an important role of PI3K class Iβ (targeted by AZD6482) in mediating cell death (Figure 5.6d). The data await replication in the A431 isogenic model.

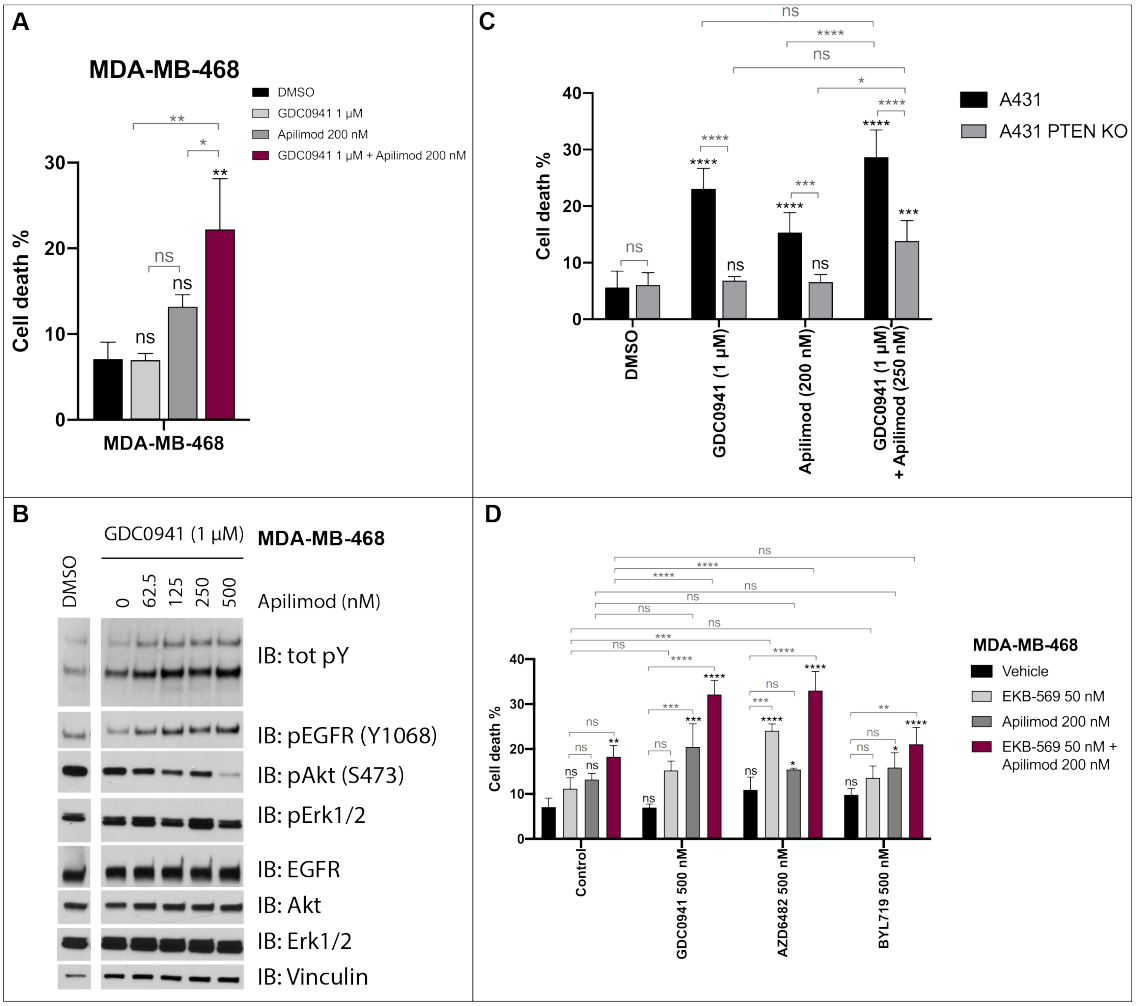

Figure 5.6 PIKfyve is an important downstream player of EGFR that, in conjunction with the PI3K pathway, may contribute to the TKI resistant phenotype of PTEN null cells.

(A) Analysis of the responses of MDA-MB-468 to 72 h treatment with pan-class-I-PI3K inhibitor, GDC0941, PIKfyve inhibitor Apilimod and the combination of the two drugs. n=3 **(B)** Western blot analysis (n=1) of MDA-MB-468 responses to 6 h treatment with Apilimod in combination with GDC0941. **(C)** Analysis of the responses of A431 parental and A431 PTEN KO to 72 h treatment with GDC0941, Apilimod and the combination of the two drugs. n=3 **(D)** Analysis of the responses of MDA-MB-468 cells to 72 h treatment with EGFR inhibitor EKB-569, PIKfyve inhibitor Apilimod, alone or in combination with class-specific PI3K inhibitors. Cell death percentages (mean ± SD) were assessed via automated trypan blue exclusion method (ViCell). ns, not significant; * significant at P <0.05; ** significant at P <0.01; *** significant at P <0.001; **** significant at P <0.0001.

Given that the investigation into the roles of PTEN-mediated TKI responses has been carried out in parallel between A431 and GTL16, we decided to test Apilimod cell toxicity properties in GTL16. To our surprise, Apilimod as a single agent was very effective in GTL16, independently of PTEN status (Figure 5.7a). This could suggest that PIKfyve is an obligate effector of MET. Apilimod and Crizotinib showed no additive effects in terms of cell toxicity, as well as target inhibition in

PTEN KO cells (Figure 5.7a and b). We could hypothesise that the loss of PTEN may affect the synergy of the two drugs. Furthermore, we found that, at the molecular level, Crizotinib achieved superior MET inhibition compared to Apilimod, as demonstrated by pMET levels (Figure 5.7c). Finally, we ruled out any off-target effects by engineering a GTL16 cell line that ectopically expresses an Apilimod-resistant PIKfyve cDNA (Figure 5.7c and d).

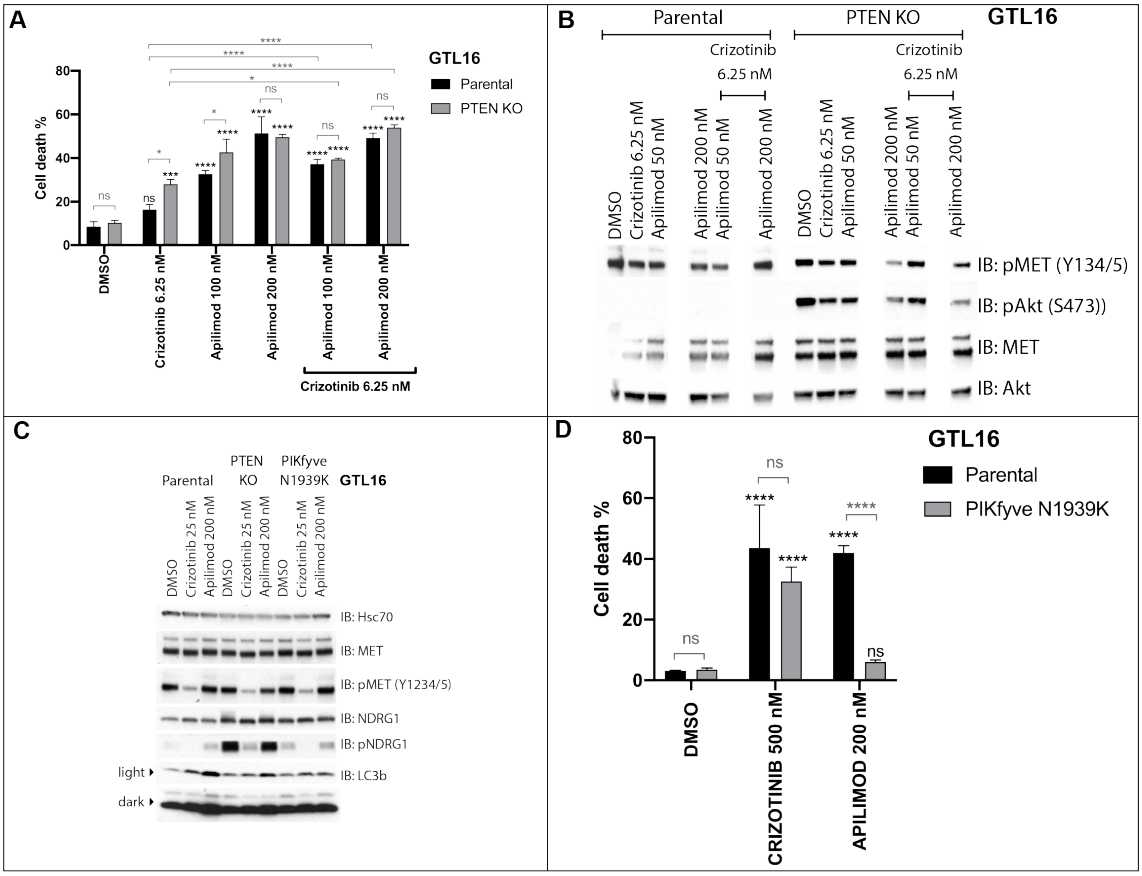

Figure 5.7 PIKfyve inhibition has anti-proliferative effects in MET-addicted cells.

(A) Analysis of the responses of GTL16 parental and GTL16 PTEN KO to 72 h treatment with Crizotinib and Apilimod alone and in combination. **(B)** Western blot analysis (n=1) of GTL16 parental and GTL16 PTEN KO responses to 6 h treatment with Crizotinib and Apilimod alone and in combination. **(C)** Western blot analysis of GTL16 parental, GTL16 PTEN KO and GTL16 Apilimod-resistant N1939K cells responses to 6 h treatment with Crizotinib or Apilimod. **(D)** Analysis of the responses of GTL16 parental and GTL16 Apilimod-resistant N1939K cells to 72 h treatment with Crizotinib or Apilimod. n=3. Cell death percentages (mean ± SD) were assessed via automated trypan blue exclusion method (ViCell). ns, not significant; * significant at *P* <0.05; ** significant at *P* <0.01; *** significant at *P* <0.001; **** significant at *P* <0.0001.

Therefore, inhibition of PIKfyve did not rescue the hypersensitisation to MET inhibitors in GTL16 PTEN KO cells, however, it showed on-target, effective toxicity against MET-addicted cells (GTL16).

5.4 Discussion

Our phosphoproteomics data is consistent with the existence of PTEN-dependent mechanisms of signal regulation and inhibitor responses, the nature of which depends on the identity of the RTK. Once again, this strengthens the hypothesis that loss of PTEN should not be used as a general biomarker for TKI resistance.
The MET, EGFR and PTEN signatures generated are hopefully a source of information for numerous follow up studies. Due to time constraints, only few of the many potential venues of investigation have been followed.

The observation that over 26% of the MET signature is similarly affected by the loss of PTEN and by Crizotinib treatment (Figure 5.1) could suggest that PTEN inactivation causes the threshold of responses to MET TKIs to be lowered. Although this hypothesis was not investigated into details, a GO analysis through DAVID has linked phosphopeptides in this 26% of the MET signature with MET downregulation and recycling. This information ties in with the previously documented deregulation of MET endocytosis following the loss of PTEN (Chapter 4).

KSEA analysis of the GTL16 samples revealed a strong signature for the kinase CK2. CK2 is a serine/threonine kinase expressed in all tissues, with over 100 physiological potential substrates. Although we are aware of the important roles that CK2 plays in multiple cellular functions, including cell proliferation, the characterisation of CK2 kinase activity remains vague. For instance, it is yet unclear whether CK2 requires phosphorylation for its own activation, or whether phosphorylation events only modulate its activity and stability (Litchfield, 2003). However, CK2 activity is known to become particularly relevant in tumorigenic cells (Ruzzene and Pinna, 2010).

Additionally, PTEN is a known CK2 substrate. Phosphorylation of PTEN on its C-terminal domain by CK2 increases protein stability (Torres and Pulido, 2001), while lowering its membrane association and overall lipid phosphatase activity (Tamguney and Stokoe, 2007). In GBM, CK2-dependent hyperphosphorylation of PTEN causes the tumour suppressor to remain in the cytoplasm, leading to a

failure in PTEN-mediated NHEJ repair pathway activation and making cells resistant to DNA-damaging agents (Kang et al., 2017). This CK2-mediated mechanism of PTEN lipid phosphatase inhibition has been linked to resistance to BRAF (Lin et al., 2018) and HER2 inhibitors (Goltsov et al., 2012). CK2 upregulation has also been reported in gastrointestinal stromal tumours (GIST) (Huang et al., 2020), but its link to MET activation and TKI responses has not been investigated.

Interestingly, the CK2 signature in our phosphoproteomics data is upregulated upon Crizotinib treatment, and downregulated with the loss of PTEN. This led us to hypothesise that CK2 is a PTEN-dependent mediator of TKI hypersensitivity in GTL16 PTEN KO cells. Unfortunately we still lack direct evidence of a relationship between PTEN and CK2 activity in our GTL16 model. However, if we assume that PTEN is phosphorylated by CK2 in GL16 cells, similarly to what has been shown in the literature (Torres and Pulido, 2001), we can start building a model for the data we have collected (Figure 5.8).

We hypothesise that CK2-phosphorylated PTEN is itself a promoter of CK2 activity. PTEN could be directly contributing to this positive feedback loop by virtue of its protein phosphatase function. Additionally, we hypothesise that MET acts as an inhibitor of PTEN-driven CK2 activation (Figure 5.8). The addition of Crizotinib would consequently result in an increase of phosphorylated-PTEN-dependent CK2 activation; this is supported by our phosphoproteomics data (Figure 5.1). At the same time, loss of PTEN would result in a decrease of CK2 activity, which is also evident from our data (Figure 5.1). The hypersensitisation to TKI observed in the PTEN KO could therefore be a result of the loss of the tumour promoting functions of phosphorylated-PTEN-dependent CK2 activation. In line with this hypothesis, the anti-proliferative activity of anti-CK2 agents combined with Crizotinib, in GTL16 parental cells, partially recapitulates the hypersensitivity phenotype of PTEN KO GTL16 cells (Figure 5.3).

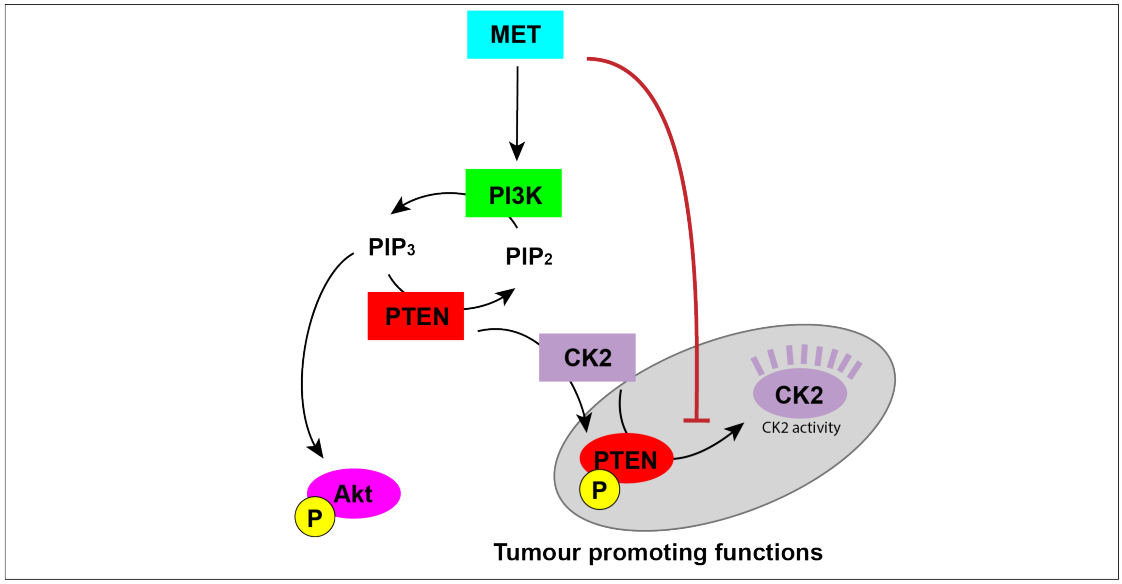

Figure 5.8 Hypothetical model for CK2-PTEN relationship in GTL16

Schematic representation of the hypothesis linking MET, PTEN and CK2.

Importantly, our model is based on the assumption that there is a functional relationship between CK2 activity and PTEN. This has not been demonstrated in GTL16 and additional experiments, such as CK2 KD or KO, are necessary to reproduce the pharmacological data generated with CX-4945. Additionally, it would be essential to determine changes in the levels of total and phosphorylated PTEN via Western blotting, as well as the effects of CK2 inhibition on PI3K pathway effectors, such as Akt.

Our preliminary data is therefore insufficient to either rule out or confirm the possibility that CK2 plays a role in modulating TKI responses in a PTEN-dependent manner. More experiments are needed to investigate this hypothesis. To this end, a lipid phosphatase dead PTEN mutant GTL16 cell line has been generated and it will help dissect the potential dual role of PTEN as both lipid and protein phosphatase.

Further to this, CK2 may still play an important role in mediating MET TKI responses, independently of PTEN status. In parental GTL16 cells, in fact, the combination of a CK2 with a MET inhibitor was more effective than the single agent Crizotinib (Figure 5.3). Although it remains to establish that CX-4945 has CK2-targeted effects in GTL16, CK2 involvement in MET TKI responses could still be

relevant, especially when considering the clinical unmet need for efficient inhibition of tumours with MET-activation. MET TKIs have failed to show clinical benefit in patients (Hughes and Siemann, 2018). Although the effect of CX-4945 combined with Crizotinib only showed a slight increase in cell death compared to Crizotinib alone, this result warrants additional work to investigate CK2 activation in MET-addicted tumours. It is in fact important that we are able to identify novel druggable targets that can improve TKI cytotoxic effects.

Unlike CK2, the second protein we decided to study in more details, NDRG1, was chosen based on its phosphorylation profile, rather than on the KSEA analysis. Similarly to CK2, NDRG1 phosphopeptides were differentially regulated by the loss of PTEN and Crizotinib treatment, and as such became good candidates for addressing the TKI hypersensitivity phenotype of GTL16 PTEN KO cells. Both total and phosphorylated NDRG1 levels were upregulated in the PTEN KO sample. Phosphorylated NDRG1 was also responsive to MET inhibition, in both parental and PTEN KO lines. Overall, this would suggest that MET and NDRG1 are somehow functionally linked in GTL16 cells.

Nonetheless, after Crizotinib treatment, the levels of total and phosphorylated NDRG1 in the PTEN KO cells remained elevated. This is suggestive of the presence of a MET-independent NDRG1 function that becomes relevant upon loss of PTEN.

NDRG1 is involved in different cellular functions including cell growth and differentiation; it is also believed to be an important suppressor of metastasis (Song et al., 2012). Although it has been linked to PTEN and cancer progression by numerous studies, there appear to be a certain degree of controversy. For instance, NDRG1 upregulation has been shown to positively correlate with PTEN downregulation in endometrial cancer (Chen et al., 2008). However, in pancreatic cancer, NDRG1 has been shown to upregulate PTEN and inhibit PI3K and Ras pathways (Kovacevic et al., 2013). Overexpression of PTEN has also been linked to NDRG1 upregulation in prostate and breast cancer (Bandyopadhyay et al., 2004). Finally, PTEN silencing caused upregulation of NDRG1 phosphorylation in prostate cancer, but not in hepatocellular carcinoma (Park et al., 2018).

It is therefore quite clear that NDRG1 is subjected to a tumour-type-dependent regulation.

Based on the phosphoproteomics data, it appears that in GTL16, similarly to endometrial cancers (Chen et al., 2008), loss of PTEN positively correlates with NDRG1 up-regulation. Although the functional significance of this remains unknown, upregulation of NDRG1 has been linked to decreased total and phosphorylated MET levels (Park et al., 2019). This model ties in with the decrease of pMET levels documented in GTL16 PTEN KO cells (Chapter 4). In the future, NDRG1 contribution to TKI responses should be assessed. Silencing NDRG1 in GTL16 PTEN KO cells could perhaps provide a strategy to understand a potential link with the TKI hypersensitivity demonstrated by these cells.

Given NDRG1 presence in multiple cellular compartments it has also been hypothesised that the protein carries out different organelle-specific functions (Park et al., 2018). A hypothesis is that NDRG1 could mediate TKI responses by affecting MET trafficking. This question could be addressed in the future by studying NDRG1 intracellular localisation. Particularly interesting, would be to investigate whether there is a link between changes in MET intracellular distribution observed upon PTEN loss (Chapter 4) and the concomitant increase in NDRG1. For the time being this remains a speculation, however, this line of research could shed more light onto the cellular dynamics underpinning the MET-dependent phenotype.

Similarly to the data for the GTL16 samples, the phosphoproteomics analysis of A431 cell lines also documented the significant signalling rewiring that follows the loss of the tumour suppressor PTEN (Figure 5.2). However, the KSEA analysis of the PTEN KO sample did not reflect the upregulation of Akt and Erk1/2 signalling activity, which was previously documented via immunoblotting (Chapter 3). The most plausible explanation for this result is the fact that KSEA is based on the upregulation of an entire group of phosphopeptides that are linked to a kinase signature. Western blotting, on the other hand, only detects the upregulation of a single phosphorylated protein. Therefore, the observed upregulation of pAkt and pErk1/2 proteins via western blotting does not necessarily imply an increase in their substrates' phosphorylation and subsequent pathway activation. Inhibition of the

PI3K/Akt or the MAPK pathway in this cell line was indeed insufficient to restore the sensitivity to EGFR inhibitors.

The Akt1 signature did emerge from the KSEA analysis. However, it was differentially regulated by Erlotinib and Lapatinib in the PTEN KO sample (Figure 5.2). Interestingly, no differences in total pAkt levels had previously been detected via immunoblotting when looking at treatments with the two inhibitors. This discrepancy could once again be explained by the difference in the nature of the techniques used. Additionally, in previous experiments, we had not considered to make a distinction between the two Akt isoforms. Therefore, it cannot be excluded that there is a difference in the phosphorylation levels of the two isoforms that goes undetected when using an antibody that targets both isoforms.

Given the different roles the two isoforms play in tumour development (Dillon et al., 2009; Riggio et al., 2017; Sahlberg et al., 2016), it also cannot be ruled out that Akt1, rather than Akt2, is the main mediator of TKI responses in A431 PTEN KO cells. A more detailed investigation is necessary to address this hypothesis. However, we have already shown that targeting Akt in combination with EGFR fails to completely re-sensitize cells to EGFR inhibitors (Figure 3.6). A contribution of Akt1 specifically to the TKI-resistance phenotype is therefore unlikely.

In addition to Akt1, the KSEA analysis of the A431 samples revealed other interesting hits, such as the microtubule affinity regulating kinase 3 (MARK3) (Figure 5.2). As the name suggests, MARK3 is a serine/threonine kinase involved in cytoskeletal dynamics. Thanks to its interaction with 14-3-3 scaffolding proteins that bind to phosphorylated serine and threonine motifs, MARK3 has also been linked to the modulation of various cellular signalling pathways (Göransson et al., 2006). Interestingly, a bioinformatics study showed that MARK3 has been associated with EGFR inhibitor resistance phenotypes in NSCLC (Kim et al., 2014). The link between the two kinases remains to be investigated, but it opens up the possibility that MARK3 upregulation also contributes to the EGFR inhibitor resistance phenotype of A431 PTEN KO cells.

A second interesting kinase emerging from the KSEA analysis, was casein kinase 1δ (CSNK1D), the signature of which was upregulated in the PTEN KO line (Figure 5.2). CSNK1D is one of the six isoforms of a big family of casein kinases. It is involved in several signalling pathways and cellular processes, such as cytoskeletal maintenance and membrane trafficking (Cheong and Virshup, 2011). Casein kinase isoforms have been linked to different tumours development. In particular aberrant CSNK1D expression has been reported in prostate, breast, colorectal and ovarian cancer (Schittek and Sinnberg, 2014). For instance, in breast cancer, suppression of CSNK1D activity decreased cellular migration and metastasis, demonstrating the role of CSNK1D in cancer progression (Bar et al., 2018). It is therefore possible that the more aggressive phenotype of EGFR-addicted PTEN-null cancers involves CSNK1D activation. This could be reflected by the upregulation of CSNK1D signature in A431 PTEN KO cells. However, no information regarding how PTEN affects the motility of A431 cells is available, and further studies are needed to determine the existence of a link between PTEN loss, CSNK1D upregulation and cellular migration.

Based on a bioinformatics study, CSNK1D also appears to positively regulate components of the PI3K/Akt signalling pathway, and to negatively regulate PTEN (Tripathi et al., 2018). It is, however, unknown whether a PTEN-driven negative feedback loop that controls CSNK1D activity exists. This model could explain the observed CSNK1D upregulation upon loss of the tumour suppressor.

Unfortunately, the contribution of CSNK1D to EGFR inhibitor responses has not been investigated. Based on the KSEA analysis, however, CSNK1D could be an interesting protein to target in the context of EGFR-addiction and PTEN-loss.

One very interesting hit that emerged from the analysis of the phosphopeptides in the A431 samples was PIKfyve (Figure 5.5). PIKfyve phosphorylation was significantly upregulated in the PTEN KO cells, but remained unchanged after treatment with EGFR inhibitors, in both the parental and PTEN KO line. As an EGFR independent hit, PIKfyve was an interesting protein to look at to explain the EGFR inhibitor resistance phenotype in the PTEN KO line, while providing a potential venue for overcoming the resistance.

The effective anti-proliferative effects obtained with the combination of the PIKfyve inhibitor, Apilimod, and an EGFR inhibitor, in both A431 PTEN KO and MDA-MB-468 cells, are overall very promising results (Figure 5.5). The evidence would support the hypothesis of PIKfyve involvement in mediating TKI resistance phenotype in EGFR-addicted PTEN-null cells. However, the PTEN-dependency of the phenotype is yet to be demonstrated.

The mechanism of PIKfyve involvement in the phenotype therefore remains elusive. However, there seem to be an interaction between the PI3K/Akt pathway and PIKfyve activation, given the synergistic effects of Apilimod and GDC0941. In the context of PTEN inactivation and EGFR addiction, the combined inhibition of PIKfyve, EGFR and PI3Kβ was found to be most effective (Figure 5.6). PTEN loss is indeed known to promote the engagement of PI3Kβ as an oncogenic mechanism to drive PI3K pathway activation (Jiang et al., 2010b; Schwartz et al., 2015; Wang et al., 2016; Wee et al., 2008). The triple combination with a PI3K-isoform-specifc inhibitor may be a desirable therapeutic option. To date, pan-PI3K inhibitors are mostly associated with dose-limiting toxicities and identifying an optimal therapeutic window for PI3K inhibitors still represents a challenge (Papa and Pandolfi, 2019; Toska and Baselga, 2016). Our preliminary result thus warrants further research in order to detail the contribution of different PI3K isoforms to the phenotype in our A431 isogenic models and in other EGFR addicted cancers.

PIKfyve has been previously shown to be a direct substrate of Akt (Emrah Er et al., 2013). It would therefore be interesting to understand whether the link we have established between PIKfyve and PI3K proteins is PI3K driven, or it is an effect of PI3K-dependent Akt activation.

PIKfyve has also been show to promote EGFR lysosomal degradation (Emrah Er et al., 2013). However, this represents a controversial subject of research. Other evidence, in fact reports that a lipid kinase deficient PIKfyve does not affect EGFR degradation patterns (Ikonomov et al., 2003a). Based on our data, we also do not seem to detect any changes in EGFR downregulation (Chapter 4). More research is needed to better delineate the relation between EGFR degradation and PIKfyve

function, but it may be a cell-type specific effect or it may involve more complex pathways.

PIKfyve could still be linked to EGFR regulation by virtue of its essential role in intracellular trafficking. PIKfyve is in fact important for the sorting of cargo in MVBs, for intraluminal vesicles formation and even for acidification of lysosomes. It carries out its activity by contributing to local phosphoinositides changes, by phosphorylating PI(3)P to PI(3,5)P_2 (Wallroth and Haucke, 2018). Defects in PIKfyve lipid kinase activity can severely disrupt intracellular trafficking. For instance, a lipid kinase deficient PIKfyve induced endomembrane vacuolation (Ikonomov et al., 2003a).

Although EGFR trafficking in relation to PIKfyve remains to be investigated in our model system, there is some evidence in the literature that establishes a connection between the two proteins. In bladder cancer for instance, MS studies have shown PIKfyve interaction with EGFR. RNA silencing experiments have also revealed PIKfyve as a mediator of EGFR transitioning to the nucleus, and its involvement in bladder oncogenesis (Kim et al., 2007).

It would therefore be interesting to explore the link between EGFR and PIKfyve in A431. We hypothesise that PIKfyve could mediate TKI responses by affecting EGFR intracellular trafficking. This could also potentially explain the changes in EGFR localization that follows the loss of PTEN (Chapter 4).
More experiments are needed to test this hypothesis. Nonetheless, given the aggressiveness of EGFR-addicted PTEN-null tumours, and the effective anti-proliferative activity of TKI-Apilimod combination, it is important to unveil the potential link between PIKfyve and EGFR.

A quite unexpected result was the observation of the anti-proliferative effects of Apilimod, as a single agent, in the GTL16 cells. Apilimod was as efficacious as Crizotinib at inducing cell death, and the two inhibitors together showed additive effects.

There may also be a link between PTEN loss and PIKfyve activation in the context of MET-addiction. The antagonistic effect between Crizotinib and Apilimod in GTL16 PTEN KO cells would support this hypothesis. More studies are needed to demonstrate that the hypersensitivity to TKI showed by the PTEN KO cells is indeed dictated by PIKfyve activity. If this hypothesis were true, then this would be an interesting research topic to explore. Understanding the mechanism behind MET-PIKfyve interaction opens up the possibility to being able to phenocopy the GTL16 PTEN KO TKI hypersensitivity in the parental model. Ultimately, this could help us to induce a more pronounced response to MET inhibitors.

PIKfyve inhibition has been previously linked to c-Met downregulation (after 2 hours of treatment), with no effects on receptor degradation (de Lartigue et al., 2009). We were unable to document a MET downregulation via western blotting, probably because of the shorter timepoint chosen. Nonetheless, the link between MET and PIKfyve is extremely appealing given the limited efficacy of MET inhibitors in the clinic.

Given the relevance of a potential role of PIKfyve in modulating MET inhibitors responses, we decided to explore this line of investigation in more details in Chapter 6.

Chapter 6. PIKfyve as a potential therapeutic target in MET-addicted cancers

6.1 Introduction

6.1.1 PIKfyve controls pleiotropic cell functions

PIKfyve is a 237 kDa evolutionary conserved protein that binds to PI and PI(3)P to synthesize PI(5)P and PI(3,5)P_2, respectively. Through its lipid kinase activity, PIKfyve plays a role in endocytic membrane genesis and regulation. PIKfyve has also been shown to have protein kinase activity, and it is therefore conceivable that it carries out additional cellular functions, the majority of which are yet to be unveiled (Shisheva, 2008). For instance, it has been proposed that PIKfyve is capable of DNA binding. This property of PIKfyve is consistent with other described nuclear functions, such as mediating the translocation of EGFR to the nucleus, a phenomenon that is observed in some cancer models (Kim et al., 2007).

One of the substrates of PIKfyve protein kinase activity is PIKfyve itself, suggesting that PIKfyve is regulated by different levels of autophosphorylation (Sbrissa et al., 2000). Phosphorylation of the C-terminal catalytic domain, however, is insufficient to stimulate PIKfyve activity. This evidence, along with the presence of a chaperonin-like domain in the protein sequence, would suggest that PIKfyve interaction with regulatory elements and other proteins is essential for its activity (Shisheva, 2008). The relevance and role of phosphorylated PIKfyve in relation to its cellular function is unclear and needs further investigation (Shisheva, 2008).

Overall PIKfyve appears to regulate important cellular processes, given the embryonic lethality of PIKfyve null mutants in *Drosophila* and *C. elegans* (Nicot et al., 2006; Rusten et al., 2006).

The lipid products of PIKfyve, PI(5)P and PI(3,5)P_2, are two very important cellular phosphoinositides that range in concentration from undetectable to approximately 5% of all cellular PIs (Ikonomov et al., 2001; Sbrissa et al., 2002a). They have been

associated not only with endocytic pathways, but also with intracellular signalling and human diseases (Hasegawa et al., 2017).

PI(5)P is found in nuclear membranes, as well as at the plasma membrane and early endocytic vesicles. It has been linked to early endosomal dynamics (Boal et al., 2015; Ramel et al., 2011), and cytoskeletal rearrangements that promote cell migration (Viaud et al., 2014). PI(5)P generation by PIKfyve has also been linked to noncanonical autophagy and to autophagosome biogenesis in HeLa cells. Noncanonical autophagy potentially exists alongside, or in some instances (such as in cancer cells) in place of, the PI(3)P-driven canonical autophagy cycle (Vicinanza et al., 2015). PIKfyve has also been implicated with the canonical PI(3)P-driven autophagy as a negative regulator of endosomal fusion (Raiborg et al., 2013).

$PI(3,5)P_2$ is the PI(3)P-derived product of PIKfyve activity. Although defects in $PI(3,5)P_2$ generation have been linked to numerous diseases, particularly neurodegenerative disorders, its cellular roles are still unclear. It is thought to localise to both early and late endosomes, as well as lysosomes and vacuoles (Takatori et al., 2016). A strong link between this phosphoinositide and vacuolation has been established; a decrease in $PI(3,5)P_2$, in fact, leads to endomembrane swelling and vacuolation (Ikonomov et al., 2002).

Given its strong links to both PI(5)P and $PI(3,5)P_2$, PIKfyve is believed to co-localise with both phosphoinositides on early and late endosomes. However, some studies, using a kinase dead PIKfyve protein, have shown that, depending on the extent of its inactivation, PIKfyve kinase activity is associated with multiple intracellular compartments. Low levels of kinase deficient PIKfyve cause the formation of large EEA1-Rab5-positive vesicles (Ikonomov et al., 2001, 2006). However, longer incubation times with the kinase deficient protein cause the formation of enlarged translucent vacuoles that may originate from late endocytic compartments (Ikonomov et al., 2003a). PIKfyve does not seem to be necessarily physically associated with these structures; nonetheless, the lack of its kinase activity is probably the source of the observed membrane trafficking imbalance.

Some work has been done to understand the spatial regulation of PIKfyve function. However, there is wide variability in PIKfyve localisation depending on cell type (Ikonomov et al., 2006; Rohn et al., 2000; Shisheva et al., 2001), expression levels and the rate of PI(3)P to PI(3,5)P_2 conversion (Ikonomov et al., 2006). There may also be additional mechanisms of PIKfyve regulation that are currently not being considered or are incompletely understood (Shisheva, 2008). For instance, a fraction of PIKfyve shows PI(3)P-independent PI3K-dependent membrane localisation, the functional relevance of which is not fully understood (Rutherford et al., 2006; Sbrissa et al., 2002b).

Importantly, the role of PIKfyve in the trafficking of cargo-loaded vesicles is likely to be relevant in the context of RTK signalling dependency. In yeast, PIKfyve is involved in cargo degradation (Odorizzi et al., 2000). However, this is not the case in mammalian systems, in which RTK degradation is not affected by a kinase dead PIKfyve (Rutherford et al., 2006), despite its association with intraluminal invaginations (Ikonomov et al., 2003a). PIKfyve instead seems to play an essential role in the formation of intermediate vesicles from early endosomes (Ikonomov et al., 2006; Sbrissa et al., 2007). These intracellular structures do not have markers of either early or late endosomes, but are essential in cargo-loaded vesicle trafficking (Gruenberg and Stenmark, 2004; Rink et al., 2005). Although PIKfyve may not contribute directly to RTK downregulation, it still plays an important role in receptor (and other cargo) internalisation and trafficking to destinations that may be different to the canonical late endocytic vesicles. The vacuolisation observed upon PIKfyve activity impairment is in fact an effect of this de-regulated membrane trafficking (Shisheva, 2008).

Apilimod is a very promising PIKfyve inhibitor currently in clinical trials as an anti-cancer drug (Harb et al., 2017).

Apilimod was originally identified as an inhibitor of Toll-like receptor-induced interleukin 12 (IL-12) and IL-23 production (Cai et al., 2013). Clinical trials were undertaken to test Apilimod's efficacy in T helper 1 (Th1) and Th17-driven diseases (Burakoff et al., 2006; Wada et al., 2012), but ultimately no efficacy was demonstrated (Krausz et al., 2012; Sands et al., 2010).

Despite the lack of success of these clinical trials, further studies started linking PIKfyve to tumour invasiveness and migration (Dupuis-Coronas et al., 2011; Oppelt et al., 2014). IL-23 itself in fact seems to be responsible for connecting inflammation-driven tumour growth to the failure of immune cells in penetrating tumours (Harris et al., 2007; Langowski et al., 2006). Since then, Apilimod has been explored as an anti-cancer drug. For instance, it has shown antiproliferative effects in NSCLC cell line models, which have been demonstrated to express IL-23 (Baird et al., 2013). Importantly, Apilimod has been shown to have selective cytotoxicity against B-cell non Hodgkin lymphoma via targeted PIKfyve inhibition (Gayle et al., 2017).

The mechanisms behind Apilimod-induced cell death are unclear, and it is still unknown whether Apilimod-mediated cell death is dependent on IL-23 expression. Apilimod-induced cell killing in cancer cells is associated with increased vacuolation and release of exosomes. Its activity has been linked to autophagy due to the autophagy-related proteins contained in the exosomes, such as p62 (Hessvik et al., 2016). One study has also shown the efficacy of Bafilomycin at reversing Apilimod-induced vacuoles formation, via counteracting endosomal fusion (Sbrissa et al., 2018). Bafilomycin inhibits H^+-ATPases and counteracts acidification of endosomes, lysosomes and phagosomes (Bowman et al., 1988). Therefore, intracellular pH may also be an important factor in Apilimod-mediated cell death.

The antiproliferative effects of Apilimod treatment in some cancer cell lines and its progress in clinical trials are encouraging. However, it is essential that we understand its mechanism of action. Particularly, given the relevance of autophagy in disease, and the possible link between PIKfyve inhibition and autophagy de-regulation, it is key that we investigate this connection.

6.1.2 Autophagy: a cellular mechanism between tumour suppression and oncogenic functions

Autophagy is a self-degradative process that cells employ to remove misfolded proteins, damaged organelles and intracellular pathogens or to balance energy resources (Glick et al., 2010). There are three main types of autophagy.

Microautophagy refers to when the lysosome itself proceeds to engulf intracellular material to degrade it. Chaperone-mediated autophagy is mediated by heat shock protein 70 (Hsc70) and cochaperons, which recognize a specific sequence on target proteins and aid their translocation onto the lysosome. Finally, macroautophagy, which will be discussed in more detail below, is the best studied and most prevalent form of autophagy in cells (Mizushima and Komatsu, 2011). We will hereafter refer to this last type of autophagic process as simply autophagy.

The formation of a phagophore marks the beginning of the autophagic process. Although the origin of the phagophore is controversial (Axe et al., 2008; Simonsen and Tooze, 2009), it seems to originate primarily from the endoplasmic reticulum (ER) (Hayashi-Nishino et al., 2009). This membrane sac engulfs intra-cellular cargo or damaged organelles forming a double-membrane autophagosome. The autophagosome then fuses with the lysosome to form the so-called autolysosome. The hydrolases contained in the acidic lysosomal compartment proceed with cargo degradation. The useful by-products of degradation, such as amino acids, are recycled back to the cytoplasm (Glick et al., 2010; Xie and Klionsky, 2007) (Figure 6.1).

The autophagic process in mammalian cells is not entirely understood, but it seems to be tightly regulated by a number of important players. The most well known protein involved in phagophore formation is Vps34, a class III PI3K. It complexes with Atg6/Beclin-1 and generates PI(3)P from PI (Backer, 2008). PI(3)P is essential to promote the recruitment of other Autophagy-related (Atg) proteins to the phagophore and thus promotes its maturation (Xie and Klionsky, 2007) (Figure 6.1).

Depending on the specific signalling events and conditions that trigger autophagy initiation, additional components can nucleate the Vps34-Beclin-1 complex. One well-characterised interactor is B-cell lymphoma 2 (Bcl-2). Bcl-2 interaction with Beclin-1 at the ER contributes to autophagy inhibition (Maiuri et al., 2007).

Key for inducing curvature into the growing phagophore and for the recruitment of microtubule-associated protein light chain 3 (LC3B) is Atg5-Atg12-Atg16L complex formation (Figure 6.1). The formation of this complex is initiated by Atg7, which

activates and transfers Atg12 onto Atg10, which in turn promotes Atg12-Atg5 binding. This complex then conjugates with Atg16L and aids the phagophore formation. After recruitment of LC3B, the complex quickly dissociates from the autophagosome (Glick et al., 2010).

The form of LC3B protein that the Atg5-Atg12-Atg16L complex recruits to the phagophore is a lipid-modified form of the cytosolic LC3B, called LC3B-II. LC3B, in fact, is cleaved after induction of autophagy by Atg4 to generate LC3B-I. LC3B-I is then activated by Atg7 and transferred to Atg3 for its conjugation to phosphatidylethanolamine (PE). This process generates LC3B-II. LC3B-II is involved in the fusion of membranes and cargo selection (Glick et al., 2010).

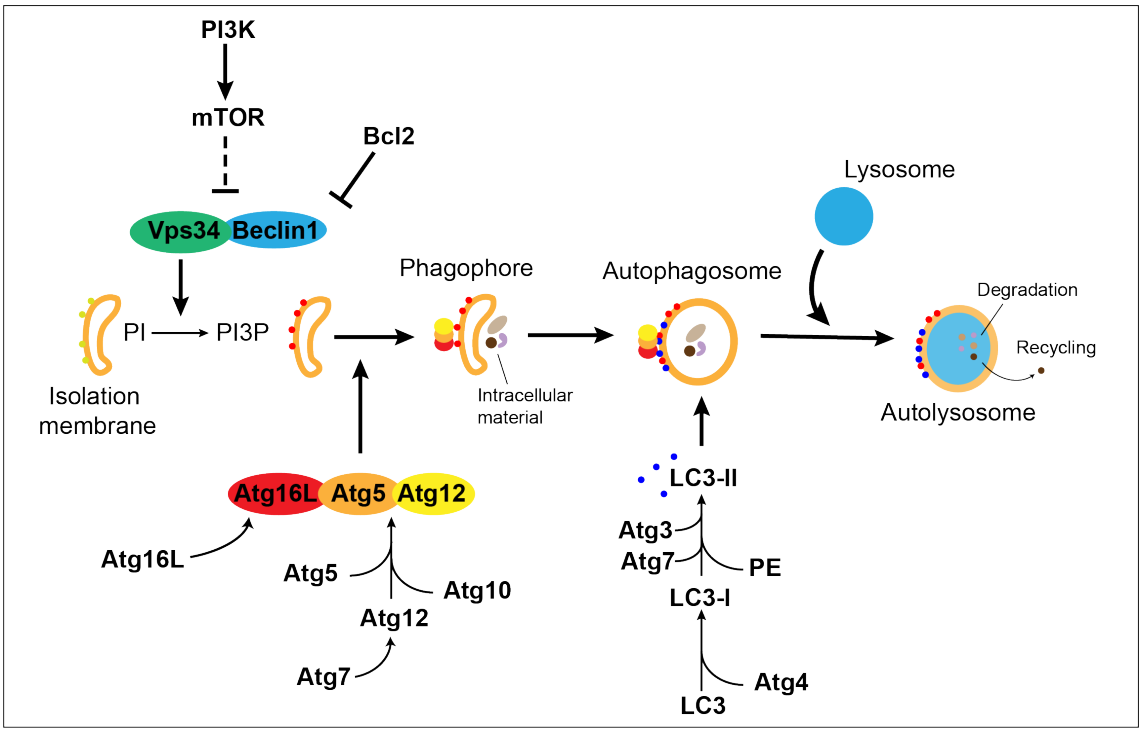

Figure 6.1 Overview of the autophagic process in eukaryotic cells

Schematic representation of the eukaryotic autophagic process.

LC3B-II regulates cargo selection with the help of accessory proteins, one of which is p62. p62 interacts with poly-ubiquitinated cargo, and with LC3B-II via an LC3-binding domain. The formation of this bridge allows for the loading of poly-ubiquitinated cargo for selective autophagy (Pankiv et al., 2007). p62 is not the only autophagy receptor, in fact roughly two dozen of them have been identified (Stolz et al., 2014), highlighting the highly regulated nature of this cellular process.

Autophagy has long been considered a Vps-34/PI(3)P-dependent process. However, Vps-34-independent autophagy has also been reported (Codogno et al., 2012; Plowey et al., 2008; Zhu et al., 2007). This non-canonical form of autophagy is potentially regulated by another phosphoinositide, PI(5)P, which also appears capable of promoting Atg5-Atg12 conjugation (Vicinanza et al., 2015).

Atg protein conjugation is also usually considered a marker of autophagy. However, this notion has recently been challenged by a mouse study that shows that inhibition of autophagy can be achieved without affecting Atg conjugation, or LC3B-II lipidation (Ueno et al., 2008). In this study, the targeted deletion of PTEN in murine hepatocytes caused inhibition of autophagy, with a reduction in both autophagosome and autolysosome numbers. However, no change in Atg5-Atg12 conjugate levels was detected (Ueno et al., 2008).

This is not the first time that PTEN has been implicated in autophagy. Some evidence suggests that PTEN loss mediates Trastuzumab resistance in breast cancer cells by causing autophagic defects (Ning et al., 2016). PTEN lipid phosphatase activity has also been shown to promote autophagy in colon cancer cells (Arico et al., 2001).

More generally the PI3K pathway has been tightly linked to autophagic processes. Akt, which is a PI3K canonical effector, is also an activator of mTOR, a negative regulator of autophagy (Cong et al., 2016). mTOR is a key player of autophagy; by mediating protein phosphorylation and localisation, it regulates several components of the autophagic machinery (Jung et al., 2010). Stimulation of the PI3K pathway indeed inhibits autophagy (Blommaart et al., 1997; Petiot et al., 2000), probably by virtue of mTOR upregulation.

Growth factor signalling therefore regulates mTOR activation through the PI3K pathway. Additionally, mTOR integrates nutrient-derived signalling via other regulators such as 5’ adenosine monophosphate (AMP)-activated protein kinase (AMPK) (Bai and Jiang, 2010; Kim and Guan, 2015). While the regulatory mechanisms of autophagy are partially known, the exact function of autophagy in cancer cells remains controversial.

Autophagy has, in fact, been shown to promote both tumour suppressing and tumour promoting functions. For instance, Beclin-1 is mono-allelically deleted in breast, ovarian and prostate cancer (Liang et al., 2006, 1999), supporting the tumour suppressor role of autophagy. It also seems to limit necrosis and inflammation, while preventing genome instability (Degenhardt et al., 2006). On the other hand, autophagy has also been linked to drug resistance and tumour cell adaptation (Amaravadi et al., 2007). For instance, in cancer cells with Ras mutations, dependency on autophagy for survival is often observed (Guo et al., 2011). Tumour cells have been shown to use autophagy as a mechanism to promote cell survival when nutrients are limited (Liu et al., 2013) and high basal levels of autophagy have been observed in numerous tumour types, suggesting it plays an important role in tumour maintenance (Kimmelman and White, 2017).

Although uninvestigated, we cannot rule out the possibility that non-canonical autophagic mechanisms, such as Vps34-independent autophagy, may also be relevant in cancer cells to escape TKI-induced cell death through novel pro-survival mechanisms (Vicinanza et al., 2015).

Despite its bivalent nature, autophagy clearly plays a role in cancer development. More research is, however, needed to better delineate its involvement in tumorigenic phenotypes and drug response. Due to its complex and dual nature, the role autophagy plays in cancer biology is unlikely to follow a uniform principle (Liu et al., 2013; Morselli et al., 2009), and we should expect for it to have different contributions in a tumour-specific manner (Ávalos et al., 2014).

6.2 Results

6.2.1 Apilimod antiproliferative effects in a panel of MET-dependent cell lines

Given the cell-killing activity of Apilimod as a single agent in GTL16 cells (Figure 5.7), we sought to investigate whether the activity of the PIKfyve inhibitor was linked to constitutive MET activity.

To this end, we tested Apilimod in multiple cell lines with known MET gene amplification and/or mutation. Overall, the inhibitor performed equally, if not better, than the MET inhibitor Crizotinib (Figure 6.2). Furthermore, Apilimod seemed to be effective in different MET-dependent gastric (GTL16, NUGC-4, Hs476T and SNU-638 gastric) and lung (EBC1, SBC5 and H1993) cancer models (Figure 6.2).

Importantly, the inhibitor showed no significant induction of cell death in a lung adenocarcinoma cell line, H596. This cell line, despite harbouring an exon 14-skipping MET mutation, behaves in a MET-independent fashion (Jorge et al., 2015; Liu et al., 2015). Additionally, Apilimod showed only mild activity in the mutant K-Ras alveolar adenocarcinoma cells, A549 (Figure 6.2). This result would indicate that Apilimod as a single agent is most effective in MET-addicted cancer lines and shows modest cell-killing activity in EGFR-mutant NSCLC cell lines. Additionally, Apilimod demonstrated low toxicity against other cell lines, most notably in non-transformed cells (Figure 6.2).

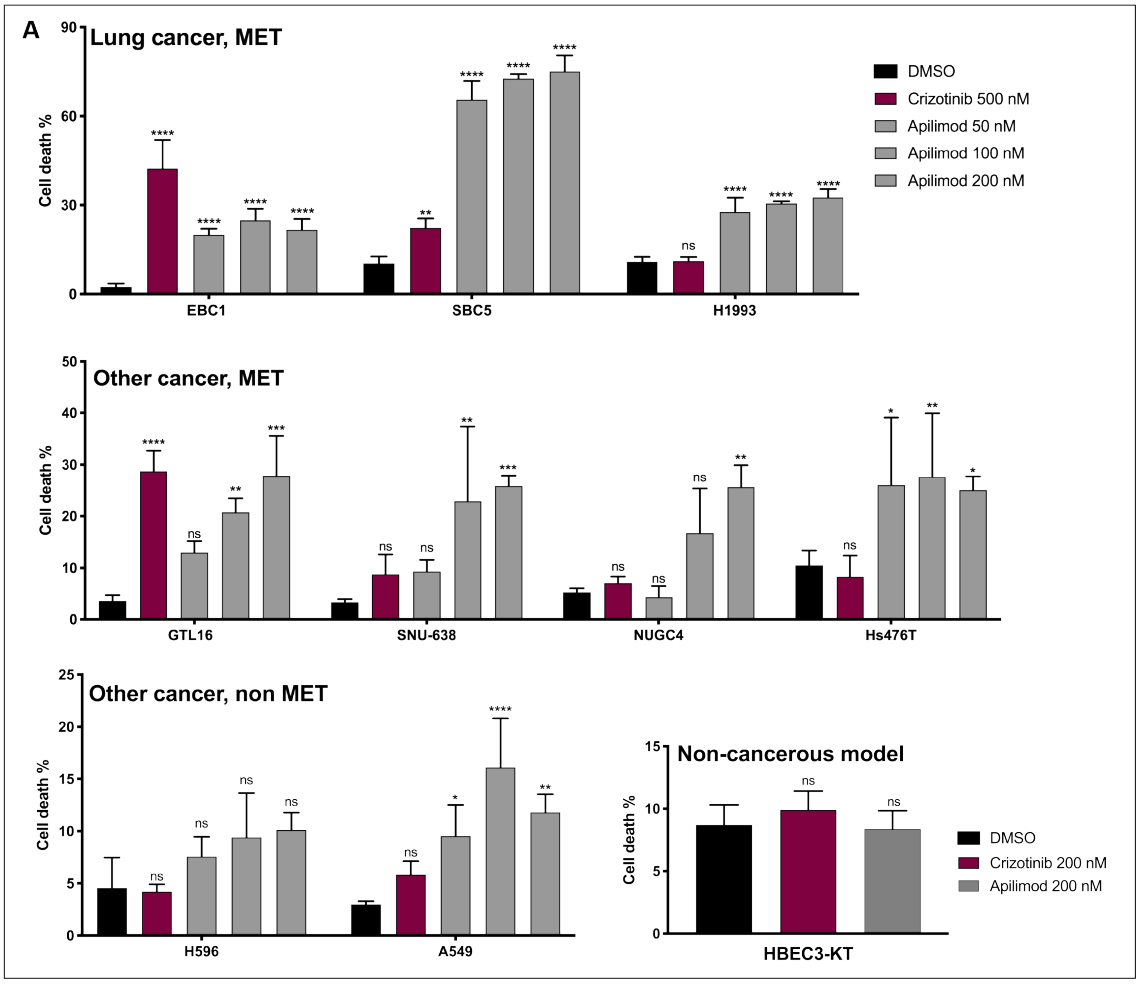

Figure 6.2 Apilimod shows antiproliferative effects on a panel of MET-addicted cancers

Analysis of the responses of a panel of cell lines to 72 h treatment with Crizotinib or Apilimod. Cell death percentages (mean ± SD) were assessed via automated trypan blue exclusion method (ViCell). n=3. ns, not significant; * significant at P <0.05; ** significant at P <0.01; *** significant at P <0.001; **** significant at P <0.0001.

A GTL16 line ectopically expressing the Apilimod-resistant PIKfyve N1939K mutant cDNA (Gayle et al., 2017) was generated to rule out the possibility that Apilimod-induced killing was due to off-target effects. Indeed, the effects of 200 ng/mL of Apilimod were fully rescued by expression of the Apilimod-resistant mutant (Figure 6.3). This cell line also showed resistance to molecular alterations triggered by Apilimod treatment (Figure 6.3).

Western blot analysis revealed that overnight Apilimod treatment affected MET receptor stability, as shown by changes in both total and phosphorylated protein levels (Figure 6.3). This supports the hypothesis that the effects of Apilimod might be linked to aberrant MET activation. Apilimod treatment also triggered

upregulation of the autophagic markers LC3B-II and p62 (Figure 6.3). An increase in LC3B-II and p62 could implicate autophagy in the yet unknown mechanism of Apilimod-driven cell death. An interesting result emerging from the Western blot analysis was the upregulation of both total and phosphorylated NDRG1 in the Apilimod treated sample. This effect was also rescued by the Apilimod resistant mutation (Figure 6.3). NDRG1 activity may therefore be linked to PIKfyve inactivation.

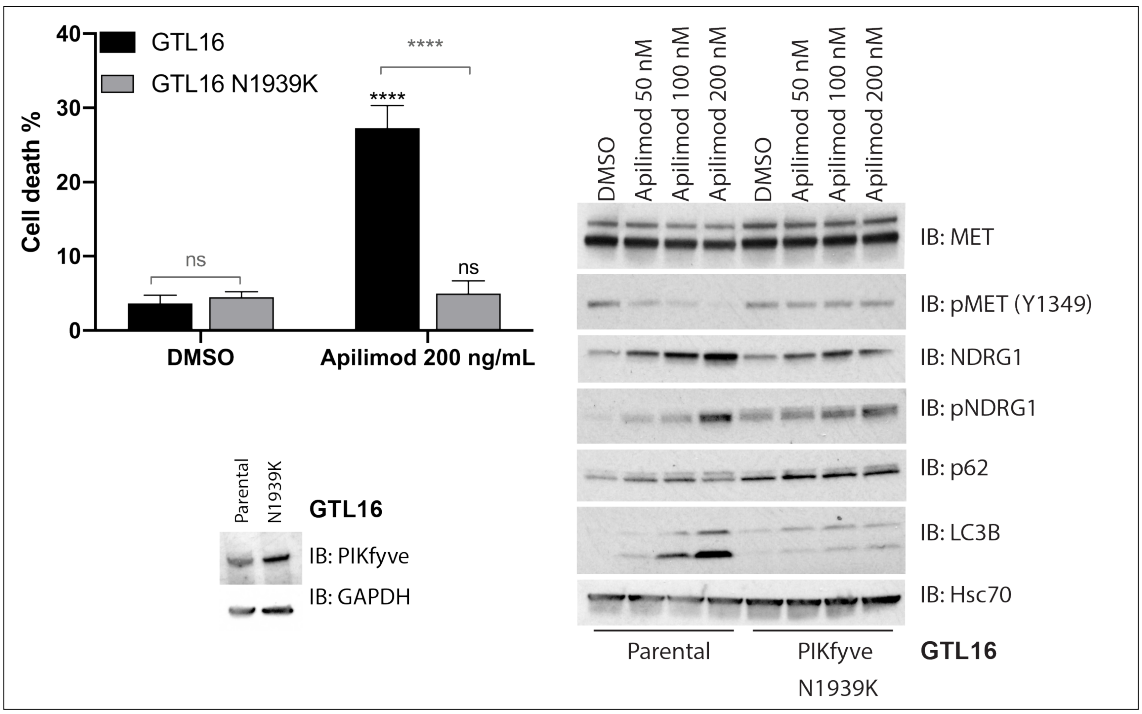

Figure 6.3 Apilimod effect is dependent on MET and may involve autophagy

Analysis of the responses of GTL16 parental and GTL16 Apilimod-resistant N1939K cells to 72 h treatment with Crizotinib or Apilimod. Cell death percentages (mean ± SD) were assessed via automated trypan blue exclusion method (ViCell). n=3. ns, not significant; * significant at P <0.05; ** significant at P <0.01; *** significant at P <0.001; **** significant at P <0.0001. Western blot analysis of GTL16 cells engineered to express an Apilimod-resistant N1939K PIKfyve construct (n=1). Western blot analysis (right) of GTL16 parental and GTL16 Apilimod-resistant N1939K cells responses to overnight treatment with Apilimod.

6.2.2 Investigating the link between Apilimod and autophagy

Given the observed upregulation of autophagic markers triggered by Apilimod treatment (Figure 6.3), we sought to investigate whether autophagy is indeed part of the mechanism of Apilimod-driven cell death.

A time course of Apilimod treatment confirmed the upregulation of LC3B-II and p62, and the concomitant downregulation of MET (Figure 6.4a). These effects were rescued in the Apilimod resistant line, showing that the molecular effects observed were indeed PIKfyve-mediated (Figure 6.4a). Once again, both total and phosphorylated NDRG1 levels were upregulated in a time-dependent manner with the PIKfyve inhibitor. Overexpression of the Apilimod-resistant form of PIKfyve caused an increase in both total and phosphorylated levels of NDRG1, which was insensitive to Apilimod treatment, unlike in the parental line (Figure 6.4a).

Using LC3B levels as a readout of autophagy in immunoblotting experiments is a controversial topic. LC3B-II, in fact, correlates with autophagosome formation, but not necessarily with autophagic flux. LC3B-II is indeed itself degraded by autophagy. (Mizushima and Yoshimori, 2007). In some cases, a comparison with known inducers and inhibitors of autophagy can help to understand the modulation of LC3B-II levels. Torin is a known inducer of autophagy, via inhibition of the mTOR pathway (Wang et al., 2015a). Bafilomycin, instead, by preventing the acidification of endosomes and lysosomes (Yamamoto et al., 1998), inhibits autophagy and leads to an upregulation of LC3B-II (Redmann et al., 2016).

Bafilomycin and Torin were therefore used alone or in combination with Apilimod to understand whether the PIKfyve inhibitor behaves like an autophagy inhibitor or as an autophagy inducer. As single agent, Apilimod resembled Bafilomycin rather than Torin, as determined by the upregulation of LC3B-II. Nonetheless, there were some Apilimod-specific effects, such as the reduction of total levels of MET and the upregulation of phosphorylated NDRG1. Bafilomycin counteracted these effects when combined with Apilimod, a puzzling result given that single agent treatments suggested a similar mode of action for these two drugs. Torin also counteracted the effects of Apilimod on MET and NDRG1 phosphorylation, and LC3B lipidation. However, this was not the case for the Bafilomycin-Torin combination that, with the exception of pNDRG1, looked different compared to the Apilimod-Torin treatment (Figure 6.4b).

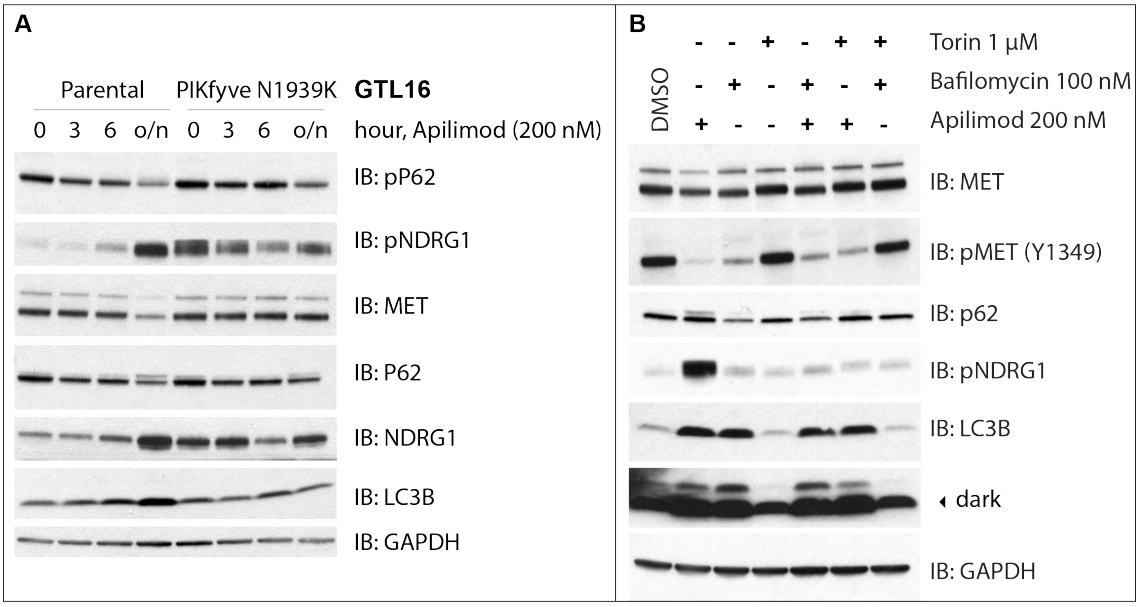

Figure 6.4 Autophagic markers are upregulated by long exposure to Apilimod

(A) Western blot analysis of GTL16 parental and GTL16 Apilimod-resistant N1939K cells responses to 0, 3, 6 h or overnight (o/n) treatments with Apilimod. **(B)** Western blot analysis of GTL16 parental cells responses to overnight treatment with Apilimod, Torin, Bafilomycin alone or in combination.

A plausible explanation for the results observed in Figure 6.4b is that Apilimod has both autophagy-dependent (i.e. LC3B lipidation) and autophagy-independent (i.e. NDRG1 phosphorylation) mechanisms of action. It therefore remains unclear whether Apilimod modulates autophagy, and whether it does so by interfering with autophagic flux.

Another inhibitor of autophagy, the Vps-34 inhibitor SAR-405, was therefore used as an additional control for the induction of p62 and LC3B-II and to compare it to Apilimod. By inhibiting Vps34, SAR-405 blocks endocytic trafficking from late endosomes to lysosomes (Pasquier, 2015). Apilimod resembled SAR-405 in LC3B-II and p62 induction, but was not as efficient at increasing p62 phosphorylation (pP62) levels (Figure 6.5a). Additionally, a mild additive effect was observed when SAR-405 and Apilimod were combined (Figure 6.5b). Overall, this could suggest that both drugs inhibit autophagy.

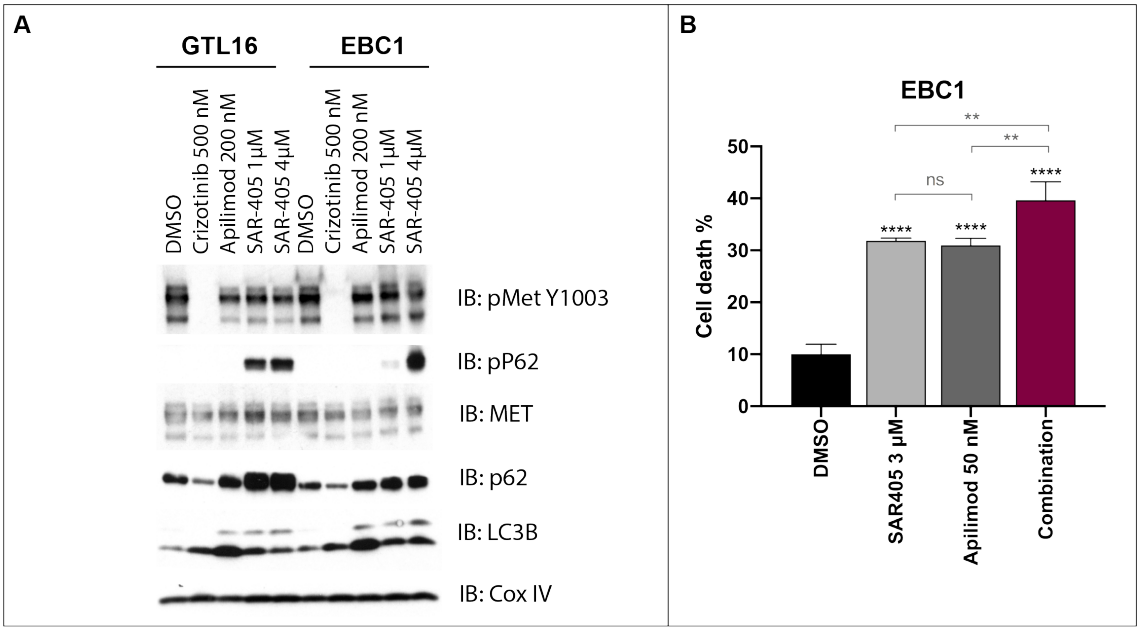

Figure 6.5 A comparison with the Vps-34 inhibitor, SAR-405, suggests that inhibition of autophagy is not the sole mechanism of action of Apilimod

(A) Western blot analysis of GTL16 and EBC1 cells responses to overnight treatment with Crizotinib, Apilimod or SAR-405. **(B)** Analysis of the responses of EBC1 to 72 h treatment with Apilimod and SAR-405 alone or in combination. Cell death percentages (mean ± SD) were assessed via automated trypan blue exclusion method (ViCell). ns, not significant; * significant at P <0.05; ** significant at P <0.01; *** significant at P <0.001; **** significant at P <0.0001.

Based on evidence in the literature, Vps34 could be the main PI(3)P source for PIKfyve activity (Ikonomov et al., 2015). This supports the hypothesis of an epistatic relationship between Vps34 and PIKfyve, which is also in line with our data (Figure 6.5b). However, the evidence still fails to definitively implicate autophagy in PIKfyve activity, and, consequently, in Apilimod-driven cell death mechanism. On the other hand, this does not exclude the possibility that Vps34 and PIKfyve may be in the same autophagy-unrelated pathway implicated in Apilimod toxicity.

In order to clarify the role of autophagy in Apilimod-driven cell death mechanism, a new strategy to measure autophagy was adopted. Measuring autophagy in general is quite complex and all available methods have caveats (Klionsky et al., 2016). However, one particular method has claimed to measure true autophagic flux in a quantitative manner (Gump and Thorburn, 2014). Cells are engineered with a mCherry-EGFP-LC3 construct that allows for quantification via a flow cytometer. The technique relies on EGFP sensitivity to low pH, such as it is found in

lysosomes or autolysosomes. The acidity found in such cellular compartments in fact causes the loss of green fluorescence from EGFP (Kimura et al., 2007). Therefore, the higher the autophagic flux, the lower the GFP signal and the higher the mCherry/GFP ratio (Figure 6.6) (Gump and Thorburn, 2014).

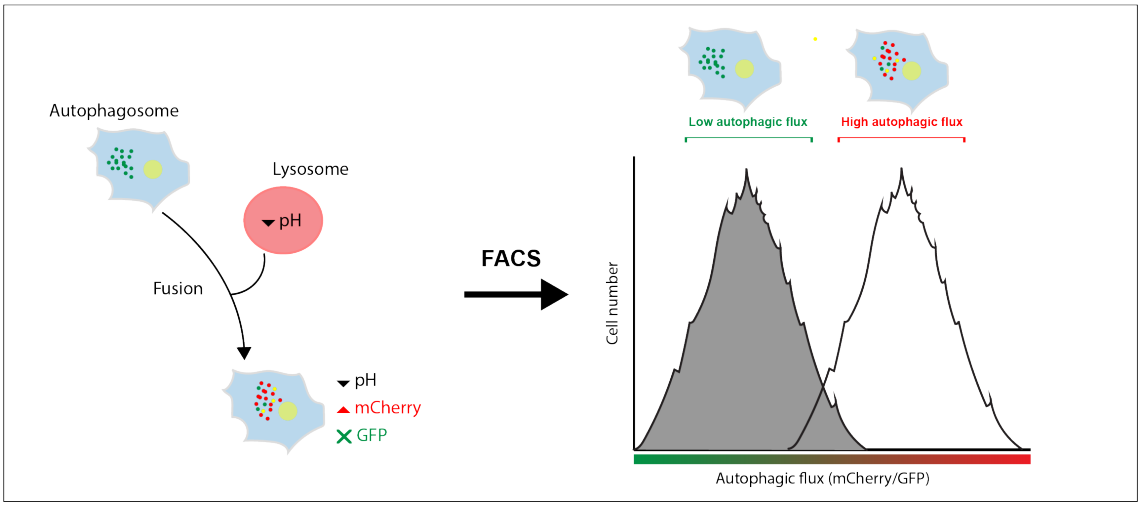

Figure 6.6 The rationale behind mCherry-EGFP-LC3 engineered lines

Cells that have been engineered with a mCherry-EGFP-LC3B construct will fluoresce green/yellow at steady state. Upon autophagy induction, due to EGFP instability in the low pH of lysosomes, cells will shift to fluoresce mainly in the red spectrum.

GTL16 cells were therefore engineered with a mCherry-EGFP-LC3 construct. An initial qualitative analysis of GTL16 cells studied with confocal microscopy showed how the EGFP signal was efficiently reduced in the Torin control. More of the red (mCherry) signal was present with the Torin treatment, indicative of higher autophagic flux, as expected. However, neither Apilimod, nor Bafilomycin, showed much distinction from the DMSO control, suggesting that in both cases there was no increase in the autophagic flux (Figure 6.7a).

Interestingly, a MET staining in this cell line revealed an Apilimod-driven change in MET localisation (Figure 6.7b). Apilimod triggered pronounced vacuolisation, with the appearance of MET-positive intracellular structures surrounded by LC3B. Unfortunately, no other marker for autophagy was used, and it is still unclear whether the vacuoles induced by Apilimod treatment are autophagic vesicles.

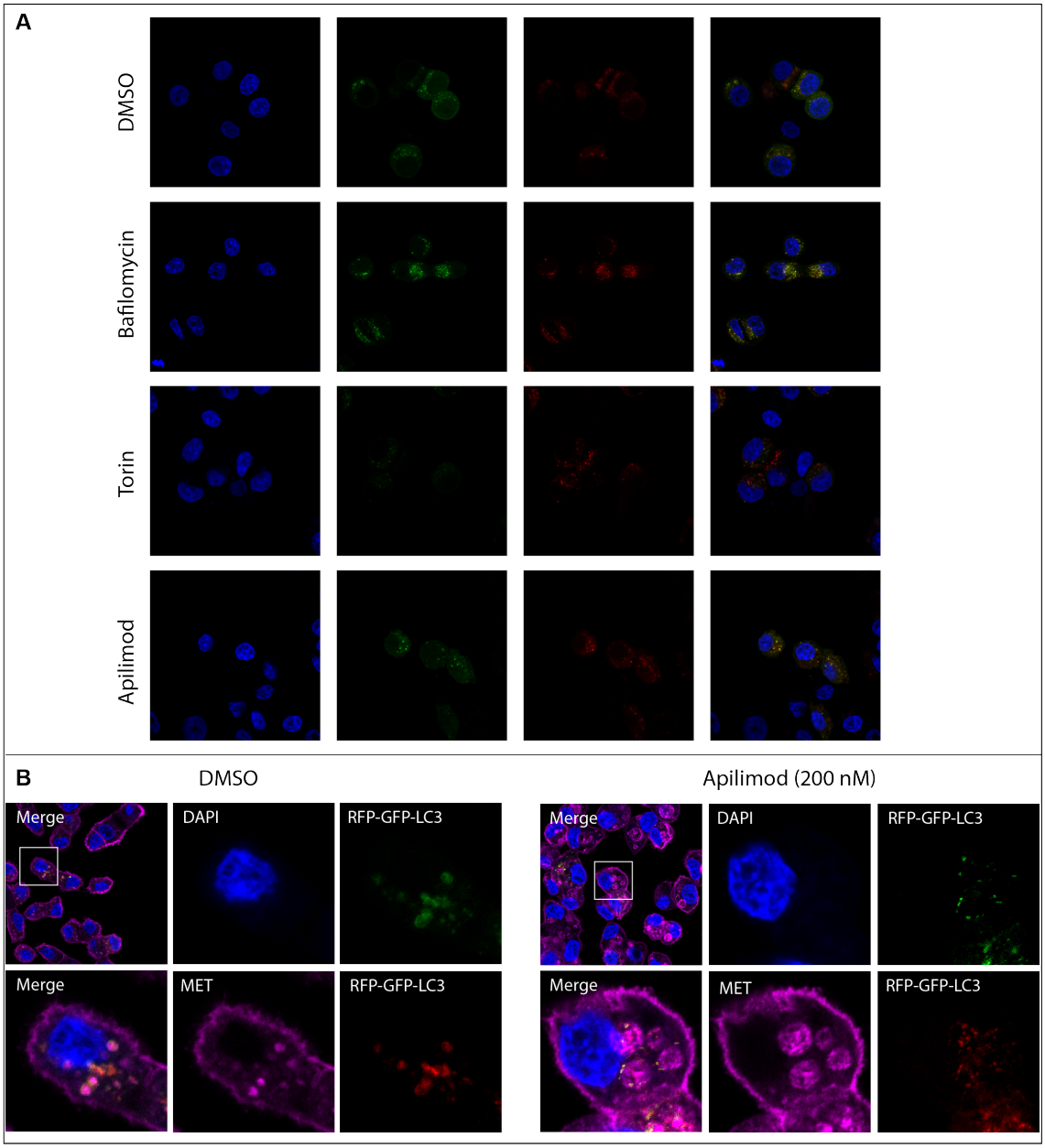

Figure 6.7 Qualitative analysis of mCherry-EGFP-LC3 GTL16 engineered line

(A) Confocal microscopy of GTL16 mCherry-EGFP-LC3B cells. Cells were treated with Bafilomycin (100 nM), Torin (1 μM) or Apilimod (200 nM) overnight. **(B)** Confocal microscopy of GTL16 mCherry-EGFP-LC3B cells co-stained with MET antibodies (magenta). Cells were treated with Apilimod (200 nM) overnight.

A more quantitative analysis of the effects of Apilimod on autophagy was carried out via flow cytometry (Figure 6.8). The effects of Bafilomycin, Torin and Apilimod on autophagic flux became clear only after overnight treatment. As expected, Bafilomycin inhibited basal autophagy, as determined by a subtle left shift in the mCherry/GFP curve. Torin instead clearly induced autophagy, given the marked

shift to the right (higher mCherry/GFP ratio). Interestingly, Apilimod did not induce a shift in the curve and it did so only very mildly after 24 hours.

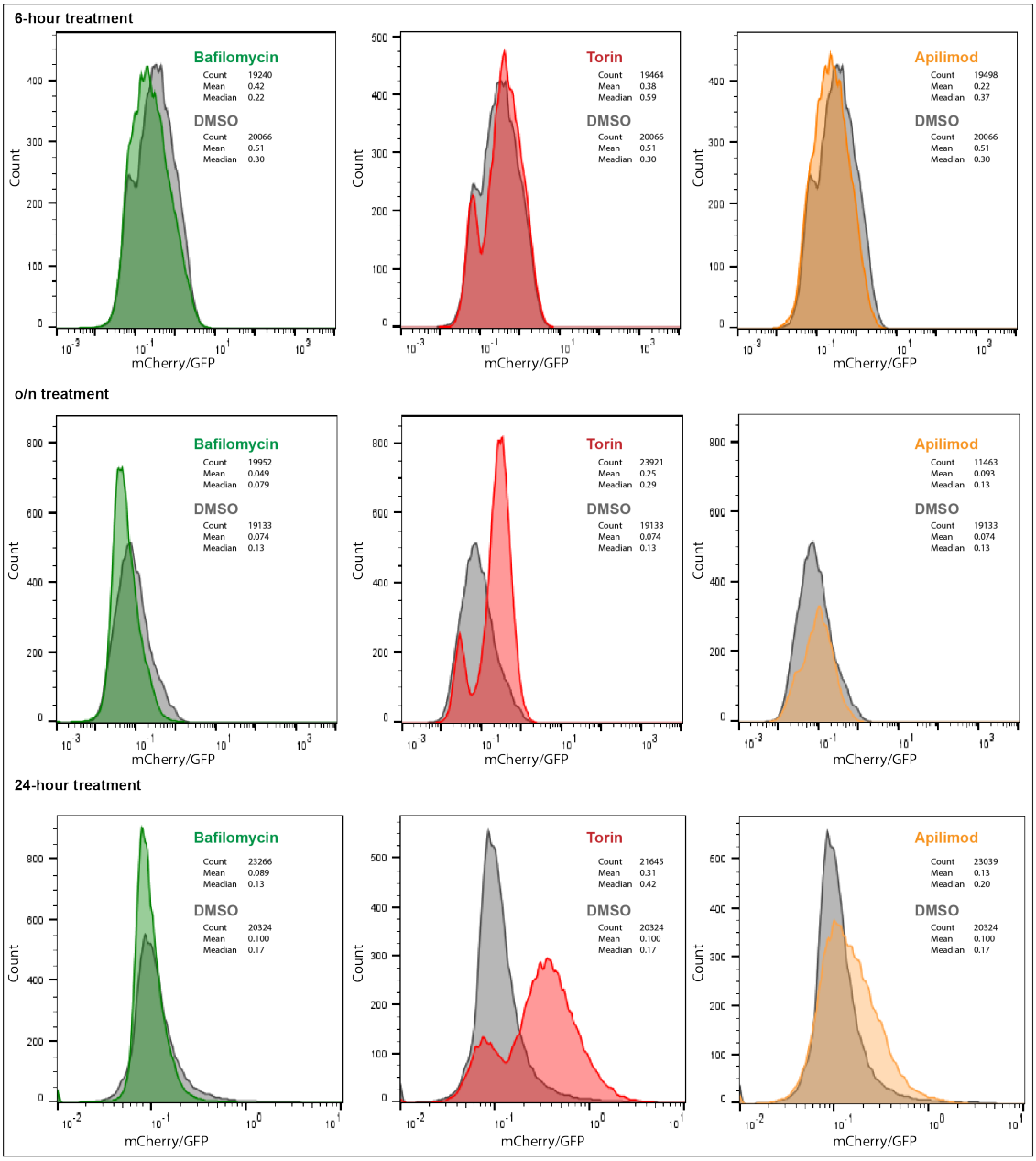

Figure 6.8 Quantitative analysis of mCherry-EGFP-LC3 GTL16 engineered line

FACS analysis of autophagic flux in GTL16 mCherry-EGFP-LC3B cells. Cells were treated with Apilimod (200 nM), Bafilomycin (100 nM) or Torin (1 μM) for 6 h, overnight or 24 h.

The quantitative analysis of mCherry-EGFP-LC3 GTL16 cells would suggest that Apilimod treatment did not increase the autophagic flux. However, given the only marginal shift in the mCherry/GFP curve caused by Bafilomycin, we cannot definitively conclude that Apilimod fully recapitulated the autophagy-inhibitor

phenotype. Nonetheless, Apilimod clearly induced dramatic vacuolisation (Figure 6.7). The nature of this vesicle defect remains unclear.

We continue to explore autophagy involvement in Apilimod-induced cell death. Some data (not shown) generated by other members of the lab provide evidence that autophagy, or at least canonical autophagy, is not involved in Apilimod-mediated cell death. For example, knocking out Atg7 in GTL16 cells, did not appear to affect Apilimod response.

The mode of action of Apilimod therefore remains an open subject of research.

6.2.3 Phosphoproteomics and proteomics: unbiased approaches to understand the mechanism of Apilimod cell-killing activity

Given that autophagy could not explain Apilimod-mediated cell death, an unbiased approach was chosen to try identifying other pathways involved in the phenotype. For reasons already explained in Chapter 5, the MS-based phosphoproteomics method was used. We chose to compare the effects of Apilimod on the phosphoproteome of both parental GTL16 cells and GTL16 cells ectopically expressing the Apilimod-resistant PIKfyve N1939K mutant cDNA. After a rapid analysis of the MS data, and due to time constraints, only one interesting phosphopeptide was chosen for further validation. Nonetheless, the data generated is currently being analysed in more detail to identify potential key modulators of Apilimod-driven cell death.

Retinoblastoma associated protein 1 (Rb1) was one of the phosphopeptides associated with a strong signature in the analysis of the phosphoproteomics data. In the GTL16 parental line, Apilimod caused Rb1 dephosphorylation. This effect was rescued in the Apilimod-resistant mutant line, suggesting the effect was PIKfyve-dependent (Figure 6.9a). Indeed Rb1 phosphorylation was reduced with Apilimod treatment, as determine by a reduction in phosphorylated Rb1 levels. This was confirmed by a shift in total Rb1 band, suggestive of a change in posttranslational motifications (Figure 6.9b).

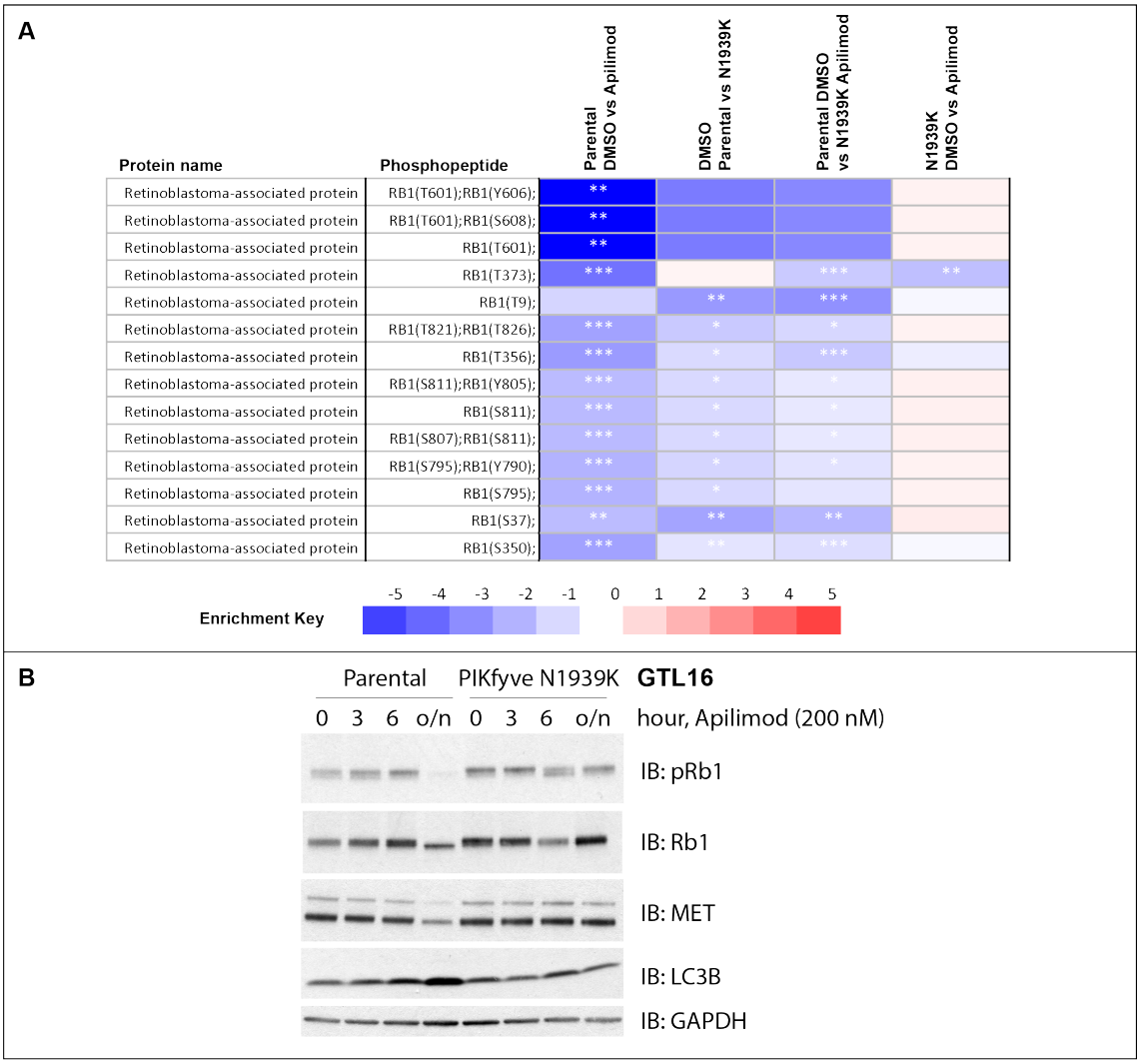

Figure 6.9 Rb1: a potential modulator of Apilimod toxicity

(A) Heatmap of fold change of KSEA analysis of Rb1. n=5. * significant at *P* <0.0400; ** significant at *P* <0.0012; *** significant at *P* <0.001; **** significant at *P* <0.0001 **(B)** Western blot analysis (n=1) of GTL16 and GTL16 Apilimod-resistant N1939K cells to Apilimod (200 nM) treatment.

Rb1 was initially chosen as an interesting hit to investigate given its important role as tumour suppressor and cell cycle regulator. Loss of Rb1 is also associated with resistance to some kinase inhibitors, including EGFR TKI (Santoni-Rugiu et al., 2019; Xing et al., 2012), and it has been linked to autophagy, as an autophagy inducer (Jiang et al., 2010a).

It remains unclear which role links Rb1 to PIKfyve activity, and whether Rb1 plays a part in Apilimod-mediated cell death, especially, as more evidence emerges against the autophagy-driven toxicity of Apilimod. However, our observations raise

the possibility that Apilimod could be used as an activator of Rb1, which could have therapeutic effects in tumours where Rb1 activity is posttranslationally suppressed.

Given the role of PIKfyve in the regulation of vesicular trafficking and autophagy, both of which are involved in protein degradation processes, we decided to explore the possibility that Apilimod-induced cell killing may be mediated by selective protein degradation. To do this, we took an unbiased approach and carried out MS-based total proteomics.

The data obtained is still under study, but a preliminary analysis revealed that the levels of a few lysosomal proteins (Cathepsin, Lysosome-associated membrane glycoprotein 2 and Sialidase) were upregulated upon Apilimod treatment (Figure 6.10). This is in line with previous work that has documented a link between PIKfyve inhibition and increased lysosome gene expression (Choy et al., 2018; Min et al., 2015). Additionally, the levels of Rab9, a small GTPase, were also upregulated upon Apilimod treatment (Figure 6.10). These data await further validation.

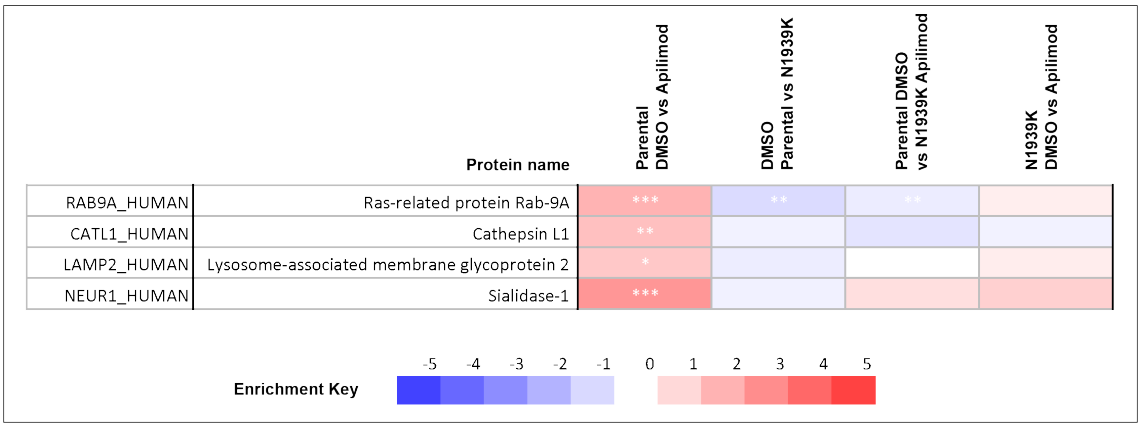

Figure 6.10 Rab9 protein levels increase with Apilimod treatment

Heatmap of fold change of proteomics analysis of Rab9. n=5. * significant at *P* <0.0400; ** significant at *P* <0.0012; *** significant at *P* <0.001; **** significant at *P* <0.0001

Interestingly, Rab9 has been shown to interact with PIKfyve to promote late endosome-to-*trans*-Golgi network trafficking (Ikonomov et al., 2003b). Nonetheless, Rab9 is also involved in lysosome biogenesis, autophagosome formation, as well as early-to-late endosomes transition (Kucera et al., 2016). To the best of our knowledge, Rab9-PIKfyve relationship at these other endosomal sites remains uninvestigated. Assuming PIKfyve interacts with Rab9 in our MET-addicted cells,

this could provide a mechanism for Apilimod-driven cell death that warrants further investigation.

6.2.4 Apilimod is a promising therapeutic strategy

Another method to try to understand the key pathways involved in Apilimod-driven cell death is by generating Apilimod resistant lines through chronic drug exposure. These cell lines will have naturally acquired resistance to the targeted therapy. The majority of the changes that the resistant lines acquire will likely be linked to essential PIKfyve-dependent pathways, and, as such, they represent potential mediators of Apilimod biology.

We therefore generated Apilimod-resistant GTL16 and EBC1 cell lines, via continuous exposure to the drug. Their resistance to Apilimod was documented in growth assays (Figure 6.11a). Additionally, GTL16 Apilimod-resistant cells displayed impaired Apilimod-induced reduction of Rb1 and MET phosphorylation, as demonstrated by western blot analysis (Figure 6.11b). However, at high dose (200 nM), Apilimod still caused upregulation of proteins such as pNDRG1 and p62 (Figure 6.11b). This could suggest that the selection of the resistant phenotype is not complete, or that cells have adopted other mechanisms of resistance, or that resistance is generated downstream or independently of these effectors.

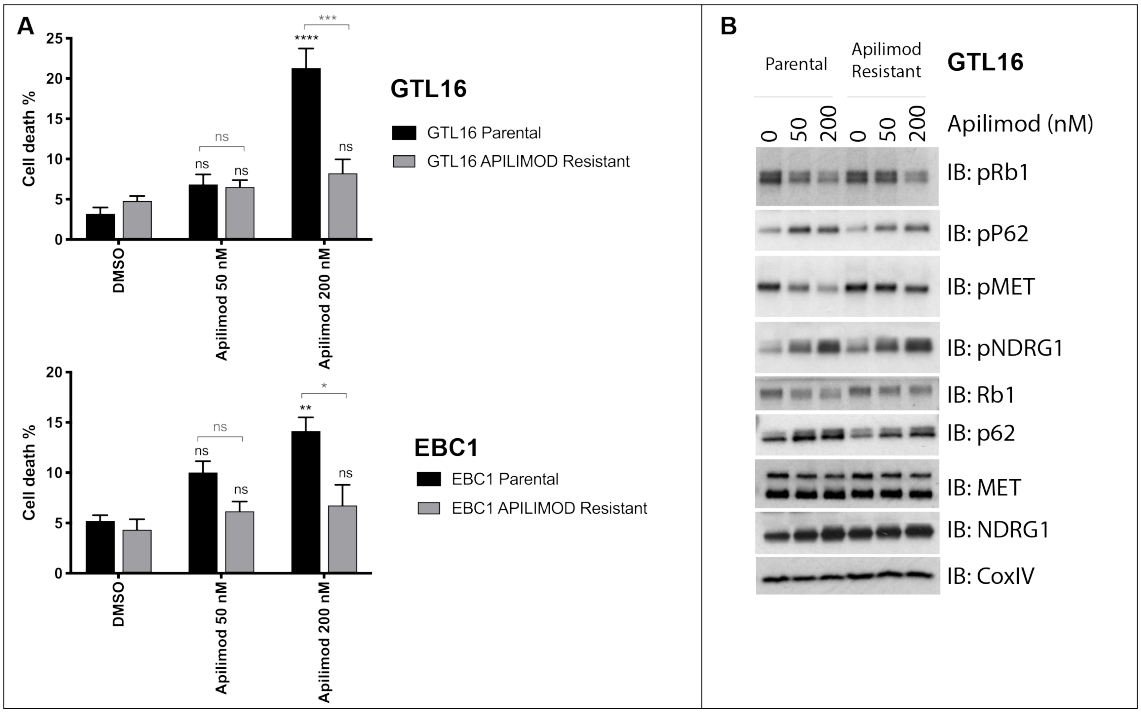

Figure 6.11 Apilimod-resistant GTL16 and EBC1 cell lines were derived by continuous exposure to the drug

(A) Analysis of the responses of GTL16 and EBC1 parental and Apilimod resistant cell lines to 72 h treatment with Apilimod. Cell death percentages (mean ± SD) were assessed via automated trypan blue exclusion method (ViCell). ns, not significant; * significant at P <0.05; ** significant at P <0.01; *** significant at P <0.001; **** significant at P <0.0001. **(B)** Western blot analysis (n=1) of GTL16 parental and Apilimod resistant cell lines responses to overnight treatment with Apilimod.

Due to time constraints, these cell lines have not undergone any further characterisation. Nonetheless, they will be invaluable tools to understand Apilimod-driven cell death and can shed light on mechanisms of acquired Apilimod resistance should this drug progress further in the clinic. Given the pronounced antiproliferative effects elicited by Apilimod, the final aim of the project is to progress the studies to xenograft models. This would allow the testing of Apilimod efficacy against cancer cells *in vivo*.

A first step towards this aim was to assess the drug toxicity in the animals. Importantly, Apilimod treatment did not cause any significant weight loss in immune-compromised mice over the treatment period (2 weeks) at either 30 or 60 mg/kg doses (Figure 6.12).

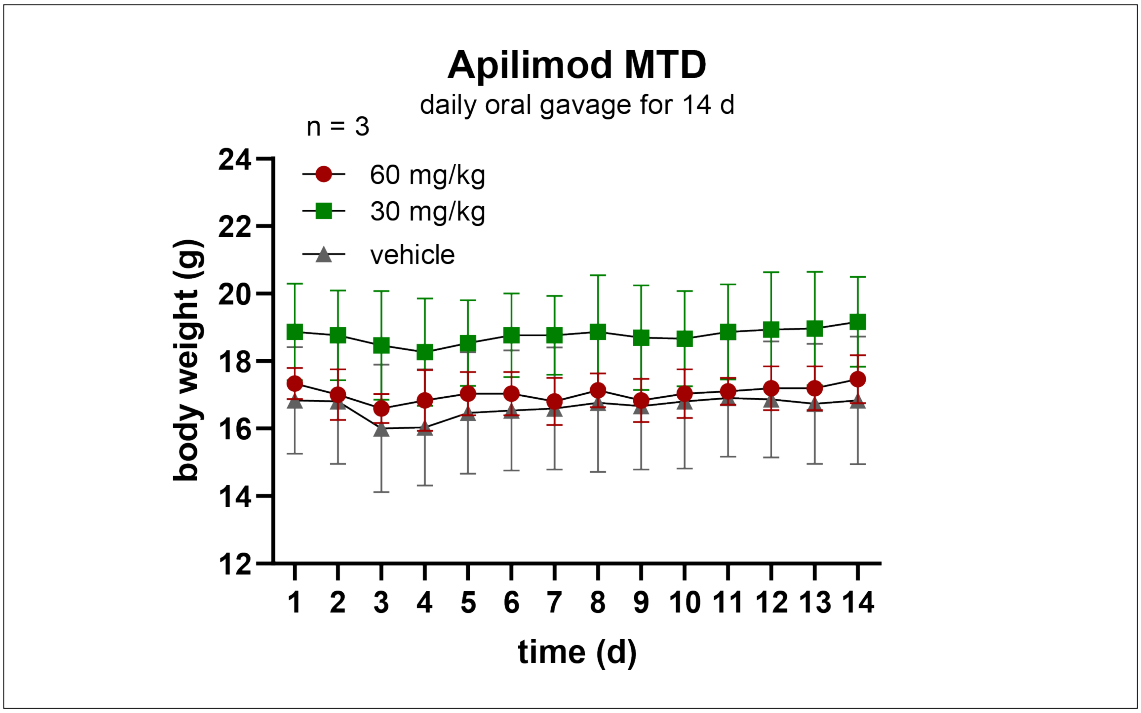

Figure 6.12 Apilimod has a low toxicity profile in mouse models

Graph of body weight of mice in Apilimod (60 mg/kg or 30 mg/kg) and vehicle treatment groups. n=3.

These promising results suggest that Apilimod is safe to use in this animal model. It now remains to be assessed whether the antiproliferative effects Apilimod had demonstrated in cell lines are also seen *in vivo*.

6.3 Discussion

To the best of our knowledge, this is the first evidence of robust single-agent cell-killing activity of Apilimod in MET-driven cancer models. We have shown the cell-killing effects of the PIKfyve inhibitor in lung, as well as gastric cancer models (Figure 6.2). Our results are also the first evidence to link Apilimod activity to the inactivation of a known oncogenic driver, MET (Figure 6.2 and Figure 6.3). These data are supported by the lack of Apilimod-driven toxicity in other non-MET cancer models (Figure 6.2). However, further research is needed to assess the nature of the connection between MET and Apilimod, and to understand whether MET-overexpression is needed for the robust single-agent cell killing activity of the drug.

An important observation is that, in various cancer cell lines with known MET gene amplification and/or mutation, Apilimod outperforms the known MET-inhibitor,

Crizotinib (Figure 6.2). At this stage, it is unclear why this is the case. One possible explanation could be that Apilimod targets a specific subpopulation of MET receptors that might be most relevant for cell survival. Understanding how Apilimod drives cell death may clarify the connection between PIKfyve and MET.

PIKfyve inhibition has previously been linked to autophagy (Hessvik et al., 2016; Sbrissa et al., 2002a), but our data failed to demonstrate the presence of a significant change in the autophagic flux (Figure 6.8). On the other hand, known autophagic markers (i.e. LC3B-II and p62) were upregulated in Apilimod treated samples and resembled the effects of two known inhibitors of autophagy, Bafilomycin and SAR-405 (Figure 6.4 and Figure 6.5). Nonetheless, combinatorial treatments with known promoters or inhibitors of autophagy led to inconclusive results (Figure 6.4 and Figure 6.5). These results seem to suggest that, if involved, autophagy may not be the only mode of action of Apilimod. Some additional preliminary data employing an Atg7 knock out model have also shown that impairing the canonical autophagy pathway does not affect Apilimod-driven cell death.

Autophagy as a mechanism of Apilimod-driven cell death cannot be completely ruled out yet. Atg7 independent autophagy has in fact been demonstrated. This cellular mechanism appears to rely on Beclin-1 (Nishida et al., 2009). We are currently investigating this hypothesis by knocking out Atg7 or Beclin-1 in GTL16 cells, both alone and in combination.

It is important to consider that, despite the fact that PIKfyve has been linked to autophagy, the kinase may have additional cellular roles. All the players in the autophagy machinery have in fact been shown to have autophagy-independent functions (Galluzzi and Green, 2019) and this possibility should be explored for PIKfyve too.

For instance, our data show a clear Apilimod-specific effect on NDRG1. Inhibition of PIKfyve, in fact, causes NDRG1 phosphorylation levels to increase; this phenotype is rescued in the Apilimod-resistant cell line (Figure 6.3 and Figure 6.4). To the best of our knowledge, a direct link between NDRG1 and PIKfyve has never

been reported. There is, however, some evidence that both share the common upstream regulator Serum/Glucocorticoid regulated Kinase 1 (SGK1). SGK1 can in fact phosphorylate both NDRG1 and PIKfyve. SGK1-mediated NDRG1 phosphorylation causes the protein to undergo degradation (Di Cristofano, 2017). When talking about NDRG1 phosphorylation, however, a distinction is necessary. Two phosphorylation sites may be relevant for the protein activity and perhaps localisation: Thr346 and Ser330. Thr346 generally marks cytoplasmic NDRG1 while Ser330 is associated with the protein that has translocated to the nucleus (Park et al., 2018). The physiological significance of these phosphorylation events is still unclear (Bae et al., 2013). This study is limited to the analysis of Thr346, and it is therefore not excluded that Ser330 phosphorylation may also have a PIKfyve-dependent role.

NDRG1 has also been linked to autophagy as a protein processing mechanism, but its functional significance is unclear (Sahni et al., 2014). Whether PIKfyve mediates NDRG1 autophagy-related activity is also an interesting hypothesis to investigate.

Another relevant piece of the puzzle is PIKfyve-dependent Rb1 phosphorylation (Figure 6.9). Rb1 is a well-known tumour suppressor gene that plays a part in a wide plethora of cellular events, including cell cycle, cell differentiation, senescence and genome stability (Chinnam and Goodrich, 2011). NDRG1 suppression in hepatocellular carcinoma (HCC) has been associated with a decrease in Rb1 phosphorylation, triggering senescence and impairing cell growth (Lu et al., 2014). In HCC, NDRG1 activity has in fact been associated with tumorigenic phenotypes, unlike in pancreatic cancer (Park et al., 2018). In GTL16 cells treated with Apilimod we also observe a decrease in Rb1 phosphorylation, which could potentially be associated with induction of cellular senescence. Given that NDRG1 activity is cancer-type dependent and that GTL16 cells have so far appeared to behave in a manner similar to pancreatic cancers, we cannot rule out that NDRG1 also contributes to the negative regulation of Rb1. Rb1 is also dependent on MET activity (Ma et al., 2003). Therefore, by suppressing MET, Apilimod could indirectly cause the observed dephosphorylation of Rb1.

Finally, total proteomics experiments suggest that Rab9 may be implicated in Apilimod-mediated cell death (Figure 6.10). We are currently investigating this

hypothesis, and we are firstly trying to determine whether PIKfyve-Rab9 relationship is indeed present in our cell line models. Assuming this interaction occurs, our current model, based on the general knowledge of Rab9 function (Ikonomov et al., 2003b), is that the interaction of the two proteins promotes late-endosome-to-*trans*-Golgi network transport. Interestingly, retrograde transport is targeted by various bacterial toxins and viral proteins to mediate cytotoxicity (Chia and Gleeson, 2011). Further to this, pharmaceutically inducing an imbalance in retrograde transport has been reported to induce cell death in cancer cells (Carew et al., 2006; Donaldson et al., 1992; Wlodkowic et al., 2009). This would suggest that retrograde transport is an important process for survival in cancer cells, and could supposedly cause cell death when, and if, inhibited by Apilimod.

However, if retrograde transport is key for general cell survival, our model fails to explain why non-transformed cells are unaffected by Apilimod treatment. One potential explanation is that PIKfyve-Rab9 relationship acquires prosurvival functions, specifically in the settings of MET-addiction. For instance, it could be playing a central role in recycling the MET receptor via retrograde transport. This could favour the accumulation of MET in endosomes, or other subcellular localisations, that might be most relevant for cell survival signalling. Some published work associating MET retrograde transport with malignant breast cancer cells (Chen et al., 2019) could support this hypothesis. The upregulation of Rab9 and some lysosomal proteins that is observed upon Apilimod treatment could be part of a compensatory mechanism triggered by loss of MET-retrograde transport or, more generally, by overall disruption of endocytic trafficking. This model awaits further investigation.

The mechanism of action of Apilimod is therefore still unclear. Research in our laboratory is ongoing using both the Apilimod-resistant lines generated (Figure 6.11), and the phosphoproteomics and proteomics data. Importantly, the Apilimod-resistant lines will also help to delineate the limitation of Apilimod as a single-agent therapeutic strategy.

The cell-killing effects of Apilimod in MET-driven cancers are exceptional. It is therefore essential that we determine whether Apilimod is indeed an effective

treatment strategy for MET-driven cancers and those tumours that have shown resistance to MET TKIs. This line of investigation is particularly relevant given the lack of success that MET inhibitors have had in clinical settings (Hughes and Siemann, 2018).

In the meantime, mouse experiments are underway to test Apilimod efficacy against MET-driven tumours *in vivo*.

Overall, the drug demonstrates a degree of specificity for MET-addicted cells *in vitro* (Figure 6.2) and has shown low levels of toxicity *in vivo* (Figure 6.12).

The data discussed in this chapter has also provided the rationale for the possible incorporation of Apilimod as a new treatment arm in the phase II genomic-driven National Lung Matrix Trial (Middleton et al., 2015), the world's largest precision medicine trial in NSCLC. This sub-study is currently being considered pending *in vivo* data demonstrating Apilimod efficacy in a NSCLC model.

Chapter 7. Discussion

RTKs are aberrantly activated in a large number of human cancers. As such, they are attractive therapeutic targets in oncology. TKIs and monoclonal antibodies (mAb) are the current main approaches to target RTKs in human cancer (Yamaoka et al., 2018). Clinical studies of various RTK-targeting agents have shown the success of these types of treatment in improving patient overall survival, as well as quality of life. However, not all patients will respond to targeted treatments, and several mechanisms of drug resistance will inevitably develop. Progressive disease therefore remains inevitable in the majority of patients who show initial benefit (Regad, 2015).

TKI resistance, mainly to EGFR and HER2 inhibitors, has been linked to the loss of PTEN. The increase in PI3K/Akt signalling outputs derived from the loss of the tumour suppressor is often considered the mechanism that drives PTEN-associated TKI resistance (Georgescu, 2010). Importantly, PTEN and PI3Ks may play nonoverlapping roles in tumorigenesis and there are controversies regarding their interplay in cancer (Chalhoub and Baker, 2009). As such, how PTEN modulates TKI responses remains an open field of investigation.

The pressing need for novel cancer treatments and the central role that RTKs and PTEN play in the progression of various cancers warrant further research on the subject.

7.1.1 PTEN loss cannot be used as a general biomarker of TKI resistance

To the best of our knowledge, this is the first time that a direct comparison between two different RTKs, MET and EGFR, has been done in the context of PTEN loss. The systematic characterisation that we have carried out has allowed us to provide the first proof-of-concept evidence that PTEN loss affects RTK physiology and TKI responses in a way that is dependent on the identity of the RTK.

Although the study is still at early stages, our data carry significant translational implications. First and foremost, based on our evidence, a re-assessment (or

refinement) of PTEN loss as a biomarker of TKI resistance is needed. Specifically, we are documenting how, in the case of MET-addiction, PTEN loss is a marker for increased TKI sensitivity.

PTEN loss-mediated sensitisation to MET TKIs has direct translational implications given the clinical failure of these drugs to-date (Hughes and Siemann, 2018). Characterising the molecular mechanisms responsible for the hypersensitivity phenotype could provide rationale to build a therapeutic strategy that aims to pharmacologically phenocopy the hypersensitivity phenotype observed in MET-models and translate it to other RTK-driven cancers.

Importantly, we also show how modulating TKI responses by targeting the canonical RTK-downstream signalling pathway is often insufficient to maximise therapeutic benefit.

7.1.2 Current hypotheses: how loss of PTEN can change receptor conformational equilibrium, signalling and localisation in an RTK-dependent manner

We have identified four potential mechanisms of PTEN-mediated resistance to EGFR TKIs:

a) a change in ATP binding:

We have shown that loss of PTEN results in a change of ATP/TKI binding to EGFR. We hypothesise that this effect is driven by an alteration in the equilibrium of membrane resident PIs due to the loss of the PI-phosphatase function of PTEN. Our evidence supports a model in which PTEN loss causes EGFR to reside in an inactive conformation more sensitive to type II inhibitors. If supported by more evidence, this result may in the future help in tailoring treatment strategies in the clinic by guiding the development of appropriate conformation-selective compounds. Our data also warrant further research on TKI-resistance with a focus on improving our understanding of receptor conformational dynamics and interactions with lipids, as these could be indirectly mediating TKI-responses.

b) a change in RTK levels:

A reduction in total and phosphorylated EGFR levels, as observed in A431 PTEN KO cells, could in itself be a mechanism of drug resistance or, more realistically, reflect the presence of one. As previously discussed, cancer cells with EGFRvIII escape TKIs and drive tumour progression (An et al., 2018; Batra et al., 1995; Moscatello et al., 1996). It is unclear if what drives EGFRvIII activity as an oncoprotein is low-level constitutive signalling (Gan et al., 2013), impaired receptor endocytosis and degradation (An et al., 2018; Grandal et al., 2007; Schmidt et al., 2003) or a combination of the above. However, we hypothesise that similarly to EGFRvIII, EGFR in A431 PTEN KO cells is maintaining low but constant activation levels. This activity, along with resistance to TKIs, is sustained by an alteration in receptor trafficking, as supported by our confocal analysis, degradation (Vivanco et al., 2010) and biophysical properties (see a above). Additionally, the possibility cannot be excluded that in the context of PTEN inactivation, kinase independent activity of EGFR may become relevant.

c) a re-wiring of EGFR-signalling including new players, such as PIKfyve:

The substantial signalling re-wiring following the loss of PTEN is evident from our phosphoproteomics analysis. We have explored one particular protein, PIKfyve, that seems to modulate TKI responses in a PTEN-dependent manner. PIKfyve is in fact upregulated upon loss of PTEN, although it is yet unclear whether it is a direct (via negative regulation) or indirect (via for instance Akt activation) effector of PTEN activity. Since PIKfyve plays an important role in endosomal trafficking pathways through its phosphoinositides kinase activity, we hypothesise that its upregulation affects TKI responses via deregulating EGFR trafficking. We have not explored this possibility in detail nor have we tested whether PIKfyve is mediating an autophagy-related mechanism of TKI resistance in A431. Nonetheless, our data suggest that PIKfyve inhibition enhances EGFR TKI activity even in the context of PTEN inactivation-driven TKI resistance.

and d) a change in LAMP1 interaction:

The clear lack of co-localisation of LAMP1 and EGFR in PTEN-deficient cells could indicate a loss of receptor downregulation. We were unable to confirm this hypothesis. Currently, we are theorizing that LAMP1-positive vesicles are sites of EGFR endocytosis and signalling. Similar to EGFRvIII, loss of PTEN could cause a decrease in EGFR endocytosis. In line with the phosphoproteomics data, loss of EGFR-LAMP1 co-localisation could be another sign of a dramatic change in patterns of cell signalling caused by the loss of PTEN.

Unlike the A431 model, loss of PTEN in GTL16 cells causes a sensitization to MET TKI. We found three main reasons for this unexpected phenotype:

a) the PI3K/Akt pathway axis acquires more importance in driving cell survival

Our data supports the hypothesis of the PI3K/Akt cascade becoming the preferred pathway for MET-mediated survival signalling in the absence of PTEN. We are currently hypothesising that uncontrolled PI3K/Akt pathway activation drives a feedback loop on the MET receptor, which ultimately causes cells to be more sensitive to MET inhibitors (see b)).

b) a change in downstream signalling

The phosphoproteomics analysis has helped to understand the extent of the change caused by PTEN inactivation on MET-dependent signalling. In particular, a large part of the PTEN KO signature resembled the signature of the parental line treated with Crizotinib. This could render PTEN KO cells more susceptible to MET inhibitors.

One particular protein we focussed on was NDRG1, as we found it to be regulated by PTEN, and also subjected to MET TKI inhibition in the absence of the tumour suppressor. We are currently using NDRG1 to build a model that, subject to further tests, would help us explain how MET TKI hypersensititvity is re-established by inhibiting the PI3K pathway (Figure 7.1). NDRG1 is in fact linked to the PI3K pathway at multiple levels: PI3K inhibition is known to restore NDRG1 expression (Bandyopadhyay et al., 2004), PTEN positively regulates NDRG1 expression

(Bandyopadhyay et al., 2004) and vice versa (Dixon et al., 2013), and NDRG1 reduces Akt phosphorylation (Sun et al., 2013). Furthermore, NDRG1 and its phosphorylated form are believed to play distinct cellular functions (McCaig et al., 2011). In view of all this, we are hypothesising that while the unphosphorylated form of NDRG1 is known to negatively regulate Akt, collaborating with PTEN, its phosphorylation may be promoted by PI3K and drive a negative feedback loop on MET (Figure 7.1). In the presence of PTEN, which may prevent NDRG1 phosphorylation, pNDRG1 levels are kept under control. However, as we have documented by phosphoproteomics and western blot analysis, loss of PTEN results in an increase of the phosphorylated form of NDRG1. This could drive MET downregulation and MET signalling inhibition, contributing to the increase in toxicity of MET TKIs. The equilibrium is re-established with PI3K inhibition by removing the NDRG1-driven negative feedback loop on MET.

It is important to understand that this interpretation of the data still awaits further confirmation and it remains unclear if and how NDRG1 negatively regulates MET.

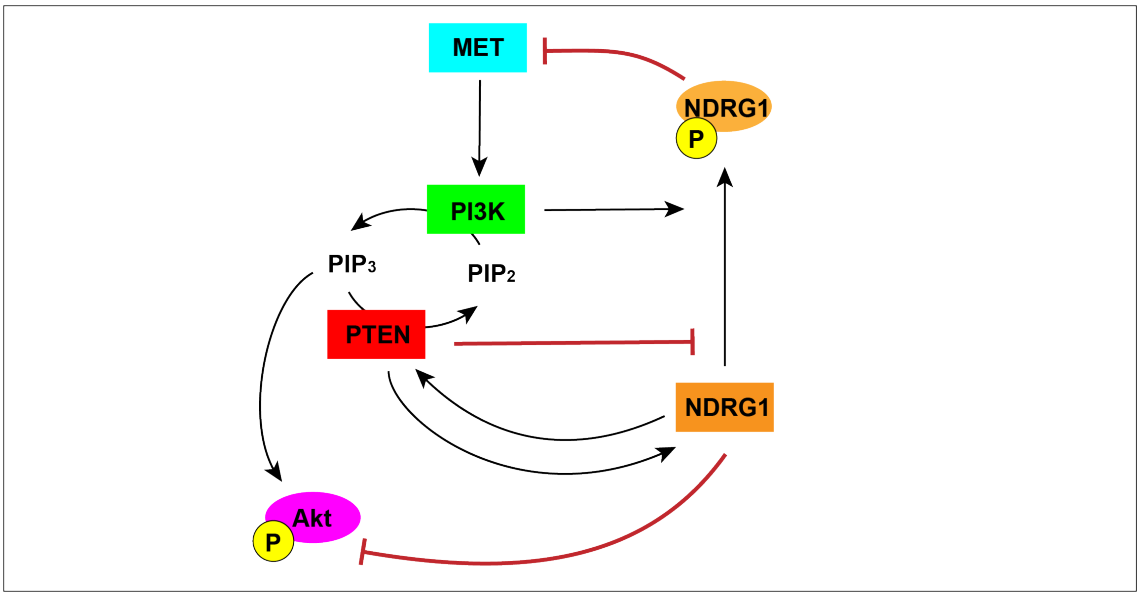

Figure 7.1 Proposed model for PTEN-dependent MET signalling rewiring

We propose that NDRG1 has a dual function in its unphosphorylated and phosphorylated forms. When unphosphorylated, NDRG1 promotes PTEN while antagonizing Akt activity. NDRG1 phosphorylation is promoted by PI3K and drives a negative feedback on MET receptor activity.

c) and MET endocytic trafficking is impaired

Based on the confocal imaging analysis we carried out, it is clear that MET endocytosis changes as a function of PTEN. Although unable to measure it, MET in

the PTEN KO cells may prevalently live on the cell-surface. The decrease in intracellular MET could partially explain the TKI hypersensitisation phenotype, because: a) more receptor could be readily available for TKI inhibition at the cell-surface; and b) MET intracellular signalling could be disrupted by the loss of MET-positive intracellular structures. We hypothesise that the formation of MET-positive vesicles is dependent on the lipid phosphatase activity of PTEN. However, we cannot rule out the possibility that PTEN, together with other factors such as NDRG1 or PIKfyve, regulates MET endocytic trafficking.

7.1.3 PIKfyve inhibition as a treatment strategy for MET addicted cancers

A serendipitous yet important finding was the identification of PIKfyve as a novel target in MET-driven cancer. This observation drove the project attention to establish the efficiency of Apilimod single-agent activity. Our data has provided the rationale for the potential incorporation of Apilimod as a new arm in the phase II genomic-driven National Lung Matrix Trial. This success was driven by Apilimod efficiency in *in vitro* studies, accompanied by the safety profile of the drug in mice experiments. Nonetheless, continuous efforts are being directed in the lab at uncovering the mechanism of Apilimod cancer cell toxicity.

Significant effort has been directed at understanding the link between Apilimod and induction of autophagy. Thanks to the data presented here, and more data generated by other members of the lab (Atg7 and Beclin-1 knock out lines), it appears that canonical autophagy is dispensable for Apilimod-mediated cell death.

Observations so far report on the accumulation of MET-positive enlarged vesicles, but no clear autophagic flux. It therefore seems that disrupting MET endocytic trafficking, without needing to involve receptor degradation, is enough to trigger toxicity.

Despite the fact that more data is needed to understand the mode of action of Apilimod in more detail, based on the results collected so far, we are starting to delineate a model to subject to further tests and experiments. For instance, an interesting observation is the contribution of PIKfyve inhibition to NDRG1 levels.

Apilimod causes the concomitant increase of pNDRG1 and decrease of MET. Given the role of PIKfyve in endocytic compartments and the fact that, in breast cancer, depletion of NDRG1 correlates with dysregulated lipid metabolism (Sevinsky et al., 2018), it may be interesting to see if MET trafficking is altered because of an interplay between NDRG1 and PIKfyve. Perhaps PIKfyve, similarly to PTEN (Figure 7.1), prevents NDRG1 from getting phosphorylated; once PIKfyve is inhibited, pNDRG1 prevails. The phosphorylated form of NDRG1 could then contribute to suppress MET signalling and/or trafficking.

Another interesting possibility is the relationship between Rab9 and PIKfyve. If proven relevant in MET-addicted models, Apilimod mode of action could be linked to the inhibition of late endosome-to-*trans*-Golgi network transport.

At this stage, the proposed links between PIKfyve, MET, NDRG1 and Rab9 remain appealing hypotheses to be tested. Given the pleiotropic effects that both NDRG1 and PIKfyve have, Apilimod mode of action in GTL16 will unlikely be a universal model, and tumour specific effects will have to be investigated. Nonetheless, we have demonstrated the impressive single-agent activity of Apilimod in MET-driven gastric and lung cancer models.

7.1.4 Current and future work

This project has allowed the generation of significant data and insights that provide the basis for a number of future projects. In fact, many are the questions that remain unanswered.

A first very important question that we wish to investigate is the dual role of PTEN and its contribution to the opposite TKI responses phenotypes we have documented in EGFR and MET addicted cells. To this end we have generated PTEN KO A431 and GTL16 cell lines reconstituted with a lipid phosphatase dead version of PTEN. These cell lines, in the future, will help determining whether TKI responses are dictated by the lipid or protein phosphatase function of PTEN.

We have provided proof-of-concept evidence that PTEN differentially regulates TKI responses and that it does so depending on the identity of the RTK. Nonetheless, we are waiting to replicate these data in more EGFR and MET models to assess the biological significance of the phenotype we have uncovered. Additionally, it would contribute greatly to our understanding of TKI resistance if we would extend the study to other RTKs.

Despite our efforts, our knowledge on the mechanism by which PTEN modulates TKI responses requires further refinement. To this end, we have generated cCbl inducible knock out lines to investigate the relevance of RTK degradation in mediating TKI responses. Additional methods, such as pulse chase experiments, could further contribute to our understanding of RTK degradation dynamics in our model systems. It would also be interesting to evaluate RTK transcript levels in both parental and PTEN KO cell lines. This study could be particularly relevant for EGFR, as it could clarify the cause of decreased receptor levels upon PTEN inactivation. Furthermore, GTL16 PTEN KO cells are in the process of being engineered with mCherry-EGFP-LC3B to try and better understand the fate of the MET receptor.

We are aware that the confocal analysis carried out so far only partially addresses the complexity of EGFR and MET intracellular localisation. The dynamics of the phosphorylated receptors are yet to be investigated, and the nature of the MET-positive intracellular structures we identified remains to be understood. Further confocal analysis with additional endocytic markers, inhibitors of endocytic trafficking, and possibly labelled growth factor probes, is therefore needed.

Finally, Apilimod mechanism of killing remains a big open question that the laboratory continues to work on, especially given the potential clinical translatability of the project. To this end, we are currently analysing both the proteomics and phosphoproteomics data, while trying to validate interesting hits, such as Rb1 and Rab9, by western blotting and confocal analysis.

At the same time, we are working to generate *in vivo* data that replicate the *in vitro* model and establish the efficacy of Apilimod against MET-addicted tumours. At the

moment the focus is prevalently on lung cancer, but we hope in the future that Apilimod-based treatments can be extended to other cancer types.

7.1.5 Concluding remarks

The development of TKIs has revolutionised the treatment of cancers with RTK driver oncogenes. However, resistance to targeted therapies inevitably limits the curative effects of TKI and warrants the development of novel strategies to overcome such resistance.

In this project we have determined that PTEN is an important modulator of TKI responses, and that its effects are determined by the identity of the RTK.
More specifically, we are proposing that PTEN can influence receptor conformation equilibrium, endocytosis and signalling and that it does so differently for the two RTKs studied, namely EGFR and MET.

We propose that PIs play an important role in regulating EGFR conformational equilibrium and endocytosis; and that PTEN, by virtue of its lipid phosphatase activity, is a major effector of these processes. TKI resistance is generated by PTEN inactivation as this powers a change in PIs-membrane composition. This affects receptor conformation (hence TKI binding) and residency in intracellular compartments. Additionally, we have demonstrated an extensive signalling rewiring as a consequence of PTEN inactivation. This suggests that a variety of downstream effectors, such as PIKfyve, can further contribute to the more aggressive phenotype of EGFR-addicted PTEN-null cancers.

Based on our model, PTEN regulation of MET-inhibitor responses mainly relies on receptor endocytosis and signalling, rather than conformation. Based on the fact that the loss of PTEN causes a signalling rewiring that resembles the one triggered by a MET inhibitor treatment, we propose that the loss of PTEN lowers the threshold of sensitivity to TKI. We hypothesise that this result is achieved by a combination of pathway rewiring (i.e. CK2 and NDRG1) and significant changes in receptor endocytosis.

Importantly, we have shown how the loss of PTEN can cause resistance to TKI in one RTK-driven model (i.e. EGFR) and hypersensitivity to TKI in another (i.e. MET). PTEN inactivation cannot therefore be considered a general biomarker of TKI resistance.

We have also generated a wealth of data for future studies with a thorough phosphoproteomics analysis that we hope can help identify novel therapeutic targets.

Finally, we have identified a potential druggable target, PIKfyve. While current efforts are still directed at understanding the exact role of this protein, PIKfyve inhibition effectively causes cell death in MET-addicted *in vitro* cancer models, and, to some extent, in EGFR-addicted PTEN null cells.

Chapter 8. Appendix

A431	
Biological source	Epidermal carcinoma of the vulva of an 85 yr old female
Growth mode	Adherent
Karyotype	Hypertriploid
Sequence variations	EGFR-PPARGC1A gene fusion, TP53 p.Arg273His
GTL16	
Biological source	Gastric adenocarcinoma derived from the liver metastasis of a 62 yr old female
Growth mode	Adherent
Karyotype	Hypotetraploid (modal chromosome number 78)
Sequence variations	MET amplification and overexpression, heterozygous for TP53 p.Arg110Cys

Supplementary Figure 1 Main properties of A431 and GTL16

The main properties of the two main cell lines used in the study are listed in the table.

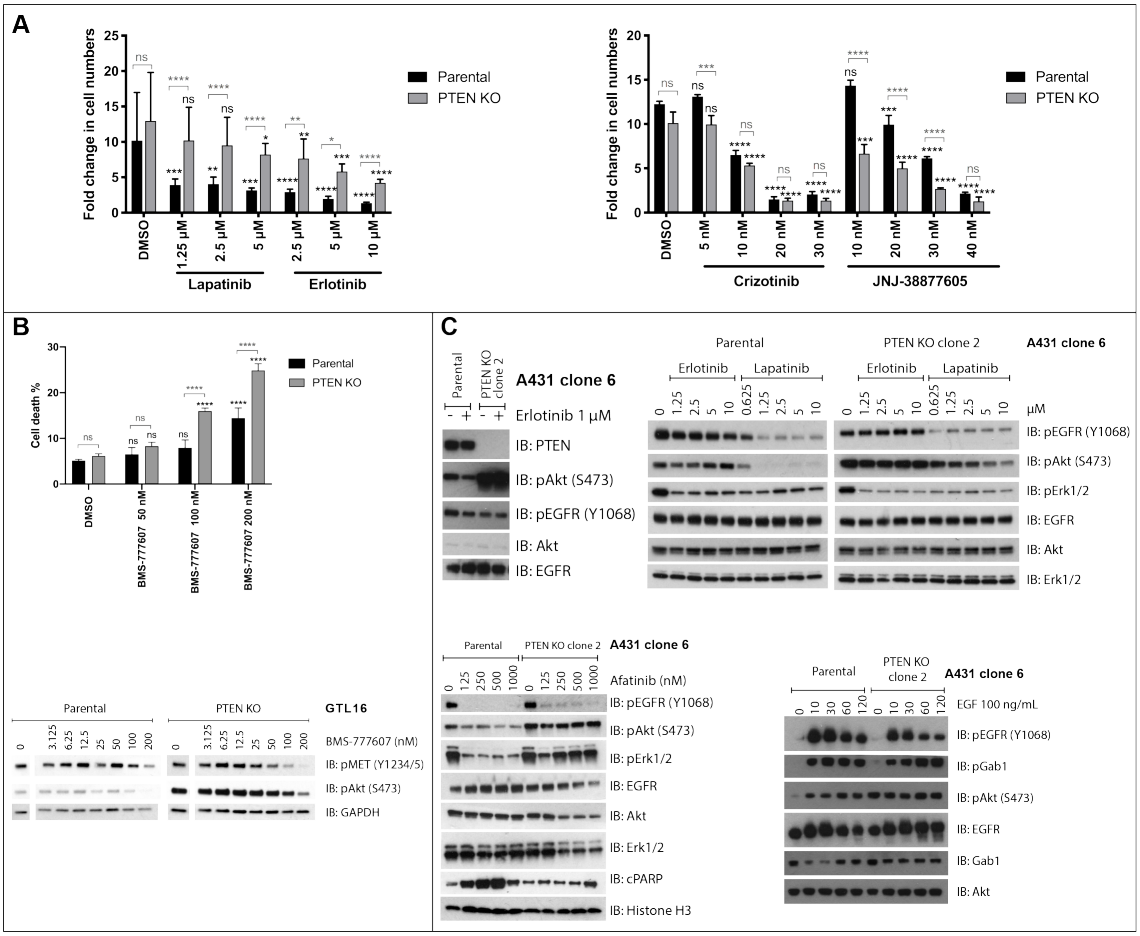

Supplementary Figure 2 Validation of EGFR and MET inhibitor responses

(A) Analysis of the responses of GTL16 parental and PTEN KO (clone 11) and A431 (clone 4) and PTEN KO (clone 3) to 72 h treatment with EGFR (Lapatinib and Erlotinib) and MET (Crizotinib and JNJ38877605) inhibitors. Fold change (mean ± SD) in the number of viable cells between the start of drug treatment and the end of the experiment was assessed via automated trypan blue exclusion method (ViCell). n=3. **(B)** Analysis of the responses of GTL16 parental and PTEN KO to a MET inhibitor, BMS-777607 via automated trypan blue exclusion method (ViCell) and western blotting. Cell death percentages (mean ± SD) are shown. **(C)** Western blot analysis of A431 clone 6 and PTEN KO clone 2 to 3 h treatments with different EGFR inhibitors (Erlotinib, Lapatinib and Afatinib) and growth factor stimulation (EGF, 100 ng/mL). ns, not significant; * significant at P <0.05; ** significant at P <0.01; *** significant at P <0.001; **** significant at P <0.0001.

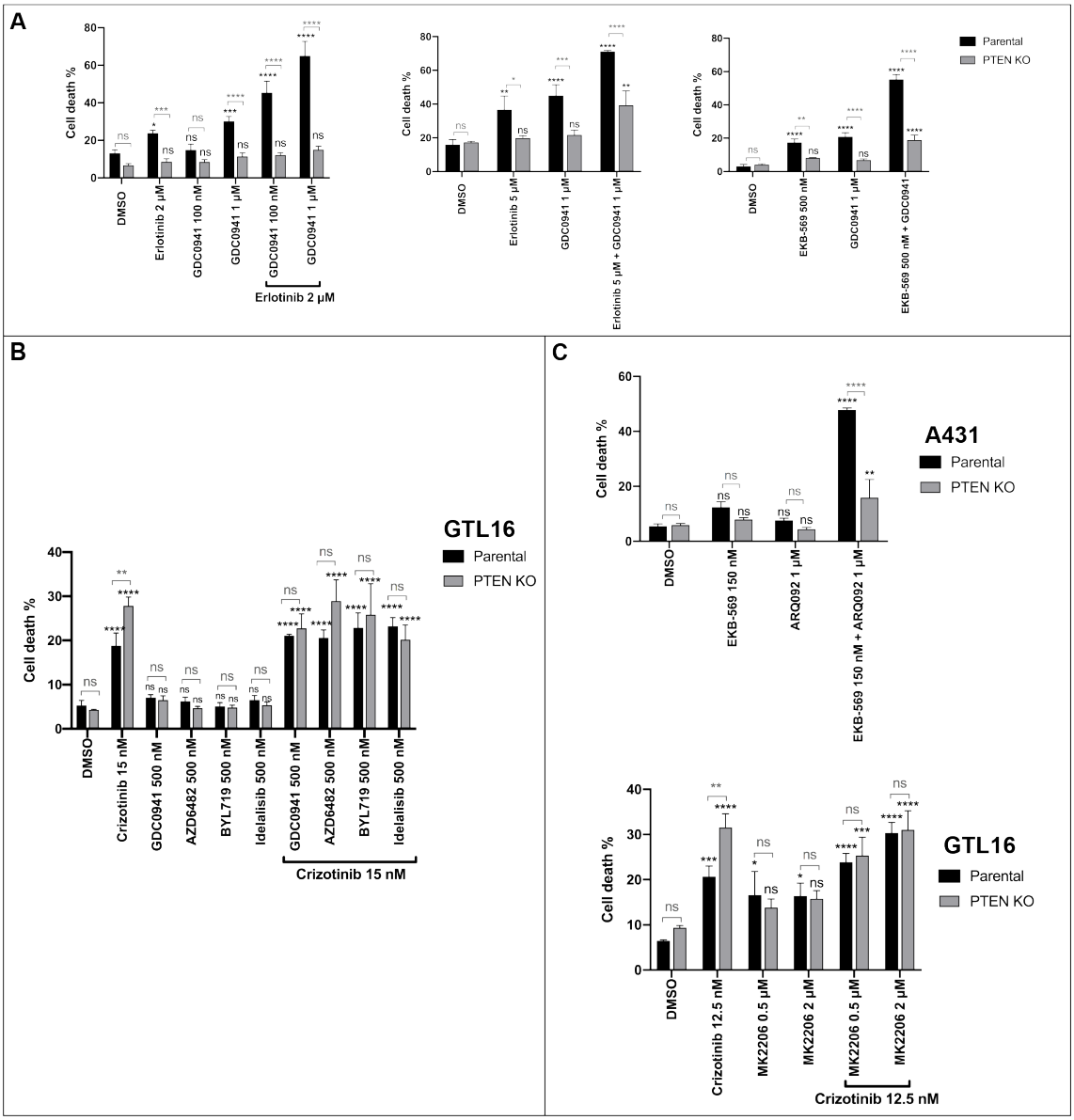

Supplementary Figure 3 PI3K pathway inhibition in the context of PTEN loss

(A) Analysis of the responses of A431 Parental and PTEN KO cell lines to 72 h treatments with EGFR inhibitors (Erlotinib and EKB-569) alone or in combination with a pan-classI PI3K inhibitor (GDC0941). **(B)** Analysis of the responses of GTL16 Parental and PTEN KO cell lines to 72 h treatments with a MET inhibitor (Crizotinib) alone or in combination with class-specific PI3K inhibitors. **(C)** Analysis of the responses of A431 and GTL16 Parental and PTEN KO cell lines to 72 h treatments with EGFR (EKB-569) or MET (Crizotinib) inhibitors alone or in combination with Akt inhibitors, ARQ092 and MK2206, respectively. Cell death percentages (mean ± SD) were assessed via automated trypan blue exclusion method (ViCell) and western blotting. ns, not significant; * significant at P <0.05; ** significant at P <0.01; *** significant at P <0.001; **** significant at P <0.0001.

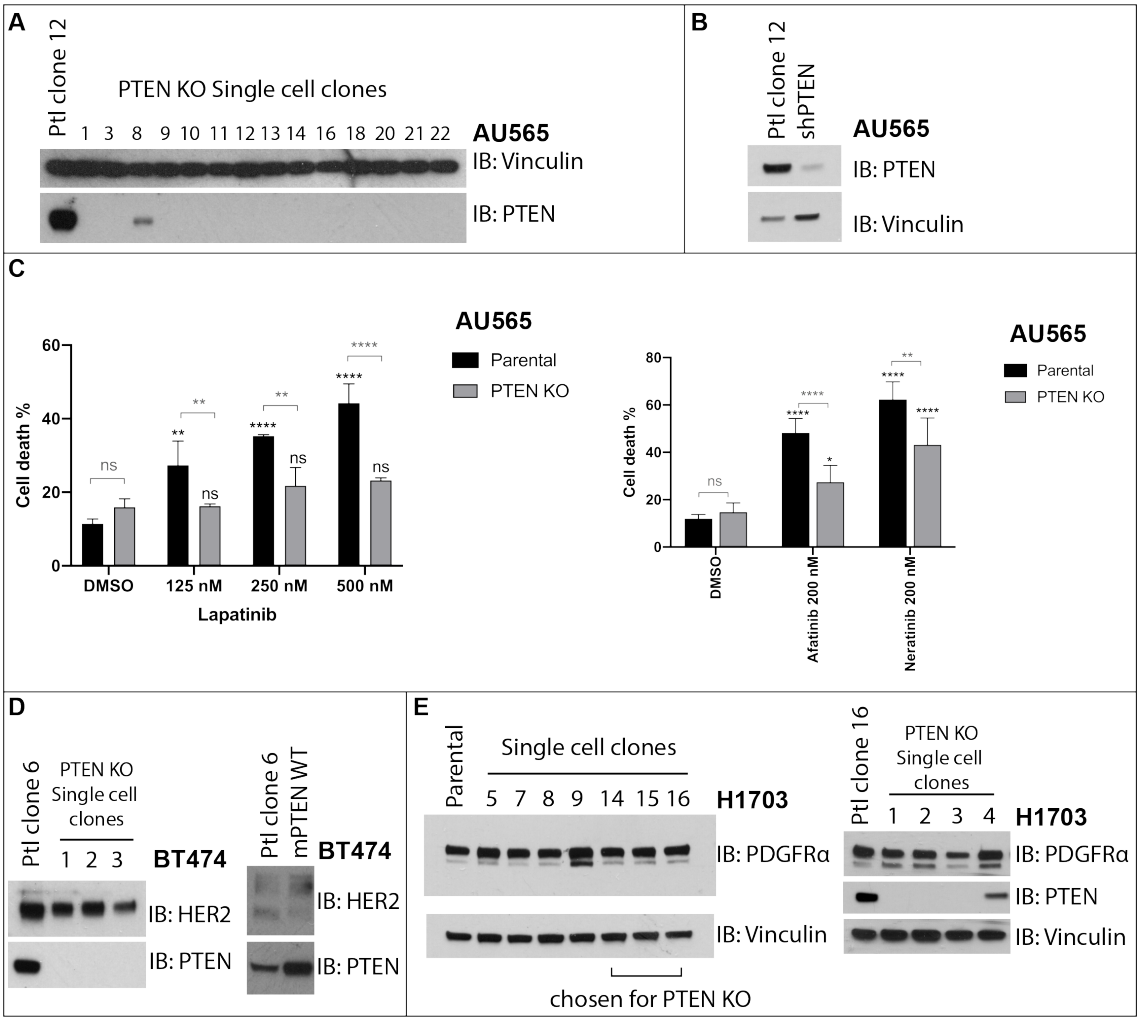

Supplementary Figure 4 Additional PTEN KO models for RTK-addicted cell lines

(A,B) Western blot confirmation of PTEN KO via CRISPR/Cas9 technology **(A)** and PTEN KD **(B)** in AU565, HER2 amplified cell line. **(C)** Analysis of the responses of AU565 parental and PTEN KO to 72 h treatment with HER2 inhibitors (Lapatinib, Afatinib, Neratinib). Cell death percentages (mean ± SD) were assessed via automated trypan blue exclusion method (ViCell) and western blotting. ns, not significant; * significant at P <0.05; ** significant at P <0.01; *** significant at P <0.001; **** significant at P <0.0001. **(D)** Western blot confirmation of PTEN KO via CRISPR/Cas9 technology and reconstitution of PTEN with a mouse cDNA (m) in BT474, a HER2 amplified cell line. **(E)** Western blot confirmation of single cell cloning and subsequent PTEN KO via CRISPR/Cas9 technology in H1703, a PDGFRα amplified cell line.

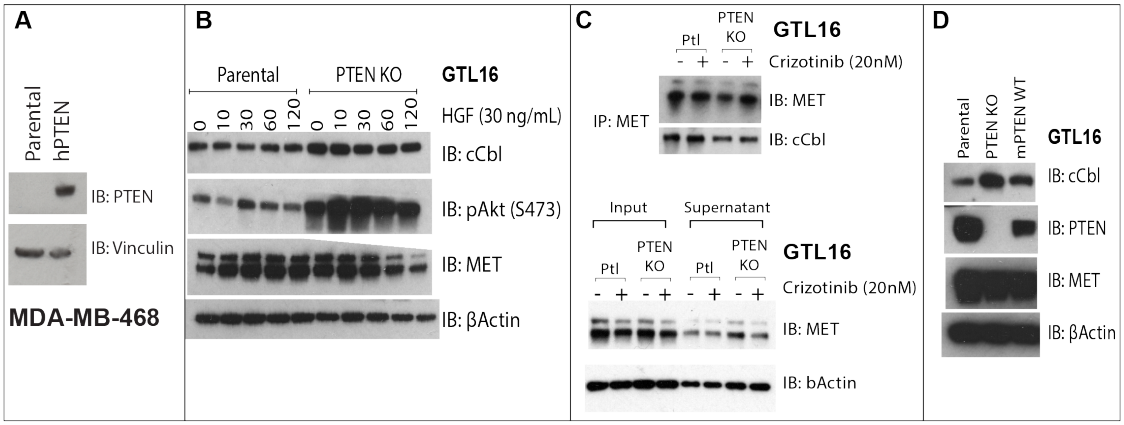

Supplementary Figure 5 PTEN inactivation is linked to cCbl activation in GTL16 PTEN KO cells

(A) Western blot analysis of human (h) PTEN reconstitution in MDA-MB-468 cells. **(B**) Western blot analysis of GTL16 Parental and PTEN KO to HGF (30 ng/mL) stimulation. **(C)** Western blot analysis of MET interaction with cCbl in GTL16 Parental and PTEN KO cells. cCbl was co-immunoprecipitated with MET in the absence and presence of the MET inhibitor Crizotinib (20 nM). **(D)** Western blot analysis of cCbl levels in GTL16 Parental, PTEN KO cells, and PTEN KO cells reconstituted with a murine (m) PTEN construct.

Reference List

Abella, J.V., Peschard, P., Naujokas, M.A., Lin, T., Saucier, C., Urbé, S., and Park, M. (2005). Met/Hepatocyte growth factor receptor ubiquitination suppresses transformation and is required for Hrs phosphorylation. Mol. Cell. Biol. *25*, 9632–9645.

Abounader, R., Reznik, T., Colantuoni, C., Martinez-Murillo, F., Rosen, E.M., and Laterra, J. (2004). Regulation of c-Met-dependent gene expression by PTEN. Oncogene *23*, 9173–9182.

Agazie, Y.M., and Hayman, M.J. (2003). Molecular Mechanism for a Role of SHP2 in Epidermal Growth Factor Receptor Signaling. Mol. Cell. Biol. *23*, 7875–7886.

Aifa, S., Aydin, J., Nordvall, G., Lundström, I., Svensson, S.P.S., and Hermanson, O. (2005). A basic peptide within the juxtamembrane region is required for EGF receptor dimerization. Exp. Cell Res. *302*, 108–114.

Ali, I.U., Schriml, L.M., and Dean, M. (1999). Mutational Spectra of PTEN/MMAC1 Gene: a Tumor Suppressor With Lipid Phosphatase Activity. JNCI J. Natl. Cancer Inst. *91*, 1922–1932.

Alimonti, A., Carracedo, A., Clohessy, J.G., Trotman, L.C., Nardella, C., Egia, A., Salmena, L., Sampieri, K., Haveman, W.J., Brogi, E., et al. (2010). Subtle variations in Pten dose determine cancer susceptibility. Nat. Genet. *42*, 454–458.

Álvarez-Garcia, V., Tawil, Y., Wise, H.M., and Leslie, N.R. (2019). Mechanisms of PTEN loss in cancer: It's all about diversity. Semin. Cancer Biol. *59*, 66–79.

Amaravadi, R.K., Yu, D., Lum, J.J., Bui, T., Christophorou, M.A., Evan, G.I., Thomas-Tikhonenko, A., and Thompson, C.B. (2007). Autophagy inhibition enhances therapy-induced apoptosis in a Myc-induced model of lymphoma. J. Clin. Invest. *117*, 326–336.

An, Z., Aksoy, O., Zheng, T., Fan, Q.-W., and Weiss, W.A. (2018). Epidermal growth factor receptor (EGFR) and EGFRvIII in glioblastoma (GBM): signaling pathways and targeted therapies. Oncogene *37*, 1561–1575.

Ardito, F., Giuliani, M., Perrone, D., Troiano, G., and Muzio, L.L. (2017). The crucial role of protein phosphorylation in cell signaling and its use as targeted therapy (Review). Int. J. Mol. Med. *40*, 271–280.

Arico, S., Petiot, A., Bauvy, C., Dubbelhuis, P.F., Meijer, A.J., Codogno, P., and Ogier-Denis, E. (2001). The Tumor Suppressor PTEN Positively Regulates Macroautophagy by Inhibiting the Phosphatidylinositol 3-Kinase/Protein Kinase B Pathway. J. Biol. Chem. *276*, 35243–35246.

Arkhipov, A., Shan, Y., Das, R., Endres, N.F., Eastwood, M.P., Wemmer, D.E., Kuriyan, J., and Shaw, D.E. (2013). Architecture and membrane interactions of the EGF receptor. Cell *152*, 557–569.

Asaoka, Y., Tada, M., Ikenoue, T., Seto, M., Imai, M., Miyabayashi, K., Yamamoto, K., Yamamoto, S., Kudo, Y., Mohri, D., et al. (2010). Gastric cancer cell line Hs746T harbors a splice site mutation of c-Met causing juxtamembrane domain deletion. Biochem. Biophys. Res. Commun. *394*, 1042–1046.

Ávalos, Y., Canales, J., Bravo-Sagua, R., Criollo, A., Lavandero, S., and Quest, A.F.G. (2014). Tumor Suppression and Promotion by Autophagy. BioMed Res. Int. *2014*.

Axe, E.L., Walker, S.A., Manifava, M., Chandra, P., Roderick, H.L., Habermann, A., Griffiths, G., and Ktistakis, N.T. (2008). Autophagosome formation from membrane compartments enriched in phosphatidylinositol 3-phosphate and dynamically connected to the endoplasmic reticulum. J. Cell Biol. *182*, 685–701.

Backer, J.M. (2008). The regulation and function of Class III PI3Ks: novel roles for Vps34. Biochem. J. *410*, 1–17.

Bae, D.-H., Jansson, P.J., Huang, M.L., Kovacevic, Z., Kalinowski, D., Lee, C.S., Sahni, S., and Richardson, D.R. (2013). The role of NDRG1 in the pathology and potential treatment of human cancers. J. Clin. Pathol. *66*, 911–917.

Bag, N., Huang, S., and Wohland, T. (2015). Plasma Membrane Organization of Epidermal Growth Factor Receptor in Resting and Ligand-Bound States. Biophys. J. *109*, 1925–1936.

Bai, X., and Jiang, Y. (2010). Key factors in mTOR regulation. Cell. Mol. Life Sci. CMLS *67*, 239–253.

Baird, A.-M., Dockry, E., Daly, A., Stack, E., Doherty, D.G., O'Byrne, K.J., and Gray, S.G. (2013). IL-23R is Epigenetically Regulated and Modulated by Chemotherapy in Non-Small Cell Lung Cancer. Front. Oncol. *3*, 162.

Balla, T. (2013). Phosphoinositides: Tiny Lipids With Giant Impact on Cell Regulation. Physiol. Rev. *93*, 1019–1137.

Bandyopadhyay, S., Pai, S.K., Hirota, S., Hosobe, S., Tsukada, T., Miura, K., Takano, Y., Saito, K., Commes, T., Piquemal, D., et al. (2004). PTEN up-regulates the tumor metastasis suppressor gene Drg-1 in prostate and breast cancer. Cancer Res. *64*, 7655–7660.

Bar, I., Merhi, A., Larbanoix, L., Constant, M., Haussy, S., Laurent, S., Canon, J.-L., and Delrée, P. (2018). Silencing of casein kinase 1 delta reduces migration and metastasis of triple negative breast cancer cells. Oncotarget *9*, 30821–30836.

Bardelli, A., Longati, P., Williams, T.A., Benvenuti, S., and Comoglio, P.M. (1999). A peptide representing the carboxyl-terminal tail of the met receptor inhibits kinase activity and invasive growth. J. Biol. Chem. *274*, 29274–29281.

Batra, S.K., Castelino-Prabhu, S., Wikstrand, C.J., Zhu, X., Humphrey, P.A., Friedman, H.S., and Bigner, D.D. (1995). Epidermal growth factor ligand-independent, unregulated, cell-transforming potential of a naturally occurring

human mutant EGFRvIII gene. Cell Growth Differ. Mol. Biol. J. Am. Assoc. Cancer Res. *6*, 1251–1259.

Batzer, A.G., Rotin, D., Ureña, J.M., Skolnik, E.Y., and Schlessinger, J. (1994). Hierarchy of binding sites for Grb2 and Shc on the epidermal growth factor receptor. Mol. Cell. Biol. *14*, 5192–5201.

Beltrao, P., Albanèse, V., Kenner, L.R., Swaney, D.L., Burlingame, A., Villén, J., Lim, W.A., Fraser, J.S., Frydman, J., and Krogan, N.J. (2012). Systematic functional prioritization of protein posttranslational modifications. Cell *150*, 413–425.

Ben-David, U., Siranosian, B., Ha, G., Tang, H., Oren, Y., Hinohara, K., Strathdee, C.A., Dempster, J., Lyons, N.J., Burns, R., et al. (2018). Genetic and transcriptional evolution alters cancer cell line drug response. Nature *560*, 325–330.

Berenjeno, I.M., Guillermet-Guibert, J., Pearce, W., Gray, A., Fleming, S., and Vanhaesebroeck, B. (2012). Both p110α and p110β isoforms of PI3K can modulate the impact of loss-of-function of the PTEN tumour suppressor. Biochem. J. *442*, 151–159.

Berns, K., Horlings, H.M., Hennessy, B.T., Madiredjo, M., Hijmans, E.M., Beelen, K., Linn, S.C., Gonzalez-Angulo, A.M., Stemke-Hale, K., Hauptmann, M., et al. (2007). A Functional Genetic Approach Identifies the PI3K Pathway as a Major Determinant of Trastuzumab Resistance in Breast Cancer. Cancer Cell *12*, 395–402.

Bi, J., Ichu, T.-A., Zanca, C., Yang, H., Zhang, W., Gu, Y., Chowdhry, S., Reed, A., Ikegami, S., Turner, K.M., et al. (2019). Oncogene Amplification in Growth Factor Signaling Pathways Renders Cancers Dependent on Membrane Lipid Remodeling. Cell Metab. *30*, 525-538.e8.

Bianco, R., Shin, I., Ritter, C.A., Yakes, F.M., Basso, A., Rosen, N., Tsurutani, J., Dennis, P.A., Mills, G.B., and Arteaga, C.L. (2003). Loss of PTEN/MMAC1/TEP in EGF receptor-expressing tumor cells counteracts the antitumor action of EGFR tyrosine kinase inhibitors. Oncogene *22*, 2812–2822.

Birchmeier, C., Birchmeier, W., Gherardi, E., and Vande Woude, G.F. (2003). Met, metastasis, motility and more. Nat. Rev. Mol. Cell Biol. *4*, 915–925.

Blommaart, E.F.C., Krause, U., Schellens, J.P.M., Vreeling-Sindelárová, H., and Meijer, A.J. (1997). The Phosphatidylinositol 3-Kinase Inhibitors Wortmannin and LY294002 Inhibit Autophagy in Isolated Rat Hepatocytes. Eur. J. Biochem. *243*, 240–246.

Boal, F., Mansour, R., Gayral, M., Saland, E., Chicanne, G., Xuereb, J.-M., Marcellin, M., Burlet-Schiltz, O., Sansonetti, P.J., Payrastre, B., et al. (2015). TOM1 is a PI5P effector involved in the regulation of endosomal maturation. J. Cell Sci. *128*, 815–827.

Bocharov, E.V., Mineev, K.S., Volynsky, P.E., Ermolyuk, Y.S., Tkach, E.N., Sobol, A.G., Chupin, V.V., Kirpichnikov, M.P., Efremov, R.G., and Arseniev, A.S. (2008).

Spatial Structure of the Dimeric Transmembrane Domain of the Growth Factor Receptor ErbB2 Presumably Corresponding to the Receptor Active State. J. Biol. Chem. *283*, 6950–6956.

Bocharov, E.V., Sharonov, G.V., Bocharova, O.V., and Pavlov, K.V. (2017). Conformational transitions and interactions underlying the function of membrane embedded receptor protein kinases. Biochim. Biophys. Acta BBA - Biomembr. *1859*, 1417–1429.

Bolte, S., and Cordelières, F.P. (2006). A guided tour into subcellular colocalization analysis in light microscopy. J. Microsc. *224*, 213–232.

Bouali, S., Chrétien, A.-S., Ramacci, C., Rouyer, M., Becuwe, P., and Merlin, J.-L. (2009). PTEN expression controls cellular response to cetuximab by mediating PI3K/AKT and RAS/RAF/MAPK downstream signaling in KRAS wild-type, hormone refractory prostate cancer cells. Oncol. Rep. *21*, 731–735.

Bowman, E.J., Siebers, A., and Altendorf, K. (1988). Bafilomycins: a class of inhibitors of membrane ATPases from microorganisms, animal cells, and plant cells. Proc. Natl. Acad. Sci. U. S. A. *85*, 7972–7976.

Brennan, C.W., Verhaak, R.G.W., McKenna, A., Campos, B., Noushmehr, H., Salama, S.R., Zheng, S., Chakravarty, D., Sanborn, J.Z., Berman, S.H., et al. (2013). The somatic genomic landscape of glioblastoma. Cell *155*, 462–477.

Bunney, T.D., and Katan, M. (2010). Phosphoinositide signalling in cancer: beyond PI3K and PTEN. Nat. Rev. Cancer *10*, 342–352.

Burakoff, R., Barish, C.F., Riff, D., Pruitt, R., Chey, W.Y., Farraye, F.A., Shafran, I., Katz, S., Krone, C.L., Vander Vliet, M., et al. (2006). A phase 1/2A trial of STA 5326, an oral interleukin-12/23 inhibitor, in patients with active moderate to severe Crohn's disease. Inflamm. Bowel Dis. *12*, 558–565.

Burgess, A.W., Cho, H.-S., Eigenbrot, C., Ferguson, K.M., Garrett, T.P.J., Leahy, D.J., Lemmon, M.A., Sliwkowski, M.X., Ward, C.W., and Yokoyama, S. (2003). An open-and-shut case? Recent insights into the activation of EGF/ErbB receptors. Mol. Cell *12*, 541–552.

Burke, J.E., and Williams, R.L. (2013). Dynamic steps in receptor tyrosine kinase mediated activation of class IA phosphoinositide 3-kinases (PI3K) captured by H/D exchange (HDX-MS). Adv. Biol. Regul. *53*, 97–110.

Cai, X., Xu, Y., Cheung, A.K., Tomlinson, R.C., Alcázar-Román, A., Murphy, L., Billich, A., Zhang, B., Feng, Y., Klumpp, M., et al. (2013). PIKfyve, a class III PI kinase, is the target of the small molecular IL-12/IL-23 inhibitor apilimod and a player in Toll-like receptor signaling. Chem. Biol. *20*, 912–921.

Cancer Genome Atlas Research Network (2014). Comprehensive molecular profiling of lung adenocarcinoma. Nature *511*, 543–550.

Carew, J.S., Nawrocki, S.T., Krupnik, Y.V., Dunner, K., McConkey, D.J., Keating, M.J., and Huang, P. (2006). Targeting endoplasmic reticulum protein transport: a novel strategy to kill malignant B cells and overcome fludarabine resistance in CLL. Blood *107*, 222–231.

Carey, K.D., Garton, A.J., Romero, M.S., Kahler, J., Thomson, S., Ross, S., Park, F., Haley, J.D., Gibson, N., and Sliwkowski, M.X. (2006). Kinetic analysis of epidermal growth factor receptor somatic mutant proteins shows increased sensitivity to the epidermal growth factor receptor tyrosine kinase inhibitor, erlotinib. Cancer Res. *66*, 8163–8171.

Carpenter, G., King, L., and Cohen, S. (1978). Epidermal growth factor stimulates phosphorylation in membrane preparations in vitro. Nature *276*, 409–410.

Carrasco-García, E., Saceda, M., and Martínez-Lacaci, I. (2014). Role of Receptor Tyrosine Kinases and Their Ligands in Glioblastoma. Cells *3*, 199–235.

Casado, P., Rodriguez-Prados, J.-C., Cosulich, S.C., Guichard, S., Vanhaesebroeck, B., Joel, S., and Cutillas, P.R. (2013). Kinase-substrate enrichment analysis provides insights into the heterogeneity of signaling pathway activation in leukemia cells. Sci. Signal. *6*, rs6.

Casado, P., Wilkes, E.H., Miraki-Moud, F., Hadi, M.M., Rio-Machin, A., Rajeeve, V., Pike, R., Iqbal, S., Marfa, S., Lea, N., et al. (2018). Proteomic and genomic integration identifies kinase and differentiation determinants of kinase inhibitor sensitivity in leukemia cells. Leukemia *32*, 1818–1822.

Casaletto, J.B., and McClatchey, A.I. (2012). Spatial regulation of receptor tyrosine kinases in development and cancer. Nat. Rev. Cancer *12*, 387–400.

Catenacci, D.V.T., Ang, A., Liao, W.-L., Shen, J., O'Day, E., Loberg, R.D., Cecchi, F., Hembrough, T., Ruzzo, A., and Graziano, F. (2017). MET tyrosine kinase receptor expression and amplification as prognostic biomarkers of survival in gastroesophageal adenocarcinoma. Cancer *123*, 1061–1070.

Chakraborty, S., Li, L., Puliyappadamba, V.T., Guo, G., Hatanpaa, K.J., Mickey, B., Souza, R.F., Vo, P., Herz, J., Chen, M.-R., et al. (2014). Constitutive and ligand-induced EGFR signalling triggers distinct and mutually exclusive downstream signalling networks. Nat. Commun. *5*, 5811.

Chalhoub, N., and Baker, S.J. (2009). PTEN and the PI3-Kinase Pathway in Cancer. Annu. Rev. Pathol. *4*, 127–150.

Chen, J., Li, S., Yang, Z., Lu, G., and Hu, H. (2008). Correlation between NDRG1 and PTEN expression in endometrial carcinoma. Cancer Sci. *99*, 706–710.

Chen, M.-K., Du, Y., Sun, L., Hsu, J.L., Wang, Y.-H., Gao, Y., Huang, J., and Hung, M.-C. (2019). H2O2 induces nuclear transport of the receptor tyrosine kinase c-MET in breast cancer cells via a membrane-bound retrograde trafficking mechanism. J. Biol. Chem. *294*, 8516–8528.

Chen, Z., Trotman, L.C., Shaffer, D., Lin, H.-K., Dotan, Z.A., Niki, M., Koutcher, J.A., Scher, H.I., Ludwig, T., Gerald, W., et al. (2005). Crucial role of p53-dependent cellular senescence in suppression of Pten-deficient tumorigenesis. Nature *436*, 725–730.

Cheng, X.-T., Xie, Y.-X., Zhou, B., Huang, N., Farfel-Becker, T., and Sheng, Z.-H. (2018). Revisiting LAMP1 as a marker for degradative autophagy-lysosomal organelles in the nervous system. Autophagy *14*, 1472–1474.

Cheong, J.K., and Virshup, D.M. (2011). Casein kinase 1: Complexity in the family. Int. J. Biochem. Cell Biol. *43*, 465–469.

Chetram, M.A., Odero-Marah, V., and Hinton, C.V. (2011). Loss of PTEN permits CXCR4-mediated tumorigenesis through ERK1/2 in prostate cancer cells. Mol. Cancer Res. MCR *9*, 90–102.

Chia, P.Z.C., and Gleeson, P.A. (2011). The Regulation of Endosome-to-Golgi Retrograde Transport by Tethers and Scaffolds. Traffic *12*, 939–947.

Chinnam, M., and Goodrich, D.W. (2011). RB1, development, and cancer. Curr. Top. Dev. Biol. *94*, 129–169.

Cho, J., Kim, S., Du, J., and Meyerson, M. (2018). Autophosphorylation of the carboxyl-terminal domain is not required for oncogenic transformation by lung-cancer derived EGFR mutants. Int. J. Cancer *143*, 679–685.

Choy, C.H., Saffi, G., Gray, M.A., Wallace, C., Dayam, R.M., Ou, Z.-Y.A., Lenk, G., Puertollano, R., Watkins, S.C., and Botelho, R.J. (2018). Lysosome enlargement during inhibition of the lipid kinase PIKfyve proceeds through lysosome coalescence. J. Cell Sci. *131*.

Chung, I. (2017). Optical measurement of receptor tyrosine kinase oligomerization on live cells. Biochim. Biophys. Acta BBA - Biomembr. *1859*, 1436–1444.

Clague, M.J., and Urbé, S. (2001). The interface of receptor trafficking and signalling. J. Cell Sci. *114*, 3075–3081.

Codogno, P., Mehrpour, M., and Proikas-Cezanne, T. (2012). Canonical and non-canonical autophagy: variations on a common theme of self-eating? Nat. Rev. Mol. Cell Biol. *13*, 7–12.

Confalonieri, S., Salcini, A.E., Puri, C., Tacchetti, C., and Di Fiore, P.P. (2000). Tyrosine Phosphorylation of Eps15 Is Required for Ligand-Regulated, but Not Constitutive, Endocytosis. J. Cell Biol. *150*, 905–912.

Cong, J., Liu, R., Wang, X., Jiang, H., and Zhang, Y. (2016). MiR-634 decreases cell proliferation and induces apoptosis by targeting mTOR signaling pathway in cervical cancer cells. Artif. Cells Nanomedicine Biotechnol. *44*, 1694–1701.

Cong, L., Ran, F.A., Cox, D., Lin, S., Barretto, R., Habib, N., Hsu, P.D., Wu, X., Jiang, W., Marraffini, L.A., et al. (2013). Multiplex Genome Engineering Using CRISPR/Cas Systems. Science *339*, 819–823.

Connell, C.M., and Doherty, G.J. (2017). Activating HER2 mutations as emerging targets in multiple solid cancers. ESMO Open *2*.

Cook, N.R., Row, P.E., and Davidson, H.W. (2004). Lysosome Associated Membrane Protein 1 (Lamp1) Traffics Directly from the TGN to Early Endosomes. Traffic *5*, 685–699.

Coskun, Ü., Grzybek, M., Drechsel, D., and Simons, K. (2011). Regulation of human EGF receptor by lipids. Proc. Natl. Acad. Sci. U. S. A. *108*, 9044–9048.

Cymer, F., and Schneider, D. (2010). Transmembrane helix-helix interactions involved in ErbB receptor signaling. Cell Adhes. Migr. *4*, 299–312.

Dai, X., Cheng, H., Bai, Z., and Li, J. (2017). Breast Cancer Cell Line Classification and Its Relevance with Breast Tumor Subtyping. J. Cancer *8*, 3131–3141.

Das, M., Scappini, E., Martin, N.P., Wong, K.A., Dunn, S., Chen, Y.-J., Miller, S.L.H., Domin, J., and O'Bryan, J.P. (2007). Regulation of neuron survival through an intersectin-phosphoinositide 3'-kinase C2beta-AKT pathway. Mol. Cell. Biol. *27*, 7906–7917.

Dawson, J.P., Berger, M.B., Lin, C.-C., Schlessinger, J., Lemmon, M.A., and Ferguson, K.M. (2005). Epidermal Growth Factor Receptor Dimerization and Activation Require Ligand-Induced Conformational Changes in the Dimer Interface. Mol. Cell. Biol. *25*, 7734–7742.

Degenhardt, K., Mathew, R., Beaudoin, B., Bray, K., Anderson, D., Chen, G., Mukherjee, C., Shi, Y., Gélinas, C., Fan, Y., et al. (2006). Autophagy promotes tumor cell survival and restricts necrosis, inflammation, and tumorigenesis. Cancer Cell *10*, 51–64.

van Delft, S., Schumacher, C., Hage, W., Verkleij, A.J., and Henegouwen, P.M.P. van B. en (1997). Association and Colocalization of Eps15 with Adaptor Protein-2 and Clathrin. J. Cell Biol. *136*, 811–821.

Deribe, Y.L., Pawson, T., and Dikic, I. (2010). Post-translational modifications in signal integration. Nat. Struct. Mol. Biol. *17*, 666–672.

Dhillon, A.S., Hagan, S., Rath, O., and Kolch, W. (2007). MAP kinase signalling pathways in cancer. Oncogene *26*, 3279–3290.

Di Cristofano, A. (2017). SGK1: The Dark Side of PI3K Signaling. Curr. Top. Dev. Biol. *123*, 49–71.

Dillon, R.L., Marcotte, R., Hennessy, B.T., Woodgett, J.R., Mills, G.B., and Muller, W.J. (2009). Akt1 and Akt2 Play Distinct Roles in the Initiation and Metastatic Phases of Mammary Tumor Progression. Cancer Res. *69*, 5057–5064.

Dixon, K.M., Lui, G.Y.L., Kovacevic, Z., Zhang, D., Yao, M., Chen, Z., Dong, Q., Assinder, S.J., and Richardson, D.R. (2013). Dp44mT targets the AKT, TGF- β and ERK pathways via the metastasis suppressor NDRG1 in normal prostate epithelial cells and prostate cancer cells. Br. J. Cancer *108*, 409–419.

Doll, S., Gnad, F., and Mann, M. (2019). The Case for Proteomics and Phospho-Proteomics in Personalized Cancer Medicine. Proteomics Clin. Appl. *13*.

Donaldson, J.G., Cassel, D., Kahn, R.A., and Klausner, R.D. (1992). ADP-ribosylation factor, a small GTP-binding protein, is required for binding of the coatomer protein beta-COP to Golgi membranes. Proc. Natl. Acad. Sci. U. S. A. *89*, 6408–6412.

Du, Z., and Lovly, C.M. (2018). Mechanisms of receptor tyrosine kinase activation in cancer. Mol. Cancer *17*, 58.

Dupuis-Coronas, S., Lagarrigue, F., Ramel, D., Chicanne, G., Saland, E., Gaits-Iacovoni, F., Payrastre, B., and Tronchère, H. (2011). The nucleophosmin-anaplastic lymphoma kinase oncogene interacts, activates, and uses the kinase PIKfyve to increase invasiveness. J. Biol. Chem. *286*, 32105–32114.

Ebbesen, S.H., Scaltriti, M., Bialucha, C.U., Morse, N., Kastenhuber, E.R., Wen, H.Y., Dow, L.E., Baselga, J., and Lowe, S.W. (2016). Pten loss promotes MAPK pathway dependency in HER2/neu breast carcinomas. Proc. Natl. Acad. Sci. *113*, 3030–3035.

Ebner, R., and Derynck, R. (1991). Epidermal growth factor and transforming growth factor-alpha: differential intracellular routing and processing of ligand-receptor complexes. Cell Regul. *2*, 599–612.

Eden, E.R., Huang, F., Sorkin, A., and Futter, C.E. (2012). The role of EGF receptor ubiquitination in regulating its intracellular traffic. Traffic Cph. Den. *13*, 329–337.

Eggeling, C., Ringemann, C., Medda, R., Schwarzmann, G., Sandhoff, K., Polyakova, S., Belov, V.N., Hein, B., von Middendorff, C., Schönle, A., et al. (2009). Direct observation of the nanoscale dynamics of membrane lipids in a living cell. Nature *457*, 1159–1162.

Ekstrand, A.J., Sugawa, N., James, C.D., and Collins, V.P. (1992). Amplified and rearranged epidermal growth factor receptor genes in human glioblastomas reveal deletions of sequences encoding portions of the N- and/or C-terminal tails. Proc. Natl. Acad. Sci. U. S. A. *89*, 4309–4313.

Emrah Er, E., Mendoza, M.C., Mackey, A.M., Rameh, L.E., and Blenis, J. (2013). AKT Facilitates EGFR Trafficking and Degradation by Phosphorylating and Activating PIKfyve. Sci. Signal. *6*, ra45.

Endres, N.F., Das, R., Smith, A.W., Arkhipov, A., Kovacs, E., Huang, Y., Pelton, J.G., Shan, Y., Shaw, D.E., Wemmer, D.E., et al. (2013). Conformational Coupling Across the Plasma Membrane in Activation of the EGF receptor. Cell *152*, 543–556.

Engelman, J.A., Luo, J., and Cantley, L.C. (2006). The evolution of phosphatidylinositol 3-kinases as regulators of growth and metabolism. Nat. Rev. Genet. *7*, 606–619.

Esteva, F.J., Guo, H., Zhang, S., Santa-Maria, C., Stone, S., Lanchbury, J.S., Sahin, A.A., Hortobagyi, G.N., and Yu, D. (2010). PTEN, PIK3CA, p-AKT, and p-p70S6K status: association with trastuzumab response and survival in patients with HER2-positive metastatic breast cancer. Am. J. Pathol. *177*, 1647–1656.

Falchook, G.S., Kurzrock, R., Amin, H.M., Xiong, W., Fu, S., Piha-Paul, S.A., Janku, F., Eskandari, G., Catenacci, D.V.T., Klevesath, M.B., et al. (2019). First-in-Man Phase I Trial of the Selective MET Inhibitor Tepotinib in Patients with Advanced Solid Tumors. Clin. Cancer Res.

Fenton, T.R., Nathanson, D., Ponte de Albuquerque, C., Kuga, D., Iwanami, A., Dang, J., Yang, H., Tanaka, K., Oba-Shinjo, S.M., Uno, M., et al. (2012). Resistance to EGF receptor inhibitors in glioblastoma mediated by phosphorylation of the PTEN tumor suppressor at tyrosine 240. Proc. Natl. Acad. Sci. U. S. A. *109*, 14164–14169.

Ferguson, K.M. (2008). A structure-based view of Epidermal Growth Factor Receptor regulation. Annu. Rev. Biophys. *37*, 353–373.

Ferguson, K.M., Berger, M.B., Mendrola, J.M., Cho, H.-S., Leahy, D.J., and Lemmon, M.A. (2003). EGF Activates Its Receptor by Removing Interactions that Autoinhibit Ectodomain Dimerization. Mol. Cell *11*, 507–517.

Ferraris, D.M., Gherardi, E., Di, Y., Heinz, D.W., and Niemann, H.H. (2010). Ligand-mediated dimerization of the Met receptor tyrosine kinase by the bacterial invasion protein InlB. J. Mol. Biol. *395*, 522–532.

Frederick, L., Wang, X.Y., Eley, G., and James, C.D. (2000). Diversity and frequency of epidermal growth factor receptor mutations in human glioblastomas. Cancer Res. *60*, 1383–1387.

Freed, D.M., Bessman, N.J., Kiyatkin, A., Salazar-Cavazos, E., Byrne, P.O., Moore, J.O., Valley, C.C., Ferguson, K.M., Leahy, D.J., Lidke, D.S., et al. (2017). EGFR Ligands Differentially Stabilize Receptor Dimers to Specify Signaling Kinetics. Cell *171*, 683-695.e18.

Fruman, D.A., and Rommel, C. (2014). PI3K and Cancer: Lessons, Challenges and Opportunities. Nat. Rev. Drug Discov. *13*, 140–156.

Fu, Y., Foden, J.A., Khayter, C., Maeder, M.L., Reyon, D., Joung, J.K., and Sander, J.D. (2013). High frequency off-target mutagenesis induced by CRISPR-Cas nucleases in human cells. Nat. Biotechnol. *31*, 822–826.

Furge, K.A., Zhang, Y.-W., and Vande Woude, G.F. (2000). Met receptor tyrosine kinase: enhanced signaling through adapter proteins. Oncogene *19*, 5582–5589.

Gajiwala, K.S. (2013). EGFR: Tale of the C-terminal tail. Protein Sci. Publ. Protein Soc. *22*, 995–999.

Galluzzi, L., and Green, D.R. (2019). Autophagy-Independent Functions of the Autophagy Machinery. Cell *177*, 1682–1699.

Gan, H.K., Cvrljevic, A.N., and Johns, T.G. (2013). The epidermal growth factor receptor variant III (EGFRvIII): where wild things are altered. FEBS J. *280*, 5350–5370.

Gandino, L., Longati, P., Medico, E., Prat, M., and Comoglio, P.M. (1994). Phosphorylation of serine 985 negatively regulates the hepatocyte growth factor receptor kinase. J. Biol. Chem. *269*, 1815–1820.

Garcia-Guzman, M., Dolfi, F., Zeh, K., and Vuori, K. (1999). Met-induced JNK activation is mediated by the adapter protein Crk and correlates with the Gab1 – Crk signaling complex formation. Oncogene *18*, 7775–7786.

Gayle, S., Landrette, S., Beeharry, N., Conrad, C., Hernandez, M., Beckett, P., Ferguson, S.M., Mandelkern, T., Zheng, M., Xu, T., et al. (2017). Identification of apilimod as a first-in-class PIKfyve kinase inhibitor for treatment of B-cell non-Hodgkin lymphoma. Blood *129*, 1768–1778.

Georgescu, M.-M. (2010). PTEN Tumor Suppressor Network in PI3K-Akt Pathway Control. Genes Cancer *1*, 1170–1177.

Gherardi, E., Sandin, S., Petoukhov, M.V., Finch, J., Youles, M.E., Ofverstedt, L.-G., Miguel, R.N., Blundell, T.L., Vande Woude, G.F., Skoglund, U., et al. (2006). Structural basis of hepatocyte growth factor/scatter factor and MET signalling. Proc. Natl. Acad. Sci. U. S. A. *103*, 4046–4051.

Ghosh, A.K., Grigorieva, I., Steele, R., Hoover, R.G., and Ray, R.B. (1999). PTEN transcriptionally modulates c-myc gene expression in human breast carcinoma cells and is involved in cell growth regulation. Gene *235*, 85–91.

Giuliano, C.J., Lin, A., Girish, V., and Sheltzer, J.M. (2019). Generating Single Cell–Derived Knockout Clones in Mammalian Cells with CRISPR/Cas9. Curr. Protoc. Mol. Biol. *128*, e100.

Glick, D., Barth, S., and Macleod, K.F. (2010). Autophagy: cellular and molecular mechanisms. J. Pathol. *221*, 3–12.

Goh, L.K., and Sorkin, A. (2013). Endocytosis of Receptor Tyrosine Kinases. Cold Spring Harb. Perspect. Biol. *5*, a017459.

Goltsov, A., Faratian, D., Langdon, S.P., Mullen, P., Harrison, D.J., and Bown, J. (2012). Features of the reversible sensitivity-resistance transition in PI3K/PTEN/AKT signalling network after HER2 inhibition. Cell. Signal. *24*, 493–504.

Gong, Q., Huntsman, C., and Ma, D. (2008). Clathrin-independent internalization and recycling. J. Cell. Mol. Med. *12*, 126–144.

Göransson, O., Deak, M., Wullschleger, S., Morrice, N.A., Prescott, A.R., and Alessi, D.R. (2006). Regulation of the polarity kinases PAR-1/MARK by 14-3-3 interaction and phosphorylation. J. Cell Sci. *119*, 4059–4070.

Gotoh, N., Tojo, A., Hino, M., Yazaki, Y., and Shibuya, M. (1992). A highly conserved tyrosine residue at codon 845 within the kinase domain is not required

for the transforming activity of human epidermal growth factor receptor. Biochem. Biophys. Res. Commun. *186*, 768–774.

Grandal, M.V., Zandi, R., Pedersen, M.W., Willumsen, B.M., van Deurs, B., and Poulsen, H.S. (2007). EGFRvIII escapes down-regulation due to impaired internalization and sorting to lysosomes. Carcinogenesis *28*, 1408–1417.

Greig, M.J., Niessen, S., Weinrich, S.L., Feng, J.L., Shi, M., and Johnson, T.O. (2015). Effects of Activating Mutations on EGFR Cellular Protein Turnover and Amino Acid Recycling Determined Using SILAC Mass Spectrometry. Int. J. Cell Biol. *2015*.

Gruenberg, J., and Stenmark, H. (2004). The biogenesis of multivesicular endosomes. Nat. Rev. Mol. Cell Biol. *5*, 317–323.

Gump, J.M., and Thorburn, A. (2014). Sorting cells for basal and induced autophagic flux by quantitative ratiometric flow cytometry. Autophagy *10*, 1327–1334.

Guo, G., Gong, K., Wohlfeld, B., Hatanpaa, K.J., Zhao, D., and Habib, A.A. (2015). Ligand-Independent EGFR Signaling. Cancer Res. *75*, 3436–3441.

Guo, J.Y., Chen, H.-Y., Mathew, R., Fan, J., Strohecker, A.M., Karsli-Uzunbas, G., Kamphorst, J.J., Chen, G., Lemons, J.M.S., Karantza, V., et al. (2011). Activated Ras requires autophagy to maintain oxidative metabolism and tumorigenesis. Genes Dev. *25*, 460–470.

Gupta, R.M., and Musunuru, K. (2014). Expanding the genetic editing tool kit: ZFNs, TALENs, and CRISPR-Cas9. J. Clin. Invest. *124*, 4154–4161.

Haapaniemi, E., Botla, S., Persson, J., Schmierer, B., and Taipale, J. (2018). CRISPR–Cas9 genome editing induces a p53-mediated DNA damage response. Nat. Med. *24*, 927–930.

Haigler, H., Ash, J.F., Singer, S.J., and Cohen, S. (1978). Visualization by fluorescence of the binding and internalization of epidermal growth factor in human carcinoma cells A-431. Proc. Natl. Acad. Sci. U. S. A. *75*, 3317–3321.

Hanawa, M., Suzuki, S., Dobashi, Y., Yamane, T., Kono, K., Enomoto, N., and Ooi, A. (2006). EGFR protein overexpression and gene amplification in squamous cell carcinomas of the esophagus. Int. J. Cancer *118*, 1173–1180.

Harb, W.A., Diefenbach, C.S., Lakhani, N., Rutherford, S.C., Schreeder, M.T., Ansell, S.M., Sher, T., Aboulafia, D.M., Cohen, J.B., Nix, D., et al. (2017). Phase 1 Clinical Safety, Pharmacokinetics (PK), and Activity of Apilimod Dimesylate (LAM-002A), a First-in-Class Inhibitor of Phosphatidylinositol-3-Phosphate 5-Kinase (PIKfyve), in Patients with Relapsed or Refractory B-Cell Malignancies. Blood *130*, 4119–4119.

Harris, R.C., Chung, E., and Coffey, R.J. (2003). EGF receptor ligands. Exp. Cell Res. *284*, 2–13.

Harris, T.J., Grosso, J.F., Yen, H.-R., Xin, H., Kortylewski, M., Albesiano, E., Hipkiss, E.L., Getnet, D., Goldberg, M.V., Maris, C.H., et al. (2007). Cutting edge: An in vivo requirement for STAT3 signaling in TH17 development and TH17-dependent autoimmunity. J. Immunol. Baltim. Md 1950 *179*, 4313–4317.

Harsha, H.C., and Pandey, A. (2010). Phosphoproteomics in cancer. Mol. Oncol. *4*, 482–495.

Hasegawa, J., Strunk, B.S., and Weisman, L.S. (2017). PI5P and PI(3,5)P2: Minor, but Essential Phosphoinositides. Cell Struct. Funct. *42*, 49–60.

Hashigasako, A., Machide, M., Nakamura, T., Matsumoto, K., and Nakamura, T. (2004). Bi-directional regulation of Ser-985 phosphorylation of c-met via protein kinase C and protein phosphatase 2A involves c-Met activation and cellular responsiveness to hepatocyte growth factor. J. Biol. Chem. *279*, 26445–26452.

Hasin, Y., Seldin, M., and Lusis, A. (2017). Multi-omics approaches to disease. Genome Biol. *18*, 83.

Hayashi-Nishino, M., Fujita, N., Noda, T., Yamaguchi, A., Yoshimori, T., and Yamamoto, A. (2009). A subdomain of the endoplasmic reticulum forms a cradle for autophagosome formation. Nat. Cell Biol. *11*, 1433–1437.

Hays, J.L., and Watowich, S.J. (2003). Oligomerization-induced modulation of TPR-MET tyrosine kinase activity. J. Biol. Chem. *278*, 27456–27463.

He, L., and Hristova, K. (2012). Physical-chemical principles underlying RTK activation, and their implications for human disease. Biochim. Biophys. Acta *1818*, 995–1005.

Hedger, G., Sansom, M.S.P., and Koldsø, H. (2015). The juxtamembrane regions of human receptor tyrosine kinases exhibit conserved interaction sites with anionic lipids. Sci. Rep. *5*, 1–10.

Heist, R.S., Wolf, J., Seto, T., Han, J.-Y., Reguart, N., Groen, H.J.M., Tan, D.S.W., Hida, T., Jonge, M.D., Orlov, S.V., et al. (2019). OA01.07 Capmatinib (INC280) in METΔEX14-Mutated Advanced NSCLC: Efficacy Data from the Phase 2 Geometry MONO-1 Study. J. Thorac. Oncol. *14*, S1126.

Heldin, C.H. (1995). Dimerization of cell surface receptors in signal transduction. Cell *80*, 213–223.

Hemmings, B.A., and Restuccia, D.F. (2012). PI3K-PKB/Akt Pathway. Cold Spring Harb. Perspect. Biol. *4*.

Hessvik, N.P., Øverbye, A., Brech, A., Torgersen, M.L., Jakobsen, I.S., Sandvig, K., and Llorente, A. (2016). PIKfyve inhibition increases exosome release and induces secretory autophagy. Cell. Mol. Life Sci. *73*, 4717–4737.

Hirsch, F.R., Varella-Garcia, M., and Cappuzzo, F. (2009). Predictive value of EGFR and HER2 overexpression in advanced non-small-cell lung cancer. Oncogene *28*, S32–S37.

Hommelgaard, A.M., Lerdrup, M., and van Deurs, B. (2004). Association with Membrane Protrusions Makes ErbB2 an Internalization-resistant Receptor. Mol. Biol. Cell *15*, 1557–1567.

Hsu, P.D., Lander, E.S., and Zhang, F. (2014). Development and Applications of CRISPR-Cas9 for Genome Engineering. Cell *157*, 1262–1278.

Hu, H., Mu, Q., Bao, Z., Chen, Y., Liu, Y., Chen, J., Wang, K., Wang, Z., Nam, Y., Jiang, B., et al. (2018). Mutational Landscape of Secondary Glioblastoma Guides MET-Targeted Trial in Brain Tumor. Cell *175*, 1665-1678.e18.

Huang, F., Kirkpatrick, D., Jiang, X., Gygi, S., and Sorkin, A. (2006). Differential regulation of EGF receptor internalization and degradation by multiubiquitination within the kinase domain. Mol. Cell *21*, 737–748.

Huang, H.-J.S., Nagane, M., Klingbeil, C.K., Lin, H., Nishikawa, R., Ji, X.-D., Huang, C.-M., Gill, G.N., Wiley, H.S., and Cavenee, W.K. (1997). The Enhanced Tumorigenic Activity of a Mutant Epidermal Growth Factor Receptor Common in Human Cancers Is Mediated by Threshold Levels of Constitutive Tyrosine Phosphorylation and Unattenuated Signaling. J. Biol. Chem. *272*, 2927–2935.

Huang, M., Yang, W., Zhu, J., Mariño-Enríquez, A., Zhu, C., Chen, J., Wu, Y., Quan, Y., Qiu, H., Li, X., et al. (2020). Coordinated targeting of CK2 and KIT in gastrointestinal stromal tumours. Br. J. Cancer *122*, 372–381.

Hubbard, S.R. (1999). Structural analysis of receptor tyrosine kinases. Prog. Biophys. Mol. Biol. *71*, 343–358.

Hubbard, S.R. (2004). Juxtamembrane autoinhibition in receptor tyrosine kinases. Nat. Rev. Mol. Cell Biol. *5*, 464–471.

Hughes, V.S., and Siemann, D.W. (2018). Have clinical trials properly assessed c-Met inhibitors? Trends Cancer *4*, 94–97.

Hughes, V.S., and Siemann, D.W. (2019). Failures in preclinical and clinical trials of c-Met inhibitors: evaluation of pathway activity as a promising selection criterion. Oncotarget *10*, 184–197.

Humphrey, S.J., James, D.E., and Mann, M. (2015). Protein Phosphorylation: A Major Switch Mechanism for Metabolic Regulation. Trends Endocrinol. Metab. *26*, 676–687.

Hwang, Y., Chumbalkar, V., Latha, K., and Bogler, O. (2011). Forced Dimerization Increases the Activity of ΔEGFR/EGFRvIII and Enhances Its Oncogenicity. Mol. Cancer Res. *9*, 1199–1208.

Ikonomov, O.C., Sbrissa, D., and Shisheva, A. (2001). Mammalian cell morphology and endocytic membrane homeostasis require enzymatically active phosphoinositide 5-kinase PIKfyve. J. Biol. Chem. *276*, 26141–26147.

Ikonomov, O.C., Sbrissa, D., Mlak, K., Kanzaki, M., Pessin, J., and Shisheva, A. (2002). Functional dissection of lipid and protein kinase signals of PIKfyve reveals

the role of PtdIns 3,5-P2 production for endomembrane integrity. J. Biol. Chem. *277*, 9206–9211.

Ikonomov, O.C., Sbrissa, D., Foti, M., Carpentier, J.-L., and Shisheva, A. (2003a). PIKfyve Controls Fluid Phase Endocytosis but Not Recycling/Degradation of Endocytosed Receptors or Sorting of Procathepsin D by Regulating Multivesicular Body Morphogenesis. Mol. Biol. Cell *14*, 4581–4591.

Ikonomov, O.C., Sbrissa, D., Mlak, K., Deeb, R., Fligger, J., Soans, A., Finley, R.L., and Shisheva, A. (2003b). Active PIKfyve Associates with and Promotes the Membrane Attachment of the Late Endosome-to-trans-Golgi Network Transport Factor Rab9 Effector p40. J. Biol. Chem. *278*, 50863–50871.

Ikonomov, O.C., Sbrissa, D., and Shisheva, A. (2006). Localized PtdIns 3,5-P2 synthesis to regulate early endosome dynamics and fusion. Am. J. Physiol. Cell Physiol. *291*, C393-404.

Ikonomov, O.C., Sbrissa, D., Venkatareddy, M., Tisdale, E., Garg, P., and Shisheva, A. (2015). Class III PI 3-Kinase is the Main Source of PtdIns3P Substrate and Membrane Recruitment Signal for PIKfyve Constitutive Function in Podocyte Endomembrane Homeostasis. Biochim. Biophys. Acta *1853*, 1240–1250.

Jean, S., and Kiger, A.A. (2014). Classes of phosphoinositide 3-kinases at a glance. J. Cell Sci. *127*, 923–928.

Jeffers, M.F., and Vande Woude, G.F. (1999). Activating mutations in the Met receptor overcome the requirement for autophosphorylation of tyrosines crucial for wild type signaling. Oncogene *18*, 5120–5125.

Jeffers, M., Fiscella, M., Webb, C.P., Anver, M., Koochekpour, S., and Vande Woude, G.F. (1998). The mutationally activated Met receptor mediates motility and metastasis. Proc. Natl. Acad. Sci. U. S. A. *95*, 14417–14422.

Jethwa, N., Chung, G.H.C., Lete, M.G., Alonso, A., Byrne, R.D., Calleja, V., and Larijani, B. (2015). Endomembrane PtdIns(3,4,5)P3 activates the PI3K–Akt pathway. J. Cell Sci. *128*, 3456–3465.

Jiang, H., Martin, V., Gomez-Manzano, C., Johnson, D.G., Alonso, M., White, E., Xu, J., McDonnell, T.J., Shinojima, N., and Fueyo, J. (2010a). The RB-E2F1 Pathway Regulates Autophagy. Cancer Res. *70*, 7882–7893.

Jiang, X., Huang, F., Marusyk, A., and Sorkin, A. (2003). Grb2 Regulates Internalization of EGF Receptors through Clathrin-coated Pits. Mol. Biol. Cell *14*, 858–870.

Jiang, X., Chen, S., Asara, J.M., and Balk, S.P. (2010b). Phosphoinositide 3-kinase pathway activation in phosphate and tensin homolog (PTEN)-deficient prostate cancer cells is independent of receptor tyrosine kinases and mediated by the p110beta and p110delta catalytic subunits. J. Biol. Chem. *285*, 14980–14989.

Jinek, M., East, A., Cheng, A., Lin, S., Ma, E., and Doudna, J. (2013). RNA-programmed genome editing in human cells. ELife *2*, e00471.

Jo, M., Stolz, D.B., Esplen, J.E., Dorko, K., Michalopoulos, G.K., and Strom, S.C. (2000). Cross-talk between Epidermal Growth Factor Receptor and c-Met Signal Pathways in Transformed Cells. J. Biol. Chem. *275*, 8806–8811.

Joffre, C., Barrow, R., Ménard, L., Calleja, V., Hart, I.R., and Kermorgant, S. (2011). A direct role for Met endocytosis in tumorigenesis. Nat. Cell Biol. *13*, 827–837.

Johnson, L.N., Noble, M.E.M., and Owen, D.J. (1996). Active and Inactive Protein Kinases: Structural Basis for Regulation. Cell *85*, 149–158.

Jorge, S.E., Schulman, S., Freed, J.A., VanderLaan, P.A., Rangachari, D., Kobayashi, S.S., Huberman, M.S., and Costa, D.B. (2015). Responses to the multitargeted MET/ALK/ROS1 inhibitor crizotinib and co-occurring mutations in lung adenocarcinomas with MET amplification or MET exon 14 skipping mutation. Lung Cancer Amst. Neth. *90*, 369–374.

Jung, C.H., Ro, S.-H., Cao, J., Otto, N.M., and Kim, D.-H. (2010). mTOR regulation of autophagy. FEBS Lett. *584*, 1287–1295.

Jura, N., Endres, N.F., Engel, K., Deindl, S., Das, R., Lamers, M.H., Wemmer, D.E., Zhang, X., and Kuriyan, J. (2009). Mechanism for Activation of the EGF Receptor Catalytic Domain by the Juxtamembrane Segment. Cell *137*, 1293–1307.

Kang, Y.-J., Balter, B., Csizmadia, E., Haas, B., Sharma, H., Bronson, R., and Yan, C.T. (2017). Contribution of classical end-joining to PTEN inactivation in p53-mediated glioblastoma formation and drug-resistant survival. Nat. Commun. *8*, 1–15.

Kaplan, M., Narasimhan, S., de Heus, C., Mance, D., van Doorn, S., Houben, K., Popov-Čeleketić, D., Damman, R., Katrukha, E.A., Jain, P., et al. (2016). EGFR Dynamics Change during Activation in Native Membranes as Revealed by NMR. Cell *167*, 1241-1251.e11.

Kaur, M., and Cole, M.D. (2013). MYC Acts via the PTEN Tumor Suppressor to Elicit Autoregulation and Genome-Wide Gene Repression by Activation of the Ezh2 Methyltransferase. Cancer Res. *73*, 695–705.

Kermorgant, S., Zicha, D., and Parker, P.J. (2003). Protein Kinase C Controls Microtubule-based Traffic but Not Proteasomal Degradation of c-Met. J. Biol. Chem. *278*, 28921–28929.

Khan, G.N., Kim, E.J., Shin, T.S., and Lee, S.H. (2017). Heterogeneous Cell Types in Single-cell-derived Clones of MCF7 and MDA-MB-231 Cells. Anticancer Res. *37*, 2343–2354.

Kim, Y.C., and Guan, K.-L. (2015). mTOR: a pharmacologic target for autophagy regulation. J. Clin. Invest. *125*, 25–32.

Kim, J., Jahng, W.J., Di Vizio, D., Lee, J.S., Jhaveri, R., Rubin, M.A., Shisheva, A., and Freeman, M.R. (2007). The Phosphoinositide Kinase PIKfyve Mediates EGF Receptor Trafficking to the Nucleus. Cancer Res. *67*, 9229–9237.

Kim, J., Kim, Y.C., Fang, C., Russell, R.C., Kim, J.H., Fan, W., Liu, R., Zhong, Q., and Guan, K.-L. (2013). Differential regulation of distinct Vps34 complexes by AMPK in nutrient stress and autophagy. Cell *152*, 290–303.

Kim, J., Vasu, V.T., Mishra, R., Singleton, K.R., Yoo, M., Leach, S.M., Farias-Hesson, E., Mason, R.J., Kang, J., Ramamoorthy, P., et al. (2014). Bioinformatics-driven discovery of rational combination for overcoming EGFR-mutant lung cancer resistance to EGFR therapy. Bioinformatics *30*, 2393–2398.

Kimmelman, A.C., and White, E. (2017). Autophagy and Tumor Metabolism. Cell Metab. *25*, 1037–1043.

Kimura, S., Noda, T., and Yoshimori, T. (2007). Dissection of the autophagosome maturation process by a novel reporter protein, tandem fluorescent-tagged LC3. Autophagy *3*, 452–460.

Klionsky, D.J., Abdelmohsen, K., Abe, A., Abedin, M.J., Abeliovich, H., Acevedo Arozena, A., Adachi, H., Adams, C.M., Adams, P.D., Adeli, K., et al. (2016). Guidelines for the use and interpretation of assays for monitoring autophagy (3rd edition). Autophagy *12*, 1–222.

Koivunen, J.P., Mermel, C., Zejnullahu, K., Murphy, C., Lifshits, E., Holmes, A.J., Choi, H.G., Kim, J., Chiang, D., Thomas, R., et al. (2008). EML4-ALK fusion gene and efficacy of an ALK kinase inhibitor in lung cancer. Clin. Cancer Res. Off. J. Am. Assoc. Cancer Res. *14*, 4275–4283.

Kokubo, Y., Gemma, A., Noro, R., Seike, M., Kataoka, K., Matsuda, K., Okano, T., Minegishi, Y., Yoshimura, A., Shibuya, M., et al. (2005). Reduction of PTEN protein and loss of epidermal growth factor receptor gene mutation in lung cancer with natural resistance to gefitinib (IRESSA). Br. J. Cancer *92*, 1711–1719.

Komada, M., and Kitamura, N. (1994). Regulatory role of major tyrosine autophosphorylation site of kinase domain of c-Met receptor (scatter factor/hepatocyte growth factor receptor). J. Biol. Chem. *269*, 16131–16136.

Kong, A., Calleja, V., Leboucher, P., Harris, A., Parker, P.J., and Larijani, B. (2008). HER2 Oncogenic Function Escapes EGFR Tyrosine Kinase Inhibitors via Activation of Alternative HER Receptors in Breast Cancer Cells. PLoS ONE *3*.

Kong-Beltran, M., Stamos, J., and Wickramasinghe, D. (2004). The Sema domain of Met is necessary for receptor dimerization and activation. Cancer Cell *6*, 75–84.

Kong-Beltran, M., Seshagiri, S., Zha, J., Zhu, W., Bhawe, K., Mendoza, N., Holcomb, T., Pujara, K., Stinson, J., Fu, L., et al. (2006). Somatic Mutations Lead to an Oncogenic Deletion of Met in Lung Cancer. Cancer Res. *66*, 283–289.

Koschut, D., Richert, L., Pace, G., Niemann, H.H., Mély, Y., and Orian-Rousseau, V. (2016). Live cell imaging shows hepatocyte growth factor-induced Met dimerization. Biochim. Biophys. Acta BBA - Mol. Cell Res. *1863*, 1552–1558.

Kosicki, M., Tomberg, K., and Bradley, A. (2018). Repair of double-strand breaks induced by CRISPR–Cas9 leads to large deletions and complex rearrangements. Nat. Biotechnol. *36*, 765–771.

Kovacevic, Z., Chikhani, S., Lui, G.Y.L., Sivagurunathan, S., and Richardson, D.R. (2013). The iron-regulated metastasis suppressor NDRG1 targets NEDD4L, PTEN, and SMAD4 and inhibits the PI3K and Ras signaling pathways. Antioxid. Redox Signal. *18*, 874–887.

Krausz, S., Boumans, M.J.H., Gerlag, D.M., Lufkin, J., van Kuijk, A.W.R., Bakker, A., de Boer, M., Lodde, B.M., Reedquist, K.A., Jacobson, E.W., et al. (2012). Brief report: a phase IIa, randomized, double-blind, placebo-controlled trial of apilimod mesylate, an interleukin-12/interleukin-23 inhibitor, in patients with rheumatoid arthritis. Arthritis Rheum. *64*, 1750–1755.

Krishnaswamy, S., Kanteti, R., Duke-Cohan, J.S., Loganathan, S., Liu, W., Ma, P.C., Sattler, M., Singleton, P.A., Ramnath, N., Innocenti, F., et al. (2009). Ethnic differences and functional analysis of MET mutations in lung cancer. Clin. Cancer Res. Off. J. Am. Assoc. Cancer Res. *15*, 5714–5723.

Kucera, A., Bakke, O., and Progida, C. (2016). The multiple roles of Rab9 in the endolysosomal system. Commun. Integr. Biol. *9*.

Kusumi, A., Suzuki, K.G.N., Kasai, R.S., Ritchie, K., and Fujiwara, T.K. (2011). Hierarchical mesoscale domain organization of the plasma membrane. Trends Biochem. Sci. *36*, 604–615.

Kwak, Y., Kim, S.-I., Park, C.-K., Paek, S.H., Lee, S.-T., and Park, S.-H. (2015). C-MET overexpression and amplification in gliomas. Int. J. Clin. Exp. Pathol. *8*, 14932–14938.

Landry, C.R., Levy, E.D., and Michnick, S.W. (2009). Weak functional constraints on phosphoproteomes. Trends Genet. TIG *25*, 193–197.

Langowski, J.L., Zhang, X., Wu, L., Mattson, J.D., Chen, T., Smith, K., Basham, B., McClanahan, T., Kastelein, R.A., and Oft, M. (2006). IL-23 promotes tumour incidence and growth. Nature *442*, 461–465.

de Lartigue, J., Polson, H., Feldman, M., Shokat, K., Tooze, S.A., Urbé, S., and Clague, M.J. (2009). PIKfyve Regulation of Endosome-Linked Pathways. Traffic Cph. Den. *10*, 883–893.

Leatherbarrow, J.R., and Halfon, M.S. (2009). Identification of Receptor-Tyrosine-Kinase-Signaling Target Genes Reveals Receptor-Specific Activities and Pathway Branchpoints During Drosophila Development. Genetics *181*, 1335–1345.

Lee, J., Tran, P., and Klempner, S.J. (2016). Targeting the MET Pathway in Gastric and Oesophageal Cancers: Refining the Optimal Approach. Clin. Oncol. *28*, e35–e44.

Lee, J.C., Vivanco, I., Beroukhim, R., Huang, J.H.Y., Feng, W.L., DeBiasi, R.M., Yoshimoto, K., King, J.C., Nghiemphu, P., Yuza, Y., et al. (2006). Epidermal growth factor receptor activation in glioblastoma through novel missense mutations in the extracellular domain. PLoS Med. *3*, e485.

Lee, Y.-R., Chen, M., Lee, J.D., Zhang, J., Lin, S.-Y., Fu, T.-M., Chen, H., Ishikawa, T., Chiang, S.-Y., Katon, J., et al. (2019). Reactivation of PTEN tumor suppressor for cancer treatment through inhibition of a MYC-WWP1 inhibitory pathway. Science *364*.

Lehmann, B.D., Bauer, J.A., Chen, X., Sanders, M.E., Chakravarthy, A.B., Shyr, Y., and Pietenpol, J.A. (2011). Identification of human triple-negative breast cancer subtypes and preclinical models for selection of targeted therapies. J. Clin. Invest. *121*, 2750–2767.

Lemmon, M.A., and Schlessinger, J. (2010). Cell signaling by receptor-tyrosine kinases. Cell *141*, 1117–1134.

Levi-Montalcini, R., and Booker, B. (1960). EXCESSIVE GROWTH OF THE SYMPATHETIC GANGLIA EVOKED BY A PROTEIN ISOLATED FROM MOUSE SALIVARY GLANDS. Proc. Natl. Acad. Sci. U. S. A. *46*, 373–384.

Levkowitz, G., Waterman, H., Zamir, E., Kam, Z., Oved, S., Langdon, W.Y., Beguinot, L., Geiger, B., and Yarden, Y. (1998). c-Cbl/Sli-1 regulates endocytic sorting and ubiquitination of the epidermal growth factor receptor. Genes Dev. *12*, 3663–3674.

Li, E., and Hristova, K. (2010). Receptor tyrosine kinase transmembrane domains. Cell Adhes. Migr. *4*, 249–254.

Li, J., Yen, C., Liaw, D., Podsypanina, K., Bose, S., Wang, S.I., Puc, J., Miliaresis, C., Rodgers, L., McCombie, R., et al. (1997). PTEN, a Putative Protein Tyrosine Phosphatase Gene Mutated in Human Brain, Breast, and Prostate Cancer. Science *275*, 1943–1947.

Li, N., Lorinczi, M., Ireton, K., and Elferink, L.A. (2007). Specific Grb2-mediated Interactions Regulate Clathrin-dependent Endocytosis of the cMet-tyrosine Kinase. J. Biol. Chem. *282*, 16764–16775.

Li, X., Wang, X., Zhang, X., Zhao, M., Tsang, W.L., Zhang, Y., Yau, R.G.W., Weisman, L.S., and Xu, H. (2013). Genetically encoded fluorescent probe to visualize intracellular phosphatidylinositol 3,5-bisphosphate localization and dynamics. Proc. Natl. Acad. Sci. *110*, 21165–21170.

Liang, C., Feng, P., Ku, B., Dotan, I., Canaani, D., Oh, B.-H., and Jung, J.U. (2006). Autophagic and tumour suppressor activity of a novel Beclin1-binding protein UVRAG. Nat. Cell Biol. *8*, 688–699.

Liang, X.H., Jackson, S., Seaman, M., Brown, K., Kempkes, B., Hibshoosh, H., and Levine, B. (1999). Induction of autophagy and inhibition of tumorigenesis by beclin 1. Nature *402*, 672–676.

Lienhard, G.E. (2008). Non-functional phosphorylations? Trends Biochem. Sci. *33*, 351–352.

Lin, R., Xia, S., Shan, C., Chen, D., Liu, Y., Gao, X., Wang, M., Kang, H.-B., Pan, Y., Liu, S., et al. (2018). The Dietary Supplement Chondroitin-4-Sulfate Exhibits Oncogene-Specific Pro-tumor Effects on BRAF V600E Melanoma Cells. Mol. Cell *69*, 923-937.e8.

Litchfield, D.W. (2003). Protein kinase CK2: structure, regulation and role in cellular decisions of life and death. Biochem. J. *369*, 1–15.

Liu, B., Bao, J.-K., Yang, J.-M., and Cheng, Y. (2013). Targeting autophagic pathways for cancer drug discovery. Chin. J. Cancer *32*, 113–120.

Liu, P., Cheng, H., Roberts, T.M., and Zhao, J.J. (2009). Targeting the phosphoinositide 3-kinase (PI3K) pathway in cancer. Nat. Rev. Drug Discov. *8*, 627–644.

Liu, P., Cleveland, T.E., Bouyain, S., Byrne, P.O., Longo, P.A., and Leahy, D.J. (2012). A single ligand is sufficient to activate EGFR dimers. Proc. Natl. Acad. Sci. *109*, 10861–10866.

Liu, X., Jia, Y., Stoopler, M.B., Shen, Y., Cheng, H., Chen, J., Mansukhani, M., Koul, S., Halmos, B., and Borczuk, A.C. (2015). Next-Generation Sequencing of Pulmonary Sarcomatoid Carcinoma Reveals High Frequency of Actionable MET Gene Mutations. J. Clin. Oncol. *34*, 794–802.

Liu, Y.J., Shen, D., Yin, X., Gavine, P., Zhang, T., Su, X., Zhan, P., Xu, Y., Lv, J., Qian, J., et al. (2014). HER2, MET and FGFR2 oncogenic driver alterations define distinct molecular segments for targeted therapies in gastric carcinoma. Br. J. Cancer *110*, 1169–1178.

Loureiro, A., and da Silva, G.J. (2019). CRISPR-Cas: Converting A Bacterial Defence Mechanism into A State-of-the-Art Genetic Manipulation Tool. Antibiotics *8*.

Lu, W.-J., Chua, M.-S., and So, S.K. (2014). Suppressing N-Myc downstream regulated gene 1 reactivates senescence signaling and inhibits tumor growth in hepatocellular carcinoma. Carcinogenesis *35*, 915–922.

Ludes-Meyers, J.H., Subler, M.A., Shivakumar, C.V., Munoz, R.M., Jiang, P., Bigger, J.E., Brown, D.R., Deb, S.P., and Deb, S. (1996). Transcriptional activation of the human epidermal growth factor receptor promoter by human p53. Mol. Cell. Biol. *16*, 6009–6019.

Luo, S.Y., and Lam, D.C. (2013). Oncogenic driver mutations in lung cancer. Transl. Respir. Med. *1*, 6.

Ma, P.C., Kijima, T., Maulik, G., Fox, E.A., Sattler, M., Griffin, J.D., Johnson, B.E., and Salgia, R. (2003). c-MET mutational analysis in small cell lung cancer: novel juxtamembrane domain mutations regulating cytoskeletal functions. Cancer Res. *63*, 6272–6281.

Ma, P.C., Jagadeeswaran, R., Jagadeesh, S., Tretiakova, M.S., Nallasura, V., Fox, E.A., Hansen, M., Schaefer, E., Naoki, K., Lader, A., et al. (2005). Functional expression and mutations of c-Met and its therapeutic inhibition with SU11274 and small interfering RNA in non-small cell lung cancer. Cancer Res. *65*, 1479–1488.

Ma, T., Sun, X., Cui, L., Gao, L., Wu, Y., Liu, H., Zhu, Z., Wang, F., and Liu, Z. (2014). Molecular Imaging Reveals Trastuzumab-Induced Epidermal Growth Factor Receptor Downregulation In Vivo. J. Nucl. Med. *55*, 1002–1007.

Maeda, R., Sato, T., Okamoto, K., Yanagawa, M., and Sako, Y. (2018). Lipid-Protein Interplay in Dimerization of Juxtamembrane Domains of Epidermal Growth Factor Receptor. Biophys. J. *114*, 893–903.

Maiuri, M.C., Le Toumelin, G., Criollo, A., Rain, J.-C., Gautier, F., Juin, P., Tasdemir, E., Pierron, G., Troulinaki, K., Tavernarakis, N., et al. (2007). Functional and physical interaction between Bcl-X(L) and a BH3-like domain in Beclin-1. EMBO J. *26*, 2527–2539.

Mali, P., Yang, L., Esvelt, K.M., Aach, J., Guell, M., DiCarlo, J.E., Norville, J.E., and Church, G.M. (2013). RNA-Guided Human Genome Engineering via Cas9. Science *339*, 823–826.

Manning, B.D., and Toker, A. (2017). AKT/PKB Signaling: Navigating the Network. Cell *169*, 381–405.

Marat, A.L., and Haucke, V. (2016). Phosphatidylinositol 3-phosphates—at the interface between cell signalling and membrane traffic. EMBO J. *35*, 561–579.

Margolis, B., and Skolnik, E.Y. (1994). Activation of Ras by receptor tyrosine kinases. J. Am. Soc. Nephrol. JASN *5*, 1288–1299.

Marmor, M.D., and Yarden, Y. (2004). Role of protein ubiquitylation in regulating endocytosis of receptor tyrosine kinases. Oncogene *23*, 2057–2070.

Martin-Fernandez, M.L., Clarke, D.T., Roberts, S.K., Zanetti-Domingues, L.C., and Gervasio, F.L. (2019). Structure and Dynamics of the EGF Receptor as Revealed by Experiments and Simulations and Its Relevance to Non-Small Cell Lung Cancer. Cells *8*, 316.

Masuda, H., Zhang, D., Bartholomeusz, C., Doihara, H., Hortobagyi, G.N., and Ueno, N.T. (2012). Role of Epidermal Growth Factor Receptor in Breast Cancer. Breast Cancer Res. Treat. *136*.

Mattoon, D.R., Lamothe, B., Lax, I., and Schlessinger, J. (2004). The docking protein Gab1 is the primary mediator of EGF-stimulated activation of the PI-3K/Akt cell survival pathway. BMC Biol. *2*, 24.

Mayer, I.A., and Arteaga, C.L. (2016). The PI3K/AKT Pathway as a Target for Cancer Treatment. Annu. Rev. Med. *67*, 11–28.

Mayinger, P. (2012). Phosphoinositides and vesicular membrane traffic. Biochim. Biophys. Acta *1821*, 1104–1113.

McCaig, C., Potter, L., Abramczyk, O., and Murray, J.T. (2011). Phosphorylation of NDRG1 is temporally and spatially controlled during the cell cycle. Biochem. Biophys. Res. Commun. *411*, 227–234.

McCain, J. (2013). The MAPK (ERK) Pathway. Pharm. Ther. *38*, 96–108.

McConnachie, G., Pass, I., Walker, S.M., and Downes, C.P. (2003). Interfacial kinetic analysis of the tumour suppressor phosphatase, PTEN: evidence for activation by anionic phospholipids. Biochem. J. *371*, 947–955.

McLaughlin, S., Smith, S.O., Hayman, M.J., and Murray, D. (2005). An Electrostatic Engine Model for Autoinhibition and Activation of the Epidermal Growth Factor Receptor (EGFR/ErbB) Family. J. Gen. Physiol. *126*, 41–53.

McPherson, P.S., Kay, B.K., and Hussain, N.K. (2001). Signaling on the Endocytic Pathway. Traffic *2*, 375–384.

Medina, P.J., and Goodin, S. (2008). Lapatinib: a dual inhibitor of human epidermal growth factor receptor tyrosine kinases. Clin. Ther. *30*, 1426–1447.

Mellinghoff, I.K., Wang, M.Y., Vivanco, I., Haas-Kogan, D.A., Zhu, S., Dia, E.Q., Lu, K.V., Yoshimoto, K., Huang, J.H.Y., Chute, D.J., et al. (2005). Molecular Determinants of the Response of Glioblastomas to EGFR Kinase Inhibitors. N. Engl. J. Med. *353*, 2012–2024.

Mellman, I., and Yarden, Y. (2013). Endocytosis and Cancer. Cold Spring Harb. Perspect. Biol. *5*.

Ménard, L., Parker, P.J., and Kermorgant, S. (2014). Receptor tyrosine kinase c-Met controls the cytoskeleton from different endosomes via different pathways. Nat. Commun. *5*, 1–14.

Miaczynska, M., Pelkmans, L., and Zerial, M. (2004). Not just a sink: endosomes in control of signal transduction. Curr. Opin. Cell Biol. *16*, 400–406.

Michailidis, I.E., Rusinova, R., Georgakopoulos, A., Chen, Y., Iyengar, R., Robakis, N.K., Logothetis, D.E., and Baki, L. (2011). Phosphatidylinositol-4,5-bisphosphate regulates epidermal growth factor receptor activation. Pflugers Arch. *461*, 387–397.

Middleton, G., Crack, L.R., Popat, S., Swanton, C., Hollingsworth, S.J., Buller, R., Walker, I., Carr, T.H., Wherton, D., and Billingham, L.J. (2015). The National Lung Matrix Trial: translating the biology of stratification in advanced non-small-cell lung cancer. Ann. Oncol. Off. J. Eur. Soc. Med. Oncol. *26*, 2464–2469.

Milella, M., Falcone, I., Conciatori, F., Cesta Incani, U., Del Curatolo, A., Inzerilli, N., Nuzzo, C.M.A., Vaccaro, V., Vari, S., Cognetti, F., et al. (2015). PTEN: Multiple Functions in Human Malignant Tumors. Front. Oncol. *5*.

Min, S.H., Weaver, L., Suzuki, A., Guzman, J., and Abrams, C.S. (2015). Pikfyve Regulates Lysosomal Biogenesis and Functions in Macrophages. Blood *126*, 887–887.

Mizushima, N., and Komatsu, M. (2011). Autophagy: Renovation of Cells and Tissues. Cell *147*, 728–741.

Mizushima, N., and Yoshimori, T. (2007). How to interpret LC3 immunoblotting. Autophagy *3*, 542–545.

Modi, V., and Dunbrack, R.L. (2018). Clustering of the structures of protein kinase activation loops: A new nomenclature for active and inactive kinase structures. BioRxiv 395723.

Mohapatra, B., Ahmad, G., Nadeau, S., Zutshi, N., An, W., Scheffe, S., Dong, L., Feng, D., Goetz, B., Arya, P., et al. (2013). Protein tyrosine kinase regulation by ubiquitination: Critical roles of Cbl-family ubiquitin ligases. Biochim. Biophys. Acta *1833*, 122–139.

Montoya, A., Beltran, L., Casado, P., Rodríguez-Prados, J.-C., and Cutillas, P.R. (2011). Characterization of a TiO2 enrichment method for label-free quantitative phosphoproteomics. Methods San Diego Calif *54*, 370–378.

Moriki, T., Maruyama, H., and Maruyama, I.N. (2001). Activation of preformed EGF receptor dimers by ligand-induced rotation of the transmembrane domain. J. Mol. Biol. *311*, 1011–1026.

Morselli, E., Galluzzi, L., Kepp, O., Vicencio, J.-M., Criollo, A., Maiuri, M.C., and Kroemer, G. (2009). Anti- and pro-tumor functions of autophagy. Biochim. Biophys. Acta BBA - Mol. Cell Res. *1793*, 1524–1532.

Moscatello, D.K., Montgomery, R.B., Sundareshan, P., McDanel, H., Wong, M.Y., and Wong, A.J. (1996). Transformational and altered signal transduction by a naturally occurring mutant EGF receptor. Oncogene *13*, 85–96.

Mosesson, Y., Mills, G.B., and Yarden, Y. (2008). Derailed endocytosis: an emerging feature of cancer. Nat. Rev. Cancer *8*, 835–850.

Mou, H., Smith, J.L., Peng, L., Yin, H., Moore, J., Zhang, X.-O., Song, C.-Q., Sheel, A., Wu, Q., Ozata, D.M., et al. (2017). CRISPR/Cas9-mediated genome editing induces exon skipping by alternative splicing or exon deletion. Genome Biol. *18*, 108.

Mousavi, S.A., Malerød, L., Berg, T., and Kjeken, R. (2004). Clathrin-dependent endocytosis. Biochem. J. *377*, 1–16.

Myers, M.P., Stolarov, J.P., Eng, C., Li, J., Wang, S.I., Wigler, M.H., Parsons, R., and Tonks, N.K. (1997). P-TEN, the tumor suppressor from human chromosome 10q23, is a dual-specificity phosphatase. Proc. Natl. Acad. Sci. *94*, 9052–9057.

Nakamura, T. (1994). Hepatocyte growth factor as mitogen, motogen and morphogen, and its roles in organ regeneration. Princess Takamatsu Symp. *24*, 195–213.

Nakanishi, Y., Walter, K., Spoerke, J.M., O'Brien, C., Huw, L.Y., Hampton, G.M., and Lackner, M.R. (2016). Activating Mutations in PIK3CB Confer Resistance to PI3K Inhibition and Define a Novel Oncogenic Role for p110β. Cancer Res. *76*, 1193–1203.

Naldini, L., Vigna, E., Narsimhan, R.P., Gaudino, G., Zarnegar, R., Michalopoulos, G.K., and Comoglio, P.M. (1991). Hepatocyte growth factor (HGF) stimulates the tyrosine kinase activity of the receptor encoded by the proto-oncogene c-MET. Oncogene *6*, 501–504.

Naslavsky, N., and Caplan, S. (2018). The enigmatic endosome – sorting the ins and outs of endocytic trafficking. J. Cell Sci. *131*.

Nicot, A.-S., Fares, H., Payrastre, B., Chisholm, A.D., Labouesse, M., and Laporte, J. (2006). The phosphoinositide kinase PIKfyve/Fab1p regulates terminal lysosome maturation in Caenorhabditis elegans. Mol. Biol. Cell *17*, 3062–3074.

Ning, L., Guo-Chun, Z., Sheng-Li, A., Xue-Rui, L., Kun, W., Jian, Z., Chong-Yang, R., Ling-Zhu, W., and Hai-Tong, L. (2016). Inhibition of autophagy induced by PTEN loss promotes intrinsic breast cancer resistance to trastuzumab therapy. Tumour Biol. J. Int. Soc. Oncodevelopmental Biol. Med. *37*, 5445–5454.

Nishida, Y., Arakawa, S., Fujitani, K., Yamaguchi, H., Mizuta, T., Kanaseki, T., Komatsu, M., Otsu, K., Tsujimoto, Y., and Shimizu, S. (2009). Discovery of Atg5/Atg7-independent alternative macroautophagy. Nature *461*, 654–658.

Odorizzi, G., Babst, M., and Emr, S.D. (2000). Phosphoinositide signaling and the regulation of membrane trafficking in yeast. Trends Biochem. Sci. *25*, 229–235.

Ogiso, H., Ishitani, R., Nureki, O., Fukai, S., Yamanaka, M., Kim, J.-H., Saito, K., Sakamoto, A., Inoue, M., Shirouzu, M., et al. (2002). Crystal Structure of the Complex of Human Epidermal Growth Factor and Receptor Extracellular Domains. Cell *110*, 775–787.

Okuda, K., Sasaki, H., Yukiue, H., Yano, M., and Fujii, Y. (2008). Met gene copy number predicts the prognosis for completely resected non-small cell lung cancer. Cancer Sci. *99*, 2280–2285.

Okur, M.N., Russo, A., and O'Bryan, J.P. (2014). Receptor tyrosine kinase ubiquitylation involves the dynamic regulation of Cbl-Spry2 by intersectin 1 and the Shp2 tyrosine phosphatase. Mol. Cell. Biol. *34*, 271–279.

Onozato, R., Kosaka, T., Kuwano, H., Sekido, Y., Yatabe, Y., and Mitsudomi, T. (2009). Activation of MET by gene amplification or by splice mutations deleting the juxtamembrane domain in primary resected lung cancers. J. Thorac. Oncol. Off. Publ. Int. Assoc. Study Lung Cancer *4*, 5–11.

Ooi, A., Takehana, T., Li, X., Suzuki, S., Kunitomo, K., Iino, H., Fujii, H., Takeda, Y., and Dobashi, Y. (2004). Protein overexpression and gene amplification of HER-2 and EGFR in colorectal cancers: an immunohistochemical and fluorescent in situ hybridization study. Mod. Pathol. Off. J. U. S. Can. Acad. Pathol. Inc *17*, 895–904.

Oppelt, A., Haugsten, E.M., Zech, T., Danielsen, H.E., Sveen, A., Lobert, V.H., Skotheim, R.I., and Wesche, J. (2014). PIKfyve, MTMR3 and their product PtdIns5P regulate cancer cell migration and invasion through activation of Rac1. Biochem. J. *461*, 383–390.

Orth, J.D., Krueger, E.W., Weller, S.G., and McNiven, M.A. (2006). A Novel Endocytic Mechanism of Epidermal Growth Factor Receptor Sequestration and Internalization. Cancer Res. *66*, 3603–3610.

Paik, P.K., Drilon, A., Fan, P.-D., Yu, H., Rekhtman, N., Ginsberg, M.S., Borsu, L., Schultz, N., Berger, M.F., Rudin, C.M., et al. (2015). Response to MET inhibitors in patients with stage IV lung adenocarcinomas harboring MET mutations causing exon 14 skipping. Cancer Discov. *5*, 842–849.

Paik, P.K., Veillon, R., Cortot, A.B., Felip, E., Sakai, H., Mazieres, J., Griesinger, F., Horn, L., Senellart, H., Van Meerbeeck, J.P., et al. (2019). Phase II study of tepotinib in NSCLC patients with METex14 mutations. J. Clin. Oncol. *37*, 9005–9005.

Palmieri, L., and Rastelli, G. (2013). αC helix displacement as a general approach for allosteric modulation of protein kinases. Drug Discov. Today *18*, 407–414.

Pankiv, S., Clausen, T.H., Lamark, T., Brech, A., Bruun, J.-A., Outzen, H., Øvervatn, A., Bjørkøy, G., and Johansen, T. (2007). p62/SQSTM1 binds directly to Atg8/LC3 to facilitate degradation of ubiquitinated protein aggregates by autophagy. J. Biol. Chem. *282*, 24131–24145.

Papa, A., and Pandolfi, P.P. (2019). The PTEN–PI3K Axis in Cancer. Biomolecules *9*.

Park, K.C., Menezes, S.V., Kalinowski, D.S., Sahni, S., Jansson, P.J., Kovacevic, Z., and Richardson, D.R. (2018). Identification of differential phosphorylation and sub-cellular localization of the metastasis suppressor, NDRG1. Biochim. Biophys. Acta BBA - Mol. Basis Dis. *1864*, 2644–2663.

Park, K.C., Geleta, B., Leck, L.Y.W., Paluncic, J., Chiang, S., Jansson, P.J., Kovacevic, Z., and Richardson, D.R. (2019). Thiosemicarbazones suppress expression of the c-Met oncogene by mechanisms involving lysosomal degradation and intracellular shedding. J. Biol. Chem. jbc.RA119.011341.

Parsons, R. (2004). Human cancer, PTEN and the PI-3 kinase pathway. Semin. Cell Dev. Biol. *15*, 171–176.

Pasquier, B. (2015). SAR405, a PIK3C3/Vps34 inhibitor that prevents autophagy and synergizes with MTOR inhibition in tumor cells. Autophagy *11*, 725–726.

Pawson, T. (1995). Protein modules and signalling networks. Nature *373*, 573–580.

Pennock, S., and Wang, Z. (2008). A Tale of Two Cbls: Interplay of c-Cbl and Cbl-b in Epidermal Growth Factor Receptor Downregulation. Mol. Cell. Biol. *28*, 3020–3037.

Petiot, A., Ogier-Denis, E., Blommaart, E.F.C., Meijer, A.J., and Codogno, P. (2000). Distinct Classes of Phosphatidylinositol 3′-Kinases Are Involved in Signaling Pathways That Control Macroautophagy in HT-29 Cells. J. Biol. Chem. *275*, 992–998.

Pines, G., Köstler, W.J., and Yarden, Y. (2010). Oncogenic mutant forms of EGFR: lessons in signal transduction and targets for cancer therapy. FEBS Lett. *584*, 2699–2706.

Plowey, E.D., Cherra, S.J., Liu, Y.-J., and Chu, C.T. (2008). Role of autophagy in G2019S-LRRK2-associated neurite shortening in differentiated SH-SY5Y cells. J. Neurochem. *105*, 1048–1056.

Ponzetto, C., Bardelli, A., Zhen, Z., Maina, F., dalla Zonca, P., Giordano, S., Graziani, A., Panayotou, G., and Comoglio, P.M. (1994). A multifunctional docking site mediates signaling and transformation by the hepatocyte growth factor/scatter factor receptor family. Cell *77*, 261–271.

Prigent, S.A., Nagane, M., Lin, H., Huvar, I., Boss, G.R., Feramisco, J.R., Cavenee, W.K., and Huang, H.-J.S. (1996). Enhanced Tumorigenic Behavior of Glioblastoma Cells Expressing a Truncated Epidermal Growth Factor Receptor Is Mediated through the Ras-Shc-Grb2 Pathway. J. Biol. Chem. *271*, 25639–25645.

Radu, A., Neubauer, V., Akagi, T., Hanafusa, H., and Georgescu, M.-M. (2003). PTEN Induces Cell Cycle Arrest by Decreasing the Level and Nuclear Localization of Cyclin D1. Mol. Cell. Biol. *23*, 6139–6149.

Raiborg, C., Schink, K.O., and Stenmark, H. (2013). Class III phosphatidylinositol 3-kinase and its catalytic product PtdIns3P in regulation of endocytic membrane traffic. FEBS J. *280*, 2730–2742.

Rakha, E.A., El-Sayed, M.E., Green, A.R., Lee, A.H.S., Robertson, J.F., and Ellis, I.O. (2007). Prognostic markers in triple-negative breast cancer. Cancer *109*, 25–32.

Ramel, D., Lagarrigue, F., Pons, V., Mounier, J., Dupuis-Coronas, S., Chicanne, G., Sansonetti, P.J., Gaits-Iacovoni, F., Tronchère, H., and Payrastre, B. (2011). Shigella flexneri infection generates the lipid PI5P to alter endocytosis and prevent termination of EGFR signaling. Sci. Signal. *4*, ra61.

Ran, F.A., Hsu, P.D., Lin, C.-Y., Gootenberg, J.S., Konermann, S., Trevino, A., Scott, D.A., Inoue, A., Matoba, S., Zhang, Y., et al. (2013). Double nicking by RNA-guided CRISPR Cas9 for enhanced genome editing specificity. Cell *154*, 1380–1389.

Razis, E., Bobos, M., Kotoula, V., Eleftheraki, A.G., Kalofonos, H.P., Pavlakis, K., Papakostas, P., Aravantinos, G., Rigakos, G., Efstratiou, I., et al. (2011). Evaluation of the association of PIK3CA mutations and PTEN loss with efficacy of trastuzumab therapy in metastatic breast cancer. Breast Cancer Res. Treat. *128*, 447–456.

Redmann, M., Benavides, G.A., Berryhill, T.F., Wani, W.Y., Ouyang, X., Johnson, M.S., Ravi, S., Barnes, S., Darley-Usmar, V.M., and Zhang, J. (2016). Inhibition of autophagy with bafilomycin and chloroquine decreases mitochondrial quality and bioenergetic function in primary neurons. Redox Biol. *11*, 73–81.

Regad, T. (2015). Targeting RTK Signaling Pathways in Cancer. Cancers *7*, 1758–1784.

Rege-Cambrin, G., Scaravaglio, P., Carozzi, F., Giordano, S., Ponzetto, C., Comoglio, P.M., and Saglio, G. (1992). Karyotypic analysis of gastric carcinoma cell lines carrying an amplified c-met oncogene. Cancer Genet. Cytogenet. *64*, 170–173.

Reungwetwattana, T., Liang, Y., Zhu, V., and Ou, S.-H.I. (2017). The race to target MET exon 14 skipping alterations in non-small cell lung cancer: The Why, the How, the Who, the Unknown, and the Inevitable. Lung Cancer *103*, 27–37.

Rickert, K.W., Patel, S.B., Allison, T.J., Byrne, N.J., Darke, P.L., Ford, R.E., Guerin, D.J., Hall, D.L., Kornienko, M., Lu, J., et al. (2011). Structural Basis for Selective Small Molecule Kinase Inhibition of Activated c-Met. J. Biol. Chem. *286*, 11218–11225.

Riggio, M., Perrone, M.C., Polo, M.L., Rodriguez, M.J., May, M., Abba, M., Lanari, C., and Novaro, V. (2017). AKT1 and AKT2 isoforms play distinct roles during breast cancer progression through the regulation of specific downstream proteins. Sci. Rep. *7*.

Rink, J., Ghigo, E., Kalaidzidis, Y., and Zerial, M. (2005). Rab conversion as a mechanism of progression from early to late endosomes. Cell *122*, 735–749.

Rodrigues, G.A., and Park, M. (1994). Autophosphorylation modulates the kinase activity and oncogenic potential of the Met receptor tyrosine kinase. Oncogene *9*, 2019–2027.

Rodrigues, G.A., Falasca, M., Zhang, Z., Ong, S.H., and Schlessinger, J. (2000). A Novel Positive Feedback Loop Mediated by the Docking Protein Gab1 and Phosphatidylinositol 3-Kinase in Epidermal Growth Factor Receptor Signaling. Mol. Cell. Biol. *20*, 1448–1459.

Rohn, W.M., Rouillé, Y., Waguri, S., and Hoflack, B. (2000). Bi-directional trafficking between the trans-Golgi network and the endosomal/lysosomal system. J. Cell Sci. *113 (Pt 12)*, 2093–2101.

Roskoski, R. (2016). Classification of small molecule protein kinase inhibitors based upon the structures of their drug-enzyme complexes. Pharmacol. Res. *103*, 26–48.

Rosselli-Murai, L.K., Yates, J.A., Yoshida, S., Bourg, J., Ho, K.K.Y., White, M., Prisby, J., Tan, X., Altemus, M., Bao, L., et al. (2018). Loss of PTEN promotes formation of signaling-capable clathrin-coated pits. J. Cell Sci. *131*.

Rusten, T.E., Rodahl, L.M.W., Pattni, K., Englund, C., Samakovlis, C., Dove, S., Brech, A., and Stenmark, H. (2006). Fab1 phosphatidylinositol 3-phosphate 5-kinase controls trafficking but not silencing of endocytosed receptors. Mol. Biol. Cell *17*, 3989–4001.

Rutherford, A.C., Traer, C., Wassmer, T., Pattni, K., Bujny, M.V., Carlton, J.G., Stenmark, H., and Cullen, P.J. (2006). The mammalian phosphatidylinositol 3-phosphate 5-kinase (PIKfyve) regulates endosome-to-TGN retrograde transport. J. Cell Sci. *119*, 3944–3957.

Ruzzene, M., and Pinna, L.A. (2010). Addiction to protein kinase CK2: a common denominator of diverse cancer cells? Biochim. Biophys. Acta *1804*, 499–504.

Sachs, M., Brohmann, H., Zechner, D., Müller, T., Hülsken, J., Walther, I., Schaeper, U., Birchmeier, C., and Birchmeier, W. (2000). Essential role of Gab1 for signaling by the c-Met receptor in vivo. J. Cell Biol. *150*, 1375–1384.

Sadowski, L., Pilecka, I., and Miaczynska, M. (2009). Signaling from endosomes: location makes a difference. Exp. Cell Res. *315*, 1601–1609.

Sahlberg, S.H., Mortensen, A.C., Haglöf, J., Engskog, M.K.R., Arvidsson, T., Pettersson, C., Glimelius, B., Stenerlöw, B., and Nestor, M. (2016). Different functions of AKT1 and AKT2 in molecular pathways, cell migration and metabolism in colon cancer cells. Int. J. Oncol. *50*, 5–14.

Sahni, S., Bae, D.-H., Lane, D.J.R., Kovacevic, Z., Kalinowski, D.S., Jansson, P.J., and Richardson, D.R. (2014). The metastasis suppressor, N-myc downstream-regulated gene 1 (NDRG1), inhibits stress-induced autophagy in cancer cells. J. Biol. Chem. *289*, 9692–9709.

Salmena, L., Carracedo, A., and Pandolfi, P.P. (2008). Tenets of PTEN Tumor Suppression. Cell *133*, 403–414.

Sanada, M., Suzuki, T., Shih, L.-Y., Otsu, M., Kato, M., Yamazaki, S., Tamura, A., Honda, H., Sakata-Yanagimoto, M., Kumano, K., et al. (2009). Gain-of-function of mutated C-CBL tumour suppressor in myeloid neoplasms. Nature *460*, 904–908.

Sands, B.E., Jacobson, E.W., Sylwestrowicz, T., Younes, Z., Dryden, G., Fedorak, R., and Greenbloom, S. (2010). Randomized, double-blind, placebo-controlled trial

of the oral interleukin-12/23 inhibitor apilimod mesylate for treatment of active Crohn's disease. Inflamm. Bowel Dis. *16*, 1209–1218.

Santoni-Rugiu, E., Melchior, L.C., Urbanska, E.M., Jakobsen, J.N., de Stricker, K., Grauslund, M., and Sørensen, J.B. (2019). Intrinsic Resistance to EGFR-Tyrosine Kinase Inhibitors in EGFR-Mutant Non-Small Cell Lung Cancer: Differences and Similarities with Acquired Resistance. Cancers *11*.

Sbrissa, D., Ikonomov, O.C., and Shisheva, A. (2000). PIKfyve lipid kinase is a protein kinase: downregulation of 5'-phosphoinositide product formation by autophosphorylation. Biochemistry *39*, 15980–15989.

Sbrissa, D., Ikonomov, O.C., Deeb, R., and Shisheva, A. (2002a). Phosphatidylinositol 5-phosphate biosynthesis is linked to PIKfyve and is involved in osmotic response pathway in mammalian cells. J. Biol. Chem. *277*, 47276–47284.

Sbrissa, D., Ikonomov, O.C., and Shisheva, A. (2002b). Phosphatidylinositol 3-phosphate-interacting domains in PIKfyve. Binding specificity and role in PIKfyve. Endomenbrane localization. J. Biol. Chem. *277*, 6073–6079.

Sbrissa, D., Ikonomov, O.C., Fu, Z., Ijuin, T., Gruenberg, J., Takenawa, T., and Shisheva, A. (2007). Core protein machinery for mammalian phosphatidylinositol 3,5-bisphosphate synthesis and turnover that regulates the progression of endosomal transport. Novel Sac phosphatase joins the ArPIKfyve-PIKfyve complex. J. Biol. Chem. *282*, 23878–23891.

Sbrissa, D., Naisan, G., Ikonomov, O.C., and Shisheva, A. (2018). Apilimod, a candidate anticancer therapeutic, arrests not only PtdIns(3,5)P2 but also PtdIns5P synthesis by PIKfyve and induces bafilomycin A1-reversible aberrant endomembrane dilation. PLoS ONE *13*.

Schaeper, U., Gehring, N.H., Fuchs, K.P., Sachs, M., Kempkes, B., and Birchmeier, W. (2000). Coupling of Gab1 to C-Met, Grb2, and Shp2 Mediates Biological Responses. J. Cell Biol. *149*, 1419–1432.

Schindelin, J., Arganda-Carreras, I., Frise, E., Kaynig, V., Longair, M., Pietzsch, T., Preibisch, S., Rueden, C., Saalfeld, S., Schmid, B., et al. (2012). Fiji: an open-source platform for biological-image analysis. Nat. Methods *9*, 676–682.

Schittek, B., and Sinnberg, T. (2014). Biological functions of casein kinase 1 isoforms and putative roles in tumorigenesis. Mol. Cancer *13*.

Schlessinger, J. (2000). Cell Signaling by Receptor Tyrosine Kinases. Cell *103*, 211–225.

Schmidt, M.H.H., Furnari, F.B., Cavenee, W.K., and Bögler, O. (2003). Epidermal growth factor receptor signaling intensity determines intracellular protein interactions, ubiquitination, and internalization. Proc. Natl. Acad. Sci. U. S. A. *100*, 6505–6510.

Schneider, C.A., Rasband, W.S., and Eliceiri, K.W. (2012). NIH Image to ImageJ: 25 years of image analysis. Nat. Methods *9*, 671–675.

Schoeberl, B., Eichler-Jonsson, C., Gilles, E.D., and Müller, G. (2002). Computational modeling of the dynamics of the MAP kinase cascade activated by surface and internalized EGF receptors. Nat. Biotechnol. *20*, 370–375.

Schubbert, S., Cardenas, A., Chen, H., Garcia, C., Guo, W., Bradner, J., and Wu, H. (2014). Targeting the MYC and PI3K Pathways Eliminates Leukemia-Initiating Cells in T-cell Acute Lymphoblastic Leukemia. Cancer Res. *74*, 7048–7059.

Schuler, M.H., Berardi, R., Lim, W.-T., Geel, R.V., De Jonge, M.J., Bauer, T.M., Azaro, A., Gottfried, M., Han, J.-Y., Lee, D.H., et al. (2016). Phase (Ph) I study of the safety and efficacy of the cMET inhibitor capmatinib (INC280) in patients (pts) with advanced cMET+ non-small cell lung cancer (NSCLC). J. Clin. Oncol. *34*, 9067–9067.

Schwartz, S., Wongvipat, J., Trigwell, C.B., Hancox, U., Carver, B.S., Rodrik-Outmezguine, V., Will, M., Yellen, P., de Stanchina, E., Baselga, J., et al. (2015). Feedback suppression of PI3Kα signaling in PTEN mutated tumors is relieved by selective inhibition of PI3Kβ. Cancer Cell *27*, 109–122.

Seo, J.-S., Ju, Y.S., Lee, W.-C., Shin, J.-Y., Lee, J.K., Bleazard, T., Lee, J., Jung, Y.J., Kim, J.-O., Shin, J.-Y., et al. (2012). The transcriptional landscape and mutational profile of lung adenocarcinoma. Genome Res. *22*, 2109–2119.

Sevinsky, C.J., Khan, F., Kokabee, L., Darehshouri, A., Maddipati, K.R., and Conklin, D.S. (2018). NDRG1 regulates neutral lipid metabolism in breast cancer cells. Breast Cancer Res. BCR *20*, 55.

Shan, Y., Eastwood, M.P., Zhang, X., Kim, E.T., Arkhipov, A., Dror, R.O., Jumper, J., Kuriyan, J., and Shaw, D.E. (2012). Oncogenic Mutations Counteract Intrinsic Disorder in the EGFR Kinase and Promote Receptor Dimerization. Cell *149*, 860–870.

Shan, Y., Arkhipov, A., Kim, E.T., Pan, A.C., and Shaw, D.E. (2013). Transitions to catalytically inactive conformations in EGFR kinase. Proc. Natl. Acad. Sci. U. S. A. *110*, 7270–7275.

Sheth, P.R., Hays, J.L., Elferink, L.A., and Watowich, S.J. (2008). Biochemical Basis for the Functional Switch That Regulates Hepatocyte Growth Factor Receptor Tyrosine Kinase Activation. Biochemistry *47*, 4028–4038.

Shinde, S.R., and Maddika, S. (2016). PTEN modulates EGFR late endocytic trafficking and degradation by dephosphorylating Rab7. Nat. Commun. *7*, 10689.

Shisheva, A. (2008). PIKfyve: PARTNERS, SIGNIFICANCE, DEBATES AND PARADOXES. Cell Biol. Int. *32*, 591–604.

Shisheva, A., Rusin, B., Ikonomov, O.C., DeMarco, C., and Sbrissa, D. (2001). Localization and insulin-regulated relocation of phosphoinositide 5-kinase PIKfyve in 3T3-L1 adipocytes. J. Biol. Chem. *276*, 11859–11869.

Shtiegman, K., Kochupurakkal, B.S., Zwang, Y., Pines, G., Starr, A., Vexler, A., Citri, A., Katz, M., Lavi, S., Ben-Basat, Y., et al. (2007). Defective ubiquitinylation of EGFR mutants of lung cancer confers prolonged signaling. Oncogene *26*, 6968–6978.

Sierra, J.R., and Tsao, M.-S. (2011). c-MET as a potential therapeutic target and biomarker in cancer. Ther. Adv. Med. Oncol. *3*, S21–S35.

Sigismund, S., Argenzio, E., Tosoni, D., Cavallaro, E., Polo, S., and Di Fiore, P.P. (2008). Clathrin-mediated internalization is essential for sustained EGFR signaling but dispensable for degradation. Dev. Cell *15*, 209–219.

Sigismund, S., Avanzato, D., and Lanzetti, L. (2018). Emerging functions of the EGFR in cancer. Mol. Oncol. *12*, 3–20.

Simonsen, A., and Tooze, S.A. (2009). Coordination of membrane events during autophagy by multiple class III PI3-kinase complexes. J. Cell Biol. *186*, 773–782.

Slamon, D.J., Clark, G.M., Wong, S.G., Levin, W.J., Ullrich, A., and McGuire, W.L. (1987). Human breast cancer: correlation of relapse and survival with amplification of the HER-2/neu oncogene. Science *235*, 177–182.

Song, M.S., Salmena, L., and Pandolfi, P.P. (2012). The functions and regulation of the PTEN tumour suppressor. Nat. Rev. Mol. Cell Biol. *13*, 283–296.

Sorkin, A., Krolenko, S., Kudrjavtceva, N., Lazebnik, J., Teslenko, L., Soderquist, A.M., and Nikolsky, N. (1991). Recycling of epidermal growth factor-receptor complexes in A431 cells: identification of dual pathways. J. Cell Biol. *112*, 55–63.

Sos, M.L., Koker, M., Weir, B.A., Heynck, S., Rabinovsky, R., Zander, T., Seeger, J.M., Weiss, J., Fischer, F., Frommolt, P., et al. (2009). PTEN Loss Contributes to Erlotinib Resistance in EGFR-Mutant Lung Cancer by Activation of Akt and EGFR. Cancer Res. *69*, 3256–3261.

Stahelin, R.V., Karathanassis, D., Bruzik, K.S., Waterfield, M.D., Bravo, J., Williams, R.L., and Cho, W. (2006). Structural and membrane binding analysis of the Phox homology domain of phosphoinositide 3-kinase-C2alpha. J. Biol. Chem. *281*, 39396–39406.

Stamos, J., Sliwkowski, M.X., and Eigenbrot, C. (2002). Structure of the epidermal growth factor receptor kinase domain alone and in complex with a 4-anilinoquinazoline inhibitor. J. Biol. Chem. *277*, 46265–46272.

Stamos, J., Lazarus, R.A., Yao, X., Kirchhofer, D., and Wiesmann, C. (2004). Crystal structure of the HGF β-chain in complex with the Sema domain of the Met receptor. EMBO J. *23*, 2325–2335.

Stolz, A., Ernst, A., and Dikic, I. (2014). Cargo recognition and trafficking in selective autophagy. Nat. Cell Biol. *16*, 495–501.

Stommel, J.M., Kimmelman, A.C., Ying, H., Nabioullin, R., Ponugoti, A.H., Wiedemeyer, R., Stegh, A.H., Bradner, J.E., Ligon, K.L., Brennan, C., et al. (2007). Coactivation of receptor tyrosine kinases affects the response of tumor cells to targeted therapies. Science *318*, 287–290.

Stoscheck, C.M., and Carpenter, G. (1984). Characterization of the metabolic turnover of epidermal growth factor receptor protein in A-431 cells. J. Cell. Physiol. *120*, 296–302.

Sturla, L.-M., Amorino, G., Alexander, M.S., Mikkelsen, R.B., Valerie, K., and Schmidt-Ullrichr, R.K. (2005). Requirement of Tyr-992 and Tyr-1173 in Phosphorylation of the Epidermal Growth Factor Receptor by Ionizing Radiation and Modulation by SHP2. J. Biol. Chem. *280*, 14597–14604.

Sun, J., Zhang, D., Bae, D.-H., Sahni, S., Jansson, P., Zheng, Y., Zhao, Q., Yue, F., Zheng, M., Kovacevic, Z., et al. (2013). Metastasis suppressor, NDRG1, mediates its activity through signaling pathways and molecular motors. Carcinogenesis *34*, 1943–1954.

Sunshine, H., and Iruela-Arispe, M.L. (2017). Membrane Lipids and Cell Signaling. Curr. Opin. Lipidol. *28*, 408–413.

Takatori, S., Tatematsu, T., Cheng, J., Matsumoto, J., Akano, T., and Fujimoto, T. (2016). Phosphatidylinositol 3,5-Bisphosphate-Rich Membrane Domains in Endosomes and Lysosomes. Traffic Cph. Den. *17*, 154–167.

Tamguney, T., and Stokoe, D. (2007). New insights into PTEN. J. Cell Sci. *120*, 4071–4079.

Tanizaki, J., Okamoto, I., Sakai, K., and Nakagawa, K. (2011). Differential roles of trans-phosphorylated EGFR, HER2, HER3, and RET as heterodimerisation partners of MET in lung cancer with MET amplification. Br. J. Cancer *105*, 807–813.

Thiel, K.W., and Carpenter, G. (2007). Epidermal growth factor receptor juxtamembrane region regulates allosteric tyrosine kinase activation. Proc. Natl. Acad. Sci. *104*, 19238–19243.

Thien, C.B.F., and Langdon, W.Y. (2005). c-Cbl and Cbl-b ubiquitin ligases: substrate diversity and the negative regulation of signalling responses. Biochem. J. *391*, 153–166.

Toker, A. (2012). Achieving Specificity in Akt Signaling in Cancer. Adv. Biol. Regul. *52*, 78–87.

Tomas, A., Jones, S., Vaughan, S.O., Hochhauser, D., and Futter, C.E. (2017). Stress-specific p38 MAPK activation is sufficient to drive EGFR endocytosis but not its nuclear translocation. J. Cell Sci. *130*, 2481–2490.

Torbett, N.E., Luna-Moran, A., Knight, Z.A., Houk, A., Moasser, M., Weiss, W., Shokat, K.M., and Stokoe, D. (2008). A chemical screen in diverse breast cancer cell lines reveals genetic enhancers and suppressors of sensitivity to PI3K isoform-selective inhibition. Biochem. J. *415*, 97–110.

Torres, J., and Pulido, R. (2001). The Tumor Suppressor PTEN Is Phosphorylated by the Protein Kinase CK2 at Its C Terminus: IMPLICATIONS FOR PTEN STABILITY TO PROTEASOME-MEDIATED DEGRADATION. J. Biol. Chem. *276*, 993–998.

Toska, E., and Baselga, J. (2016). Pharmacology in the Era of Targeted Therapies: The Case of PI3K Inhibitors. Clin. Cancer Res. Off. J. Am. Assoc. Cancer Res. *22*, 2099–2101.

Tovar, E.A., and Graveel, C.R. (2017). MET in human cancer: germline and somatic mutations. Ann. Transl. Med. *5*.

Tripathi, K.P., Piccirillo, M., and Guarracino, M.R. (2018). An integrated approach to infer cross-talks between intracellular protein transport and signaling pathways. BMC Bioinformatics *19*, 58.

Trotman, L.C., Niki, M., Dotan, Z.A., Koutcher, J.A., Di Cristofano, A., Xiao, A., Khoo, A.S., Roy-Burman, P., Greenberg, N.M., Van Dyke, T., et al. (2003). Pten dose dictates cancer progression in the prostate. PLoS Biol. *1*, E59.

Trusolino, L., Bertotti, A., and Comoglio, P.M. (2010). MET signalling: principles and functions in development, organ regeneration and cancer. Nat. Rev. Mol. Cell Biol. *11*, 834–848.

Ueno, T., Sato, W., Horie, Y., Komatsu, M., Tanida, I., Yoshida, M., Ohshima, S., Mak, T.W., Watanabe, S., and Kominami, E. (2008). Loss of Pten, a tumor suppressor, causes the strong inhibition of autophagy without affecting LC3 lipidation. Autophagy *4*, 692–700.

Uings, I.J., and Farrow, S.N. (2000). Cell receptors and cell signalling. Mol. Pathol. *53*, 295–299.

Ullrich, A., and Schlessinger, J. (1990). Signal transduction by receptors with tyrosine kinase activity. Cell *61*, 203–212.

Ullrich, A., Coussens, L., Hayflick, J.S., Dull, T.J., Gray, A., Tam, A.W., Lee, J., Yarden, Y., Libermann, T.A., and Schlessinger, J. (1984). Human epidermal growth factor receptor cDNA sequence and aberrant expression of the amplified gene in A431 epidermoid carcinoma cells. Nature *309*, 418–425.

Ung, P.M.-U., and Schlessinger, A. (2015). DFGmodel: Predicting Protein Kinase Structures in Inactive States for Structure-Based Discovery of Type-II Inhibitors. ACS Chem. Biol. *10*, 269–278.

Vanhaesebroeck, B., Guillermet-Guibert, J., Graupera, M., and Bilanges, B. (2010). The emerging mechanisms of isoform-specific PI3K signalling. Nat. Rev. Mol. Cell Biol. *11*, 329–341.

Veenstra, C., Pérez-Tenorio, G., Stelling, A., Karlsson, E., Mirwani, S.M., Nordensköljd, B., Fornander, T., and Stål, O. (2016). Met and its ligand HGF are associated with clinical outcome in breast cancer. Oncotarget *7*, 37145–37159.

Vega, Q.C., Cochet, C., Filhol, O., Chang, C.P., Rhee, S.G., and Gill, G.N. (1992). A site of tyrosine phosphorylation in the C terminus of the epidermal growth factor receptor is required to activate phospholipase C. Mol. Cell. Biol. *12*, 128–135.

Viaud, J., Lagarrigue, F., Ramel, D., Allart, S., Chicanne, G., Ceccato, L., Courilleau, D., Xuereb, J.-M., Pertz, O., Payrastre, B., et al. (2014). Phosphatidylinositol 5-phosphate regulates invasion through binding and activation of Tiam1. Nat. Commun. *5*, 4080.

Vicinanza, M., Korolchuk, V.I., Ashkenazi, A., Puri, C., Menzies, F.M., Clarke, J.H., and Rubinsztein, D.C. (2015). PI(5)P Regulates Autophagosome Biogenesis. Mol. Cell *57*, 219–234.

Vijayan, R.S.K., He, P., Modi, V., Duong-Ly, K.C., Ma, H., Peterson, J.R., Dunbrack, R.L., and Levy, R.M. (2015). Conformational Analysis of the DFG-Out Kinase Motif and Biochemical Profiling of Structurally Validated Type II Inhibitors. J. Med. Chem. *58*, 466–479.

Vivanco, I., Palaskas, N., Tran, C., Finn, S.P., Getz, G., Kennedy, N.J., Jiao, J., Rose, J., Xie, W., Loda, M., et al. (2007). Identification of the JNK Signaling Pathway as a Functional Target of the Tumor Suppressor PTEN. Cancer Cell *11*, 555–569.

Vivanco, I., Rohle, D., Versele, M., Iwanami, A., Kuga, D., Oldrini, B., Tanaka, K., Dang, J., Kubek, S., Palaskas, N., et al. (2010). The phosphatase and tensin homolog regulates epidermal growth factor receptor (EGFR) inhibitor response by targeting EGFR for degradation. Proc. Natl. Acad. Sci. U. S. A. *107*, 6459–6464.

Vivanco, I., Robins, H.I., Rohle, D., Campos, C., Grommes, C., Nghiemphu, P.L., Kubek, S., Oldrini, B., Chheda, M.G., Yannuzzi, N., et al. (2012). Differential Sensitivity of Glioma- versus Lung Cancer–Specific EGFR Mutations to EGFR Kinase Inhibitors. Cancer Discov. *2*, 458–471.

de Vos, A.M., Ultsch, M., and Kossiakoff, A.A. (1992). Human growth hormone and extracellular domain of its receptor: crystal structure of the complex. Science *255*, 306–312.

Wada, Y., Cardinale, I., Khatcherian, A., Chu, J., Kantor, A.B., Gottlieb, A.B., Tatsuta, N., Jacobson, E., Barsoum, J., and Krueger, J.G. (2012). Apilimod Inhibits the Production of IL-12 and IL-23 and Reduces Dendritic Cell Infiltration in Psoriasis. PLoS ONE *7*.

Wagner, M.J., Stacey, M.M., Liu, B.A., and Pawson, T. (2013). Molecular Mechanisms of SH2- and PTB-Domain-Containing Proteins in Receptor Tyrosine Kinase Signaling. Cold Spring Harb. Perspect. Biol. *5*.

Wallroth, A., and Haucke, V. (2018). Phosphoinositide conversion in endocytosis and the endolysosomal system. J. Biol. Chem. *293*, 1526–1535.

Wandinger-Ness, A., and Zerial, M. (2014). Rab Proteins and the Compartmentalization of the Endosomal System. Cold Spring Harb. Perspect. Biol. *6*.

Wang, C., Wang, X., Su, Z., Fei, H., Liu, X., and Pan, Q. (2015a). The novel mTOR inhibitor Torin-2 induces autophagy and downregulates the expression of UHRF1 to suppress hepatocarcinoma cell growth. Oncol. Rep. *34*, 1708–1716.

Wang, Q., Liu, P., Spangle, J.M., Von, T., Roberts, T.M., Lin, N.U., Krop, I.E., Winer, E.P., and Zhao, J.J. (2016). PI3K-p110α mediates resistance to HER2-targeted therapy in HER2+, PTEN-deficient breast cancers. Oncogene *35*, 3607–3612.

Wang, W., Marimuthu, A., Tsai, J., Kumar, A., Krupka, H.I., Zhang, C., Powell, B., Suzuki, Y., Nguyen, H., Tabrizizad, M., et al. (2006a). Structural characterization of autoinhibited c-Met kinase produced by coexpression in bacteria with phosphatase. Proc. Natl. Acad. Sci. *103*, 3563–3568.

Wang, W., Marimuthu, A., Tsai, J., Kumar, A., Krupka, H.I., Zhang, C., Powell, B., Suzuki, Y., Nguyen, H., Tabrizizad, M., et al. (2006b). Structural characterization of autoinhibited c-Met kinase produced by coexpression in bacteria with phosphatase. Proc. Natl. Acad. Sci. U. S. A. *103*, 3563–3568.

Wang, W., Xu, S., Yin, M., and Jin, Z.G. (2015b). Essential roles of Gab1 tyrosine phosphorylation in growth factor-mediated signaling and angiogenesis. Int. J. Cardiol. *181*, 180–184.

Wang, Y., Gao, J., Guo, X., Tong, T., Shi, X., Li, L., Qi, M., Wang, Y., Cai, M., Jiang, J., et al. (2014). Regulation of EGFR nanocluster formation by ionic protein-lipid interaction. Cell Res. *24*, 959–976.

Wee, P., and Wang, Z. (2017). Epidermal Growth Factor Receptor Cell Proliferation Signaling Pathways. Cancers *9*.

Wee, S., Wiederschain, D., Maira, S.-M., Loo, A., Miller, C., deBeaumont, R., Stegmeier, F., Yao, Y.-M., and Lengauer, C. (2008). PTEN-deficient cancers depend on PIK3CB. Proc. Natl. Acad. Sci. *105*, 13057–13062.

Weihua, Z., Tsan, R., Huang, W.-C., Wu, Q., Chiu, C.-H., Fidler, I.J., and Hung, M.-C. (2008). Survival of Cancer Cells Is Maintained by EGFR Independent of Its Kinase Activity. Cancer Cell *13*, 385–393.

Weinstein, I.B. (2002). Cancer. Addiction to oncogenes--the Achilles heal of cancer. Science *297*, 63–64.

Westerfield, J.M., and Barrera, F.N. (2019). Membrane receptor activation mechanisms and transmembrane peptide tools to elucidate them. J. Biol. Chem. jbc.REV119.009457.

Wiley, H.S. (1988). Anomalous binding of epidermal growth factor to A431 cells is due to the effect of high receptor densities and a saturable endocytic system. J. Cell Biol. *107*, 801–810.

Williams, R. (2007). PIP2 in endocytosis. J. Cell Biol. *177*, 185.

Wirbel, J., Cutillas, P., and Saez-Rodriguez, J. (2017). Phosphoproteomics-Based Profiling of Kinase Activities in Cancer Cells. Methods Mol. Biol. Clifton Nj *1711*, 103–132.

Wlodkowic, D., Skommer, J., McGuinness, D., Hillier, C., and Darzynkiewicz, Z. (2009). ER-Golgi network– a future target for anti-cancer therapy. Leuk. Res. *33*, 1440–1447.

Xie, Z., and Klionsky, D.J. (2007). Autophagosome formation: core machinery and adaptations. Nat. Cell Biol. *9*, 1102–1109.

Xing, F., Persaud, Y., Pratilas, C., Taylor, B., Janakiraman, M., She, Q.-B., Gallardo, H., Liu, C., Merghoub, T., Hefter, B., et al. (2012). Concurrent loss of the PTEN and RB1 tumor suppressors attenuates RAF dependence in melanomas harboring V600EBRAF. Oncogene *31*, 446–457.

Xu, Z., Hu, J., Cao, H., Pilo, M.G., Cigliano, A., Shao, Z., Xu, M., Ribback, S., Dombrowski, F., Calvisi, D.F., et al. (2018). Loss of Pten synergizes with c-Met to promote hepatocellular carcinoma development via mTORC2 pathway. Exp. Mol. Med. *50*, e417.

Yamamoto, A., Tagawa, Y., Yoshimori, T., Moriyama, Y., Masaki, R., and Tashiro, Y. (1998). Bafilomycin A1 prevents maturation of autophagic vacuoles by inhibiting fusion between autophagosomes and lysosomes in rat hepatoma cell line, H-4-II-E cells. Cell Struct. Funct. *23*, 33–42.

Yamaoka, T., Kusumoto, S., Ando, K., Ohba, M., and Ohmori, T. (2018). Receptor Tyrosine Kinase-Targeted Cancer Therapy. Int. J. Mol. Sci. *19*.

Yan, B., Lim, M., Zhou, L., Kuick, C.H., Leong, M.Y., Yong, K.J., Aung, L., Salto-Tellez, M., and Chang, K.T.E. (2013). Identification of MET genomic amplification, protein expression and alternative splice isoforms in neuroblastomas. J. Clin. Pathol. *66*, 985–991.

Yang, J., Nie, J., Ma, X., Wei, Y., Peng, Y., and Wei, X. (2019). Targeting PI3K in cancer: mechanisms and advances in clinical trials. Mol. Cancer *18*, 26.

Yarden, Y. (2001). The EGFR family and its ligands in human cancer: signalling mechanisms and therapeutic opportunities. Eur. J. Cancer *37*, 3–8.

Yarden, Y., and Ullrich, A. (1988). Growth factor receptor tyrosine kinases. Annu. Rev. Biochem. *57*, 443–478.

Yokouchi, M., Kondo, T., Houghton, A., Bartkiewicz, M., Horne, W.C., Zhang, H., Yoshimura, A., and Baron, R. (1999). Ligand-induced ubiquitination of the epidermal growth factor receptor involves the interaction of the c-Cbl RING finger and UbcH7. J. Biol. Chem. *274*, 31707–31712.

Yu, X., Sharma, K.D., Takahashi, T., Iwamoto, R., and Mekada, E. (2002). Ligand-independent Dimer Formation of Epidermal Growth Factor Receptor (EGFR) Is a Step Separable from Ligand-induced EGFR Signaling. Mol. Biol. Cell *13*, 2547–2557.

Zeng, S., Xu, Z., Lipkowitz, S., and Longley, J.B. (2005). Regulation of stem cell factor receptor signaling by Cbl family proteins (Cbl-b/c-Cbl). Blood *105*, 226–232.

Zhang, W., and Liu, H.T. (2002). MAPK signal pathways in the regulation of cell proliferation in mammalian cells. Cell Res. *12*, 9–18.

Zhang, J., Adrián, F.J., Jahnke, W., Cowan-Jacob, S.W., Li, A.G., Iacob, R.E., Sim, T., Powers, J., Dierks, C., Sun, F., et al. (2010). Targeting Bcr-Abl by combining allosteric with ATP-binding-site inhibitors. Nature *463*, 501–506.

Zhang, S., Huang, W.-C., Li, P., Guo, H., Poh, S.-B., Brady, S.W., Xiong, Y., Tseng, L.-M., Li, S.-H., Ding, Z., et al. (2011). Combating trastuzumab resistance by targeting SRC, a common node downstream of multiple resistance pathways. Nat. Med. *17*, 461–469.

Zhang, X., Gureasko, J., Shen, K., Cole, P.A., and Kuriyan, J. (2006). An Allosteric Mechanism for Activation of the Kinase Domain of Epidermal Growth Factor Receptor. Cell *125*, 1137–1149.

Zhang, Y., Xia, M., Jin, K., Wang, S., Wei, H., Fan, C., Wu, Y., Li, X., Li, X., Li, G., et al. (2018). Function of the c-Met receptor tyrosine kinase in carcinogenesis and associated therapeutic opportunities. Mol. Cancer *17*, 45.

Zhen, Z., Giordano, S., Longati, P., Medico, E., Campiglio, M., and Comoglio, P.M. (1994). Structural and functional domains critical for constitutive activation of the HGF-receptor (Met). Oncogene *9*, 1691–1697.

Zheng, H., Ying, H., Yan, H., Kimmelman, A.C., Hiller, D.J., Chen, A.-J., Perry, S.R., Tonon, G., Chu, G.C., Ding, Z., et al. (2008). p53 and Pten control neural and glioma stem/progenitor cell renewal and differentiation. Nature *455*, 1129–1133.

Zhu, J., Horbinski, C., Guo, F., Watkins, S., Uchiyama, Y., and Chu, C.T. (2007). Regulation of Autophagy by Extracellular Signal-Regulated Protein Kinases During 1-Methyl-4-Phenylpyridinium-Induced Cell Death. Am. J. Pathol. *170*, 75–86.